DOCTOR OF PHILOSOPHY

Identification of OATP1B3 as a potential therapeutic target in Recessive Dystrophic Epidermolysis Bullosa Associated Squamous Cell Carcinoma

Cole, Clare Louise

Award date:
2011

DOCTOR OF PHILOSOPHY

Identification of OATP1B3 as a potential therapeutic target in Recessive Dystrophic Epidermolysis Bullosa Associated Squamous Cell Carcinoma

Clare Louise Cole

2011

University of Dundee

Identification of OATP1B3 as a Potential Therapeutic Target in Recessive Dystrophic Epidermolysis Bullosa Associated Squamous Cell Carcinoma

Clare Louise Cole

Doctor of Philosophy

University of Dundee

1 December 2011

Declaration

I hereby declare that this thesis has been composed entirely by myself. This thesis is a true record of all work performed by me. This work has not previously been submitted for any other higher degree. The work presented here is completely my own and all referenced work has been duly recognized and acknowledged.

This investigation was carried out under the supervision of Dr Andrew South and Professor Irene Leigh in the Centre of Oncology and Molecular Medicine, at the University of Dundee.

Clare Louise Cole

I confirm that Clare Louise Cole has undertaken all work described herein at the University of Dundee under my supervision. She has fulfilled all criteria for Ordinance 39 and is qualified to submit this thesis for the Doctor of Philosophy degree.

Dr Andrew P South

Professor Irene Leigh

Acknowledgements

I have been indebted to my supervisor, Dr Andrew South of the University of Dundee for his guidance, and patience throughout the preparation of this thesis. His support and wealth of knowledge and experience has been invaluable to me.

I am extremely grateful to my colleagues and past and present members of “team skin”, especially to Dr Stephen Watt, Dr Celine Pourreyron and Dr Carol Hogan who have provided me with support, help and their expertise in the lab throughout my PhD.

My family, especially my parents have provided me with constant support both emotionally and morally as well as given me encouragement to keep me going over the past 4 years. Finally, to Charlotte Killick; who has been a pillar of support throughout the final months of my thesis – thank you.

Table of Contents

List of Tables

List of Figures

Abbreviations

A	Adenine
aa	Amino acid
Ab	Antibody
ABI	Applied Biosystems
AGE	Agarose Gel Electrophoresis
AK	Actinic Keratosis
AP	Alkaline Phosphatase
ATP	Adenosine triphosphate
BCC	Basal Cell Carcinoma
BMZ	Basement membrane zone
bp	Base pair
BSA	Bovine serum albumin
C	Cytosine
$CaCl_2$	Calcium Chloride
CDKN2A	Cyclin-dependent kinase inhibitor 2A
cDNA	Complementary DNA
CGH	Comparative genomic hybridization
Ci	Currie
CO_2	Carbon dioxide
COL7A1	Type VII Collagen

CPD	Cyclo pyrimidine dimers
CpG	Cytosine guanine dinucleotide
cSCC	Cutaneous squamous cell carcinoma
Ct	Cycle Threshold
DAPI	4', 6-diamido-2-phenylindole
ΔΔCt	Delta delta Ct
DEB	Dystrophic epidermolysis bullosa
DDEB	Dominant dystrophic epidermolysis bullosa
dH_2O	Distilled H_2O
DNA	Deoxyribonucleic acid
dNTPs	Deoxynucleotide Triphosphates
DMEM	Dulbecco's modified eagle medium
DTT	Dithiothreitol
EBK	Epidermolysis Bullosa Keratinocytes
EBS	Epidermolysis Bullosa Simplex
EBS-S	Suprabasal EBS
EBS-B	Basal EBS
ECL	Enhanced chemiluminescence
ECM	Extracellular matrix
EDTA	Ethylenediaminetetraacetic acid
EGF	Epidermal growth factor

ELISA	Enzyme linked immunosorbent assay
EM	Electron microscopy
ER	Endoplasmic reticulum
ESC	Embryonic stem cells
EST	Expressed sequence tag
ETOH	Ethanol
ExoI	Exonuclease I
ExoSap	Exonuclease I and Shrimp Alkaline Phosphatase
F	Forward
FBS	Fetal bovine serum
FCS	Fetal Calf Serum
FFPE	Formalin fixed paraffin embedded
FU	Fluorescence units
G	Guanine
g	Gram
GAPDH	Glyceraldehyde 3-phosphate dehydrogenase
gDNA	Genomic DNA
GO	Gene ontology
HCL	Hydrochloric acid
HD	Homozygous deletion

HH	Hedgehog
HIV	Human immunodeficiency virus
HNSCC	Head and neck squamous cell carcinoma
HPV	Human papilloma virus
HRP	Horse radish peroxidase
IC	Immunocompetent
IF	Immunofluorescence
IG	Immunoglobulin
IHC	Immunohistochemistry
IPA	Ingenuity pathway analysis
iPSC	Induced pluripotent stem cells
IS	Immunosuppression
JEB	Junctional epidermolysis bullosa
JEB-H	Herlitz JEB
JEB-O	Other JEB
Kb	Kilobase
KCl	Potassium chloride
kDa	Kilodalton
KH_2PO_4	Potassium dihydrogen phosphate
KRT	Keratin

KS	Kindler syndrome
l	Litre
Log	Logarithmic
LOH	Loss of heterozygosity
µ	Micron
µg	Microgram
µl	Microlitre
µM	Micromolar
m	Metre
M	Molar
mA	Milliamps
Mb	Megabase
MD	Moderately differentiated
MDM2	Double minute 2 protein
Met	Metastatic
mg	Milligram
MGB	Minor groove binder
$MgCl_2$	Magnesium Chloride
$MgSO_4$	Magnesium sulphate
Mins	Minutes
miRNA	MicroRNA

ml	Millilitres
mM	Millimolar
MMP	Matrix Metalloproteinase
mRNA	MessengerRNA
NaCl	Sodium chloride
NC	Non-collagenous
NER	Nucleotide excision repair
ng	Nanogram
nM	Nanomole
NMSC	Non melanoma skin cancer
ORF	Open reading frame
OTR	Organ transplant recipients
PBS	Phosphate buffered saline
PBST	PBS with Tween
PCR	Polymerase chain reaction
PCD	Programmed cell death
PD	Poorly differentiated
PEG	Polyethylene glycol 8000
PFA	Paraformaldehyde
pg	Picogram

pmol	Picomole
PTC	Premature termination codon
qRT-PCR	Quantitative real time-PCR
R	Reverse
RE	Restriction enzyme
RBI	Retinoblastoma
RDEB	Recessive Dystrophic Epidermolysis Bullosa
RDEB-O	Generalised other RDEB
RIN	RNA integrity number
RNA	Ribonucleic acid
ROS	Reactive oxygen species
RPM	Revolutions per minute
RT	Reverse Transcriptase
RT-PCR	Reverse Transcriptase PCR
Sap	Shrimp alkaline phosphatase
SCC	Squamous cell carcinoma
Sec	Seconds
Sev-gen RDEB	Severe generalised RDEB
SNP	Single nucleotide polymorphism

T	Thymine
TBE	Tris-borate-ethylenediaminetetraacetic acid
TBS	Tris buffered saline
Tm	Melting temperature
TNF	Tumour necrosis factor
TP53	Tumour protein 53
TSG	Tumour suppressor gene
U	Units
UPD	Uniparental disomy
UTR	Untranslated region
UV	Ultraviolet
V	Volts
vs.	Versus
WB	Western blotting
WD	Well differentiated
WT	Wild-type
x	Times

Abstract

Epidermolysis Bullosa encompasses a group of inherited heterogeneous diseases involving trauma induced blistering of the skin. Recessive Dystrophic Epidermolysis Bullosa (RDEB) is one of the most debilitating variants of the disease and patients are predisposed to developing aggressive cutaneous Squamous Cell Carcinoma (SCC). Unlike SCC in the general population, the primary cause of RDEB associated SCC is not UV-radiation. SCC in RDEB patients has poor prognosis due to a high frequency of recurrence and metastasis. 70% of all severe generalized RDEB patients die from SCC by the age of 45, compared to only 1.25% of all patients with UV-induced SCC in the general population (Fine et al. 2008), making SCC the leading cause of death in these RDEB patients.

The aim of this investigation was to identify therapeutic targets for RDEB associated SCC. Global gene expression studies identified 36 candidate genes which were differentially regulated in RDEB SCC (n=4) compared with non-RDEB SCC (n=5) primary keratinocyte cultures. The validation of these genes by qRT-PCR in replicate cultures of RDEB SCC (n=3), non-RDEB SCC (n=3) keratinocytes and normal human keratinocytes as a control, deduced 5 genes to be significantly differentially regulated. Of particular interest, is the over-expression of *SLCO1B3* by 6.25 fold in RDEB SCC keratinocytes (p = 0.035). *SLCO1B3* encodes the organic anion transporter OATP1B3, which is normally exclusively expressed on the basolateral membrane of hepatocytes. qRT-PCR revealed the mRNA expression level of *SLCO1B3* is reduced in RDEB SCC keratinocyte cultures when *COL7A1*, the causal gene mutated in RDEB, is re-expressed, suggesting that *COL7A1* which encodes the Type VII Collagen protein and is secreted into the extracellular matrix, may suppress the transcription of *SLCO1B3*. Immunofluorescent staining of RDEB SCC keratinocytes and

tissue identified OATP1B3 expression, whilst qRT-PCR using mRNA isolated from freshly frozen skin and SCC tissue samples from both RDEB and non-RDEB individuals identified increased *SLCO1B3* mRNA expression in RDEB SCC *in vivo.*

Over expression of *SLCO1B3* and increased activity of OATP1B3 is associated with breast, colon and pancreatic cancer and is a known transporter of chemotherapeutic agents, such as Methotrexate and Paclitaxel. These observations have led to speculation that, as a transporter over expressed in cancer and capable of introducing drugs into cells, OATP1B3 represents a potential therapeutic target. Preliminary results from a cell viability assay suggest that exposing RDEB SCC cells to Microcystin-LR specifically reduces cell viability in a *SLCO1B3* dependent manner. This supports the conclusion that *SLCO1B3* represents a viable RDEB SCC specific therapeutic target and provides a pathway which can be exploited to deliver anti-cancer drugs directly to tumour cells whilst reducing the systemic toxicity of these agents.

Chapter 1

Introduction

1.1 Skin, structure and function

The skin is the largest organ of the body and its crucial function is to protect the body from damage. It does this by creating a self-renewing physical barrier against the environment and thus provides protection against pathogens, guards the underlying muscles, bones, ligaments and internal organs and prevents dehydration and nutrient loss (Poumay and Coquette 2007).

The uppermost layer of the skin, known as the epidermis, is mainly composed of keratinocytes that can undergo proliferation and differentiation. This is a progressive maturing of the cells to create the 4 layers of the epidermis; the stratum corneum being the outermost layer followed by the granular, spinous and finally the basal layer (Figure 1.0). Keratinisation occurs when cells are formed by mitosis in the basal layer and daughter cells migrate up through the strata. During terminal differentiation of these cells, they undergo morphological changes from undifferentiated proliferative cuboid cells to a squamous morphology of the cornified layer (Poumay and Coquette 2007). The epidermis also consists of other minor cell types including; merkel cells that when in the presence of neurons create synapses (Shimohira-Yamasaki et al. 2006), antigen-presenting langerhans cells and pigment producing cells known as melanocytes (Pittelkow and Shipley 1989).

Beneath the epidermis is the dermis; however separating these two layers is the basement membrane zone (BMZ), which securely connects the two layers. The BMZ is composed of a number of proteins, including keratins, plakins, laminin 332 and collagens, to name a few, that are responsible for the structural integrity and association of the epidermis to the underlying dermis (Uitto and Richard 2005).

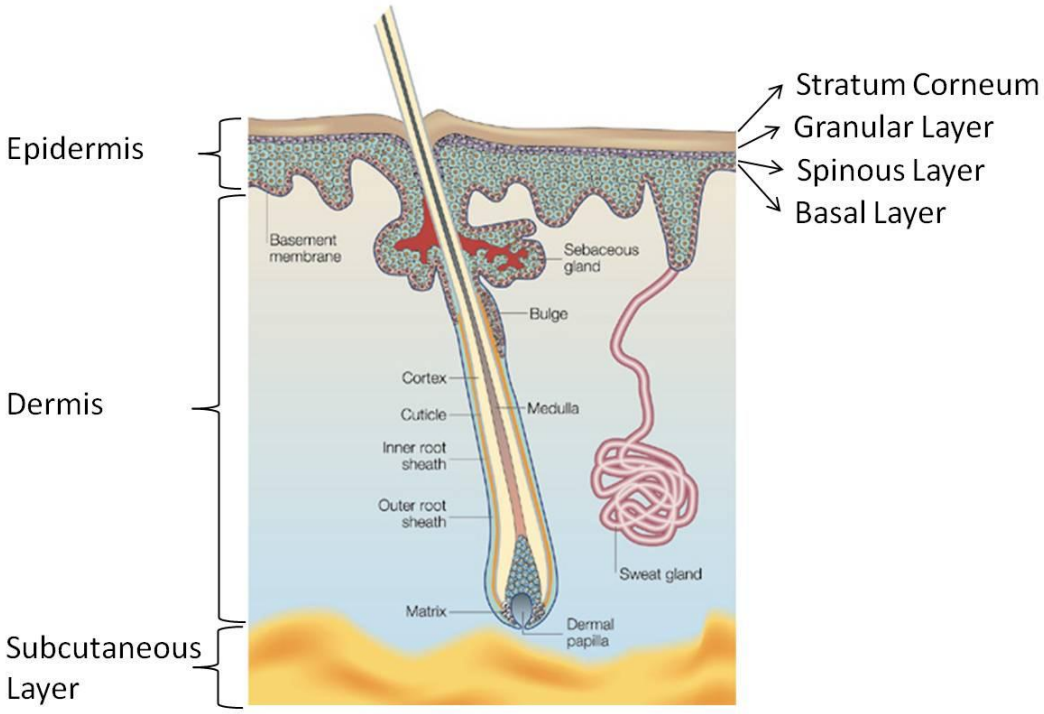

Figure 1.0 Basic Skin Structure

The skin is composed of 2 layers, the dermis followed by the overlying epidermis, comprising of 4 layers; basal layer, spinous layer, granular layer and stratum corneum which are primarily composed of keratinocytes at different stages of differentiation. The two skin layers are separated by the basement membrane zone. Figure adapted from (Fuchs and Raghavan 2002).

The dermis is composed of cells dispersed among an extracellular matrix containing connective tissue, hair follicles, sebaceous glands, apocrine glands and blood vessels (Aumailley et al. 2006). Structurally it can be divided into 2 sections; first an area of loose areolar connective tissue known as the papillary dermis followed by a thick layer of dense irregular connective tissue known as the reticular region which has strength, extensibility and elasticity.

Finally, although not considered to be a separate layer of the skin; the subcutaneous layer composed of loose connective tissue and elastin attaches the skin to the underlying bone and muscle. This layer supplies the skin with blood vessels and nerves, and is mainly comprised of fibroblasts, macrophages and adipocytes.

The skin is a dynamic and resilient organ that is able to constantly renew and heal itself. However, the skin's function becomes compromised and challenged when mutations in the molecular makeup of this tissue occur. The altered DNA sequences of genes involved in the skin can cause a wide array of cutaneous diseases most of which are caused by germline mutations, an example of which is the rare genetically inherited disease Epidermolysis Bullosa, which this thesis focuses on.

1.2 Epidermolysis Bullosa

Approximately 5000 people in the UK suffer from a rare genetic condition known as Epidermolysis Bullosa (EB) (Pillay 2008). EB encompasses a complex group of genetic skin diseases affecting approximately 1 in 17,000 live births, with an estimated 500,000 cases worldwide (Featherstone 2007). EB was first described by Kobner in 1886, however it wasn't until the 1960's that a distinct classification of the disease was established (Pearson 1962). The manifestations of the disease are heterogeneous and many subtypes of the condition exist. Briefly, EB consists of a group of mechanobullous diseases involving trauma induced blistering and chronic erosions of the skin. There is also extracutaneous involvement where blistering affects a number of specialised mucosal membranes such as those of the oral cavity, pharynx, oesophagus and gastrointestinal tract (Briggaman and

Wheeler 1975; Uitto et al. 1992). All variants of EB are produced as a result of dysfunctional cell adhesion molecules.

The EB classification system has been under recurrent revision since the first categorisation of the disease, with the most recent review occurring in 2009. Current classification states four major types of the disease exist, which can be distinguished by identifying the plane of cleavage through the dermal-epidermal BMZ (Fine et al. 2009). The subtypes of EB can be diagnosed and distinguished by electron microscopy (EM) of the skin, but it has been suggested that for an accurate diagnosis to be made by EM, this can only be provided by a person experienced in using this technique, and therefore it is likely to play a lesser role in diagnosis of EB in the future (Fine et al. 2009). However, the definitive diagnosis is ultimately dependent on DNA mutational analysis (Sawamura et al. 2010).

EB diagnosis generally begins with immunoflourescence and electron microscopy of skin tissues followed by analysis of the proteins and antigen mapping by immunofluorescence microscopy. Diagnosis of the specific subtypes is essential, as in neonates the disease subtypes may present with similar clinical features but the actual prognosis of the disease is very different depending on the variant of EB. Furthermore, many genetic therapies require accurate knowledge of the specific mutations of a particular patient and therefore it is important that a definitive molecular diagnosis is made. This is also beneficial for developing an understanding of the disease mechanisms, allowing progress to be made in employing accurate mouse and cell models of EB for research investigations. Skin biopsies allow identification of the level of separation occurring and protein deficiencies can be seen using monoclonal antibodies, an important step in the pursuit of a correct diagnosis of EB

subtype. Prenatal diagnosis is offered when one or both parents are patients and have already had one affected pregnancy. The test comprises of taking a sample of free-fetal DNA in the plasma faction of maternal blood, which represents 3-6% of the total DNA in maternal plasma.

1.2.1 Subtypes of EB

The four entities include EB Simplex (EBS), Junctional EB (JEB), Dystrophic EB (DEB) and Kindler Syndrome (KS). The main types of EB can be further sub-classified based on the mode of inheritance and clinical features of the disease, as outlined in Table 1.0. The majority of pathogenic mutations in EBS are within the *KRT5, KRT14* and *PLEC1* genes, where cleavage of the BMZ occurs in the basal keratinocyte (Figure 1.1). JEB has separation at the level of the lamina lucida with the main mutations occurring in *LAMA3*, *LAMB3, LAMC2, COL17A1* and α6β4 *integrin* (Pfendner and Lucky 1993). DEB is exclusively caused by mutations of the *COL7A1* gene and is identified by blister formation below the lamina densa, as shown in Figure 1.1. Finally, KS has mutations of the *KIND1* gene (Fine et al. 2008), with cleavage occurring in multiple regions of the BMZ. Although EB encompasses a wide spectrum of skin fragility diseases, the main focus of this introduction will be Recessive Dystrophic Epidermolysis Bullosa (RDEB).

1.2.2 Epidermolysis Bullosa Simplex

EB Simplex is the mildest and most common form of EB and with an occurrence of 1 in every 25,000 live births (Coulombe et al. 2009). There are several phenotypes of EBS, and these can be confined to two broad subtypes; suprabasal (EBS-S) and basal (EBS-B). EBS was the first disorder shown to be caused by mutations in a gene encoding an intermediate

filament protein and also the first epithelial skin fragility condition to have its etiology revealed (Coulombe et al. 2009). EBS is chiefly inherited in an autosomal dominant pattern although recessive inheritance has been reported (Pfendner and Bruckner 1993).

Major EB Type	Major EB Subtype	Minor Sub-classifications
EB Simplex	Suprabasal	Lethal ancatholytic EB
		Plakophilin deficiency
		EBS superficialis
	Basal EBS	EBS, localised
		EBS, Dowling-Meara
		EBS, generalised other
		EBS with mottled skin pigmentation
		EBS with muscular dystrophy
		EBS with pyloric atresia
		EBS, autosomal recessive
		EBS, Ogna
		EBS, migratory circinate
Junctional EB	JEB-Herlitz	N/A
	JEB, other	JEB, non-Herlitz generalised
		JEB, non-Herlitz localised
		JEB with pyloric atresia
		JEB, inversa
		JEB, late onset
		LOC syndrome
Dystrophic EB	Dominant DEB	DDEB, generalised
		DDEB, acral
		DDEB, pretibial
		DDEB, pruriginosa
		DDEB, nails only
		DDEB, bullous dermolysis of the new born
	Recessive DEB	RDEB, severe generalised
		RDEB, generalised other
		RDEB, inversa
		RDEB, pretibial
		RDEB, pruriginosa
		RDEB, centri petalis
		RDEB, bullous dermolysis of the new born
Kindler Syndrome	N/A	

Table 1.0 Epidermolysis Bullosa subtype lineage

The main EBS subtypes are EBS-generalised other, which is characterised by blisters that occur all over the body. EBS-localised is normally used to describe the condition when blisters are confined to the hands and feet. Finally, EBS Dowling-Meara is the most severe form of this EB subtype. Patients suffer from generalised skin involvement, which can appear as hemorrhagic clusters of blisters (Coulombe et al. 2009). The causal gene mutations give rise to cluster formation in the helix initiation motif or termination motif of *KRT5* and *KRT14* whereas the less severe EBS-localised generally result from mutations in the same genes but within H1 and H2 domains (Titeux et al. 2006). *KRT5* and *KRT14* genes produce Keratin 14 or 5 proteins, which produce type I and II intermediate filament proteins that assemble into cytoskeletal intermediate filaments. The group termed Suprabasal EBS, contains other classifications of EB caused by *PKP1* and *DSP* gene mutations. These genes encode the desmosomal proteins; Plakophilin-1 and Desmoplakin proteins (O'Shaughnessy and Christiano 2004).

A rare recessive form of EBS is associated with Muscular Dystrophy, a severe neuromuscular disease, with known mutations of the *PLEC1* gene encoding the protein plectin (Smith et al. 1996). Plectin is a cytolinker protein that integrates various cytoskeletal and cell-adhesive elements into a functionally unified network (McLean et al. 1996).

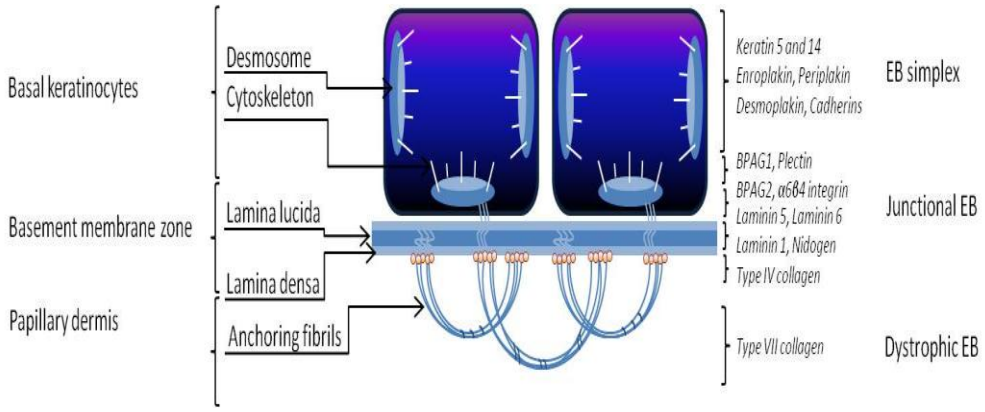

Figure 1.1 Schematic diagram of structural components of the skin important in EB

The interactions between basal keratinocytes, basement membrane protein and the papillary dermis are important factors in EB. The diagram represents the basic structural interactions and the genes which are involved in each layer and the corresponding EB subtype.

1.2.3 Junctional Epidermolysis Bullosa

Junctional EB is inherited recessively and is quite rare, affecting approximately only 500 patients worldwide (Pfendner et al. 2007). Herlitz-JEB (JEB-H) often carries the hallmark of prolific granulation tissue (Fine et al. 2008), however lesions generally heal with very mild or no scarring. The other-JEB (JEB-O) group contains sub-classifications of JEB commonly associated with mutations of *COL17A1*, *ITGB4* and *ITGA6* (Pfendner et al. 2007).

1.2.4 Kindler Syndrome

Kindler Syndrome (KS) is an autosomal recessive condition that has recently been added to the EB classification due to the clinical appearance of the disease which mimics that of H-JEB and DEB in the neonate period (Fine et al. 2008). Onset of the disease starts at birth,

with generalized skin involvement, blisters, nail dystrophy (Siegel et al. 2003), progressive poikiloderma which is where hyperpigmentation of the skin which leads to a mottled appearance, skin atrophy (Jobard et al. 2003) and varying degrees of photosensitivity (Jobard et al. 2003; Ashton 2004). These latter specific clinical features distinguish KS from the other types of EB (Burch et al. 2006). The condition arises due to mutations in the *KIND1* gene, encoding the protein Kindlin-1, a molecule involved in actin cytoskeleton attachment through focal contacts (Ashton et al. 2004; Burch et al. 2006). Approximately 17 different mutations have been identified in *KIND1* in over 40 families (Ashton et al. 2004; Burch et al. 2006). Unlike other subtypes types of EB, KS has multiple planes of cleavage within the basal keratinocytes, lamina lucida and aberrations of the lamina densa (Shimizu et al. 1997).

1.2.5 Dystrophic Epidermolysis Bullosa

Dystrophic EB (DEB) can be clinically characterised by trauma induced blistering, resulting in chronic ulcerations and scarring of the skin (Hovnanian et al. 1997). There are 3 main subtypes that come under the category of DEB; firstly the autosomal Dominant DEB (DDEB) and the two autosomal recessive subtypes; severe-generalised RDEB (sev-gen RDEB), previously referred to as Hallopeau-Siemens RDEB, and the final subtype is classed as generalised-other RDEB (RDEB-O) (Fine et al. 2008). In general, the clinical severity is widely variable ranging from minor dystrophy of the nails to major skin fragility. The RDEB phenotype is more severe than that of DDEB, and in the most severe cases patients present with recurrent wounds, infections, scarring, failure to thrive and development of Squamous Cell Carcinoma (SCC) which can result in death (Mallipeddi 2002).

Defective *COL7A1* which encodes the extracellular matrix protein Type VII Collagen is the exclusive causal defect that results in the development of all dystrophic EB variants (Sawamura et al. 2010). *COL7A1* is a complex gene that consists of 118 exons and a transcribed mRNA sequence of 9.2 kb in length (Christiano et al. 1994). It is an excreted protein produced primarily by keratinocytes (Yuspa and Epstein 2005). Type VII Collagen is the main component of anchoring fibrils (Sakai et al. 1986), the proteins assemble into these functional structures by associating into a homotrimeric ultra structural protein that consists of a central triple helical collagenous domain, with non-collagenous (NC) domains at both the amino and carboxyl ends, known as the NC1 and NC2 domains, respectively (Hovnanian et al. 1997) (Figure 1.2). Type VII Collagen molecules assemble to form anti-parallel dimers that overlap at the NC2 domain which then produce anchoring fibrils (Bruckner-Tuderman et al. 1995) (Figure 1.3). These fibrils are key structures in the integrity of the BMZ of the skin and are responsible for providing structural stability by forming bands that trap dermal extracellular matrix proteins and bind them to the basement membrane and thus securing the epidermis to the underlying dermis (Burgeson 1993).

Molecular research into DEB has revealed a wide spectrum of *COL7A1* mutations that cause separation of the basement membrane below the lamina densa, with over 300 mutations having been reported (Dang and Murrell 2008; Almaani et al 2011.). Separation in the skin occurs as a result of absent or a reduced number of functional anchoring fibrils which are truncated as a result of the various mutations causing reduced adherence and weak attachment of the epidermis to the dermis (Rodeck and Uitto 2007). Glycine substitutions on one allele of the *COL7A1* gene are strongly associated with DDEB (Christiano et al. 1994). Although pathogenic heterozygous mutations cause DDEB, non-sense mutations,

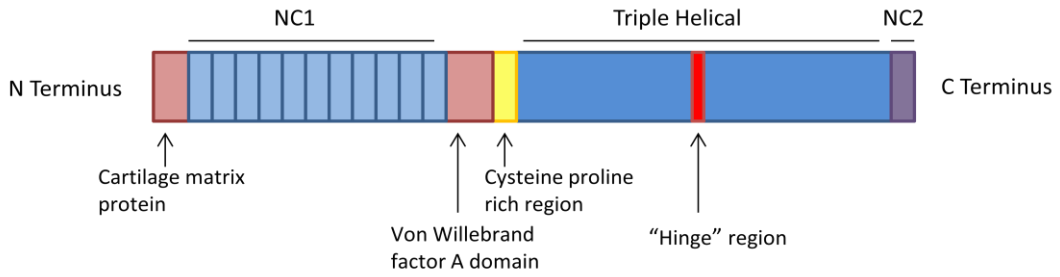

Figure 1.2 Structure of Type VII Collagen polypeptides

Type VII Collagen is a complex protein consisting of 118 exons. The domain organisation of Type VII Collagen polypeptides has been deduced from the 9.2kb cDNA sequence. It indicates that each polypeptide consists of a triple-helical domain which contains a 39 amino acid non-collagenous "hinge" region. This domain is flanked by an amino terminal non-collagenous (NC1) domain and carboxy terminal non-collagenous (NC2) domain.

frameshift, or splice site mutations on both alleles are required for the development of RDEB. However, it has emerged that genotype-phenotype correlations in DEB exist in which glycine substitutions in the triple helix may lead to diagnostic difficulties as certain mutations can result in either dominant or recessive DEB. In particular four newly identified glycine missense mutations; p.Gly1483Asp, p.Gly1770Ser, p.Gly2213Arg and p.Gly2369Ser which can lead to both DDEB and RDEB (Almaani et al. 2011). Sev-gen RDEB shows a complete absence of Type VII Collagen expression at the basement membrane (Bruckner-Tuderman et al. 1989), with a previous study postulating that loss of *COL7A1* identified by lack of antibody binding suggests inadequate synthesis of Type VII Collagen or excessive breakdown (Leigh et al. 1988) this is a likely explanation given that in the most severe form of RDEB, premature termination codons (PTC) occur on both alleles of *COL7A1*. PTC can occur in milder forms on one allele but are usually accompanied by a further

missense mutation or in-frame mutation on the other allele, in which case some Type VII Collagen expression is observed (Christiano et al. 1993).

1.2.5.1 Dominant Dystrophic Epidermolysis Bullosa

DDEB patients suffer from trauma-induced blistering which is confined to the hands, feet, knees and elbows and is accompanied by nail dystrophy and milia. This is one of the mildest forms of DEB therefore blisters are generally innocuous but nevertheless heal with scars. Typically, glycine substitutions in the collagenous triple helical domain of Type VII collagen occur, which subsequently causes poor folding of the triple helices and disruption of anchoring fibril assembly (Varki et al. 2007). Furthermore, shortened Type VII Collagen polypeptides are sometimes seen in DDEB and are produced by genomic deletions within *COL7A1* exons (Mellerio 1999).

1.2.5.2 Recessive Dystrophic Epidermolysis Bullosa

The 3 main types of RDEB are; severe-generalized RDEB (sev-gen RDEB), which is the most debilitating classification of DEB with the milder forms are known as generalized-other RDEB (RDEB-O) and pruriginosa RDEB (Fine et al. 2008). Many patients suffer from chronic blistering induced by mild trauma and is often accompanied by complications including; anaemia, scarring and fusion of digits (pseudosyndactyly) (Bodemer et al. 2003).

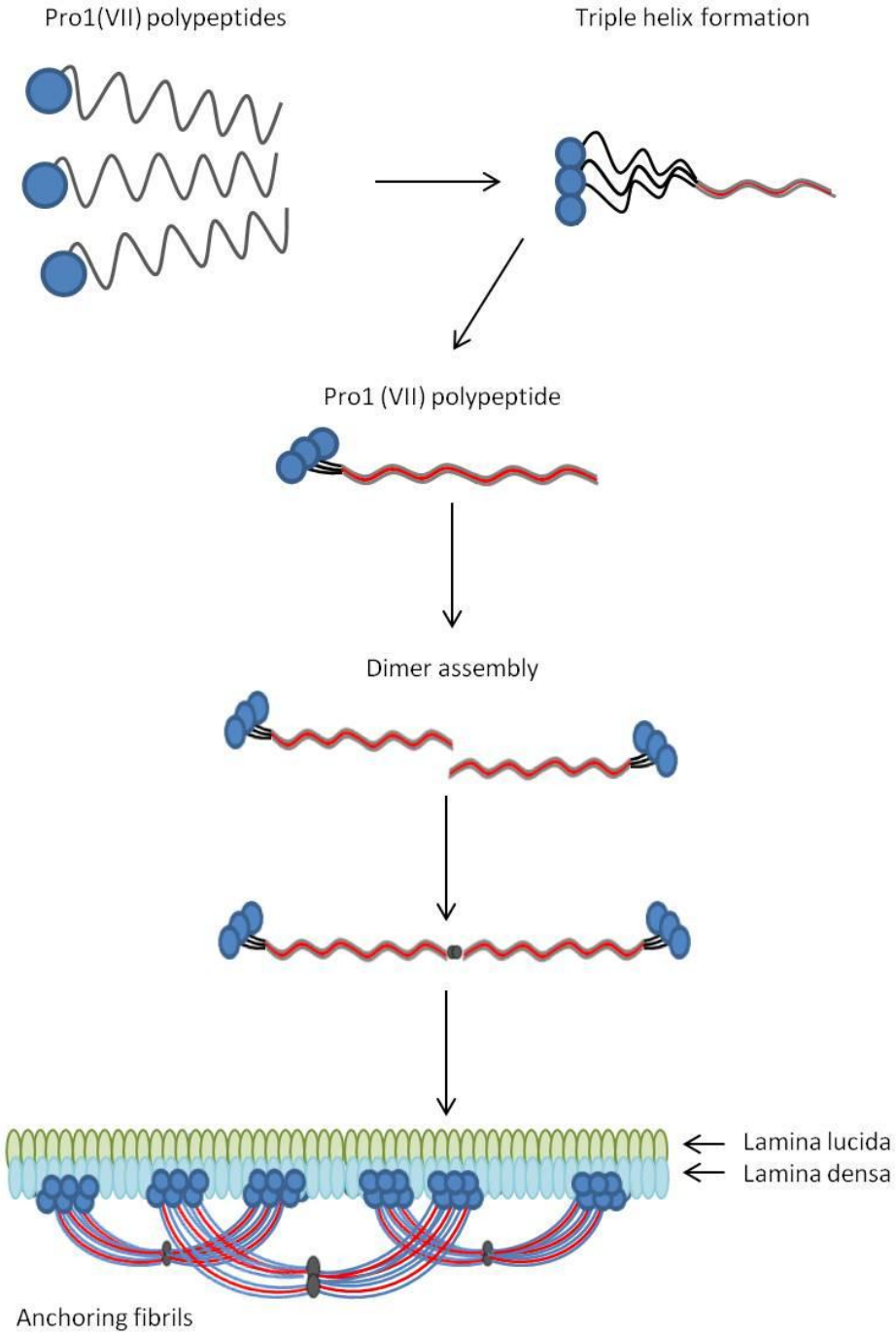

Figure 1.3 Schematic presentation of anchoring fibril formation under normal physiological conditions. Firstly, pro-α1(VII) polypeptides are synthesized and then three polypeptides associate through their carboxy-terminal end and collagenous domains to form triple helices. These polypeptides are then secreted into the extracellular space, whereby the triple helical type VII collagen molecules form anti-parallel dimers, after which the carboxy terminal is proteolytically cleaved and dimer assembly is stabilised by disulfide bonds. Several dimers then laterally assemble to form cross-striated anchoring fibrils with the NC1 amino-terminal domain attached to the lamina densa thus stabilising the association with the underlying dermis.

RDEB-O can result from glycine substitutions on one allele and a premature termination codon (PTC) on the other allele, which results in a small quantity of partially functional Type VII Collagen protein (Pfendner et al. 2007). Milder phenotypes of RDEB can also be produced by amino acid substitutions, but it is almost impossible to generalise which mutations cause a certain characteristic of RDEB-O as widely variable phenotypes have been observed and over 500 mutations have been reported (Mellerio 1999).

Severe-generalised RDEB can be clinically characterised by severe and haemorrhagic blistering induced by mild trauma with chronic unhealing wounds and extensive scarring (Tomlinson 1983). It is accompanied by complications including; malnutrition, anaemia, oesophageal strictures, corneal erosions, recurrent infections such as pneumonia and pseudosyndactyly in which the digits fuse together during wound healing and scar formation (Bodemer *et al.,* 2003; Csikos et al., 2003). Incidence of sev-gen RDEB is reported to be 0.4-0.6 cases per million live births in the United States (Vendrell et al. 2011).

The molecular hallmark of sev-gen RDEB is PTCs on both alleles of the *COL7A1* gene (Christiano et al. 1993). PTCs are the result of insertion, deletion or substitution mutations which lead to a frame shift of the DNA sequence up or downstream of the alteration. These mutations tend to be span across the entire length of the *COL7A1* coding sequence (Rodeck and Uitto 2007). However, as mentioned already, glycine substitutions have been reported to cause both DDEB and RDEB (Almaani et al. 2011).

Although, sev-gen RDEB is one of the most mutilating forms of EB, clinical management of the disease and its complications has greatly improved, with fewer patients dying from the primary disease. However, it has become evident over the last 20 years at least that this subset of patients have a grossly increased susceptibility to developing aggressive cutaneous Squamous Cell Carcinoma (SCC). They have a 90% lifetime risk of developing metastatic SCC which is closely mirrored by an 80% risk of mortality by SCC thus representing the prevalent cause of death in RDEB patients (Fine et al. 2009). With no curative treatment and tumour excision as the main treatment modality there is a universal need for the development of new more effective treatment strategies, this patient group and complication is the primary focus of this thesis. This will be discussed in section 1.3 and 1.5.

1.1.6 Epidermolysis Bullosa Treatment

The heterogeneity of these diseases and the various genes involved in their pathogenesis mean that no single treatment is likely to treat or cure EB. However, extensive research is ongoing in this area with varying degrees of success.

Recent attention has been drawn to cell based therapies ranging from cutaneous injections of fibroblasts to autologous gene corrected bone marrow transplants (Woodley et al. 2003; Woodley et al. 2007; Fritsch et al. 2008; Wong et al. 2008; Kern et al. 2009; Tolar et al. 2009). One new report looked at the use of induced pluripotent stem cells (iPSCs) as a useful substitute for embryonic stem cells (ESCs) which have the potential of unlimited proliferative capacity and extensive differentiation capability (Itoh et al. 2011). Itoh and colleagues used autologous iPSCs generated from an individual's somatic cells and

exogenously expressed defined transcription factors to generate cells with similar biological characterisations to ESCs (Itoh et al. 2011). They created these cells from both normal and RDEB fibroblasts and were able to generate 3D skin equivalents using iPSC derived keratinocytes. This study demonstrated a new potential source for cells for regenerative therapies for use in RDEB patients which would circumvent ethical issues raised from the use of ESCs and immunological rejection possibilities.

Gene-corrected RDEB keratinocytes have also been used for cell therapy in which they are harvested and injected intradermally into immunocompetent mice. This study revealed retention of Type VII Collagen for up to 2 months, supported by positive staining in the basement membrane zone (Woodley et al. 2004). This study was followed by another which tested the clinical efficacy of this application by treating 5 RDEB patients with a single intradermal injection of allogenic fibroblasts (Wong et al. 2008). Results showed an increase in anchoring fibrils after 3 months that were lacking normal morphology but still increased adherence at the dermal-epidermal junction (Wong et al. 2008).

Gene therapy is an attractive treatment option for EB, by theoretically restoring the function of an absent or abnormal gene with a normal healthy gene. Du Luca's (Phase I/II clinical trial) reported the first ever successful gene therapy for treatment of EB (De Luca et al. 2009). Several genetically modified epidermal sheets were grown in culture and transplanted onto both legs to cover a total area of 500cm^2, curing areas of skin on the legs of a non-Herlitz JEB patient. The epidermal sheets were grown from the patient's own laminin 332-β3-chain-deficient epidermal stem cells taken from palm biopsies and transfected *ex vivo* with a retroviral vector expressing the normal laminin 332. The

epidermal sheets were prepared using the same method used for preparing skin grafts for burn patients. The JEB patient had a low level of basal laminin expression which helped prevent graft rejection; this clinical trial showed success in complete epidermal regeneration after 8 days and retained a normal epidermis for 1 year (De Luca et al. 2009). There has been continual research in this area, looking at both *in vivo* and *ex vivo* approaches. *Ex vivo* models using retroviral vectors in animal models of JEB has had some success, however using retroviral vectors limits the size of the target gene and with cumbersome genes such as *COL7A1*, retroviral expression although is not impossible is often unsustainable (Pfendner et al. 2007). A significant challenge of gene therapy is delivery not only to the skin, but cell linings of the mouth, oesophagus, gastrointestinal tract and other affected internal sites (Featherstone 2007).

Paradoxically, dermal fibroblasts have been suggested to be a more suitable target for gene therapy rather than keratinocytes, which *in vivo* are the predominant source of Type VII Collagen. The reason being that when gene corrected DEB skin cells are made into a skin equivalent and transplanted onto rodents, Type VII Collagen from fibroblasts contributes substantially more to the basement membrane (Goto et al. 2006). A recent investigation by Woodley and colleagues (2007) has shown intravenous injection of RDEB fibroblasts re-expressing *COL7A1* in athymic mice led to improved wound healing compare to non-corrected RDEB fibroblasts (Woodley et al. 2007).

Other potential treatments include using gene corrected skin grafts which have demonstrated stable delivery of Type VII Collagen in mouse models (Chen et al. 2002; Ortiz-Urda et al. 2002). This method has been shown to have clinical success for the treatment of

JEB through the sustained delivery and expression of LAMB3 (Mavilio et al. 2006). It has been reported that matrix metalloproteinases (MMP) 1, 2, 3 and 9 are highly expressed in RDEB, suggesting that pharmacological MMP inhibitors could be beneficial to RDEB patients with greater MMP activity (Bodemer et al. 2003). MMPs are a family of zinc dependent endopeptidases. Implicated in the degradation of extracellular matrix molecules, they are also known to play a pivotal part in tissue remodelling, cell migration, wound healing, inflammation and cancer invasiveness (Titeux et al. 2008). A SNP in the promoter of MMP1 causes an up-regulation of MMP1 and has been found to have a strong genetic association with RDEB disease severity (Titeux et al. 2008). *Col7a1* null mice were used to study the effects of repetitive intradermal injections of recombinant full length Type VII Collagen (Remington et al. 2009). They reported that Type VII Collagen was incorporated into the epidermal-dermal junction and was found at distant sites but was still present in the skin for 2 months. Over the 2 months there was significant improvement of the phenotype shown by decreased blistering and prolonged survival of the mice (Remington et al. 2009).

1.3 Squamous Cell Carcinoma

RDEB patients have a high propensity to develop aggressive cutaneous squamous cell carcinomas that readily metastasize. This type of cancer forms part of a group of tumours known as non melanoma skin cancer (NMSC). Non-melanoma skin cancer in the general population is the most common cancer in the USA, with 80% being accounted for by Basal Cell Carcinoma (BCC) and the other 20% being Squamous Cell Carcinoma (SCC) (Kwa et al. 1992). Cutaneous SCC is the second most common human cancer among Caucasians (Alam and Ratner 2001) and there is the general perception that these tumours develop from a multi-step process (Boukamp 2005), with the primary causative agent being ultraviolet (UV) radiation (Armstrong and Kricker 2001). SCC can develop in several tissues and organs,

such as; the skin, lips, mouth, oesophagus, bladder and lungs. The tumours develop in the squamous epithelium and in the skin they are derived from keratinocyte transformation (Dazard et al. 2003).

In the multistep process of carcinogenesis, initiation is brought about by cumulative UV radiation primarily from sun exposure causing the development of UV specific mutations in target genes, followed tumour promotion by clonal expansion of the damaged cells and finally progression through uncontrolled proliferation and invasion (Dazard et al. 2003). UV specific mutations occur in *TP53* and $p16^{ink4a}$, two of the body's main tumour suppressor genes. These specific mutations are known as UV-signature mutations; which will be explained in further detail in Chapter 3. The body has its own surveillance system to protect itself in the event of harmful DNA damage; under normal circumstances UV induced DNA damage to normal skin cells is detected and a process is initiated whereby the p53 signalling cascade is activated to commence cell cycle regulation to prevent replication and initiate apoptosis thus destroying the aberrant cells to thwart further damage from occurring. However when mutations go unnoticed and another mutation occurs in the *p53* gene resulting in a faulty protein function, the surveillance and protection mechanism becomes defective and the cell is unable to initiate DNA repair mechanisms or apoptosis. Therefore, promoting tumour formation in the tissue as the cell is able to undergo cell division and proliferate uncontrollably causing premalignant lesions such as Actinic Keratoses (AK) that can develop further into malignancy.

1.3.1 Incidence

Of all skin cancers; 80% are accounted for by basal cell carcinoma (BCC), 16% are SCC and 4% are melanoma (Alam and Ratner 2001). The lifetime risk of developing SCC is 9-14% for men and 4-9% amongst women (Miller and Weinstock 1994).

1.3.2 Molecular Mechanisms

The tumour suppressor gene *TP53,* encodes the p53 tumour suppressor protein and is most studied aberration in skin cancer and is mutated in 90% of SCCs (Brash 2006). This tumour suppressor protein has many functions primarily aimed at protecting cells against damage (Vousden and Lane 2007). Two such mechanisms are DNA repair and the induction of apoptosis (Hofseth et al. 2004). The *TP53* gene carries UV-signature mutations in sporadic SCC; traditionally this involves the transition of cytosine to thymine nucleotides, where two pyramidines are adjacent in the DNA sequence. When the *TP53* gene becomes mutated its normal function which is activated by cellular stress, is altered in a dominant negative fashion and causes genomic instability and thus contributes to cancer initiation and progression. p53 function will be discussed at greater length in Chapter 3. Also implicated in the pathogenesis of SCC is the cyclin-dependent kinase inhibitor known as $p16^{INK4a}$ also a tumour suppressor protein, is located within in the 9p22 chromosomal region that is frequently altered in cancer (Suzuki et al. 2007). This protein inhibits progression of the G1 phase of the cell cycle by blocking cyclin-dependent kinase 4 from phosphorylating the retinoblastoma protein (Brown et al. 2004).

Studies have shown a paradox in the role of NF-κB in tumourigenesis. A report has shown inhibition of NF-κB in skin can lead to increased cell proliferation and even cancer (Dajee et

al. 2003). Conversely, in other cell lineages NF-κB is known to play a role in promoting cell proliferation and protecting against apoptosis (Bolotin and Fuchs 2003). Mutations of *CYLC* gene encoding a regulator of protein degradation in the NF-κB pathway predispose people to head and neck tumours known as cylindroma (Yuspa and Epstein 2005).

The human papillomavirus (HPV) is a small DNA virus that infects epithelial cells and can induce a variety of proliferative lesions, such as warts, laryngeal papillomas, and cervical carcinoma (Masini et al. 2003). Additionally, they are known to be associated with skin cancer in individuals with epidermodysplasia verruciformis (EV), a rare inherited condition characterized by widespread HPV infection and eventual development of multiple SCCs, predominantly on sun-exposed sites (Masini et al. 2003). One study suggested that individuals from the general population with positive serologic findings for HPV-8 had a 3 fold risk of cSCC (Masini et al. 2003).

1.3.3 Premalignant Lesions

Actinic Keratoses (AK) are premalignant neoplasms that sometimes precede SCC. They contain UV induced *p53* mutations. The site at which AKs occur generally show field change, whereby an area of skin between 2-6cm becomes scaly, involuted, and is more easily felt than seen. Usually patients have many lesions and although p53 is known to be mutated the molecular mechanisms that cause these lesions to evolve into malignant neoplasms is unknown. Other premalignant lesions include kerato-acanthoma and Bowen's disease (Lanssens and Ongenae 2011).

1.3.4 Treatment

Total body examination of the skin is the only screening test available for cutaneous SCC. Early detection of the disease provides a good prognosis for patients. The main treatment of SCC is wide local surgical excision which can be followed by dissection of regional lymph nodes and adjuvant radiation therapy (Clayman et al. 2005). Other standard dermatologic management treatments can also be used for lower risk SCCs such as cryoablation therapy and topical cytotoxic therapy (Martinez and Otley 2001). Electrodessication, curettage, excision or cryosurgery can eliminate up to 90% of local tumours with a low risk of metastasis (Martinez and Otley 2001). Whilst cryosurgery, electrodessication and curettage are relatively inexpensive to perform, surgical excision and Moh's surgery provide lower rates of recurrence and metastasis for patients with higher risk tumours but both are more costly to perform.

1.3.5 Metastasis/Recurrence

Invasive SCC has the potential to re-occur and metastasize. The 5 year recurrence rate for primary cutaneous lesions is 8%, and the 5 year metastasis rate is 5% (Rowe et al. 1992). The 5 year survival rates for metastatic SCC is 25-50% (Veness 2006). There is a correlation between tumour size and location and the risk of metastasis. Tumours at high risk of metastasis include those >2cm, poorly differentiated tumours and invasive tumours infiltrating into or beyond the dermis (Kwa et al. 1992; Rowe et al. 1992).

1.4 RDEB associated SCC

RDEB associated SCC is very aggressive and has a high rate of metastasis, consequently prognosis is often poor with many patients dying within 5 years of the first SCC diagnosis

(Fine 2004). It is known that even well differentiated tumours can be aggressive and have high metastatic potential (Fine et al. 2009). Although most SCCs arise in the skin other areas can be affected by SCC development including the tongue, lips and hard palate (Fine et al. 2008).

1.4.1 Incidence

RDEB associated SCC has a short latency and tumours can develop in early adolescence (Fine et al. 2009). There has even been a report of tumour development as early as 6 years of age (Shivaswamy et al. 2009). Recent reports conveyed a 75% risk of developing SCC by the age of 45 for sev-gen RDEB (Fine et al. 2009).

1.4.2 Pathogenesis and molecular mechanisms of RDEB associated SCC

Some reports have suggested that chronic wound healing represents the driving force for the development of highly malignant SCCs in both the general population and RDEB patients (Rodeck and Uitto 2007). Malignant lesions that present in RDEB patients are often difficult to diagnose as they are found within the margins of non-healing ulcerations (Arbiser et al. 2004), with some individuals presenting with multiple primary tumours.

Gene expression studies aimed at identifying genes present in chronic EB wounds has identified a 5-fold increase in L-arginine (*ARG1*) (Wessagowit et al. 2004). This involves changes in arginine metabolism and arginine-nitric oxide synthase pathway which is thought to impair wound healing. Not only would this contribute to the chronic non-healing ulcerations often seen in RDEB patients but also contribute to their susceptibility to malignant transformation.

No definitive molecular mechanisms have been identified as causal in the pathogenesis of RDEB associated SCC. Research shows that *TP53* is mutated in 30% of RDEB SCC samples in one cohort and was not associated with UV radiation (Arbiser et al. 2004), whilst, hypermethylation of *p16* has been seen in some RDEB SCC samples (Arbiser et al. 2004).

One gene that has been implicated in RDEB associated SCC is insulin growth factor binding protein (*IGFBP-3*), an average reduction of 5.8 fold in RDEB SCC was seen compared to non-RDEB SCC (Mallipeddi et al. 2004). In a normal state, IGFBP-3 plays an important role in cancer cell apoptosis which is mediated through retinoid X receptor alpha (*RXRα*). It has long been hypothesised that the absence of Type VII Collagen in RDEB is a major contributor to the aggressive nature of SCC (McGrath et al. 1992), furthermore knock-down of *COL7A1* in non-RDEB SCC keratinocytes *in vitro* resulted in increased migration and invasion, decreased terminal epithelia differentiation and enhanced mesenchymal transition all characteristics of tumorigenesis (Martins et al. 2009). However one study specifically implies that the NC1 fragment of Type VII Collagen is essential for transformation of RDEB keratinocytes to malignancy (Ortiz-Urda et al. 2005). However, following this, a separate study investigated *COL7A1* expression in RDEB SCC (Pourreyron et al., 2007). Contrary, to those results presented by Ortiz Urda (2007), this study showed RDEB patients developed SCC regardless of *COL7A1* expression, this was proven by examination of Type VII Collagen expression in 17 SCC tumours excised from 11 patients, 2 of which harboured heterozygous mutations within the region of COL7A1 encoding the NC1 domain (Pourreyron et al. 2007). This evidence suggests *COL7A1* expression is not a reliable predictor of SCC development and would not be useful biomarker of tumourigenesis.

The cellular pathways that predispose these patients to develop aggressive cSCC remain undefined, but the following have been implicated; p53 gene, suppression of p16 activity, increased collagenase activity and increased Basic Fibroblast Growth Factor (bFGF) in some patients (Arbiser et al. 1998; Arbiser et al. 2004). Increased BFGF was seen in 51% of RDEB patients, and it has been postulated that this may promote tumour initiation though mitogenic and angiogenic effects, although increased levels of BFGF was also be detected in unaffected family members (7 of 33 RDEB unaffected family members) (Arbiser et al. 1998).

It can be speculated that the molecular mechanisms of RDEB associated SCC may arise from the interplay of many signals and proteins that control the wound healing process. RDEB skin is chronically blistered and therefore there is a constant turnover of cells due to activated wound healing processes in the skin. Normal wound healing involves a complex process of activating signals and proteins being expressed to specifically enhance the repair of the skin. Initially, open wounds are plugged by platelet activation and aggregation providing a bolus of secreted proteins. Signals are initiated to increase the migration of cells to close up the wound. It is interesting that SCC in RDEB develop within non-healing wounds, therefore suggesting that wound healing is directly linked to the initiation of tumourigenesis in these patients. It could be postulated that because RDEB skin is in a constant state of repair the signalling that aids the healing process also enhances the growth and survival of rogue cells, which remain undetected by the immune system.

Not only is migration enhanced in wound healing but angiogenesis is activated in which new blood vessels develop. Again, this could further contribute to the survival of tumour

cells, as angiogenesis has been reported to be required for tumour development and metastasis (Nishida et al. 2006). Wounds are also associated with inflammation, some genes and proteins that are specifically seen in inflammatory environments include; TGFβ, selectins, chemokines and their appropriate receptors. They have also been reported to be expressed in tumour cells and furthermore have be shown to promote invasion and metastasis (Coussens and Werb 2002). Another example of this association between inflammation and cancer is the tumour microenvironment which is orchestrated by inflammatory cells that are essential for neoplastic conversion and is known to increase migration, proliferation and survival. Sustained proliferation of cells in an inflammatory environment which contains growth factors and activated stroma can potentiate the risk of cancer. Normally wound healing is a self-limiting process, dysregulation of any of these factors can lead to abnormalities which could eventually enhance the pathogenesis of tumour development (Arwert et al. 2011). The process of wound healing, angiogenesis and inflammation may be exploited by rogue pre-malignant cells in RDEB patients and greatly increase the risk of neoplastic transformation of the cells, thereby enhancing the SCC incidence in these patients.

1.4.3 Treatment

It is well established that chronic non-healing ulcerations, like those common in RDEB patients should be closely monitored for malignant change. Multiple biopsies are essential as only part of the chronic ulceration may undergo malignant change, and further more the tumour may appear asymptomatic and are indistinguishable from chronic ulcerations of the RDEB phenotype.

The main treatment of RDEB associated SCC is surgical excision (Mallipeddi 2002). However, despite taking a large excision margin, malignant lesions can recur and metastases are often seen. RDEB patients require frequent monitoring of chronic wounds for malignant changes, as they are often indistinguishable from normal RDEB phenotypic blistering and multiple biopsies are taken. Treatment by surgical excision is attributed to the fact that there is often difficulty in distinguishing premalignant lesions from non-malignant lesions and accurate diagnosis requires histological analysis (Mallipeddi 2002).

Some combination therapies have been used; however they have shown minimal effectiveness (Mallipeddi 2002). There are a few reports of radiotherapy being used to treat SCC in DEB patients (McGrath et al. 1992; Bastin et al. 1997). Bastin and colleagues reported the use of radiotherapy in 12 DEB patients delivering a total dose between 12-60Gy over 9-47 days (Bastin et al. 1997). Only 54% of irradiated tumours in the study showed a partial response, and poor wound healing and skin erosions were apparent at a total dose of around 45Gy (Bastin et al. 1997). Furthermore, the use of chemotherapy is generally avoided due to the risk of systemic toxicity. One report documents two DEB patients treated with Cisplatin which produced a partial response in relation to the reduction in axillary lymphadenopathy, the patient then went on to have a lesion on her chest surgically excised and the patient was alive 1 year after treatment (Lentz et al. 1990). The second patient chose to withdraw from the treatment and died just under 4 weeks later (Lentz et al. 1990). The few reports that document combination therapies and the use of radio- and chemo- therapy suggest that there is a narrow therapeutic index in the treatment. Further evidence of this is documented by Fine and colleagues who used Isotretinoin to treat DEB patients with SCC, this caused several patients to have increased

mechanical skin fragility when a sustained dose of Isotretinoin was administered (Fine et al. 2004).

1.5 Other patient groups with higher risk of SCC

1.5.1 Other EB subtypes with increase SCC risk

JEB and DDEB patients have exhibited SCC but metastasis or death was not observed. Up until 2004, there had been 6 reported cases of SCC in non-Herlitz JEB patients (Mallipeddi et al. 2004). Although this patient group are not presented with as great a risk as the RDEB patients, it is important to note that other EB types do develop SCC, so that they are aware of changes to blisters and erosions which may be indicative of malignant transformation. Kindler syndrome patients have a 20% increase in SCC.

1.5.2 Immunosuppression is implicated by a higher incidence of NMSC in OTRs

It has long been established that immunosuppression in the setting of solid organ transplantation has been implicated as the main etiological factor for an increased risk of developing non-melanoma skin cancer in organ transplant recipients (OTRs) (Penn and Starzl 1972; Preciado et al. 2002). There is a strong predisposition specifically for renal transplant patients to have a higher incidence of cutaneous SCC (Euvrard et al. 2003), with up to a 100 fold greater risk of developing SCC in comparison to the general population of a comparable age range (Penn and Starzl 1972; Jensen et al. 1999).

Unlike the general population, and in parallel to RDEB patients tumours that develop in OTRs have much earlier onset with studies showing the mean age of development of

epithelial tumours being 35 years old (Penn and Starzl 1972). There have been varying reports of the average lag time of tumour development after transplantation including; between 3-5 years after transplantation (Blohme and Larko 1990), followed with a more recent study identifying a 8.4 year interval (Preciado et al. 2002). A long-term retrospective study evaluating the risk of cancer in 1098 renal OTRs, indicated a 7% risk of tumour development after 1 year of immunosuppression therapy, which is significantly increased to 75% risk after 20 years (Preciado et al. 2002). Although there is a prevalence of cutaneous SCC in OTRs, there is also a 3 fold, 84 fold, and 20 fold increased incidence of melanoma, Kaposi's sarcoma and SCC of the lip, respectively (Jensen et al. 1999).

Although immunosuppression has been eluded to be the leading cause of SCC development in this patient group, the exact pathogenesis is unknown. Suggestions have been that the immunosuppressing agents themselves are carcinogenic or that they potentiate the effect of environmental carcinogens such as UV light in these patients. Parallels can be drawn between SCC development in OTRs and RDEB patients when compared to the general population. Firstly they both develop earlier in life, secondly both groups can present with multiple primary tumours, with an Australian study demonstrating an average of 7.5 primary tumours being presented per patient in their cohort of OTRs (Bouwes Bavinck et al. 1996). Further still, like SCCs associated with RDEB patients, these tumours tend to be more aggressive (Stasko et al. 2004).

The increased incidence of SCC in OTR, and together with an decreased T cell population in EB patients (Chopra et al. 1992) implies that although the oncogenic mechanisms in these patients are undoubtedly multi-factorial a lowered immune surveillance could aid the carcinogenesis in both subsets of patients. A reduction in immunological function could

lead to poorer efficiency in immune mediated destruction of tumour cells. Consistent with the theory that poor immune surveillance leads to cancer susceptibility, is supported by increased incidence in patients suffering from immunodeficiency diseases such as HIV (Veness 2006).

1.5.3 Increased risk of SCC in burn scars

SCC commonly occurs in the background of chronically injured and diseased skin, the SCC that develops in RDEB patients is a prime example. Skin affected by; long term ulcers, radiation dermatitis and vaccination scars all provide cutaneous defects that are more liable to become SCCs (Alam and Ratner 2001).

Further to this, epidermoid cancers that develop in non healing scars, known as Marjolin's ulcers (Sabin et al. 2004) are a rare occurrence but present another subset of patients with higher risk of aggressive SCC development, with a high tendency for local recurrence, lymphatic metastasis (Sabin et al. 2004; Kadir 2007) and general metastatic rate of approximately 30-34% compared to only 0.5-3% in the general population (Novick et al. 1977; Moller et al. 1979). One case study, of a 47 year old woman, following the excision of a septic ischial bursa sinus, 20 years later presented with a keratinized squamous carcinoma which was excised but unfortunately recurred, metastasized and caused death 8 months after diagnosis (Cruickshank et al. 1963), demonstrating a 27 year lag period in cancer development and then the aggressive and rapidly invasive nature of these SCCs. There are varying reports about the average latency period after the initial ulceration; with reports of between 20-40 years (Kowal-Vern and Criswell 2005), which is higher than that of OTRs but similar in some respects to the interval seen in RDEB patients. A recent report of 16,903

Danish patients presents a conflicting report that no increased risk of cutaneous malignancies is seen in their burns patient cohort (Mellemkjaer et al. 2006). This could be a direct result of improved initial treatment and management of burns.

Although SCC is the most common malignancy in burns patients, other cancers can develop as a result of scarring including BCC, melanoma, liposarcoma and adenocanthoma (Kadir 2007). Various etiologies have en implicated in the malignant transformation of burn scars including; toxin production from tissue damage, immunological factors, poor vascularisation, weaker lymphatic systems which may lead to poorer immunological defence and DNA mutations (Lindelof et al. 2008). A prolonged wound healing environment which can lead to increased proliferation of cells and abnormal keratinocyte behaviour has also been implicated in burn scar malignant transformation; this is similar to the circumstances of keratinocyte cell biology associated with SCC development in RDEB patients.

1.5.4 Xeroderma Pigmentosum patients have a high frequency of cSCC

Mutations of DNA repair machinery predispose to many cancers (Yuspa and Epstein 2005). A rare recessive genodermatoses known as Xeroderma Pigmentosum (XP) is characterised by amplified sensitivity to UV light with exaggerated sun burning and a high susceptibility to cutaneous malignancies (Kraemer et al. 1987). It is now known that this disorder is caused by defective DNA repair due to aberrations in the Nucleotide Excision Repair (NER) pathway in most patients (van Steeg and Kraemer 1999). XP sufferers develop malignancies at very high frequency; with a 2000 fold increase in incidence compared to the general population (Kraemer 1993).

A comprehensive literature review of XP patients between 1974 and 1982 showed 45% of XP patients developed SCC or BCC. Contrasting to RDEB associated SCC, the tumours that develop in XP patients do develop earlier with the median age of 8 years, but they generally have good prognosis with a 70% probability of survival and metastasis is rare (Kraemer et al. 1987). The molecular pathology behind the development of SCC is known in this patient group, as mentioned earlier the NER pathway is defective. Tumours occur mainly on sun-exposed sites and damage to the DNA via UV radiation is ineffectively repaired leading to the development of a mutant population of cells.

Other conditions exist that have a higher malignancy incidence, including some inflammatory disorders such as discoid lupus erythematosus, lichen sclerosis, lichen planus and cutaneous tuberculosis which have all been reported to predispose patients to development of skin tumours (Alam and Ratner 2001).

Although the process of cancer initiation which seems to be activated in all these conditions, and for reasons that remain unknown in a number of skin diseases, it is possible to theorise that this is due to a complex array of aberrations and interplay involving genetics, tumour microenvironment and immune function. Whilst these diseases share similarities in incidence of cutaneous SCC and parallels to RDEB in terms of pathophysiology of chronic wound environments and a compromised immune system, no similarities in the molecular pathogenesis of cutaneous malignancies in these patient groups have been identified.

1.5.5 Other malignancies in RDEB SCC

Malignant melanoma is uncommon in RDEB but still poses significant risk (Mallipeddi 2002), one report outlined an RDEB patient with melanoma (Chorny et al. 1993). National EB Registry (NEBR) data analysis between 1986 and 2006 revealed melanoma arose in 2% of DDEB patients and 2.1% of sev-gen RDEB (Fine et al. 2009). 3 RDEB patients with melanoma were between 2 and 12 years of age. This study shows a total cumulative risk of melanoma development in RDEB patients of 2.5% by age 12 (Fine et al. 2009), compared to a risk of 1.15% in the US general population (Rigel et al. 1996).

Basal cell carcinoma (BCC) is the most common NMSC in the general population; but remains relatively low risk in EB patients. NEBR demonstrated between 1986 and 2006 there were no reported cases of BCC in sev-gen RDEB but 2 cases in RDEB-O (Fine et al. 2009). Within EB diseases, BCC is most common in EBS patients with a cumulative risk of 8% by the age of 40 (Fine et al. 2009). No significant risk is posed for RDEB patients to develop of internal malignancies (Fine et al. 2009).

1.6 Aims of Thesis

As of yet, no distinct biomarkers of RDEB SCC development or progression have been identified. New investigative methods such as higher resolution expression arrays and next generation sequencing will hopefully move this research forward. Signalling pathways already implicated in sporadic SCC include epidermal growth factor receptor, mitogen activated protein kinases, phosphotidylinositol 3-kinase (Featherstone 2007). One similarity of RDEB SCC and non-RDEB SCC manifestations is the up-regulation of the transmembrane glycoprotein MUC1 (Cooper et al. 2004; Rodeck et al. 2007). It is necessary

to continually strive to identify the key pathways involved in the initiation of SCC development in these patients in the hope of targeting these pathways for potential preventative and combative therapies.

One initial aim of this thesis is to investigate *TP53* expression in RDEB. In light of recent research on the *p53* gene and the identification of beta, gamma and delta isoforms (Bourdon et al. 2005) along with only a few studies on *TP53* status in RDEB SCC, this outlines an interesting avenue to establish for the first time the *TP53* isoform status in RDEB SCC. If present, mutation analysis would enlighten as to whether they are fully functional or abnormal proteins in these tumours.

Microarrays have been utilised in thousands of studies to compare expression profiles between diseased and normal tissues. To determine genetic pathways implicated in initiation, progression and maintenance of disease, the aim of this project is to utilise the results from a global gene expression array performed by previous members of Dr Andrew South's laboratory using RDEB SCC keratinocytes, Normal Human Keratinocytes and non-RDEB SCC keratinocytes to establish candidate therapeutic targets of RDEB associated SCC. All SCC cell lines were generated from primary tumours and SNP mapping confirmed the samples were of neoplastic origin rather than normal untransformed cells. The initial hypothesis being that RDEB SCC represents a distinct phenotype of SCC compared to sporadic non-RDEB SCC due to the clinical presentation of the disease and its aggressive nature.

Knowing which genes are expressed and at what levels are key questions in understanding many diseases at the molecular level. Microarrays provide a platform that can give an insight into the expression profiles of many disease states to help decipher the cause and consequence of genetic aberrations, identify therapeutic gene targets and the effects of drugs on cells. This is a versatile method which is capable of analysing the mRNA expression levels of thousands of genes simultaneously thus giving a global view of a sample's transcriptome in a single experiment. This method, and in fact this microarray study has been used to investigate changes between SCC (including UV-induced and RDEB associated SCC as one sample group) and NHK (grouped including RDEB keratinocytes), which has ultimately derived a 435 gene signature of SCC and identified 2 definitive therapeutic targets of SCC; *PLK1* and *c20orf20* (Watt et al. 2011). Thereby validating the use of this array as a suitable method for discovering real genetic differences between RDEB SCC keratinocytes and non-RDEB SCC keratinocytes, in the quest to identify therapeutic targets of the aggressive SCC that develop in RDEB patients. Validation of the genes identified by the microarray as being differentially regulated between RDEB SCC keratinocytes and non-RDEB SCC keratinocytes were then subjected to further analysis to establish if they are affected by the expression of Type VII Collagen, which thereby implies whether or not dysregulation of certain genes are a direct consequence of the RDEB phenotype or as a result of the genetic instability associated with cancer cells. One particular gene of interest; *SLCO1B3*; which encodes an organic anion transporter; OATP1B3 was carried forward and interrogated on its suitability as a target of RDEB SCC and is discussed in detail in Chapter 5. The ultimate aim of this investigation was to identify potential therapeutic targets of RDEB associated SCC.

1.7 Significance of Research

Clinical data suggest there is a defined pathology unique to RDEB SCC yet numerous studies imply only similarities via molecular and histological studies (Arbiser et al. 2004; Cooper et al. 2004; Mallipeddi et al. 2004; Kivisaari et al. 2008). To date no single study has identified a distinct difference in histology or expression of markers both at the mRNA or protein level when comparing RDEB to non-RDEB SCC. SCC is the greatest cause of death in RDEB patients. Although huge resources are being spent on research into the treatment of EB, it is only recently that better treatment strategies providing long term therapies against the primary disease RDEB have become available, but these treatments which target the blistering phenotype have not yet been used for long enough to establish if they reduce the risk of SCC in the long term in this set of patients. Furthermore, the generic squamous cell carcinoma treatment strategies used to deal with sporadic SCC in the general population have proved of little use in the treatment of SCC that arise in the background of RDEB, with surgical treatment being primarily palliative (Uitto et al. 2010) and 41.9% of sev-gen RDEB patients having to undergo surgical amputation of part of their affected limbs due to the regional spread of SCC (Fine et al. 2009). Therefore effective treatment strategies are a substantial clinical need which remains unmet for these patients. Whilst we are still unable to prevent the development of SCC or to prevent the metastatic potential of the mutagenic keratinocytes in RDEB patients it is unequivocally of utmost importance to identify therapeutic targets of RDEB SCC and to ultimately develop treatment modalities that provide patients with a better prognosis if not cure for their cancer.

Chapter 2

Material and Methods

2.1 General Materials

2.1.1 Specialised materials

3mm Whatman paper	Whatman
Filter flasks	Nunc, Denmark
Hybond ECL nitrocellulose membrane	Amersham, UK
NuPage 4-12% Bis-Tris gels	Invitrogen
NuPage novex Tris-Acetate mini gels	Invitrogen
Top10 One Shot electrocomp cells	Invitrogen
Cryo 1°C freezing container	NalGene, USA
CryoVials	Nunc, Denmark

2.1.2 General reagents

100bp DNA ladder	Invitrogen, UK
1kb DNA ladder	Invitrogen, UK
Alkaline phosphatase (AP)	Roche, Germany
Calcium Chloride	Fluka Biochemika, Switzerland
COL7A1 Taqman probes	Applied Biosystems
Dulbeccos modified Eagles medium	Life Technologies, UK

ECL plus western blotting detection reagent	Amersham, UK
EDTA	Fluka Biochemika, Switzerland
EDTA-free protease inhibitor cocktail tablets	Roche, Germany
Electrophoresis grade agarose	Invitrogen, UK
Hepes	Fischer Scientific, UK Ltd
Human genomic DNA	Roche, Germany
Human liver total RNA	Clontech, CA, USA
Isopropanol	Fischer Scientific, UK Ltd
Lipofectamine 2000	Invitrogen, UK
M-MLV reverse transcriptase	Promega, USA
Rainbow marker	Invitrogen, UK
Random primers	Invitrogen, UK
RNase-free water	Invitrogen, UK
RNasin plus RNase inhibitor	Promega, USA
Set of dNTPs	Promega, USA
Taqman universal PCR master mix, no UNG	Applied Biosystems
T4 poly nucleotide kinase	Invitrogen, UK
Trypsin	GibCo BRL

Phosphate buffered solution	Fischer Scientific, UK Ltd
Sodium Chloride	Fischer Scientific, UK Ltd
Tris-Base	Fischer Scientific, UK Ltd
Triton X-100	Fischer Scientific, UK Ltd
Versene	GibCo BRL

2.1.2 Assay kits

Cell titer 96 AQeous One solution cell proliferation assay	Promega, USA
Dual luciferase reporter assay system	Promega, USA
ECL advance western blotting detection kit	Amersham, UK
FastStart high fidelity PCR System	Roche, Germany
QIAquick gel extraction kit	Qiagen, Germany
QIAquick maxi prep kit	Qiagen, Germany
RNeasy mini kit	Qiagen, Germany
TOPO TA cloning kit	Invitrogen, UK
Wizard plus mini preps DNA purification system	Promega, USA

All other chemicals used in the following experiments were purchased from Sigma Aldrich (Poole, Dorset, UK) unless otherwise stated.

2.1.3 Antibodies

All primary antibodies used for the detection of proteins are listed in Table 2.1, secondary antibodies used and their appropriate dilutions for each method are listed in Table 2.2.

Antibody	Host	Supplier
Anti-Collagen Type VII	Rabbit Polyclonal IgG	Calbiochem, Darmstadt, Germany
Beta-Actin	Mouse Monoclonal IgG	Abcam
OATP8	Rabbit Polyclonal IgG	Professor B. Steiger, University Hospital, Zurich
OATP8 C14	Goat Polyclonal IgG	Santa Cruz
OATP8 D16	Goat Polyclonal IgG	Santa Cruz
OATP8 H-52	Rabbit Polyclonal IgG	Santa Cruz
OATP8 MDQ	Mouse Monoclonal IgG	Novus Biologicals, Littleton, CO, USA
p16 (c20)	Rabbit Polyclonal IgG	Santa Cruz
p53 (DO-1 SC126)	Mouse Monoclonal IgG	Santa Cruz

Table 2.1 Table of primary antibodies (Ab) used for investigating protein expression

Antibody	Dilutions	Supplier
Donkey-anti-goat IgG HRP (H&L)	WB/IMF 1:2000	Jackson ImmunoResearch, Suffolk, UK
AlexaFluor 594 goat-anti-rabbit	1:800 IMF	Molecular Probes, Eugene, USA
AlexaFluor 488 goat-anti-mouse	1:250 IMF	Molecular Probes, Eugene, USA
Polyclonal rabbit-anti-mouse	WB 1:2000	Dako, Denmark
Polyclonal swine-anti-rabbit	WB 1:4000	Dako, Denmark

Table 2.2 All secondary antibodies used, their dilutions and suppliers

2.1.4 General buffers

10x Phosphate Buffered Saline (PBS)

0.2M phosphate buffer (1 part 0.2M $NaH_2PO_4H_2O$ and 4 parts 0.2M $NaHPO_42H_2O$) + 1.5M NaCl, pH 7.4

10X TBE

104g Tris Base + 55g Boric Acid +40ml 0.5M EDTA

Tris tween buffer solution (TTBS)

50mM Tris/HCl (ph8.0), 0.1% (v/v) tween, 150mM NaCl

Transfer Buffer

14.4g glycine + 3.03g tris (hydroxymethyl) methylamine dissolved in 400ml dH_2O then make up to 800ml with dH_2O and add 200ml methanol

RIPA buffer

150 mM sodium chloride +1.0% Triton X-100 + 0.5% sodium deoxycholate + 0.1% SDS (sodium dodecyl sulphate) + 50 mM Tris, pH 8.0

2.1.5 Fixatives

4% (w/v) paraformaldehyde (Merck, Darmstadt, Germany) made up in PBS. The powder was dissolved in water by stirring at 60°C and adding drops of NaOH until the solution had cleared.

Methanol Acetone made up from 1:1 ratio of methanol (VWR, France) and acetone (VWR, France).

2.2 Methods

2.2.1 Cell Culture

2.2.1.0 SCC Cell Lines

A list of SCC cell lines used for all experiments performed in this thesis, are listed in table 2.1.

2.2.1.1 Maintenance and storage of cell lines

Maintained at 37°C, 5% humidified atmosphere with 5% CO_2. Cells were grown in keratinocyte medium containing; 300ml DMEM with 100ml Ham F12, 40ml FBS and 4ml RM+ (growth factors). Cells are maintained in 75cm^2 Nunc filter flasks (Nunc, Roskilde, Denmark), and grown to approximately 75% confluency before routine passaging. Growth media was changed approximately every 2 days.

Phoenix cells were used as a packaging line for retroviral transfections and were maintained at 37°C, 5% humidified atmosphere with 5% CO_2 in media containing only 90% DMEM and 10% FBS.

2.2.1.2 Cell passaging

Cells were passaged by aspirating off media and washing cells with 5ml PBS. Cells were then incubated with 1.5ml Versene and 1.5ml dH_2O for 2-3 minutes to remove any contaminating fibroblasts, cells were then washed again in PBS and dissociated from the

Sample	Patient	Age	Sex	Tumour Location	Differentiation State	Metastasis
RDEB SCC 1	RDEB *COL7A1* c.3832-1G>A	54	M	n/a	Poorly differentiated	No
RDEB SCC 2	RDEB COL7A1 p.R525X; p.R578X	36	F	Left forearm	Moderately differentiated	No
RDEB SCC 3	RDEB COL7A1 c.8244insC	32	F	Shoulder	Unknown	n/a
SCC 1	Renal Transplant	unknown	M	Forearm	Well differentiated	No
SCC 2	Cardiac Transplant	unknown	M	Hand	Well differentiated	No
SCC 3	Renal Transplant	unknown	M	Hand	Moderately differentiated	Yes
SCC 4	Renal Transplant	unknown	M	Ear	Poorly differentiated	Yes
SCC 5	Immunocompetent	unknown	M	Right temple	Moderately differentiated	Yes

Table 2.3 SCC cell lines use for experiments. RDEB SCC refers to SCC cell lines generated from Recessive Dystrophic Epidermolysis Bullosa Patients; SCC refers to cells lines from non-RDEB individuals.

plastic surface by incubation with 3ml Trypsin. Cells were centrifuged at 1200rpm for 3 minutes. Media was aspirated off the cell pellet which was then re-suspended in approximately 5ml of fresh keratinocyte media. Approximately, 10^6 cells were plated into a

new 75cm^2 Nunc filter flask containing 10ml Keratinocyte media, and maintained in culture. Remaining cells were prepared for cryostorage.

2.2.1.3 Cryostorage of cells

Cells were resuspended at a concentration of a minimum of 1 million cells per ml in Freezing media (FBS + 10% DMSO). Cells were aliquoted in 1ml volumes into cryovials (Nunc), and placed in a Cryo 1°C freezing container (NalGene, Rochester, NY, USA) and placed at -80°C for a few days before to slowly bring down the temperature prior to long term storage in liquid nitrogen.

To bring up cells from cryostorage, vials were thawed quickly in a 37°C water bath and added to 5ml of cold keratinocyte media, as the DMSO in the freezing media is toxic to cells at room temperature. Cells were then centrifuged at 1200rpm for 3minutes, then aspirating of the media. Cells were re-suspended in fresh keratinocyte media and plated out in either 25 or 75cm^2 filter flasks and maintained in culture.

2.2.1.4 Cell counting

Experiments which required cells to be plated out at specific densities, cells were counted using a Casy Counter (Roche Diagnostics Ltd, West Sussex, UK); a cell counting machine which utilises multiple channel technology to give highly accurate cell counts. 100µl of cell suspension is diluted in 900µl CasyTon and placed under the capillary. Readings were given in cells/ml.

2.2.1.5 siRNA Transfections

SLCO1B3 knockdown experiments were performed by transfecting RDEB SCC keratinocytes with siRNA using Lipofectamine 2000 (1mg/ml) (Invitrogen, UK), following the manufacturers's protocol. Briefly, the day before transfection cells were plated out in 6-well plates at a density of 300,000 cells per well in 2ml of keratinocyte medium. Generally for high transfection efficiencies it is recommended that cells are transfected at approximately 90-95% confluency to minimise toxicity to cells. The most important aspect of transfecting cells is maintaining the correct ratio of DNA:Lipofectamine2000 when preparing each complex. For each well, the following volumes of reagents were used; 5µl of Lipofectamine2000 diluted in 250µl of Opti-Mem I reduced serum media (Opti-Mem) and incubated for 5 minutes, whilst a total of 5µg DNA was diluted in 250µl Opti-Mem. Both complexes were mixed together and incubated at room temperature for 20minutes. The total 500µl complex was added to the well, and cells incubated at 37° in CO_2 humidified incubators for 6 hours, before changing the media for 2.5mL fresh keratinocyte medium and maintained in culture for 48 hours.

2.2.1.6 Cell fixation

Cells were plated out onto glass cover slips in 24 well plates, at a density of 0.5 million cells per ml of media, and 1ml of cell suspension was added to each well. Cells were grown for 2 days prior to fixation. To fix cells using methanol acetone, first the media was aspirated and cells washed with 1ml PBS. 500µl of ice-cold methanol acetone was added to each well and placed at -20°C for 20 minutes. Methanol acetone was removed and cells were washed 3 times for 5 minutes with 1ml of PBS. 24-well plates contained fixed cells were stored at 4°C in PBS until needed.

2.2.2 RNA/DNA Manipulations

2.2.2.0 RNA isolation

Keratinocyte cell lines were grown to 2 days post-confluency in 75mm dishes, washed in phosphate buffered saline (PBS), and detached from the culture dish by adding 2ml of RNA-Bee (Biogenesis, Poole, England) and physically removing cells with a cell scraper (Sarstedt, Newton, NC, USA). Cell lysates were then collected and aliquoted 1ml into two 1.5ml microcentrifuge tubes. 20% chloroform (200µl/ml) was added to each aliquot and shaken vigorously for 30 seconds. Tubes were placed directly on ice for 5 minutes, prior to being pelleted via centrifugation at 13,000rpm, at 4°C for 15 minutes. The aqueous phase was collected and removed to a fresh microcentrifuge tube and an equal volume of isopropanol was added. RNA was then precipitated overnight at 4°C or stored at -80°C for long term storage. RNA was pelleted at 13,000rpm, for a further 15 minutes, and the pellet was washed in 70% ethanol (ETOH) followed by air drying for 5 minutes. RNA was resuspended in 100µl dH_20, and quantified using the Nanodrop. Approximately, 50µl of RNA was purified using the Qiagen DNaseI treatment protocol followed by the Qiagen RNA mini kit, no more than 100µg of RNA can be added to a single RNA mini column, therefore volumes of starting RNA may vary. RNA was eluted from the column in 50-100µl dH_20. RNA was re-quantified using the Nanodrop, and stored at -80°C in single use aliquots to prevent freezing thawing which may cause degradation of the RNA.

2.2.2.1 RNA isolation from tissue

RNA was extracted from tissue samples by the Tayside Tumour Bank (Ninewell's Hospital, Dundee, UK). Poor quality RNA can greatly hamper and compromise gene expression results and differences between the sample qualities can cause misinterpretation of results.

The tumour bank tested the quality of each RNA using the Agilent 2100 Bioanalyser, to electrophoretically separate the sample which is then detected via laser induced fluorescence. This method of examining RNA quality is by far the most accurate. Principally, good quality RNA will have high 18S and 28S peaks and low 5s peaks (Figure 2.0), the RIN (RNA integrity number) is then derived from the electropherogram curve and samples are assigned a number from 1-10; with 1 showing the most degradation of RNA and 10 showing the least (Fleige and Pfaffl 2006).

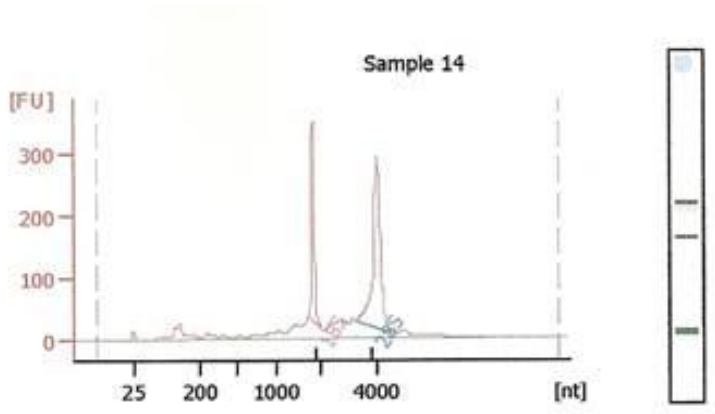

Figure 2.0 RNA integrity electropherogram

An example of an RNA integrity electropherogram for one of the RDEB SCC tissue samples, this particular sample shows high 18S and 28S peaks and was assigned a RIN of 8.4

2.2.2.2 cDNA synthesis

2.5ug of total RNA was used as a template for first strand cDNA synthesis. Briefly, RNA was diluted in up to 20µl of dH_20. Next, the following components were added to the RNA prior to incubating at 65°C for 10 minutes:

7µl 5 x M-MLV RT-buffer (Promega, Madison, WI)

4µl 10mM dNTPs (Promega, Madison, WI)

1µl RNasin (Promega, Madison, WI)

1µl random primers (OD 90, Invitrogen)

Heating the reaction denatures the RNA and allows the dNTPs and random primers to bind to the single stranded RNA. After initial incubation period, reactions are placed directly on ice. 2µl of M-MLV reverse transcriptase (equivalent to 400 units) (Promega) was added or in the case of control samples, 2µl of dH_20 was added to a duplicate sample. Samples were then incubated at 42°C for 90 minutes. cDNA was then quantified via spectrophotometry and its purity tested by running a standard RT-PCR reaction using the desmoplakin (*DSP*) gene to identify if samples are contaminated by genomic DNA (gDNA) prior to its use in further investigations. The primer sequences for *DSP* were; Forward: 5'-CTG AGG TCT TCT TCA ATC CC-3' and Reverse 5'-TGC GGA TGG CAT CTG AAT G-3' and had an annealing temperature of 57°C. PCR products were visualised on an agarose gel and as the primers are able to amplify cDNA and gDNA with amplicons of 178bp and 1.25kb, respectively, as seen in Figure 2.1.

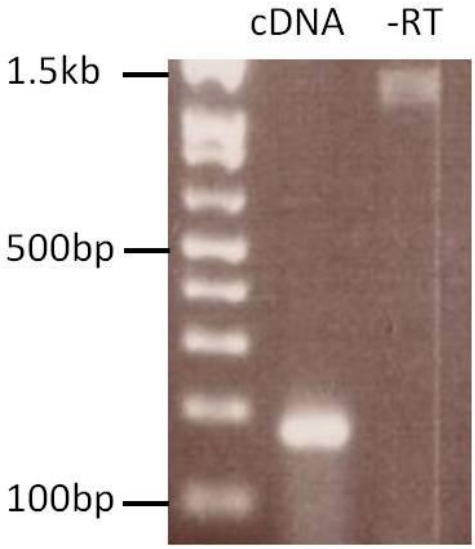

Figure 2.1 Genomic contamination identified by AGE of cDNA and –RT samples. *Desmoplakin* amplification in SCC 2 should produce a product of 178bp as seen in the cDNA lane, whilst the control cDNA; -RT (without reverse transcriptase) showed an amplified band of approximately 1.25kb signifying genomic contamination of this sample.

2.2.2.3 Spectrophotometry

DNA and RNA were both quantified using the Nanodrop 2000 (Labtech, International, UK). dH_20 was used as a blank to adjust for any background.

2.2.2.4 Primer design

Oligonucleotide primers were manually designed for all genes tested for gene expression, unless otherwise stated. Primer pairs were designed to amplify a product that spanned an exon-exon boundary to reduce the risk of amplifying genomic DNA. All primers were designed in a 5' to 3' orientation from the plus to minus strand of DNA and the following parameters were taken into account to design the most efficient primer sets:

- Primers ranged between 18-24 nucleotides in length, which was dependent on GC content within each sequence. Where possible >4 consecutive GC's were avoided. Ideally 50% GC content was achieved to give greater stability but still maintains a unique sequence. A range of 40-60% GC could be used if necessary.

- Primer pairs were designed to amplify a product of 80-200bp, which is the range that is most easily amplified using standard PCR thermal cycling parameters.

- All primer pairs were searched for in the BLASTN (Altschul et al. 1997), to locate similarities between sequences, and to identify homologous matches. This ensures the specificity of the primers to amplify a single product.

- Primers designed to amplify genes identified by the microarray, were made specifically to pick up the same transcript variant(s) that the Illumina array probe sequence would hybridise to.

Finally, all primers were ordered in a lyophilised format from MWG eurofins (Germany), and reconstituted in dH_2O at a concentration of 1nm/µl stock concentration. Primer annealing temperatures could be calculated manually; if the recommended temperature was not successful in amplifying a product, in which case the following formula was used:

$$69.3\ (0.41(GC\%)) - 650/oligo.length$$

2.2.2.5 Reverse transcriptase PCR

Standard PCR (RT—PCR) was carried out in 25 or 50µl reaction volumes. Each 50µl reaction contained; 5µl 10x PCR Buffer (HT Biotechnology), 1µl forward primer (20pMol/µl), 1µl reverse primer (20pMol/µl), 1µl dNTPs (10nM), 3µl of cDNA, 0.5µl SuperTaq (HT Biotechnology) and 38.5µl dH_2O. If performing a number of PCR reactions, make a master

mix for number of reactions you will use plus one, to reduce pipetting errors. Standard cycling conditions were used and can be found in Table 2.4 and were performed on the DNA Engine Tetrad 2 (BioRad, Nottingham, UK).

Step	Temperature	Time (seconds)	Number of Cycles
Enzyme Activation	94°C	2minutes	1
DNA Denaturing	94°C	10	
Annealing	55-65°C*	10	34
Extension	72°C	†	
Final Extension	72°C	5minutes	1

Table 2.4 Standard PCR cycling parameters. *Annealing temperatures were determined uniquely for each primer set used and was dependent on length and GC content of primer sequences. †Extension times could vary depending on the length of amplicon, generally 1kb products required 1 minute for extension.

2.2.2.6 Agarose gel electrophoresis

PCR products were ran on an agarose gel, where they were subjected to a voltage that caused the migration of DNA from the cathode to anode and visualised under ultraviolet (UV) light in a method called agarose gel electrophoresis (AGE). The percentage of agarose used is dependent on the size of products being visualised, usually larger products require a lower percentage gel to allow easier migration of fragments through the gel matrices. As a general rule; a 2% agarose gel is adequate for 0.1-1kb fragments, whilst 1-5kb fragments are better ran on 0.8-1% agarose gels. Briefly, electrophoresis grade agarose was mixed

with 100ml 0.5% Tris-borate-EDTA-acid (TBE) buffer and heated until the agarose has dissolved, before cooling prior to adding 6µl ethidium bromide (0.1mg/ml), a DNA intercalating dye. Agarose solutions were poured in gel trays and allowed to set. PCR products were prepared with 10x loading buffer containing glycerol and bromophenol blue, subsequently 5-10µl of sample was loaded per well. Gels were run at 70 volts (v) for approximately 1.5 hours and visualised using a UV light transilluminator. The GeneGenius, (Synergy) gel imaging machine was used to document the results if required (Figure 2.2)

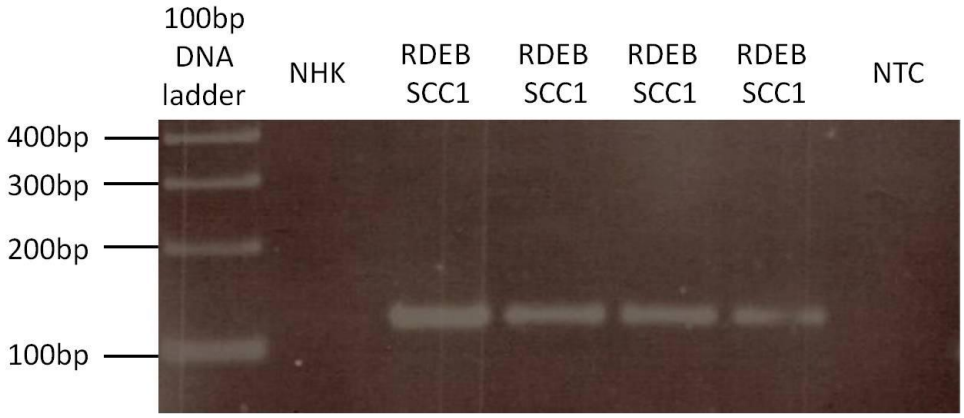

Figure 2.2 Example of an agarose gel. Gel was loaded with 6.5µl 100bp DNA ladder, followed by 10µl of each sample and run at 70 volts for 1.5 hours. All samples show an amplified product of correct size at approximately 125bp and no contamination is present in the no template control (NTC).

2.2.2.7 Direct sequencing

Prior to direct sequencing, PCR products were purified using an ExoSap protocol, which utilises two hydrolytic enzymes; Exonuclease I (ExoI) and Shrimp alkaline Phosphatase (Sap). ExoI is used to remove residual single stranded primers and DNA whilst Sap eliminates unused dNTPs from PCR products. Briefly, both ExoI and SapI were diluted in their corresponding buffers at a ratio of 1:50 and 1:20, respectively. Then, equal volumes of ExoI and Sap were mixed to create the ExoSap solution, of which 2µl was added to each purification reaction containing 5µl of PCR product. Reactions were incubated at 37°C for 15 minutes, followed by heat inactivation at 80°C for 15 minutes. Samples were aliquoted and sent to the DNA Analysis Facility at Dundee University (Ninewells Hospital, Dundee) for direct sequencing by Capillary Electrophoresis using the 3730 DNA Analyser (Applied Biosystems, UK). Both PCR products and plasmid preps were sequenced by the DNA Analysis Facility, and the concentrations required for the different samples are listed in Table 2.5.

Template	Quantity/µl
PCR Products	
100-200bp	1-30ng
200-500bp	3-10ng
500-1000bp	5-20ng
1000-2000bp	10-40ng
>2000bp	20-50ng
Plasmid DNA	
Double Stranded	150-300ng

Table 2.5 Required template concentrations for DNA sequencing

2.2.2.8 High fidelity PCR

The *SLCO1B3* ORF and promoter fragments were amplified using the FastStart High Fidelity PCR Kit (Roche, Germany). Each 50µl PCR reaction was setup using each component listed in Table 2.6. Reactions were then run on the DNA Tetrad 2 (BioRad) using the cycling conditions outline in Table 2.7

Reaction Component	Volume Required
cDNA template	1µl
High Fidelity Reaction Buffer	5µl
dNTPs (10mM)	2µl
Forward Primer (20pMol/µl)	1µl
Reverse Primer (20pMol/µl)	1µl
High Fidelity Enzyme	0.5µl
dH2O	39.5µl

Table 2.6 High Fidelity FastStart PCR reaction components and required volumes

Step	Temperature	Time	Number of Cycles
Enzyme Activation	95°C	5mins	1
DNA Denaturing	95°C	30sec	40
Annealing	55-65°C*	30sec	
Extension	72°C	2.5mins†	
Final Extension	72°C	5mins	1

Table 2.7 Cycling conditions for High Fidelity PCR reactions * Annealing temperature was dependent on the primer set used, †Extension times varied on the length of the amplified product, approximately 1kb is extended in 1 minute

2.2.2.9 SYBR Green qRT-PCR

There are 3 stages of any PCR amplification: the baseline, exponential and plateau phase (Figure 2.3). Quantitative Real-Time PCR (qRT-PCR) allows the entire amplification process to be observed unlike in standard RT-PCR in which the end point, or plateau phase which occurs when all reagents are exhausted is examined by AGE. Therefore qRT-PCR which measures expression during the early exponential phase is able to detect smaller changes in gene expression. qRT-PCR was used to determine and validate the relative gene expression levels of all the genes identified by global gene expression array analysis using the DyNAmo SYBR green PCR kit (Finnzymes, Finland).

SYBR green is a DNA intercalating dye which, upon binding to dsDNA, fluoresces. Basically, primers extend the target DNA sequence, then multiple molecules of SYBR green bind to the dsDNA product and emit fluorescence. The fluorescence is dependent on the amount of DNA and therefore longer products will generate great fluorescence. This provides a versatile and inexpensive method for investigating gene expression.

Primers for all genes used in this investigation are listed in Table 2.8. To examine the gene expression levels using qRT-PCR: 10µl 2x SYBR Green Master Mix was mixed with 8pmol of each primer and 5µl cDNA (80ng/µl) in a total volume of 20µl. Reactions were performed in triplicate for each sample and primer set, alongside an endogenous control which was *EF1α* and ran on the MiniOpticom Real-Time PCR System (BioRad, Hertfordshire, UK). Cycling parameters are outline in Table 2.9 and follow the recommended DyNAmo SYBR Green Kit conditions. Data was collected in “real-time” by measuring the fluorescent signal at the

end of each cycle, and in this case was taken at two points 72°C and 80°, followed by the generation of a melting curve to identify non-specific products by ramping the temperature

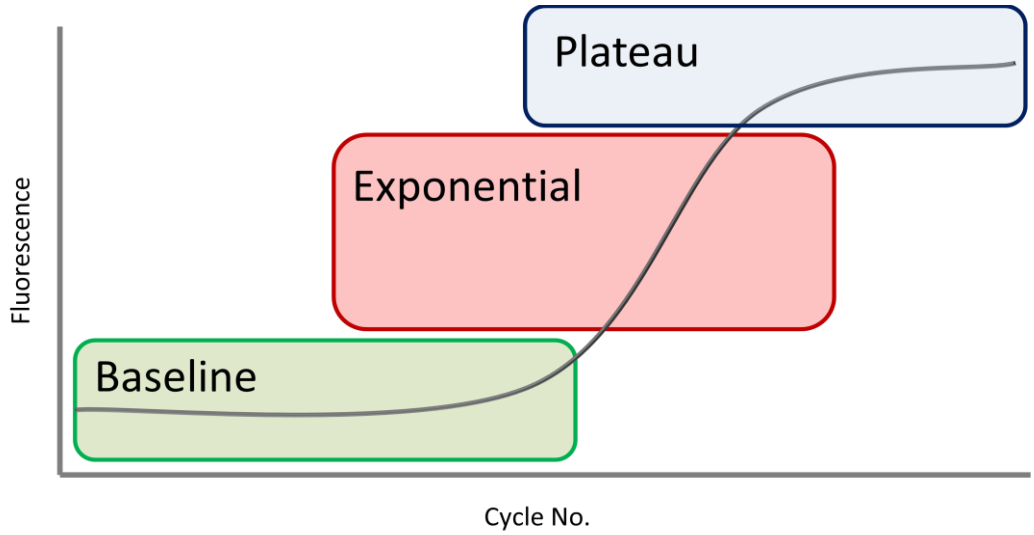

Figure 2.3 PCR amplification plot. Three stages of amplification baseline, exponential and plateau phase. qRT-PCR readings are taken during the exponential phase whilst standard RT-PCR only gives a reading from the final plateau phase

from 70°C to 90°C and collecting data every 4 seconds. The cycle threshold (Ct), which is the number of cycles it takes for the fluorescence to cross the threshold on the amplification plot and was determined by setting the baseline to subtract the background fluorescence seen in the initial PCR cycles prior to the detection of an increase in fluorescence from a PCR product amplification, then manually setting the threshold level in the log view of the amplification curve in during exponential phase. Relative expression was determined using the ΔΔCt method (Livak and Schmittgen 2001).

Table 2.8

Gene	Primer Sequence 5' – 3'	Tm (°C)
AAMP	F: GTG GAG TCC TTG GGC TTC TG R: GCC TAA GAG TCT GCG TAG CC	61
ADFP	F: GCT CTA CCT CTC ATG GGT AG R: CCT TGG ATG TTG GAC AGG AG	59
BCS1L	F: CCT GGT TGC GGA AAG AGC AG R: GCT CAG CAG GTG GTT GAG TC	61.4
C14orf156	F: CAG CCG GTT GCT TTT GTG AG R: CTC TGT GAA AGC CAG TCT CC	59
C1orf135	F: GCA TTG CTT CCT TCT TCA CC R: GGA TCA AAT GGT CTA GCT GG	57.3
C7orf27	F: CCT GAG AGT TAT GTC CGA GC R: GAG TCT ACG GAG AGG ATGTG	59
CCNA1	F: GAC CTC AGC AAG CAA TTA GG R: GAA GTT CTG GAA GTG CTT CC	57
DNAJB14	F: GAT GCC TGT ATA CTG GGT ATG R: GCC ACC CTA TCT AGC ATT CTC	57.9
DNMT3B	F: CAG ATG AGA AGT CTG CTA CC R: CCT GTC ATC TCT CAG ATG TG	57
DUSP23	F: CTT CGT GCA GAT CGT GGA C R: CTT CAC CAG GTA ACA GGC C	59

ERH	F: GAT GAT CTG GCA GAC CTC AG R: CAC TAC AGC ACG CTG TAC AC	60
FST	F: GGA ATG ATG GAG TCA CCT AC R: GCA CTG GAT ATC TTC ACA GG	57
FTH1	F: CTT GGC ATA TCT CTT TG R: GAA ATT AGC CCG AGG CTT AG	56.3
G3BP2	F: GAC TCT GAA CCA GTT CAG AG R: CAT TGC GCC TAA TAT CCC TG	57
GSDMDC1	F: GGC ACT GAC CAT GCT GAG TG R: CAC TCT GCT CCA AGA GGC TG	58.2
HOXA5	F: CGC AAG CTG CAC ATA AGT C R: GAG AGG CAA AGA GCA TGT G	57
HSPC244	F: GAG CTG TGC TAT ACC TGT CC R: GTT GTG GAA CTC AGT CTC CG	59.4
IFITM1	F: CTT CTT GAA CTG GTC CTG TCT G R: GAA TCC AAT GGT CAC GAG GATG	60
ITGB1	F: GTG CTT TCT GTC ACC TCT TC R: CAA AGT AAG ACT CGC GTA GG	57.3
KRT8	F: CCT CCA GGG CCG TGG TTG R: CCG CAG CTG TTC ACT TGG	60
LOC116412	F: CAA CGC TCC AAC CTC AAC R: GTT ACA AAC GTT GGT GGG	54.9

MGAT4B	F: GAG AGG TGG ACC CAG CCT TCG R: CAG GGT ACC CTC AGA AGC CCG	60
MXD4	F: GCA GCA GGA GCA TCG TTT CC R: CAC CAG GGC CAA ACT CCA TG	61
OAS3	F: CAT CTG CCC TGT GCT GCA TG R: GGG CTG GTG TCC ATC TTC TC	61
POFUT1	F: CCC AGT CGG TCT ACG TTG C R: GAC CTG TAC ATC CTC GGC C	61
PPP1R3E	F: GTT CAA GAT CGC ACA GCT AG R: CAT CAT GGT TAC ACA GAG GC	57.3
RPL23	F: CCA GTG TCC TTT GAA TCG AC R: GAA ATC CGG AAT TTC GCA CC	57.3
SLCO1B3	F: GTT CTC TGC AAC AGG AGG TAC R: GGA GCT AGA ATT CCT CCT AG	58
SLC25A11	F: GAA TCC AGA ACA TGC GGA TG R: CGT AGC GGA CAA CTT TGA AC	63.7
SNRPN	F: GGA TCG CTT ACA CCT GAG AC R: GCA CCG GAG GAA GAA AGA GG	60
SNURF	F: GGA GAT GCC TGA CGC ATC TG R: GGT GTA AGC GAT CCC TTG CC	61.4
STOML2	F: GAT AAA TGA GGC AGC AGG AG R: CAG TGA AGC TGC TGC ATC TC	58

TJAP1	F: CTGGAAGAGCTCAATGAGCG R: CGAACCATGTCCTGTAGCTC	59
TTC7B	F:GCA CTG TCG GAA GTG GCT TC R: CTG TGG CTT CTG CAG GCT TC	61.4
VWA1	F: GGC AAC TTC CTG GAG CTG TC R: CAT CGC GTC AAT GGA GC	61
EF1α	F: GAG AGC TTC TCA GAC TAT CC R: GTC CAC TGC TTT GAT GAC AC	58

Table 2.8 List of all primers used for qRT-PCR. All primer sequences and recommended annealing temperatures.

Step	Temperature	Time (mins)	No. of Cycles
Enzyme Activation	95°C	10 mins	1
DNA Denaturing	94°C	10 secs	40
Annealing	55-65°C*	20 secs	
Extension	72°C	30 secs (Plate Read)	
2nd Extension	80°C	2 secs (2nd Plate Read)	
Final Extension	72°C	5 mins	1
Melting Curve	70-95°C	Read every 4 secs, hold for 2 secs	1
Incubation	72°C	5 mins	

Table 2.9 DyNAmo Sybr Green qRT-PCR cycling parameters *Annealing temperature was specific to each primer set

2.2.2.10 TaqMan qRT-PCR

TaqMan reagents utilises 2 primers and a probe which must hybridise to the target and is therefore considered a highly sensitive and has greater specificity and accuracy than standard gene expression assays. This method uses an assay mix specific to a particular gene of interest which consists of a non-extendable DNA probe which is labelled with both a fluorescent reporter and 3' quencher. The quencher prevents the Taq polymerase from extending along the DNA. Once both the primers have attached, they are extended by the 5' to 3' exonuclease activity of the polymerase, which also hydrolyses the probe causing the fluorophore and quencher to dissociate from the target DNA. This spatial separation of the reporter/quencher disrupts their ability to absorb energy emitted by the reporter and therefore creates an increase in the reporter dye fluorescence which is measured during the extension of each cycle. The more abundant a gene target, the more binding occurs thus the higher the fluorescence emission.

qRT-PCR for *COL7A1* (5' and 3') and *GAPDH* was performed using TaqMan probes sets Hs001574739_g1, Hs00982422_g1 and Hs001922876_u1 (Applied Biosystems, UK), respectively. These assays all contained a probe which had a minor groove binder (MGB) at the 3' end of the probe, as well as a FAM reporter dye at the 5' end and a non-fluorescent quencher at the 3'. For each reaction 2.5µl (25ng/µl) cDNA was added to 12.5µl 2x TaqMan master mix (AbiGene, UK), 1.25µl assay primer and probe mix and made up to 25µl dH_2O, on ice. Reactions were carried out in 96-well plates, in triplicate for each sample and assay set. PCR reactions were carried out by the DNA Analysis Facility at the University of Dundee (Dundee, UK), using the 7900HT Fast Real-Time PCR System (Applied Biosystems, UK).

2.2.3 Gene Cloning

2.2.3.0 Transformations into *E.coli*

Electrocompetent *E.coli* (similar to DH10B strain) were electroporated, a method in which foreign DNA is introduced into host cells by applying high voltage electric pulses which create a pore like structure in the cell wall of the host cells, this increases the permeability allowing for easier uptake of DNA. Briefly, 0.5µl DNA was added to 20µl Top10 electrocompetent cells (similar to DH10B strain) (Invitrogen, UK) in a 2mm electroporation cuvette (PeqLab, Germany) on ice. The cuvette was then dried and placed in the GenePulser (BioRad, Hemel Hempstead, UK) and electroporated at 20v. The time constant was checked after each electroporation and should equate to ~4.6. Cuvettes were immediately placed on ice after electroporation and 750mL LB broth was added. The LB broth was then aliquoted into a microcentrifuge tube and placed in a shaking incubator at 37°C for 45 minutes to recover.

The transformed *E.coli* was then spread on to agar plates containing 0.1mg/ml Ampicillin using aseptic technique. Plates were incubated overnight at 37°C.

2.2.3.1 Inoculation of colonies

Colonies that had grown on agar plates were inoculated by using a pipette tip to pick single colonies (perfectly circular colonies, with no other colonies around) and placed in 5ml LB broth containing 0.1mg/ml Ampicillin. Cultures were grown at 37°C o/n before creating glycerol stocks and purifying DNA using small scale plasmid DNA purification protocol (see section 2.2.3.2).

2.2.3.2 Small scale purification of plasmid DNA

To purify DNA from small 5ml plasmid cultures, 1.5ml of LB Broth was aliquoted into two microcentrifuge tube and centrifuged at 9,500rpm for 5 minutes. The supernatant was removed and then the Wizard Plus Prep DNA purification system (Promega) was used by following the manufacturers instruction to fully lyse and clear cells and effectively use a column to bind the DNA and purified by multiple wash steps. The DNA was eluted in 30µl of dH_2O, quantified by spectrophotometry (see section 2.2.2.4) and finally run on a 0.8% agarose gel to confirm size after restriction enzyme digestion (see section 2.2.3.4).

2.2.3.3 Large scale purification of plasmid DNA

Using the QIA maxi prep kit (Qiagen) and following the manufacturer's protocol, DNA was purified from plasmid cultures of between 50-100mL in volume. The kit utilizes a "QIAcatridge" and "HiSpeed Maxi Tip" along with lysate cleaning of cell debris and isopropanol precipitation of DNA which is then bound to the HiSpeed tip to wash and lyse cells, and remove cell debris and bind DNA prior to further wash steps and final elution of DNA from the Maxi tip with 1mL of dH_2O, which delivers a yield of approximately 500µg DNA.

2.2.3.4 Restriction enzyme digestions of plasmid DNA

Restriction enzymes are endonucleases that recognise specific sequences of DNA and cleave dsDNA. These enzymes are often used in cloning experiments in the preparation of target DNA and vector DNA, prior to ligating the DNA of the two fragments together. RE digestions are also useful and quick tools for confirming the size of constructs by creating linear DNA which can migration evenly through an agarose gel, unlikely supercoiled DNA, and the use of multiple enzymes in a reaction can create specific fragment lengths that can

be used to confirm the orientation of an inserted piece of DNA in a vector. In brief, 10µl reactions were set up using a maximum of 10% enzyme in each. The following components were added to a 0.2mL PCR tube:

1µl RE Buffer (specific to each enzyme)

1-8µl DNA

0.5-1µl RE

Make up to 10µl with dH2O

Reactions were incubated at 37°C for 1 hour for a quick digest or for complete digestion; o/n, unless otherwise stated by the RE datasheet. Table 2.10 lists all RE used for the experiments discussed in this thesis. If using only one RE for the digestion of a vector which will subsequently be used in a ligation reaction, it was necessary to incubate the digested vector with alkaline phosphatase (AP) (Roche), a hydrolase enzyme that removes the phosphate groups from DNA which prevents the re-annealing of the vector DNA. In brief, 0.5µl of AP plus 1µl AP buffer and 8µl dH2O were added to the digested vector DNA and incubated at 37°C for 2 hours, then heat inactivated at 85°C for 30 minutes.

2.2.3.5 DNA purification by gel extraction

PCR products and plasmid digestions that required purification were loaded onto agarose gels of appropriate percentage for the size of product and ran at 100v for approximately 1 hour, or until bands had completely separated. Half of the gel lane containing the product of interest was visualised using a UV light transilluminator and then aligned with the remaining gel where the fragment of interest was excised using a sterile scalpel. The gel remaining gel can then be viewed to establish is complete excision of the fragment was achieved. The whole gel was not viewed under UV light to prevent DNA degradation and

damage by the UV light. Excised products were then purified following the standard protocol of the QIAquick Gel Extraction Kit (Qiagen) and DNA was eluted in 30µl dH_2O.

Restriction Enzyme	Recognition Sequence	Temperature (°C)	Supplier
BsmI	GAATG CN▼ CTTAC▲GN	65	New England Biolabs, Hertforshire, UK
BstXI	CCAN NNNN▼NTGG GGTN▲NNNN NACC	50	New England Biolabs, Hertforshire, UK
HindIII	A▼AGCT T T TCGA▲A	37	Invitrogen, UK
PvuI	CG AT▼CG GC▲TA GC	37	New England Biolabs, Hertforshire, UK
SacI	G AGCT▼C C▲TCGA G	37	New England Biolabs, Hertforshire, UK
XhoI	C▼TCGA G G AGCT▲C	37	Invitrogen, UK

Table 2.10 Restriction Enzymes used for cloning experiments. Closed triangles in the recognition sequences show where the DNA is excised on each strand in a 5' to 3' direction.

2.2.4.6 Ligations

Ligation reactions of previously digested and purified vector and insert DNA were setup according to the manufacturer's protocol for the Sigma ligation kit. A ratio of 1:10 for vector to insert was used in a total volume of 10µl and incubated overnight at 16°C.

Reactions were then electroporated in Top10 electrocompetent cells and grown overnight at 37°C on Ampicillin agar plates. Appropriate controls were performed including using the vector alone, insert alone and vector minus ligase.

2.2.4.7 Retroviral transduction

Using healthy phoenix cells, $3.5x10^6$ cells per T25 flask per transfection and leave to settle and grow over night. Next day, change the media to 2.5ml pre-warmed phoenix cell media. Using the standard Lipofectamine2000 (Lipo2000) transfection protocol, make up the following components; 230µl OptiMem mixed with 20µl Lipo2000, and 2.5µg DNA (*SLCO1B3* ORF in pBabe puro vector) in 250µl OptiMem. Mix Lipo2000 and OptiMem and incubate at room temperature for 5 minutes. Both complexes were then mixed together and incubated for a further 20 minutes at room temperature. The 500µl mix was then added to the phoenix cells and incubated overnight. The next day, the media was replaced for fresh phoenix cell media and incubated overnight. The following day, the transfected phoenix cells were split into a larger T150 flask and left to expand and grow. Two days later the media was replaced for 16ml of keratinocyte media and collect the media overnight at 32°C. Meanwhile RDEB keratinocytes were seeded at a low density of $2x10^4$ cells per well of a 6 well plate and grown over night at 37°C.

The following day, conditioned media from the phoenix cells was collected and replaced and continued to grow 32^oC. The collected conditioned media was filter through a.4.2µM Nalgene syringe filter (Thermoscientific, Leicestershire) to removed cells, and 8µg/ml polybrene was added. The media on the RDEB SCC keratinocytes was replaced with 2ml of the conditioned media, centrifuged at 300g for 1 hour at 32^oC. After which cells were

immediately place the cells at 32^{o}C for another 1 hour before replacing the media with fresh-pre-warmed 37^{o}C media and incubated at 37^{o}C overnight. Infection cycles were repeated for 3 days, and then 48 hours later the cells were selected for recombinant expression by adding 2µg/ml puromycin. If cells express the recombinant protein they should also express the puromycin resistance gene encoding in the vector DNA, and therefore only cells expressing the vector will survive after puromycin selection.

2.2.4 Protein Expression

2.2.4.0 Whole cell lysate extraction

Cells were grown in 25mm filter flasks to until 2 days post confluence (see section 2.3). To isolate whole cell lysates firstly, the growth media was aspirated and cells were washed in 3ml of PBS. After removing all PBS, 3ml of Trypsin was added and flasks were incubated at 37°C for 3 minutes to dissociation adherent cells from the plastic surface. An addition 2ml of media was added to the flask and the cell suspension was aliquoted into a falcon tube and centrifuged at 1200rpm for 3 minutes. Cell pellets were re-suspended in1ml of ice-cold PBS and aliquoted into a fresh 1.5ml microcentrifuge tube. Cell suspensions were centrifuged at 10,000rpm for 1 minute and the supernatant removed. Cell pellets were re-suspended in 100µl RIPA buffer containing complete mini protease inhibitors, and mix well by aspirating up and down. Solutions were then incubated on ice for 30 minutes to obtain completely lysed cells, prior to centrifugation at 13,000rpm for 15 minutes at 4°C. The supernatant was then collected in a fresh microcentrifuge tube and stored at -80°C.

2.2.4.1 Protein quantification

Concentration of protein in cell lysates was quantified using the Bradford assay. In brief, bovine serum albumin (BSA) standards of known protein concentrations between 0.1-1.4mg/ml were prepared; 5µl of each standard was then added to separate wells of a 96 well plate. Unknown samples were diluted in RIPA buffer, to be approximately within the range of 0.1-1.4µg/ml. Five microlitres of each unknown sample was added to the 96-well along with triplicate wells of RIPA buffer alone to act as a blank to enable the background to be subtracted. To each well, 250µl of Bradford reagent (Invitrogen, UK) was added, and

the plate was mixed briefly on a shaker for 30 seconds. Samples were then incubated at room temperature for 5minutes prior to measuring the absorbance of each well at 595nm using the VersaMax tuneable microplate reader (Molecular Devices). A standard curve of the net absorbance versus the protein concentration was generated from the BSA standards, and used to extrapolate the protein concentrations of all unknown samples, taking into account the original dilution factor.

2.2.4.2 Immunoblotting

For analysis OATP1B3 that has a molecular weight of 120kDa was ran on a 10% Bis-Tris gel (Invitrogen). Samples were prepared in a total volume of 20µl to the required concentration (20-50µg), and mixed with 4x NuPage LDS sample buffer (Invitrogen) plus and incubated at 95° for 5 minutes. Samples were centrifuged briefly before loading onto the gel, gel tank was filled with running buffer (14.4g Glycine, 3.03g Tris (hydroxymethyl) methylamine, 800ml dH_2O and 200ml methanol) and run at 120V until the rainbow marker (Invitrogen) had ran through the gel and separated completely. The gel was removed and sandwiched into a cassette along with materials pre-soaked in transfer buffer and layered in a specific order, see Figure 2.4. Air bubbles were removed by gently rolling over the layers as the sandwich was assembled, before firmly securing into a cassette which was placed in a transfer tank (BioRad, Hertfordshire, UK) and ran over night at a current of 25mA. This is known as a wet transfer, in which the proteins migrate from the gel onto the nitrocellulose membrane due to the negative charge of particles and the current applied.

Following transfer, the membrane was removed and placed in a tray containing 5% dried non-fat milk (Marvel, Dublin, ROI) in PBS with 0.1% tween20 (PBS-T) for 1 hour on a rocking

platform to block non-specific binding. The primary OATP1B3 antibody (Ab) was diluted to the appropriate dilution in 5% milk PBS-T and incubated overnight at 4°C. After incubation with the primary Ab, the membrane was washed 3 times for 5 minutes each in 5% PBS-T prior to incubating for 1 hour with the appropriate secondary Horse Radish Peroxidase (HRP) linked antibody that was made up in 5% PBS-T. The membrane was then placed in 5% PBS-T for 2 minutes on a rocking platform, and then washed 4-5 times for 10 minutes each in PBS-T at room temperature on a rocking platform. The membrane was placed on cling film and excess PBS-T was removed with tissue, 1ml of ECL advance western blotting detection kit was incubated for 1 minute, which is a chemiluminescent detection system based on peroxide oxidation of the lumigen substrate to produce light. Excess ECL was removed with tissue and the clingfilm folded over. The membrane was place into a dark cassette and exposed for autoradiography, using Hyperfilm autoradiography film (GE Healthcare, Little Chalfont, UK).

Figure 2.4 Immunoblotting transfer setup. The figure represents the order in which the transfer cassette for western blotting is set up, and the direction of current.

2.2.4.3 Immunofluorescent staining of cells

Parafilm was taped down onto the work surface and cover slips with previously fixed cells were rehydrated in 8µl of PBST (Tween 20 0.1%) for 5minutes. Cover slips were then incubated on 8µl of PBST with 3% BSA for 20 minutes. Primary antibodies were made up in PBST-BSA, and cover slips were incubated on 10µl of appropriate Ab for 1 hour in a humidified atmosphere, control samples were incubated in 10µl of PBST-BSA. Cover slips were then washed 3 times in 8µl PBS, for 5 minutes each time. Each cover slip was then incubated on 10µl of secondary antibody for 45 minutes in a dark container, prior to another three PBS washes each of which was 5 minutes and slides were incubated in a box to prevent exposure to the light. Each cover slip was then placed on a 4µl drop of Mounting (Invitrogen) on a glass slide and the edges of each cover slip were coated with nail varnish to prevent movement of the cover slips. Cells were then viewed for immunofluorescent staining of specific proteins using a fluorescent microscope.

2.2.4.4 Immunofluorescent staining of tissue sections

Frozen tissue sections were fixed onto glass slides by placing them in a slide holding containing ice-cold methanol acetone and placed at -20°C for 5 minutes. Slides were then air dried for 2 minutes in a humidified atmosphere. Each section was then outlined using a wax pen and each slide appropriately labelled with the name of sample, antibody, Ab dilution and date.

Sections were rehydrated with PBS for 2 minutes, and then covered with BSA, a protein to prevent non-specific binding and incubated in a humid atmosphere for 20 minutes. Primary antibodies were reconstituted in BSA solution to the required dilution. 10µl of primary

antibody was added to appropriate sections, and BSA solution was added to negative controls, and incubated for 1 hour. Antibodies and BSA were removed from the sections, and slides were subjected to 3 washes in PBS each for 5 minutes. The appropriate "AlexaFluor" secondary antibodies were made up to the required dilutions and 10µl was added to all sections, and incubated for 45 minutes in a dark container. Slides were then subjected to 3 more PBS washes. 2 drops of Mountin (Invitrogen) containing Dapi nucleic stain was added to each section and then each section was covered with a square glass cover slip and left in a dark container until set. Tissue sections could then be examined for protein expression using a fluorescent microscope.

2.2.5 Functional Assays

2.2.5.0 Cell viability assays

Microcystin-LR (MC-LR) a cyano-bacterial toxin was purchased from Alexis Biochemical's (Nottingham, UK) and was used to investigate if SCC keratinocytes could be selectively killed based on the expression of OATP1B3. A colorimetric assay was used to determine changes in cell viability after exposure to MC-LR using the cell titer 96 aqueous one solution cell proliferation assay (Promega, Madison, CA) which is an MTS-based assay, which basically utilises the ability of living cells to produce NADH and NADPH which is able to reduce the tetrazolium 3-(4,5-dimethylthiazol-2-yl)-5-(3-carboxymethoxyphenyl0-2-(4-sulfophenyl)-2H-tetradzolium, inner salt (MTS) product to a soluble formazan in culture. When cells die, they lose their ability to reduce the MTS, and therefore the amount of formazan produced in proportional to the number of viable cells.

To perform the assay, cells were plated at 3000 cells per well in 50µl of keratinocyte media and seeded into 96-well plates. The following day, 50µl of media containing various concentrations of MC-LR (0.001-1µM) were added to each well. Appropriate controls were performed and included; adding 50µl media alone and 50µl media containing the drug vehicle (1% DMSO). Cells were then grown for 24-48 hours at 37°C. Cell viability was determined at time of seeding (T0) and after 24 and 48 hours by adding 20µl MTS solution and incubated for 3 hours, prior to reading the absorbance at 495nm in the VersaMax tuneable microplate reader (Molecular Devices, UK).

2.2.5.1 siRNA knockdown

The expression of *SLCO1B3* was knocked-down by transfecting RDEB SCC 2 cells with a pool of 3 *SLCO1B3* specific siRNAs (Sigma Aldrich, UK). Transfections were optimised and carried out in 6-well plates. Each well required 5µl of Lipofectamine2000 to be diluted in 250µl Opti-Mem and incubated for 5 minutes, followed by diluting a total of 4.0µg siRNA (1.33µg of each siRNA) in 250µl of Opti-Mem. Each complex was then mixed together gently and incubated for 20 minutes prior to adding to the appropriate well of the 6-well plate. 3 controls were performed for this experiment and included; control cells with just 500µl Opti-Mem added, mock transfected cells which only had the Lipofectamine complex added to an addition 250µl Opti-Mem and a final control, known as a non-targeting siRNA in which a scrambled siRNA was diluted in Opti-Mem and complexed with Lipofectamine. Cells were maintained in culture for 6 hours prior to changing the media for 2.5mL fresh keratinocyte medium. RNA was then isolated at specific time points after transfection, and converted into cDNA using the same method outlined in section 2.2.2.0 and 2.2.2.1, followed by determining if knock-down of *SLCO1B3* expression was successfully achieved via qRT-PCR using the protocol in section 2.2.2.9**.**

2.2.5.2 Fluo-3 Uptake Assay

The fluorescent calcium indicator; 1-[2-Amino-5-(2,7-dichloro-6-hydroxy-3-oxo-3Hxanthen-9-yl)]-2-(20-amino-50-methylphenoxy)ethane-N,N,N0N0-tetraacetic acid tetra ammonium salt (Fluo-3) (Invitrogen, Carlsbad, CA) is a substrate of OATP1B3 and was used to investigate the transport activity of OATP1B3 in SCC keratinocytes.

Briefly, SCC keratinocytes were grown in culture and plated at as density of 400,000 cells per well in 24-well plates. Cells were grown at 37°C in a humidified 5% CO_2 atmosphere for 24 hours prior to the start of the uptake experiment. Cells were washed in 0.5mL of pre-warmed (37°C) and filtered Fluo-3 uptake buffer composed of 142mM NaCl, 5mM KCl, 1mM KH2PO4, 1.2mM MgSO4, 1.5mM CaCl2, 5mM glucose and 12.5mM HEPES, pH 7.4. Then, 1ml Fluo-3 uptake buffer was added to each well, with or without 50µM of the inhibitor Rifampicin and incubated at 37°C in a humidified 5% CO_2 atmosphere for 1 hour. After 1 hour, the uptake before was removed and replaced by 1ml of fresh uptake buffer containing various concentrations of Fluo-3, ranging from 0.125 to 50µM. Cells were incubated for 1 hour at 37°C. After the incubation period, uptake was stopped by removing the uptake buffer containing the substrate and washing cells 3 times using ice-cold uptake buffer followed by adding 500µl 10% SDS in 1mM $CaCl_2$ to lyse the cells. Uptake was the determined by measuring the fluorescence in a HT synergy 2 multi-mode microplate reader (BioTek, USA) at an excitation wavelength of 485nm and an emission wavelength of 530nm.

2.2.5.3 Tritiated β-estradiol Uptake Assay

Radiolabelled [3H] estradiol-17β-glucuronide (39.8Ci/mmol) was purchased from PerkinElmer Life Sciences (Boston, MA). SCC keratinocytes were grown at 37°C in a humidified 5% CO2 atmosphere, and plated at 80,000 cells per well on 24-well plates, 24 hours later the cells were used in the uptake assay.

Initially, cells were washed 3 times in 0.5mL pre-warmed uptake buffer containing 116.4mM NaCl, 5.3mM KCl, 1mM NaH2PO4, 0.8mM MgSO4. 5.5mM D-Glucose and 20mM Hepes, pH7.4. Uptake was initiated by adding 200µl of uptake buffer containing the 20nM

[3H]-estradiol-17β-glucuronide, in the presence or absence of OATP8 substrates; Clotrimazole and Rifampicin. Cells were incubated for 1 hour at 37°C in a humidified 5% CO2 atmosphere. Uptake was stopped by removing the uptake solution, and washing cells 4 times with 0.5ml of ice-cold uptake buffer. Cells were then lysed using 500uL 1% Triton X-100, and physically removing the cells of the plastic using a cell scraper. Lysates were homogenized by pipetting up and down. Finally, 300µl of cell lysate was added to emulsifier (PerkinElmer, Buckinghamshire, UK) and used for liquid scintillation counting.

Chapter 3

TP53 Expression and Mutation Status in SCC

3.1 Background

3.1.1 Tumour Suppressor Genes

Tumour suppressor genes (TSGs) encode proteins that protect cells from damage which can cause cancer to development. When TSGs become mutated this may result in loss of phenotypic function and if accompanied by several other genetic changes the cell can undergo cancerous transformation. TSGs generally operate to prevent cellular damage by promoting cell cycle arrest and apoptosis. The general dogma regarding dysfunctional tumour suppressor genes is that of Knudson's "two-hit hypothesis" in which both alleles that encode a TSG must be affected for an effect to be apparent (Knudson 1971). The reason being that the mutated alleles of a TSG are most commonly recessive and therefore if only one allele is mutated the other allele is still capable of producing a functional protein. Although there are exceptions to this rule, examples of which are talked about in greater detail when discussing *TP53* mutations further on in this chapter.

3.1.1.1 Gatekeeper TSGs

TSGs can be divided into 3 distinct classes; gatekeepers, caretakers and landscapers (Macleod 2000). Gatekeepers include all genes that act directly to inhibit cell growth, whether that is by suppressing cell proliferation, the induction of apoptosis or by promoting differentiation. This category can be further divided into initiation, progression and metastatic gatekeepers, depending on the stage at which the genes act to prevent tumour growth (Macleod 2000). There are two main points that can define a gatekeeper TSG. Firstly they act directly to prevent tumour growth; loss of function of a particular

gatekeeper is a rate limiting step in tumourigenesis and finally the restoration of the function of these TSGs in tumour cells can suppress neoplastic growth (Macleod 2000).

3.1.1.2 Caretaker TSGs

Caretakers act indirectly to suppress growth by certifying the fidelity of the DNA through effective repair of DNA damage or prevention of genomic instability. This group of TSGs include many genes involved in DNA repair, such as *MSH2*, *MLH1* and *ATM* protein kinase which respond to ionizing radiation by activating p53 (Giaccia and Kastan 1998). The functional loss of a caretaker TSG can predispose to cancer by increasing the DNA mutation rate and thereby increasing the risk that the function of gatekeeper tumour suppressor genes will be lost as more mutations occur. By restoring the function of these genes tumour growth is not prevented, as mutations of gatekeeper genes may have already occurred as a consequence of the original caretaker function loss (Kinzler and Vogelstein 1998). Interestingly, the *TP53* gene can be classified as both a gatekeeper and caretaker TSG. As p53 induces apoptosis, it would appear to act as a gatekeeper, however whilst acting as "guardian of the genome" it prevents genomic instability and therefore would then be referred to as a caretaker TSG (Lane 1992).

3.1.1.3 Landscaper TSGs

Finally, landscaper TSGs are predicted to act by controlling the microenvironment in which tumour cells grow. The term landscaper TSG was first described following observations in juvenile polyposis syndrome (JPS) a disease characterised by polyps in the gastrointestinal tract that occur in childhood whereby initiating lesions were found in stromal cells

surrounding the tumour rather than directly in the tumour cells (Kinzler and Vogelstein 1998; Whittle et al. 2010). Landscaper TSGs can act by directly or indirectly regulating extracellular matrix proteins, cell surface markers, adhesion proteins, or secreted growth factors. The loss of function of these TSGs can result in irregular microenvironment growth and function, thus promoting transformation of the epithelia in which it surrounds.

3.1.2 *TP53*

TP53 is a tumour suppressor gene that encodes the protein p53, it was discovered over 30 years ago through the interaction of p53 with the oncogenic T antigens from the SV40 virus and has since become one of the most widely studied genes (Lane and Crawford 1979). Initially, *TP53* was thought to be an oncogene, this discrepancy in classification was due to initial studies being inadvertently carried out using a mutant form of *TP53*. Later studies revealed that the primary function of p53 was that of a TSG (Levine and Oren 2009). It is reported that 40% of human tumours express the mutant form of p53 (Goh et al. 2010). However, the role in which it plays in RDEB SCC is somewhat little understood and has only been reported in two papers (Slater et al. 1992; Arbiser et al. 2004). However, it has been well studied in cutaneous SCC, and has been reported to be mutated in up to 90% of tumours and deep sequencing of micro-dissected skin has revealed 14% of all epidermal cells harboured accumulated p53 mutations (Brash et al. 1991; Stahl et al. 2011). The p53 protein is normally expressed at low levels under normal conditions but its expression is induced in response to cellular stress. Many different stress signals can activate the expression of p53, where the protein undergoes post translational modification thereby stabilising the protein and allowing it to accumulate within the nucleus of cells where it can activate downstream target genes that are involved in cell cycle control, maintenance of

genetic integrity, proliferation and differentiation (Figure 3.0) (Giaccia and Kastan 1998; Giglia-Mari and Sarasin 2003; Goh et al. 2010).

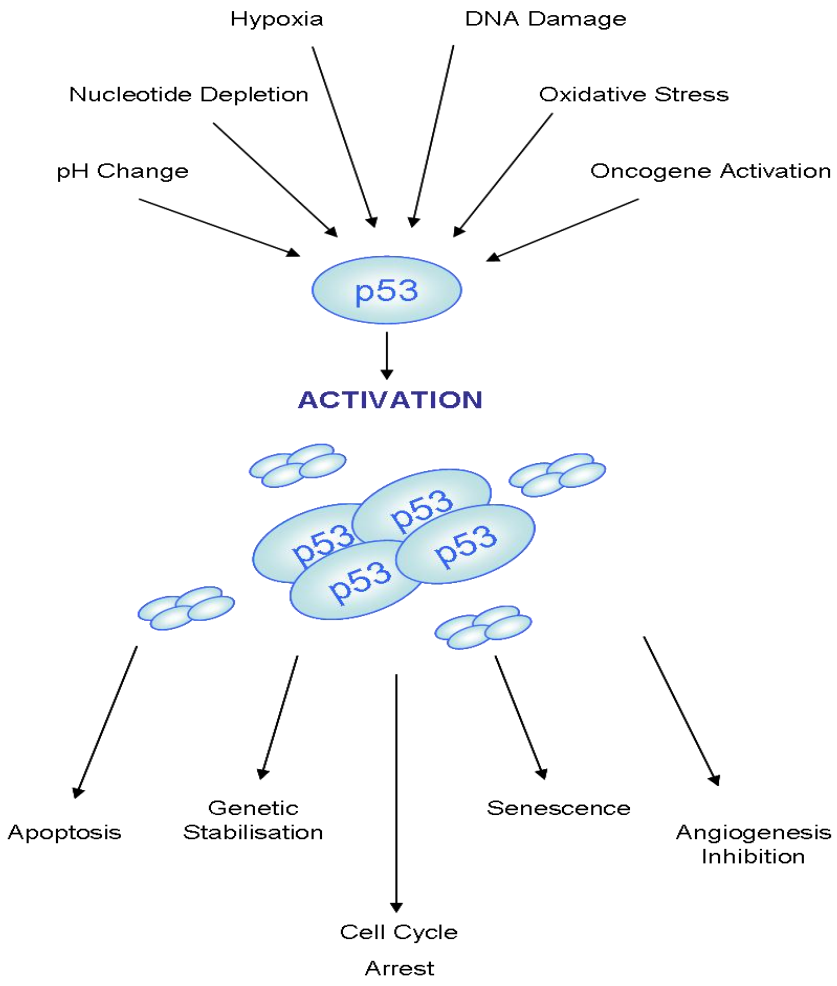

Figure 3.0 p53 expression is induced by many stress signals and as a result initiates a response to prevent cellular damage. The schematic diagram above depicts the stress signals that can activate p53 expression which is usually low under normal conditions. Activation causes the protein to accumulate in the nucleus and form stabilised tetramers whereby it can then bind to co-factors and induce a stress response.

3.1.2 1 p53 structure

Over the past few years it was established that there are as many as 9 p53 protein isoforms encoded by the *TP53* gene through splicing and an alternative transcriptional initiation site (Bourdon et al. 2005), the structure of which is shown in Figure 3.1. The expression of the p53 isoforms is not well studied in either RDEB SCC or non-RDEB SCC and it is interesting to investigate the expression of these isoforms in our sample cohort, to establish if mutations are present and to identify if there is a specific mutation spectrum in the RDEB SCC samples that could lead to higher rates of cell proliferation or if common mutations are found this could be used as a target in the development of RDEB SCC cancer therapies. It has been reported that p53 isoforms are expressed in normal tissue but in a tissue dependent manner suggesting the expression of the isoforms can be selectively regulated and have been reported to be differentially expressed in various cancers including breast tumours and head and neck squamous cell carcinoma (Bourdon et al. 2005; Boldrup et al. 2007). Presence of multiple splice variants is a probable cause for discrepancies in research showing difficulty in linking p53 status to the mechanisms and sensitivities of different human cancers (Bourdon et al. 2005).

3.1.2.2 *TP53* mutations

TP53 mutations are the most frequent genetic aberrations in human cancer (Kato et al. 2003). *TP53* aberrations are reported to be the most frequent genetic mutations in cutaneous SCC, with 50% incidence (McGregor et al. 1997; Boukamp 2005). They are also considered to be an early event in cutaneous SCC, due to a study showing that over 50% of AKs harbour *TP53* mutations (Nelson et al. 1994). Germline mutations of *TP53* have been

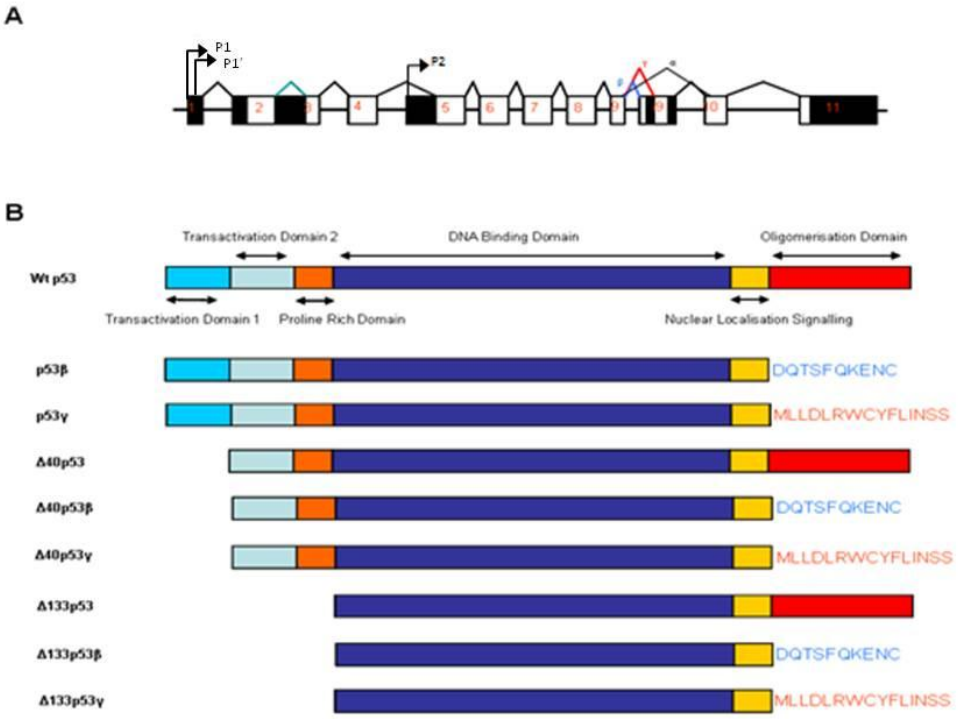

Figure 3.1 Schematic diagram illustrating that *p53* can encode at least 9 protein isoforms

(A) Shows the intron/exon structure of p53 containing 11 introns. The wild-type p53, p53β, p53γ and Δ40 proteins are encoded by P1 and P1' promoters, whilst Δ133 protein isoforms are encoded by the P2 alternative promoter. The C-terminus can be alternatively spliced to produce 3 isoforms, denoted by red, blue and black arrow above the intron/exons boxes. (B) The top band shows the full length wild-type p53, followed by β and γ gamma isoforms produced by splicing of intron 9. Then the three Δ40 isoforms produced by alternative splicing of intron 2 and alternative initiation of translation sites. Finally the last three isoforms are produced by use of an alternative promoter in intron 4 to create Δ133 isoforms.

definitively linked to a predisposition to cancer development; such is the case in an autosomal dominant hereditary disorder known as Li-Fraumeni syndrome (Malkin 1993).

The majority of mutations, approximately 80%, occur within the DNA-binding domain which is important for the folding and stabilization of the tertiary structure of p53 (Kato et al. 2003; Marcel and Hainaut 2009; Peltonen et al. 2010). Within this domain 6 "hotspot" mutations have been identified (Petitjean et al. 2007). Most of the mutations occurring in the *TP53* coding sequence are predominantly missense mutations; these are point mutations which results from the substitution of a single nucleotide within the DNA sequence.

Many different mutations within this gene can result in very different consequences to the function of the protein; some studies have worked solely on establishing the effects of particular mutations on p53 function in mice models (Lozano 2007). The consequences of mutations can cause loss of tumour suppressor function (LOF) (Blagosklonny et al. 1997); gain of oncogenic function (GOF) (Dittmer et al. 1993) and furthermore, some mutant *TP53* alleles can exhibit a dominant-negative effect over the wild-type copy (de Vries et al. 2002).

3.1.2.3 Dominant-negative *TP53* Mutations

Studies using knock-in mouse models have demonstrated the ability of mutant p53 to drive tumour formation, invasion and metastasis through dominant-negative inhibition of wild-type p53 (Goh et al. 2010). The concept of dominant-negative inhibition is just one example of the complexity of mutant p53 in driving tumour progression. Dominant-

negative effects occur due to the fact that p53 binds to form functional tretramers, which when wild-type and mutant p53 bind they show weakened DNA association and reduced transcriptional activity (Milner and Medcalf 1991), thus the mutant p53 prevents the function of the wild-type protein.

3.1.2.4 Gain of function *TP53* mutations

TP53 also has 'gain of function' properties which is an oncogenic effect. To test p53 mutants which exhibit GOF effects, mutant p53 alleles can be introduced into mice which do not express endogenous p53, and then test for an acquired tumour phenotype. Using this basic model, Dittmer and colleagues (1993) were able to show mutant p53 tumours confered a gain of function that provided these cells with a growth advantage over p53-null tumours. Some GOF properties may also be attributed to mutant p53 being able to inhibit the function of p53 family member's p63 and p73 (Strano et al. 2002).

Mutant p53 can also acquire additional functions that allow it to interact with other proteins, eliminating or altering their activities (Lozano 2007). Many of the proteins targeted by GOF are those which are part of the general transcriptional machinery, such as kinases and acetylases that modify p53, and others are negative regulators of p53 itself (Appella and Anderson 2001). p53 mutants that possess new functions that are not shared by the wild-type p53 protein can be defined as GOF mutants. Rather than transactivating normal p53 target genes, GOF mutant p53 activates a different subset of genes, such as MDR1 and MYC (Vousden and Prives 2005), these newly activated proteins provide survival and growth advantages for to tumour cells. For example MDR1 is a multi-drug resistance

protein which provides a transport mechanism in tumour cells that causes efflux of anti cancer drugs and effectively pumps the drug back out of the cell making them resistant to certain treatments.

3.1.3.5 Effect of UV radiation on TP53

It has been clearly demonstrated that UV radiation of the skin by exposure to both UVA and UVB light causes skin cancer (Brash et al. 1991). This is evident from skin tumours which occur mainly on sun-exposed sites, and occur at a higher frequency in fair skinned individuals (Salasche 2000). It is common to find UV molecular signatures in the DNA of SCCs. These signatures mutations are specifically caused by UV and are common in the *TP53* gene. It is thought that sunburnt skin harbours cells with *TP53* mutations and that these mutant cells undergo clonal expansion and can give rise to a tumour. Molecular signature mutations can also be found in premalignant conditions such as Actinic Keratoses (AK), which can develop into SCC. Studies have shown that 1 in 1000 AKs progress into a SCC (Marks et al., 1996). Together this suggests that *TP53* mutations are an early event in SCC development. Xerodermo Pigmentosa (XP), is a nucleotide excision repair (NER) deficient condition, predisposes patients to a 4000-fold increased risk of developing skin cancers and these tumours have a high frequency of molecular signatures found in the *TP53* (Benhamou and Sarasin 2000).

3.1.4 *TP53* in RDEB SCC

Only 2 studies have investigated p53 expression in RDEB SCC. Neither of which have investigated the expression of the different p53 isoforms. The first study showed 26% of

RDEB SCC samples labelled positively for up regulation of the p53 protein (Slater et al. 1992). Furthermore, 12 out of 15 of the well differentiated tumours within the sample cohort were negative. Whilst 63% of the moderately to poorly differentiated tumours had positive labelling. This study concluded that mutant p53 protein expression correlates with poorer tumour differentiation states. Differentiation refers to the state of the tumour cells and how much they resemble the surrounding normal tissue. Those with poor differentiation are likely to be mature tumour cells or highly invasive metastatic tumour cells which lack the morphological structure and function of normal healthy cells. The second paper, demonstrated 3 of 8 tumours had *TP53* mutations, however this study only investigated exons 3-8 of the DNA sequence and not the whole open reading frame (Arbiser et al. 2004). In our sample cohort, p53 protein expression has been previously reported and over-expression can be seen in 5 of 8 SCC samples (Figure 3.2).

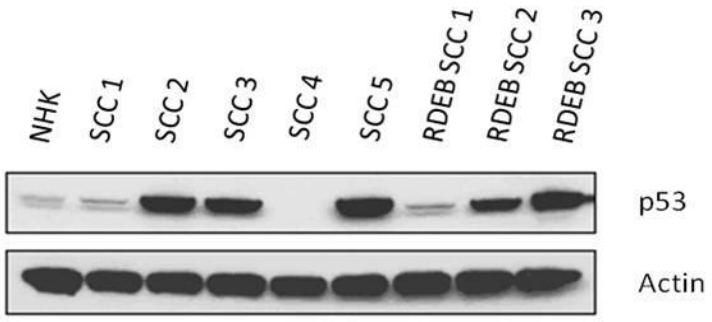

Figure 3.2 p53 protein expression by western blotting (Watt et al. 2011)

Western blotting performed by Dr Carol Hogan, shows the protein expression of p53 in the same samples used throughout this thesis. The immunoblot shows amplification of p53 protein in 5 of 8 SCC samples, and complete loss in 1 of 8 SCC samples.

3.1.5 Single Nucleotide Polymorphisms in RDEB SCC

Single nucleotide polymorphisms (SNP) are variations in a single base within the DNA code. SNP mapping is a high-throughput, rapid and accurate technique that utilises microarray technology to provide whole-genome wide analysis of allelic alterations within the DNA of a given sample (Purdie et al. 2007). Arrays have been used to detect SNP and identify disease related chromosome loci, including those in several human cancers. Such as the identification of frequent 3p11-p12 loss in oral tongue SCC (Zhou et al. 2005) and conserved loss of heterozygosity (LOH); which is the loss of a normal functional allele at a heterozygous locus (Tischfield 1997) at 9p21and 6p23-27 in BCC (Teh et al. 2005). Only one published study has reported SNP mapping in cutaneous SCC, in which their results showed LOH at 9p, in 81% of samples; along with recurrent but less frequent changes at 3p, 2q, 8p and 13 (Purdie et al. 2007).

Unpublished data from a SNP mapping experiment from Dr Andrew South's laboratory has identified recurrent LOH of chromosome 17p13 (5 of 12 RDEB SCC and 6 of 12 SCC) this chromosomal loci is known to harbour the TSP; *TP53*. SNP results showing allelic losses, gains and uniparental disomy (UPD) which results from the inheritance of both homologous chromosomes from one parent, for each of the samples used within this study are summarized in Table 3.1.

3.1.6 Aim

The aim of this chapter was to identify the mRNA expression status of the main tumour suppressor gene *TP53* in RDEB SCC samples and evaluate whether there is a difference

between *TP53* mutation status in RDEB SCC compared to non-RDEB SCC. This is brought about by identification of SNPs in RDEB SCC and non-RDEB SCC samples and the increased p53 protein expression in our samples cohort (Figure 3.2) (Purdie et al. 2007; Watt et al. 2011). Identifying a different mutational spectrum between the two SCC types could identify different molecular origins of these tumours and would allow specific RDEB SCC therapies to be developed by targeting mutations that are common in RDEB SCC tumours.

In this study, the mRNA expression of full length wild-type (wt) *p53, p53β, p53γ and the Δ133 p53* isoforms was investigated followed by mutational analysis of the amplified products. Results suggest that no distinct mutational spectrum was identified in either SCC type. Whilst all tumour samples harboured at least one mutation, each was a heterogenous mutation which was not observed in the other samples.

Sample	Loss	Gain	UPD
RDEB SCC 1	4p, 4q, 8p, 10p, 11p, 13q, X	8q, 11p, 12q, 22q	3q, 4p, 4q, 9p, 12p, 13q, 17p, 18q
RDEB SCC 2	3p, 4p, 4q, 5q, 6p, 7q, 8p, 10p, 21p, X	14p, 14q, 22p, 22q	1p, 1q, 2q, 4p, 5q, 8q, 9p, 9q, 11q, 13q, 15q, 17p
RDEB SCC 3	3p, 4p, 4q, 8p, 13q	5q	2p, 4p, 5q, 6q, 7p, 7q, 8q, 9p, 10p, 10q, 12p, 12q, 14q, 17p, 19q, 21q, X
SCC 1	3p, 8p, 18p	1q, 3p, 7p, 8q, 9q	8p, 9q
SCC 2	3, 9p, 18q	3q, 9p	-
SCC 3	3p, 5q, 8p, 9p, 11p, 17p	3q, 5p, 7p, 8q, 11p, 17q	7q, 9p, 9q, 17p
SCC 4	1q, 2q, 7q, 9q, 10p, 11q, 14p, 22p, 22q	13p, 13q, 17p, 17q	1p, 6p, 6q, 9q, 14q, 20q, X
SCC 5	2q, 9p, 18p, 18q, 19p, 19q	8q, 11p, X	-

Table 3.1 Overview of chromosomal aberrations as identified by SNP mapping

Summary of SNP locations identified by SNP array (Dr Andrew South), and previously reported by Purdie and colleagues (2007) for UV induced SCC samples. Chromosome locations showing loss, gain and/or uniparental disomy (UPD) are noted for each sample used throughout this thesis. p and q refers to the arm of the chromosome where SNPs were identified.

3.2 Methods and Results

Nested RT-PCR was used to amplify the *p53* isoforms. Briefly, 50µl reactions were setup using standard RT-PCR protocol as outlined in Chapter 2 Section 2.2.2.5. The first PCR reaction used primers E2.1 and RT1 to amplify the *TP53* ORF using the following conditions outlined in Table 3.2, using the DNA Tetrad 2. A second PCR reaction was then performed using the 1µl of the PCR product from the first reaction as the template. The following primer combinations were used; E2+RT2, E2+p53b and E2+p53g to amplify wtp53, p53β and p53γ, respectively. Δ133p53 variants were also amplified using nested PCR. The initial reaction utilised primers i4f1 and RT2, followed by a second reaction using the following combinations of primers; Δ133p53: i4f2 and RDNp53, Δ133p53β: i4f2 and p53β and Δ133p53γ: i4f2 and p53γ. All primer sequences are outlined in Table 3.3.

Step	Temperature	Time	Number of Cycles
Enzyme Activation	94°C	3mins	1
DNA Denaturing	94°C	30sec	35
Annealing	64°C	45sec	
Extension	72°C	1.5mins	
Final Extension	72°C	8mins	1

Table 3.2 Cycling conditions p53 nested RT-PCR

Primer Name	Primer Sequence (5'---3')
E2.1	GTC ACT GCC ATG GAG GAG CCG CA
RT1	GAC GCA CAC CTA TTG CAA GCA AGG GTT C
E2	ATG GAG GAG CCG CAG TCA GAT
i4f1	CTGAGG TGT AGA CGC CAA CTC TCT CTA G
RT2	AAT GTC AGT CTG AGT CAG GCC CTT CTG TC
i4f2	GCT AGT GGG TTG CAG GAG GTG CTT ACA C
p53β	TTT GAA AGC TGG TCT GGT CCT GA
p53γ	TCG TAA GTC AAG TAG CAT CTG AAG G
RDNp53	CTC ACG CCC ACG GAT CTG A

Table 3.3 *TP53* nested RT-PCR primers

3.2.1 *TP53* isoforms are expressed in cutaneous SCC

The expression of *TP53* mRNA isoforms in SCC was investigated using nested qPCR. No previous publications have documented the expression of *TP53* isoforms in cutaneous SCC. RNA was extracted from cultures of 3 independent RDEB SCC, 1 normal human keratinocyte (NHK) and 5 non-RDEB SCC keratinocyte samples 2 days post confluence (for methodology see Chapter 2.2.2.2). NHK was used to determine the normal expression pattern of the isoforms in keratinocyte cells. Primer sets, have been previously published and were used to amplify isoforms of *TP53* cDNA (Bourdon et al. 2005). Nested PCR revealed expression of full length *TP53* in NHK, all 3 RDEB SCC and 4 out of 5 non-RDEB SCC samples. An example of the amplified products is seen in Figure 3.3.

PCR amplification showed mRNA expression of the p53β in NHK and all 8 SCC keratinocyte samples. The expression of the isoform at the mRNA level for each sample is summarized in Table 3.4. Interestingly, SCC 4 showed only expression of the β-isoform. Whilst p53γ mRNA expression wasn't present in NHK, but was present in all 3 RDEB SCC samples and 3 of 5 non-RDEB SCC samples. The Δp53 and Δp53β were both expressed at the mRNA level in NHK, but not Δp53γ. The Δp53 mRNA isoforms were all expressed in RDEB SCC keratinocyte samples, apart from RDEB SCC 2 which showed no expression of any of the three Δp53 isoforms. Δp53 isoforms were expressed in the majority of non-RDEB SCC samples, with the exception of Δp53γ which was not detected in SCC 1 and again only the Δp53β isoform was detectable in SCC 4.

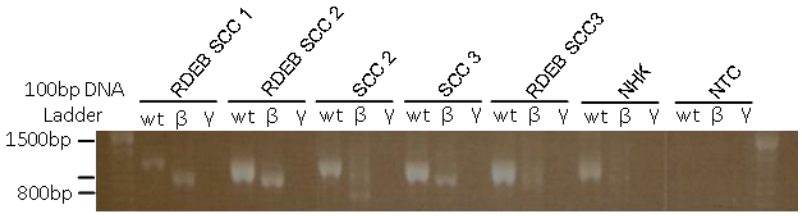

Figure 3.3 Agarose gel showing PCR amplification of full length p53, p53β, and p53γ

TP53 isoforms were amplified by nested PCR. wt represents amplified full length p53, followed by beta, for the beta isoform, and y for the gamma isoform, for each of the 6 samples used which are labelled above the 3 corresponding lanes. NHK represents normal human keratinocytes used as a control samples and NTC is a no template control used to identify any contamination. All other gel photos can been seen in appendix 1.0.

3.2.2 RDEB SCC keratinocytes express mutant p53 transcripts

All amplified PCR products were purified using an ExoSap protocol followed by direct sequencing to identify mutations within the ORF of *TP53* isoforms. Sequencing of the PCR products revealed single point mutations in all 3 RDEB SCC samples. Chromatographs of each mutation can be seen in Figure 3.4, all mutations are homozygous missense mutations that occur within the DNA-binding domain. Codon 173 is mutated in RDEB SCC 1 in which the original valine amino acid is changed to a leucine once the first G nucleotide of the codon is substituted by a T nucleotide. In RDEB SCC 2 the second nucleotide of codon 273 is changed from a G to A nucleotide resulting in a histidine amino acid residue being produced instead of an arginine residue. Finally, RDEB SCC 3 contained a double CC to TT substitution of the first two nucleotides of codon 152 resulting in the proline residue being replaced by a leucine amino acid residue.

Interestingly, repeated PCR reactions duplicate RNA from these samples sometimes demonstrated different results. One a number of occasion's samples which showed expression in one PCR run didn't necessarily demonstrate expression of the same isoform on a second run. In these cases, at least 3 independent PCR reactions were performed and if the expression was seen in 2 out of 3 runs then the results were recorded as that isoform was expressed in the sample.

It is intriguing to note that the p53γ isoform is expressed in RDEB SCC samples and not non-RDEB SCC samples suggesting a possible gain of function phenotype may be acquired in these cells. But NHK also showed expression of this isoform, however in retrospect the use

of only one NHK control limits the conclusions which can be drawn directly from this experiment. Therefore it would be necessary to repeat this experiment with a greater number of NHK samples, so establish a greater understand of the normal isoform expression in normal human keratinocytes.

Sample	*p53*	*p53β*	*p53γ*	*Δp53*	*Δp53β*	*Δp53γ*
NHK	Yes	Yes	X	Yes	Yes	X
RDEB SCC 1	Yes	Yes	Yes	Yes	Yes	Yes
RDEB SCC 2	Yes	Yes	Yes	X	X	X
RDEB SCC 3	Yes	Yes	Yes	Yes	Yes	Yes
SCC 1	Yes	Yes	X	Yes	Yes	X
SCC 2	Yes	Yes	Yes	Yes	Yes	Yes
SCC 3	Yes	Yes	Yes	Yes	Yes	Yes
SCC 4	X	Yes	X	X	Yes	X
SCC 5	Yes	Yes	Yes	Yes	Yes	Yes

Table 3.4 Summary of the SCC samples which express the *TP53* mRNA isoforms

The table shows which *TP53* isoforms were expressed in each of the SCC samples. A "yes" indicates an amplified product was observed when samples were run on agarose gels whilst an "x" means no amplified products were seen.

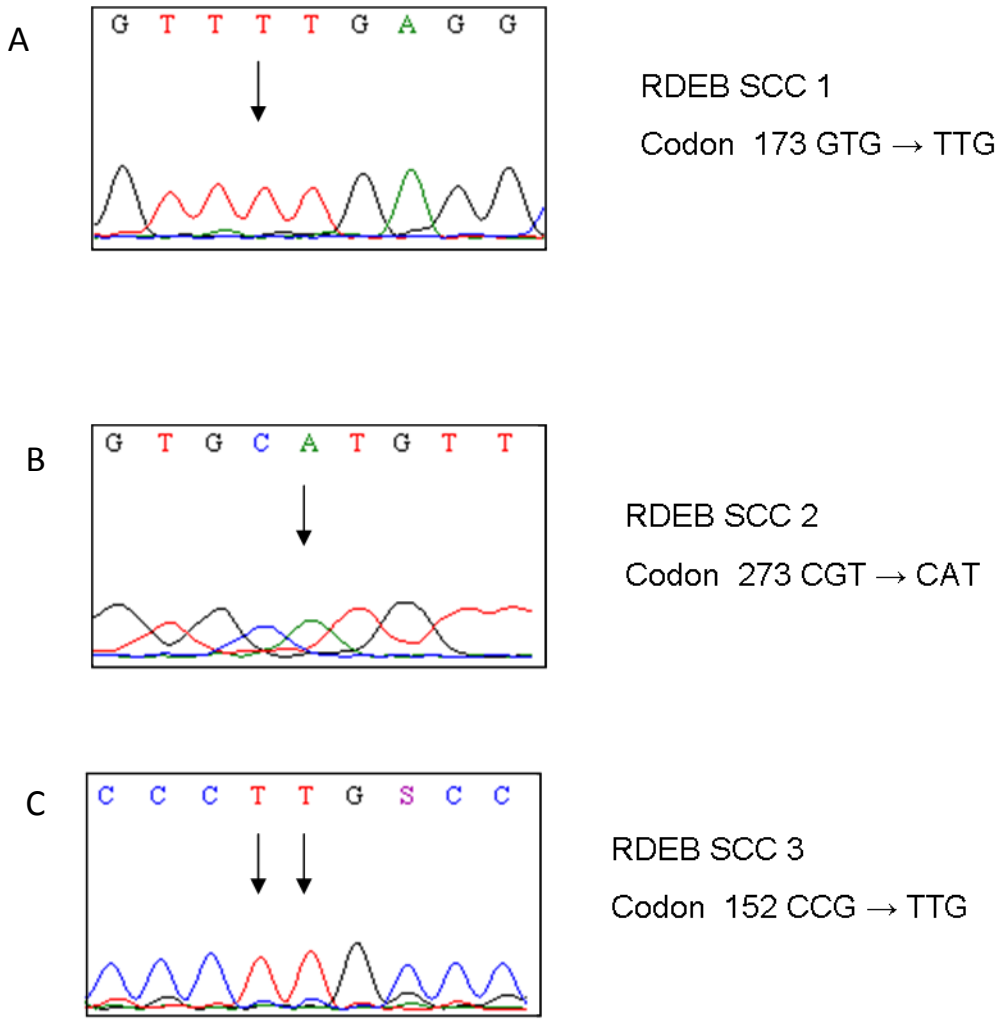

Figure 3.4 RDEB SCC keratinocytes harbour missense mutations in p53, p53β and p53γ

Direct sequencing of PCR amplified *TP53* products revealed homozygous missense mutations in each of the RDEB SCC samples. The arrow indicates the mutated nucleotide(s) and each codon affected is underlined. (A) Codon 173 is mutated in RDEB SCC 1, in which the first base is changed; C>T. (B) Codon 273 is mutated in RDEB SCC 2, in which the second base is changed; G>A. (C) Codon 152 is mutated in RDEB SCC 3, in which the first two bases are changed; CC>TT. Each of the mutations were present in full length p53**,** p53β and p53γ.

3.2.3 SCC express mutant *TP53* transcripts

Non-RDEB SCC keratinocyte samples (SCC 1-5) all express mutant *TP53* transcripts, chromatographs of each mutation are shown in Figure 3.5. SCC 1 contained a single heterozygous mutation at codon 234, which results in the amino acid being changed to a serine residue on one allele. SCC 2 contained a homozygous CC to TT mutation that results in a phenylalanine amino acid being produced instead of a proline residue. SCC 3 also contained a homozygous mutation, although this alteration in the DNA sequence was present in codon 216 in which the original valine residue is changed to a methionine due to the first G nucleotide of the codon being substituted for an A nucleotide. SCC 4 contained a single nucleotide deletion, in which the first T nucleotide of codon 91 is absent from the DNA sequence. Lastly, SCC 5 was the only sample to contain more than one mutation, and harboured 3 heterozygous mutations. Firstly; codon 179 contained a C to T transition which results in the amino acid being changed to a tyrosine, codon 247 also contained a C to T substitution which was a silent mutation in which the mutation resulted in a codon encoding the same asparagine amino acid as the original codon and finally, codon 248 contained a C to T substitution resulting in a tryptophan residue instead of an arginine.

Both heterozygous mutations occurred in samples with no apparent LOH at chromosome 17 (Table 3.1 and Figure 3.5A and E). Also, SCC 1 was the only non-RDEB SCC sample to show normal p53 protein level (Figure 3.2). SCC 2 also showed no abnormalities of chromosome 17 by SNP mapping, but did show over-expression at the protein level (Table 3.1 and Figure 3.5) indicating that p53 may be mutated, which was the case. SCC 3 showed some loss of 17p and UPD, and over-expression at the protein level, and so it was expected to be mutated. SCC 4 showed some gain of 17p, and no protein expression (Table 3.1 and Figure 3.5) This sample contained a single nucleotide deletion in codon 91 of the proline-

rich domain resulting in a frameshift of the DNA sequence immediately after the deletion and subsequently alters all codons after the original mutation. This would be an explanation for why no protein is seen when western blotting is performed to look for p53, although it could also be due to non-sense mediated decay of the transcript. It is important to note that the western blot seen in Figure 3.2 was conducted using a p53 antibody which does not distinguish between different protein isoforms. After the deletion the subsequent frameshift results in the generation of four STOP codons (Figure 3.6), which are likely to cause non-sense, mediated decay of the transcript, thus, preventing the expression of the protein.

3.2.3 Mutation spectrum is unique to each tumour sample

Each of the samples contained different mutations, suggesting that the mutation spectrum in the SCC samples in our cohort is unique to the each tumour. From this study it is impossible to distinguish between RDEB SCC and non-RDEB SCC based on the expression or mutations of *TP53*. The majority of mutations detected were homozygous, and probably result from loss of one *TP53* allele and a mutation occurring in the other. All but one of the mutations occurred within the DNA-binding domain, with the other mutation occurring upstream in the proline rich domain (Table 3.5). Intriguingly, two mutations; codon 273 in RDEB SCC 2 and codon 248 in SCC 5 are the two most commonly reported mutations out of all the mutations identified in this study.

3.2.4 UV signature mutations are most prevalent in sporadic SCC rather than RDEB SCC

As expected, more UV signature mutations were identified in the non-RDEB SCC samples, where 57% (4 of the 7) of mutations identified in non-RDEB SCC are classed as UV signature mutations as they occur at dipyrimidine locations within the DNA sequence, whereas only 1 of the 3 mutations identified in RDEB SCC is classified as a UV signature mutation.

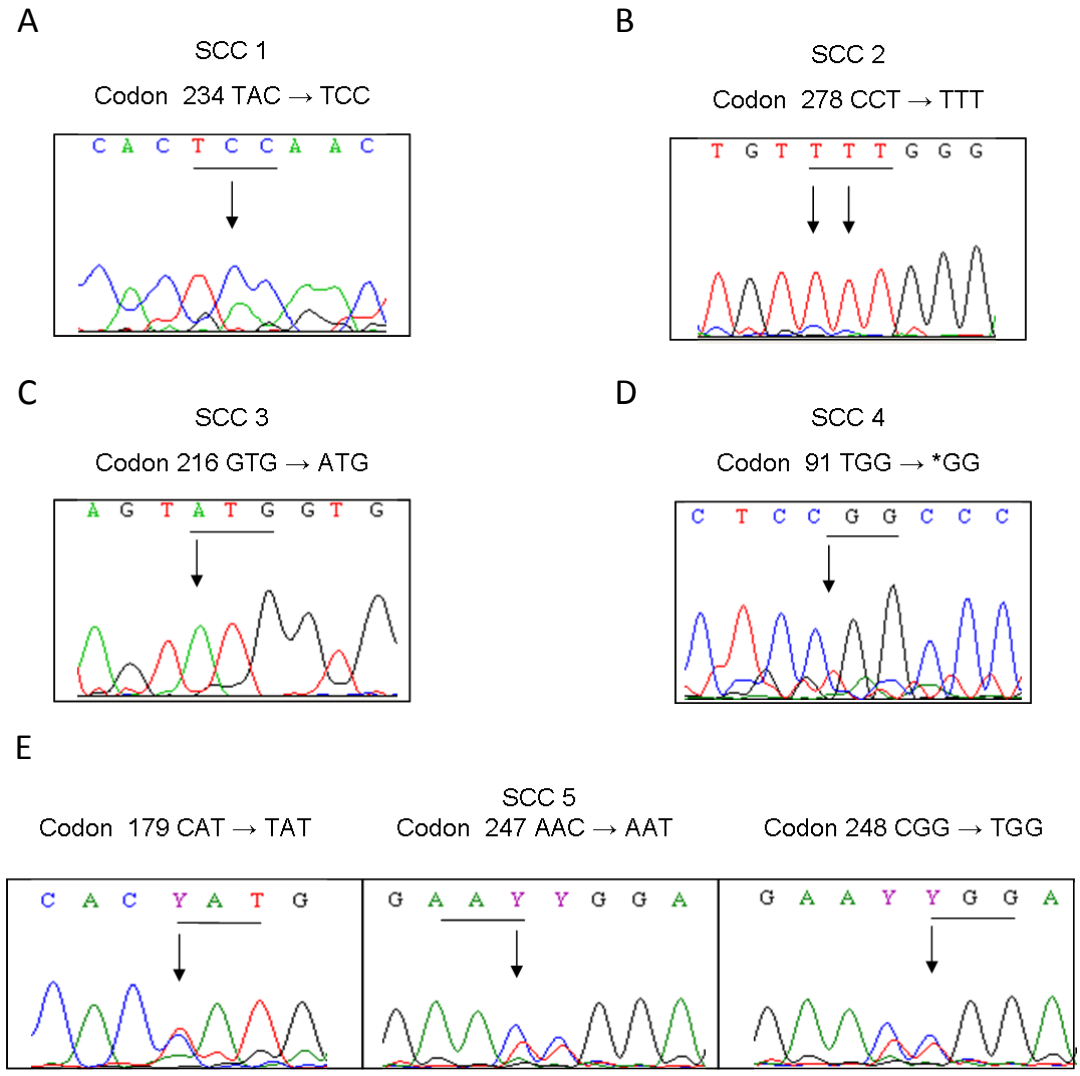

Figure 3.5 Non-RDEB SCC keratinocytes harbour mutations in p53, p53β and p53γ

Direct sequencing of the PCR amplified *p53* products revealed homozygous mutations in 3 of the 5 SCC samples and heterozygous mutations in 2 of 5 SCC samples. The arrow indicates the mutated nucleotide(s) and each codon affected is underlined. Each of the mutations was present in wtp53, p53β and p53γ, unless otherwise stated. (A) Codon 234 is mutated in non-RDEB SCC1, in which the second base is changed; A>C. (B) Codon 278 is mutated in non-RDEB SCC2, in which the first two bases are changed; CC>TT, a classic UV signature mutation. (C) Codon 216 is mutated in non-RDEB SCC3, in which the first base is changed; G>A. (D) Codon 91 is changed in non-RDEB SCC4 in which only the p53β isoform is expressed, this is a deletion of the first base TGG>*GG. (E) Codons 179, 247 and 248 show heterozygous mutations in non-RDEB SCC. Each codon displays a C>T substitution

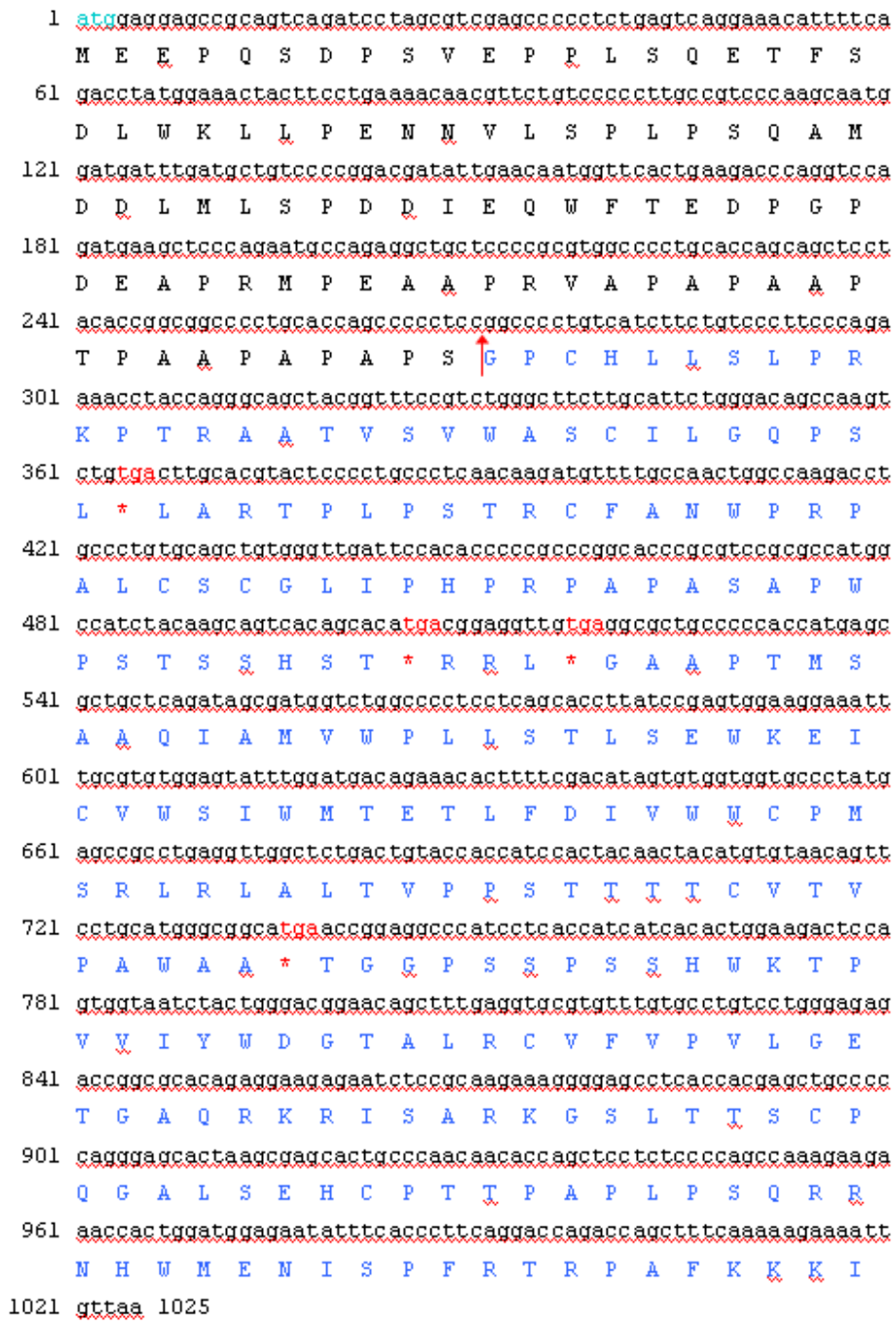

Figure 3.6 mutant expression of p53β in SCC4 is caused by a deletion of nucleotide 271

Deletion of nucleotide 271 in the coding sequence of p53β results in an altered amino acid sequence. The deletion of the T nucleotide occurs at the position denoted by the red arrow, after which the new codon sequence is shown in blue writing along with the generation of 4 STOP codons highlighted by the red writing and *.

Sample	Type of Mutation	Coding Sequence	Exon	Domain	Protein Sequence	Mutation Effect	Structural Motif	CpG Site	No. Of Mutation Reports
RDEB SCC 1	Homozygous	c.517G>T	5	DNA Binding Domain	p.V173L	Missense	L2	No	65
RDEB SCC 2	Homozygous	c.818G>A	8	DNA Binding Domain	p.R273H	Missense	S10	Yes	812
RDEB SCC 3	Homozygous	C454-455CC>TT	5	DNA Binding Domain	p.P152L	Missense	L	No	3
SCC1	Heterozygous	c.701A>C	7	DNA Binding Domain	p.Y234S	Missense	S8	No	7
SCC 2	Homozygous	c.832-833CC>TT	8	DNA Binding Domain	p.P278F	Missense	H2	No	10
SCC 3	Homozygous	c.646G>A	6	DNA Binding Domain	p.V216M	Missense	S7	No	76
SCC 4	Homozygous	c.271del1	4	Proline Rich Domain	N/A	Frameshift	S3	No	2
SCC 5	Heterozygous	c.535C>T	5	DNA Binding Domain	p.H179Y	Missense	H1	No	107
SCC 5	Heterozygous	c.741C>T	7	DNA Binding Domain	p.N247N	Silent	L3	No	15
SCC 5	Heterozygous	C742C>T	7	DNA Binding Domain	p.R248W	Missense	L3	No	707

Table 3.5 Summary of all *TP53* mutations.

The table summarises all mutations identified in all SCC samples. The number of mutations reported was provided by the IARC p53 mutation database (Petitjean et al. 2007).

3.3 Discussion

3.3.1 *TP53* isoforms are expressed in SCC

The expression of *TP53* isoforms at the mRNA level was investigated to determine the pattern of expression in RDEB SCC and non-RDEB SCC compared to NHK (Table 3.4). No previous publications have reported expression of the *TP53* isoforms in cutaneous SCC, although full length *TP53* has been investigated in; pre-cancerous lesions AKs and Bowen's disease, cutaneous SCC and in two reports in RDEB SCC (Brash et al. 1991; Slater et al. 1992; Campbell et al. 1993; Arbiser et al. 2004). *TP53* isoform expression has been investigated in head and neck SCC in which they concluded that all *TP53* variants except the Δp53 were expressed in some tumour samples and in normal epithelium (Boldrup et al. 2007), this is concordant with no expression of Δp53 in NHK, suggesting that in 6 of the 8 SCC samples transcription of Δp53 is activated.

3.3.2 Internal hotspot mutations present in RDEB SCC

A single point mutation was identified in each of the RDEB SCC keratinocyte samples. Codon 173 was mutated in RDEB SCC1 (Figure 3.4A) this mutation occurs within the DNA-binding domain, and more specifically within the L2 domain which is responsible for the correct folding and stabilisation of the central part of the protein (Cho et al. 1994).

Interestingly, the mutation of codon 273 discovered in RDEB SCC2 (Figure 3.4B), has been reported to be a "hotspot" mutation often seen in internal malignancies (Khromova et al. 2009). Internal hotspots are generally situated where there is cytosine methylation which blocks the formation of (6-4) photo products and are therefore generally not associated

with UV (Ziegler et al. 1993). Hotspot mutations are classified as amino acid residues involved in either making direct contact with DNA or in supporting the structural binding surface of the DNA. According to the IARC p53 database, this mutation has been reported on 636 occasions and in several cancers (Petitjean et al. 2007), reports identified in the database suggest mutation R273H possesses oncogenic gain of function in which mutant p53 is able to transactivate reporter genes suppressed by wt-p53. This particular mutation changes the amino acid from an arginine to histidine has been reported to increase angiogenesis of colon cancer xenografts harbouring this hotspot mutation identified by having a higher number of blood vessels which is correlated with accelerated tumour growth (Khromova et al. 2009). Given that this *TP53* mutant is classed as a "contact" residue it is possible to expect that this mutant retains the overall structure of the DNA binding domain but directly interferes with p53's ability to bind to DNA and thus transactivate target genes (Joerger and Fersht 2007; Olivier et al. 2010).

Intriguingly, the mutation of codon 152 identified in RDEB SCC 3 is a classic example of a UV-signature mutation (Figure 3.4C). This is an interesting mutation, as RDEB patient's skin is bandaged for prolonged periods of time due to chronic blistering. This would suggest that they are not exposed to high levels of UV light and therefore you would not expect to see UV induced mutations in these samples. However, it is most likely that this mutation was caused through other means than by UV-exposure, but as this mutation involves the substitution of two nucleotides it would be interesting to see if photoproducts were generated at this location within the DNA of these cells. This can be done by measuring the cyclobutane pyrimidine dimers and pyrimidine-pyrimidone (6-4) photoproducts in the DNA to establish if indeed photoproducts were generated and demonstrating if this was a UV induced mutation (Douki and Cadet 2001; Kim et al. 2010).

3.3.3 Heterozygous mutations present in SCC with retained heterozygosity at 17p

Unlike the RDEB SCC samples which contained only homozygous mutations, two of the non-RDEB SCC keratinocytes samples contained heterozygous mutations. In SCC5 3 heterozygous mutations were present; all three mutations are UV signatures as they are C-T substitutions at dipyrimidine locations in the DNA sequence (Figure 3.5E). The mutation at codon 179 occurs within the DNA-binding domain at zinc binding residue, in yeast based functional assays its transactivation activity is reported as partially functional (Kato et al. 2003). Mutant codon 247 is a silent mutation, in which the single base pair substitution which still codes for the same amino acid as the original codon and therefore results in wild-type protein being translated rather than a mutant protein, this is also known as a synonymous mutation.

The final mutation in SCC 5 is another example of a contact "hotspot" mutation, in which the residue is required for direct interaction of the DNA. This mutation is a hotspot of both internal and UV associated malignancies (Ziegler et al. 1993). The IARC database documents that this mutation has been observed 597 times and allows reporter genes repressed by wt-p53, whilst inhibiting the actions of p63 and p73 (Petitjean et al. 2007; Goh et al. 2010). There are two mouse models available for this mutant; one constructed in BALB/c genetic background transgenic mice with mutant p53 G245W the mice equivalent to human mutant p53 R248W, which fused with a haemagglutinin (HA)-tag to allow it to be distinguished from wt-p53 (Krepulat et al. 2005) and a more recent model by Song and colleagues (2007) in which they introduced the R248W allele into humanized p53 knock in (HUPKI). The HUPKI model showed abolished tumour suppressor activity and evidence to indicate these p53 mutants have acquired GOF by the interaction with the nuclease Mrell

and suppression of binding which leads to impaired activation of *Ataxia-telangiectasia mutated* (ATM) (Song et al. 2007).

Interestingly, the identification of only heterozygous mutations in this samples correlates with SNP mapping data showing no alterations and retained heterozygosity at 17p. SCC1 also contained a heterozygous mutation which also showed no alteration on chromosome 17 (Figure 3.5A).

3.3.4 A single nucleotide deletion in p53β of cutaneous SCC

One of the ten mutations identified in this study was a deletion of a single T nucleotide in SCC 4 a non-RDEB SCC sample, in the p53β isoform (Figure 3.5D). A single deletion (or insertion) of any nucleotide ultimately results in a frameshift of the remaining nucleotide sequence after the mutation. Under normal conditions, the majority of non-sense transcripts, such as those which result from an insertion or deletion of a nucleotide are recognised and degraded by the cell in a process known as non-sense mediated decay (NMD) (Frischmeyer and Dietz 1999). Our results indicate that at the mRNA level only the p53β and Δp53β isoforms were detectable and furthermore, Dr Carol Hogan was only able to demonstrate expression of the p53β variant at the protein level via immunoblotting (Appendix 1.1). This conforms to the hypothesis that the full length p53, p53γ and the corresponding Δp53 isoforms undergo NMD as a result of the deletion of the T nucleotide in codon 91 which is predicted to be detected by the cell during proof-reading of the mRNA transcript and identified as a non-sense transcript.

3.3.5 Further Work

Our results imply that the p53 isoforms are expressed in NHK and in cutaneous SCC. In accordance with other reports that suggest approximately 75% of p53 mutations are classified as missense, our study demonstrated that 100% of RDEB SCC samples contained missense mutations whereas only 85% of the non-RDEB SCC harboured mutations. The higher percentages of missense mutations in our study are likely to be due to the small sample size, and a more representative percentage could be acquired by investigating the mutations of a greater number of samples. Arbiser et al., (2007) identified only 3 of 8 RDEB SCC by single-strand conformation polymorphism (SSCP) analysis using an electrophoresis unit in which a mutation was identified by a shifted band pattern, samples indicating mutation were then further analysed by direct sequencing of the PCR products.

The only other study that has investigated p53 in RDEB SCC is that by Slater and colleagues (1992), in which, they used anti-serum to p53 protein to detect for up-regulation of the protein in 26 SCC samples from 6 patients. Only 26% of these labelled positively for mutant p53 protein, they speculated that the low percentage of mutant p53 identified was due to most tumours in the cohort being well differentiated and showed no p53 staining. Our study has shown that even samples which show normal p53 protein expression harbour mutations in the mRNA which supports Kusters-Vandevelde's report that positive staining of p53 is not synonymous with p53 mutations (Kusters-Vandevelde et al. 2010). Although, over-expression of the protein is indicative of mutation as missense mutations lead to the synthesis of a more stable mutant protein than the wild type-protein resulting in the higher levels detectable by the antibody.

As a therapeutic target of RDEB SCC, *TP53* does not represent a unique pathway, although the mutations identified in *TP53* of these samples were different to those in non-RDEB SCC, no common mutations were identified. Having a common mutation within a sample set would allow an anticancer strategy to be developed, whereby p53 pathway is reactivated by targeting that specific mutation in a gene therapy approach. However, it would be interesting to investigate these mutants further to elucidate the structural and functional consequences of each mutant. To do this nuclear magnetic resonance (NMR) spectroscopy and x-ray crystallography could be utilised to examine the structure, followed by yeast based functional assays to predict the impact of the mutant on the protein function.

All samples in this study harbour mutant *TP53*; therefore this suggests that SCC tumours in general could be selectively targeted based on this finding. Given that p53 is mutated in over 40% of all cancers, it has been a popular target for therapeutic research. Many strategies are being employed to treat cancers with aberrations of the p53 pathway (Lane et al. 2010). Research currently ongoing in this area includes work on p53 vaccines (Roth et al. 1996; Nemunaitis et al. 2009). Based on the high expression and frequent mutations of p53 in tumour cells the immune system could recognise it as an antigen, this has led to research into immunising patients with large peptides derived from p53 (Cheok et al. 2011). This is so far the only approved p53 therapy, with a vaccine known as Gendicine being permitted for use in China. Other interesting therapeutic approaches include; using small molecules to inhibit MDM2 and p53 interactions. A group of cis-imidazoline analog small molecules known as Nutlins are proving to be useful by inhibiting MDM2 and thus inducing p53 (Vassilev et al. 2004). Specifically Nutlin-3, which competes to bind to MDM2 causing displacement of p53 and resulting in the induction of apoptosis in malignant cells (Kojima et al. 2005; Secchiero et al. 2008). However, this treatment strategy is mainly effective in

tumours that do not harbour *TP53* mutations such a haematological malignancies (Cheok et al. 2011).

Having identified that all SCC samples harbour mutations in *TP53,* the generation of p53 therapies that target mutant p53 and restore its activity are of particular interest (Brown et al. 2011). This is potentially effective in tumours with inactive mutant p53, particularly those with mutations within the core DNA binding domain which accounts for 87.5% of the samples studied in this investigation, these mutations are known to cause the thermal destabilisation of p53 (Brown et al. 2011). Peptides that stabilise mutant p53 can restore the biological conformation and potentially restore wt-p53 alleles, an example of this is p53C a peptide derived from the c-terminal domain that has a stimulatory effect on p53 DNA binding activity. *In vitro* this peptide has restored activity of some p53 DNA contact mutants and several destabilised mutants (Hupp et al. 1995). As a therapy for SCC in general further experiments could be done to establish the effect of mutant p53 on the tumours, to provide further evidence to support the use of p53 targeted therapies. Such models could initially include p53 knock-down in SCC cell cultures to evaluate the effect on tumour cell viability, this could be further supported by knock-out mouse models. Another experiment to knock in specific p53 mutants could be used to establish the effect of certain mutants, with particular interest in the expression of p53γ and the possibility of a gain of function.

SCC in RDEB patients arise in areas of severe inflammation (Mallipeddi 2002; Arbiser 2007), and studies have shown p53 to be mutated in other cancer-prone chronic inflammatory diseases. An example of which is Barrett's oesophagus whereby the normal squamous

epithelium of the windpipe transforms into intestinal columnar epithelium due to repeated attack from acid reflux from the stomach (Kong et al. 2010), and has been shown to be contain mutated p53 (Keswani et al. 2006; von Holzen et al.). Together, with evidence of p53 mutations in premalignant conditions of the skin, as mentioned earlier, and owing to recent research revealing the accumulation of multiple non-synonymous p53 mutations in normal epithelial skin cells (Stahl et al. 2011) it would be of interest to investigate p53 in status in unaffected and affected (scarred) RDEB skin. Another reason for doing this, along with investigating p53 expression in SCC tissue is that it is known that in culture p53 can be activated, and therefore the expression we see and subsequent mutation specific is an artefact of culturing the cells. Therefore it would be crucial to evaluate whether p53 expression is seen as a result of culturing.

To conclude this study, *TP53* and its isoforms are expressed in RDEB SCC and non-RDEB SCC. Furthermore, each sample contains at least one mutation, each sample hosts a unique mutation and no common alterations were identified. The mutation spectrum of RDEB SCC was different to non-RDEB SCC. Although *TP53* does not have a unique mutation status in RDEB SCC, and therefore does not offer a specific target for RDEB associated SCC, it does in fact offer an abrogated pathway which could be targeted for SCC therapy in general.

Chapter 4

Markers of RDEB SCC keratinocytes identified by global gene expression analysis

4.1 Background

As already mentioned in Chapter 1, cancer originates from an accumulation of several genetic mutations (Hanahan and Weinberg 2000). In studying the genetic alterations that occur in cancer cells it allows researchers to develop an understanding of the originating genetic changes that cause cancer growth, and to identify those changes that allow the metastatic spread of the disease. Identifying expression changes of various genes can also identify pathways that are aberrantly regulated in cancer cells, which can then be used to directly target the cancer cells with therapeutics. An example of a therapy developed to target genetic mutations is the discovery of the BCR-ABL fusion gene caused by a reciprocal translocation of two chromosomes and is responsible for the development of chronic myeloid leukaemia (CML) (Pane et al. 2002). This mutant protein displays constitutive tyrosine kinase activity which is crucial for the transformation of haematopoietic cells and has led to the development of tyrosine kinase inhibitors used for CML treatment (Daley et al. 1990; Lugo et al. 1990; Druker et al. 2001). One such inhibitor is Imatinib, which targets the oncogenic protein BRC-ABL and is routinely used for the treatment of CML, with studies showing 90% of low and 83% of high risk patients having 5 year progression free survival after this treatment (Hasford et al. 2011).

Frequently in cancer cells, alterations occur in the expression of genes through the amplification and deletions of genomic DNA; resulting in over-expression and reduced expression of genes that may drive tumour development (Akkiprik et al. 2009; Medina et al. 2009). Global gene expression arrays can be used to investigate the RNA expression levels of thousands of genes (Schena et al. 1995; Shalon et al. 1996). Over 15 years ago, DNA microarrays were developed which now provide a powerful tool capable of simultaneously analysing the expression of thousands of genes (Maskos and Southern 1992). Microarrays

have become a mainstream technique for the study of gene expression in many disease states, not only cancer (Meltzer 2001; Mohr et al. 2002).

4.1.1 Concept of Microarray Experiments

The main principle of a microarray relies on the hybridization of two complementary DNA strands. If there is a high degree of similarity between the two sequences, it allows strong non-covalent bonds to form between complementary base pairs. The target samples are fluorescently labelled and these directly bind to the probe sequences which are attached to a substrate generally made from glass or silicon. After binding, the substrates are washed to remove any non-specific binding. The hybridized sequences generate a fluorescent signal which can vary in intensity depending on the amount of target sample binding to the probe. Some arrays utilize two fluorophores, to create a two colour hybridisation which are detected by a fluorescent scanner allowing amplifications and reductions in gene expression to be synchronously measured (Shalon et al. 1996). The raw values are given as a relative quantization intensity which has been compared to the intensity of the same feature under different conditions.

4.1.1.1 Microarray Studies

Many microarray studies have focused on detection of biomarkers capable of distinguishing disease stages (Bomprezzi et al. 2003), prognosis (Subramanian and Simon 2010; Cho et al. 2011) and response to therapeutics (Maxwell et al. 2003; Chiaretti et al. 2004). Also, countless studies have centred on the genetic alterations between disease and normal samples to identify genes and genetic pathways that are altered in cancer and could be used as targets for new therapies (Huang 1999). The importance of this is just starting to become recognised, as a greater spotlight is focused on; individualised molecular

medicines, the capability of predicting an individual's drug response, and targeting specific proteins and pathways within an individual's tumour. Microarray studies provide a solid foundation for these studies.

In parallel to microarrays the emergence of next generation sequencing provides the only alternative platform to offer "global" identification of genetic changes (Schuster 2008; Reis-Filho 2009). This new technology offers simultaneous data collection on a cell's genome; and provides identification of somatic mutations, accurate copy number analysis and information on any balanced or unbalanced chromosome rearrangements (Shah et al. 2009; Stratton et al. 2009).

4.1.1.2 Microarray Studies in SCC

Many studies of SCC have utilised microarray technology (Daley et al. 1990; Dooley et al. 2003; Hudson et al. 2011; Watt et al. 2011). Microarrays used for the investigation of cutaneous SCC have identified increased expression of epidermal differentiation complex genes on chromosome 1q21, a hallmark of SCC (Hudson et al. 2011), and the use of both *in vivo* and *in vitro* conditions has demonstrated biomarkers of SCC common to both experimental conditions (Dooley et al. 2003). Watt and colleagues (2011) used expression array analysis in an integrated approach to elucidate therapeutic targets of cutaneous SCC. The study used a microarray to identify markers of SCC *in vitro* and *in vivo* which were followed up by siRNA screening resulting in the identification of 2 genetic targets both of which have inhibitors that can reduced tumour volume in mice xenografts (Watt et al. 2011). This study demonstrated the robust use of gene expression analyses in the identification of biomarkers of disease and target identification.

4.1.2 Cancer therapy for RDEB SCC is limited

As detailed in Chapter 1, cutaneous SCC is the leading cause of death in RDEB patients (Arbiser et al. 2004). RDEB patients often die from the disease, unlike in the general population where SCC treatments for example Moh's surgery provide a positive outcome and have a good cure rate in those who develop UV-induced SCC, including high risk tumours (Kwa et al. 1992; Fleming et al. 1995; Leibovitch et al. 2005).

4.1.3 Microarray data comparing SCC to RDEB SCC

Global gene expression array data from our laboratory, produced prior to the start of this investigation, made comparisons of RDEB SCC keratinocytes to non-RDEB SCC keratinocytes. The array contained approximately 50,000 probes that are complementary to 40,000 genes. Four groups of samples were hybridized to the array. The samples originated from early passage primary cultured keratinocytes and the groups composed of; 4 independent NHK, 3 EBK, 4 RDEB SCC and 5 non-RDEB SCC keratinocyte samples.

For this investigation the array data was used to compare the gene expression profiles of RDEB SCC and non-RDEB SCC keratinocytes to identify differentially regulated genes between the two samples sets. This comparison tested the following hypothesis that based on the clinical presentation and localisation of the SCC tumours that arise in RDEB patients, and their aggressive nature, these tumours are significantly genetically different to the SCC tumours that arise in the general population.

Initial findings, based on clustering analysis of the samples suggested that RDEB SCC and non-RDEB SCC cannot be distinguished base on the transcriptional profiles in culture, as seen in Figure 4.1, which demonstrates that the 4 different sample sets do not cluster separately which would have indicated that each group of samples could be distinguished based on their gene expression profiling. The closer two samples cluster the more similarities they share.

4.1.3.1 Analysis of DNA microarray

The microarray data was initially analysed using Illumina's BeadStudio Data Analysis Software to generate normalized signal intensities for each of the probes on the array. These signal intensities were then analysed by performing the student's T-Test using Excel (Microsoft). The array identified a total of 36 genes to be differentially regulated between RDEB SCC and non-RDEB SCC keratinocytes. This is not a significant number of transcripts and only represents approximately 0.007% of the total number of transcripts tested on the array. When comparing all SCC (grouped RDEB SCC and non RDEB SCC) samples in this experiment against to normal samples (NHK and RDEBK) identified a 365 gene signature for SCC which has been validated and is able to distinguish SCC samples from non-SCC samples in culture, thus validating the reliability of the array results (Watt et al. 2011). The small number of genes identified as being differentially regulated between RDEB SCC and non-RDEB SCC also conforms to clustering analysis of the array data shown in Figure 4.0, taken from study by Watt and colleague's (2011) study which confirms that RDEB SCC and non-RDEB SCC are not genetically different. However, the genes that have been identified as being differentially regulated in RDEB SCC keratinocytes may prove to be useful targets for new therapeutics that specifically aimed at tumour cells that arise in RDEB patients and form that basis of this chapter.

The 36 genes were derived from the array used strict filtering criteria. Initial interrogation of the data to expose the differentially regulated transcripts in RDEB SCC in comparison to non-RDEB SCC; derived 18 transcripts (Table 4.0) that were identified due to alterations in fold change, expression level and *p* value using the following 3 categories:

1: *p* value < 0.001, fold change >2.5

2: *p* value <0.001, fold change >1.5, expression >100

3: *p* value 0.001 – 0.005, fold change >2.5, expression >50

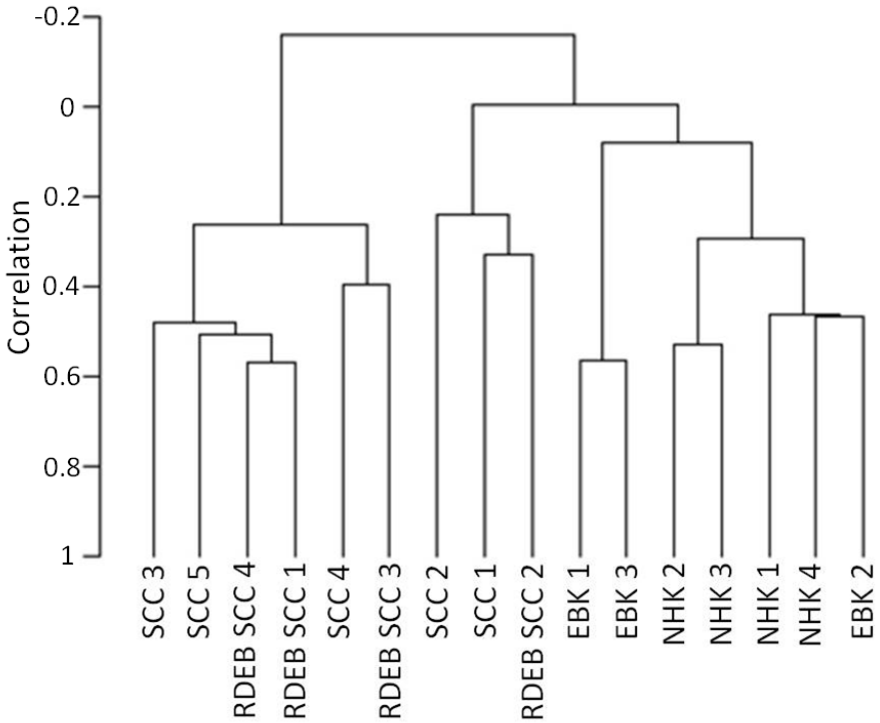

Figure 4.0 Dendrogram showing clustering of RDEB SCC and non-RDEB SCC indicative of genetic similarties. Normalised array signal intensities were subjected to unsupervised clustering using (BRB-ArrayTools v3.8.1). The closer two samples are to one another on the dendrogen demonstrates more similarities between samples. This provides evidence that samples clearly separate based on tumour status. However RDEB SCC cannot be segregated from non-RDEB SCC based on their gene expression profiles. Adapted from ((Watt et al. 2011).

GI Number	Gene Name	Functional Name	Chromosome Location	Fold Change RDEB SCC vs Non-RDEB SCC	*p* value RDEB SCC vs Non-RDEB SCC
GI_4557228-S	*AAMP*	Angio-associated migratory cell protein	2q35	**1.80**	0.000877
GI_34577058-S	*ADFP*	Adipose differentiation-related protein	9p22.1	**0.08**	0.004119
GI_28559062-A	*DNMT3B*	DNA (cytosine-5-)-methyltransferase 3 beta	20q11.2	**2.81**	0.000244
GI_32261290-S	*DUSP23*	Dual specificity phosphatase 23	1q23.2	**0.14**	0.001571
GI_30148196-S	*FAM41C*	Family with sequence similarity 41, member C	7p15-14	**0.21**	0.000148
GI_24497516-S	*HOXA5*	Homeobox A5	1p36.33	**0.37**	0.003794
GI_19923799-S	*HSPC244*	HSPC244	11q13.1	**0.27**	0.004538
GI_4504918-S	*KRT8*	Keratin 8	5q35	**4.45**	0.004491
GI_16915933-A	*MGAT4B*	Mannosyl (alpha-1-3)-glycoprotein beta-1,4-N-acetylglucosamine transferase, isozyme B	12q13	**0.47**	0.000320
GI_10947033-S	*MXD4*	MAX dimerisation protein 4	4p16.3	**0.26**	0.002232
GI_45007006-S	*OAS3*	2-5-oligodenylate synthetase 3, 100kDa	12q24.2	**4.34**	0.002258
GI_27436888-I	*POFUT1*	Protein O-fucosyltransferase 1	20q11	**2.48**	0.000491
GI_34147649-S	*SLC25A11*	Solute carrier family 25 member 11	12p12	**1.60**	0.000106
GI_9790232-S	*SLCO1B3*	Solute carrier organic anion family, member 1B3	17p13.3	**9.06**	0.000115
GI_29540556-A	*SNRPN*	Small nuclear ribonucleoprotein polypeptide N	15q11.2	**0.15**	0.001527
GI_1302654-A	*SNURF*	SNRPN upstream reading frame	15q12	**0.12**	0.001920
GI_18079315-S	*TJAP1*	Tight junction associated protein 1	6p21.1	**0.61**	0.000997
GI_37545980-S	*TTC7B*	Tetratricopeptide repeat domain 7B	14q32.11	**2.74**	0.001625

Table 4.0 Microarray analyses based on three sets of criteria, identified 18 genes that are differentially regulated in RDEB SCC compared to non-RDEB SCC keratinocytes.

3 sets of criteria taking into account p value and fold change were used as an indicator of statistically significance in regard to differentially regulated genes between the two sample sets. Fold changes highlighted in red are up regulated in RDEB SCC whilst those in green are down regulated.

18 transcripts is not a significant number of transcripts, and therefore suggests that the SCC that present in RDEB patients are not significantly genetically different to those that present in the general population. Further interrogation of the data was performed to prevent any differences between the two sample sets being overlooked. The three additional sets of filtering criteria used to identify differentially regulated transcripts in RDEB SCC, are listed below:

1: Further interrogation of microarray data using a modification of the Mann-Whitney U test, identified transcripts with wide variation but the expression value for the close sample from the Non-RDEB SCC sample group to the RDEB SCC sample group was higher than 50, which is the level of intermediate expression on the Illumina array, and at least 50% of the value (Table 4.1). This was able to identify genes which showed a wide variation in expression levels in the samples which would be missed using the t-test which assumes a normal distribution.

2: Differentially expressed genes were identified based on differences between SCC versus normal between RDEB and non-RDEB samples. *P* values for all genes are within the original filtering criteria for category C, and have *p* values below 0.005 (Table 4.2). This derived 3 genes that were not significantly different when comparing RDEB SCC to non-RDEB SCC but clearly showed significant expressional differences between tumour and normal samples for each SCC group.

3: Non parametric ranking was used to identify genes with the highest level of dysregulation in RDEB SCC. Each sample on the array was assigned a number from 1-16 based on their level of dysregulation, 16 being highly dysregulated. Genes showing the highest level of dysregulation in all RDEB samples were identified as markers of RDEB SCC (Table 4.3).

Gene	Average Non-RDEB SCC	Average RDEB SCC	RDEB SCC Fold Change	*P* Value	SCC				RDEB SCC				Difference
					1	2	3	4	1	2	3	4	
FST	143	626	4.4	0.02	210	59	150	89	367	572	415	1149	157
IFITM1	141	893	6.3	0.005	11	99	17	280	698	426	1291	1156	129
Hs.448642	1076	600	0.5	0.004	946	874	1309	983	769	550	552	527	104
FTH1	600	792	1.32	0.008	1246	1268	1521	1232	610	913	1146	499	87
ITGB1	1440	950	0.6	0.016	1323	1266	1849	1239	801	1158	761	1081	81
VWA1	109	582	5.3	0.006	50	195	73	31	269	513	658	888	74
RPL26	1643	2430	1.5	0.009	1606	1753	1694	1989	2902	2494	2268	2055	66
C14ORF156	1884	2704	1.4	0.007	1983	1673	2258	1824	3215	2428	2320	2854	62
ERH	548	864	1.5	0.006	618	454	540	715	1031	775	779	870	60
C7ORF7	245	135	0.55	0.001	219	246	264	279	165	157	90	129	51

Table 4.1 Modified Mann-Whitney U test used to identify a further 10 markers of SCC

Further interrogation of microarray data using a modification of the Mann-Whitney U test, identified transcripts with wide variation but the expression value for the closest sample from the Non-RDEB SCC and RDEB SCC sample group was higher than 50, which was the level of intermediate expression on the Illumina array and at least 50% of the value.

Gene	Fold Change RDEB SCC vs Non-RDEB SCC	Fold Change All SCC vs NHK	Fold Change RDEB SCC vs EBK	*P* Value RDEB SCC vs Non-RDEB SCC	*P* Value All SCC vs NHK	*P* Value RDEB SCC vs EBK
G3BP2	1.64	2.94	0.46	0.00649	0.00288*	0.00072*
DNAJB14	1.92	1.49	0.28	0.00714	0.00386*	0.00387*
PPP1R3E	5.82	13.42	0.18	0.011717	0.00806	0.00009*

Table 4.2 Differentially expressed genes based on differences between SCC versus Normal comparing RDEB and Non-RDEB samples

p values for the different groups were significant based on Category C of the original filtering criteria, and had values below 0.005. Significance denoted by *

Gene	SCC 1	SCC 2	SCC 3	SCC 4	SCC 5	RDEB SCC 1	RDEB SCC 2	RDEB SCC 3	RDEB SCC 4
C1orf135	10	9	12	11	7	15	16	13	14
BCSIL	10	7	12	8	11	15	16	13	14
GSDMDC1	8	9	12	10	11	13	16	14	15
STOML2	10	8	12	5	11	16	14	15	13
LOC116412	9	12	8	5	11	15	13	14	16

Table 4.3 Genes identified by level of dysregulation for all SCC samples

Non parametric ranking was used to assign each sample with a number from 1-16 based on the level of dysregulation, 16 being the greatest level of dysregulation. Those genes with the highest levels of dysregulation for all for RDEB SCC samples were derived as markers of RDEB SCC.

4.1.4 Aim

As the array suggests that these genes are uniquely regulated in RDEB SCC, they could potentially hold the key to therapeutic pathways that are valuable targets in the treatment of SCC in RDEB patients, as these tumours are resistant to conventional cancer therapies, and elucidate the reasons why these tumours are more tolerable of conventional therapies. This small set of genes may also harbour dysregulated genes which encode proteins that provide a growth and survival advantage to neoplastic cells in RDEB patients, thus contributing to the aggressive and invasive nature of these tumours, the pathogenesis of which remains unknown.

The aim of this chapter is to identify genetic targets of cutaneous SCC that specifically arise in RDEB patients that could potentially be objectified for therapeutic intervention. The strategy for this investigation included; identifying common pathways among the 36 genes through gene ontology and pathway analysis. Following on from microarray analysis, the 36 genes identified as being significantly dysregulated in RDEB SCC were validated using replicate cultures of the RDEB SCC and non-RDEB SCC keratinocytes samples used for the original array experiment. Concordant expression of genes from on the microarray and qRT- PCR validation experiment were followed up and the expression levels of each examined *in vivo* and in RDEB SCC keratinocyte cultures re-expressing Type VII Collagen.

4.2 Methods and Results

4.2.1 Pathway analysis identifies *HNF4A* and *TGFβ1* to be enriched in RDEB SCC

The gene ontology (GO) of the 36 genes identified by the microarray was explored using the NCBI gene database (http://www.ncbi.nlm.nih.gov/gene) to look through the literature annotations and conserved protein domains to categorise the genes based on their biological functions. Literature on each gene was explored and function was curated into 1 of 16 functional processes. Of the 36 genes 44.4% were previously reported to be linked to cancer (16 of 36 genes), showing an enrichment for tumour related genes. The biological function grouping revealed the two largest functional groups to be; firstly unknown function with 30.6% of the genes being within this category and secondly 13.9% of the genes were involved in the regulation of transcription (Figure 4.1).

Ingenuity Pathway Analysis (IPA) software (Ingenuity, USA) was accessed in July 2008 and used to investigate the pathways predicted by the literature between the genes identified by the microarray. Additionally *COL7A1* although was not identified by the array as being dysregulated was added to the gene list to help identify pathways directly linked to RDEB. This software uses a database generated by published scientific reports to correlate and link proteins based on biological and chemical interactions. No one specific pathway was indentified from the 36 genes (Figure 4.2). However, 2 “hubs”; *HNF4A* and *TGFβ1* were identified as being enriched with interactions associated with the genes identified by the array. This suggests that these two pathways could be of importance in the development of cutaneous SCC in RDEB patients.

4.2.2 qRT-PCR Optimisation

Quantitative real time-PCR (qRT-PCR) was performed using 1 NHK sample, 3 independent RDEB SCC and 3 non-RDEB SCC keratinocyte samples, to validate the array results of the 36 genes identified as being differentially regulated in the microarray experiment. This allowed real changes in RDEB SCC gene expression to be identified by reproducing the same results in an independent mRNA expression study. Both the microarray and qRT-PCR experiments were performed using RNA harvested from primary SCC keratinocytes cultures 2 days post confluence. This model mimics *in vivo* cell-cell contact and interaction and reduces variation in expression levels caused by different rates of proliferation.

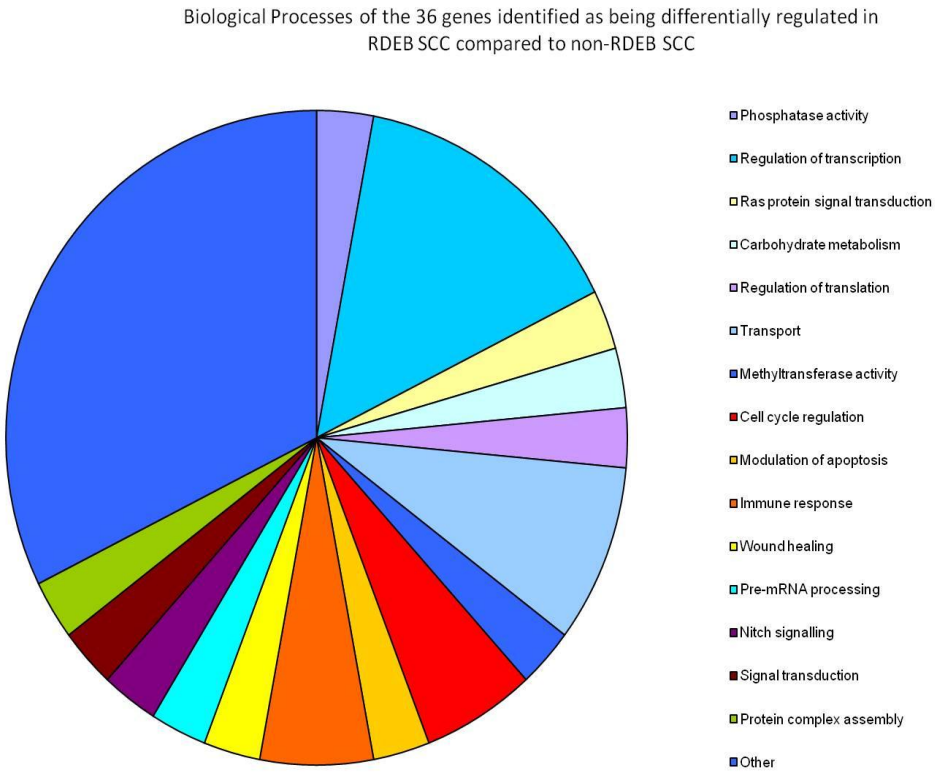

Figure 4.1 Regulation of transcription is an enriched biological process in RDEB SCC. Categorising genes based on their biological function and processes, identified genes involved in regulation of transcription to be enriched in this gene group and over 25% to have unknown function.

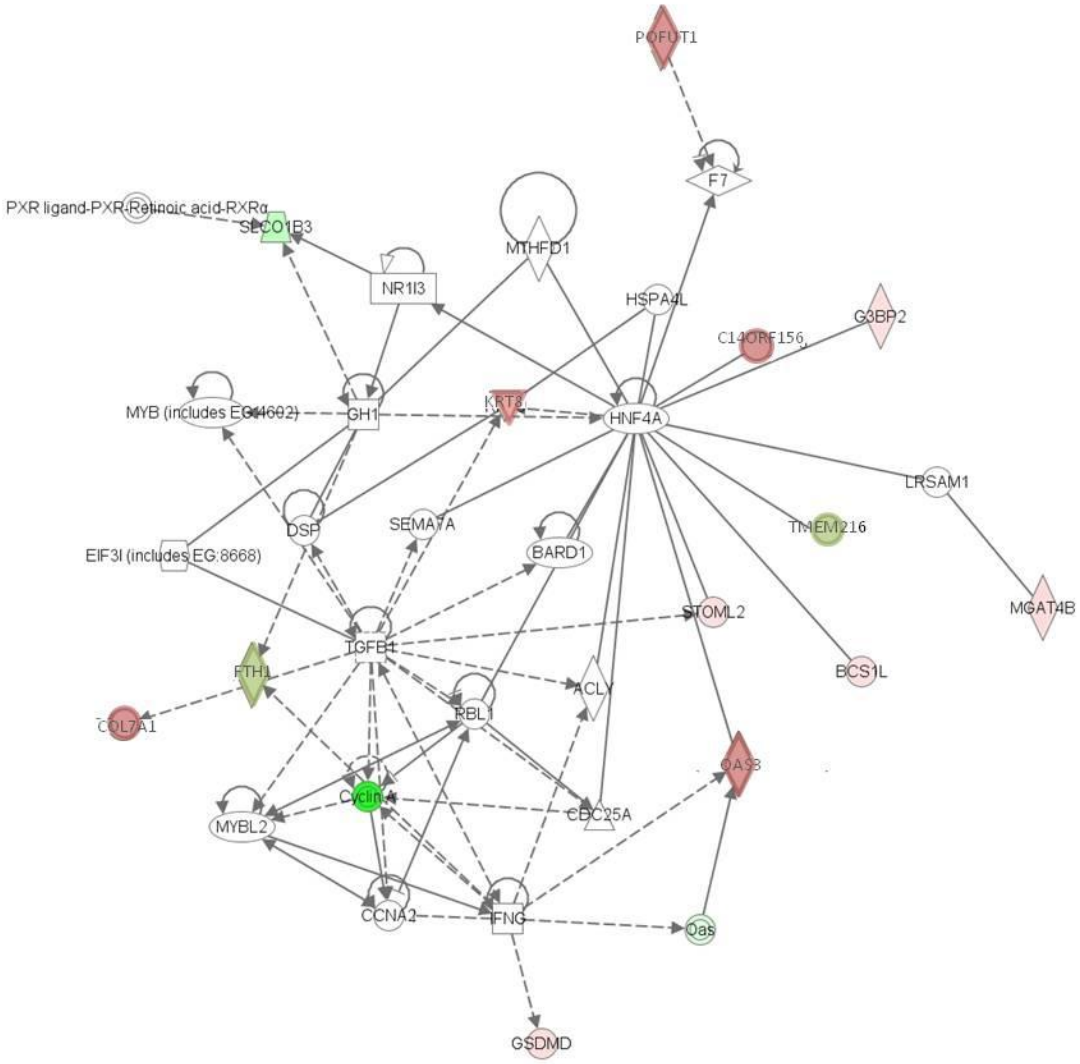

IPA - accessed July 2008

Figure 4.2 IPA identified HNF4A and TGFβ1 as "hubs" involving genes dysregulated in RDEB SCC compared to non-RDEB SCC. Two hubs were identified; *TGFβ1* and *HNF4A.* Each gene pathway is associated with several interactions. Genes in green are those which are up-regulated in RDEB SCC and those in red are down-regulated in RDEB SCC. The genes in white boxes are not identified as differentially regulated by the microarray analysis. The shape of each box represents a different functional class; solid lines indicate direct interactions whilst dotted lines are indicative of indirect interactions between proteins.

Primers were designed to amplify a 100-200bp amplicon for each of the 36 genes. Primer design specifications are detailed in Chapter 2, Section 2.2.2.4. Briefly, primers crossed an exon-exon boundary to prevent the amplification of genomic DNA and were located in the 3' region of the coding sequence of each gene so that they were in close proximity to the probes used on the Illumina microarray (Primer sequences are listed in Chapter 2, Table 2.9). Primers were tested first using RT-PCR to verify the correct product was amplified and to identify any non-specific products (Figure 4.3A). Before running samples using qRT-PCR a temperature gradient was performed to optimise primer annealing temperatures for generating products with the highest yield whilst having low background and amplification of non-specific products (Figure 4.3B).

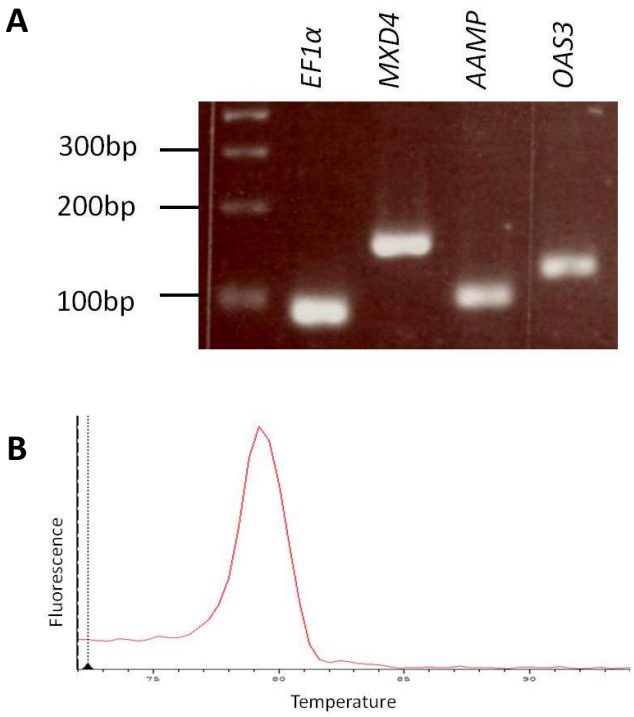

Figure 4.3 Primer optimisation. A) Shows an example of an agarose gel used to visualise RT-PCR products using NHK as a template to test primer pairs. Amplicons between 100-200bp were amplified for the 4 genes; *EF1α, MXD4, AAMP* and *OAS3*. B) Demonstrates an ideal melting curve at 60°C from the temperature optimisation gradient using *EF1α* primers for a qRT-PCR Run. The melting curve shows a single product was amplified.

Accurate PCR analysis requires an internal control, such as a gene which is constitutively expressed in all cells at similar levels. When designing the qRT-PCR validation experiment, using replicate samples as those used on the array, a reference gene was chosen by establishing the level of expression of a number of routinely used reference genes (Dheda et al. 2004; Radonic et al. 2004). The average expression levels of several reference genes including *GAPDH* and *β-Actin* were explored in NHK, EBK, non-RDEB SCC and RDEB SCC keratinocytes on the microarray to elucidate a suitable control for qRT-PCR experiments. The *EF1α* gene was chosen as the most appropriate reference gene for this experiment due to having the lowest standard deviation as expressed as a percentage of the expression level (Figure 4.4). Therefore the level of expression of this gene varies the least between this particular sample cohort.

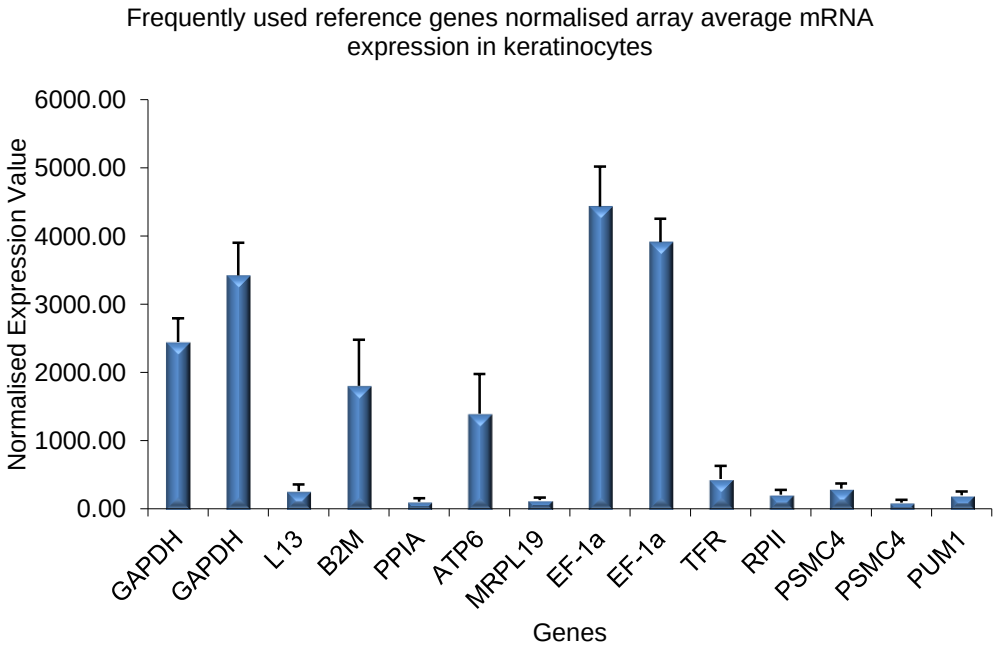

Figure 4.4 *EF1α* a suitable reference gene that shows the least change in expression

Graph showing normalised microarray expression ratios for commonly used qRT-PCR reference genes, each value is given as an average expression level for the whole sample set (n=16) and error bars represent the standard deviation of the samples expressed as a percentage. *EF1α* had the smallest variation in expression throughout all samples used on the microarray.

4.2.3 qRT-PCR confirms 14 genes to be differentially regulated between RDEB SCC and non-RDEB SCC keratinocytes in culture

Quantitative RT-PCR validation identified 14 genes that showed the same pattern of expression as seen in the microarray analysis (Table 4.4), however only 5 of those were significantly different in the microarray experiment and the qRT-PCR confirmation screen. The 5 biomarker genes; *SLCO1B3*, *DUSP23*, *TJAP1*, *SNRPN* and *SNURF* are significantly differentially regulated between RDEB SCC keratinocytes and non-RDEB SCC keratinocytes at the mRNA level.

4.2.4 Five genes are significantly dysregulated in RDEB SCC *in vitro*

Microarray analysis identified a 9 fold increase in expression of *SLCO1B3* in RDEB SCC keratinocytes. Subsequent qRT-PCR validated the up-regulation of this gene, showing an average 7.8 fold increase in mRNA expression in RDEB SCC keratinocytes in comparison to both non-RDEB SCC and NHK (*p* value 0.035) (Figure 4.5A).

DUSP23 mRNA expression was significantly reduced in RDEB SCC compared to non-RDEB SCC keratinocytes with a down regulation of expression by 0.39 fold in RDEB SCC (*p* value 0.004) (Figure 4.5B). However, the actual dysregulation of *DUSP23* is seen more so in non-RDEB SCC keratinocyte samples in comparison to NHK, whereas RDEB SCC and NHK show similar expression of *DUSP23*.

mRNA expression of *TJAP1* is altered in opposing ways in RDEB SCC compared to non-RDEB SCC keratinocytes in relation to the normal expression seen in NHK (Figure 4.5C).

Table 4.4 Continued

	NHK	RDEB SCC 1	RDEB SCC 2	RDEB SCC 3	SCC 1	SCC 2	SCC 5	RDEB SCC avg.	NHSCC avg.	Fold Change	*p value*
AAMP	0.0138	0.0185	0.0201	0.0195	0.0228	0.0266	0.0310	0.0193	0.0268	0.7226	0.037453
ADFP	0.0087	0.0030	0.0120	0.00329	0.0125	0.0135	0.0024	0.0061	0.0095	0.6418	0.500274
BCSIL	0.0298	0.0337	0.0408	0.0733	0.0615	0.0648	0.0840	0.1479	0.2103	0.7033	0.213549
C1orf135	1.2050	1.6600	1.1240	1.850	1.1980	1.1430	1.0940	1.5446	1.1450	1.3490	0.142651
C7orf27	0.0205	0.0357	0.0198	0.02362	0.0321	0.3326	0.3785	0.0263	0.2477	0.1065	0.111502
C14orf156	0.1188	0.1452	0.1924	0.2555	0.1369	0.2260	0.3774	0.1977	0.2467	0.8011	0.559243
CCNA1	0.0181	0.0145	0.0142	0.0212	0.0129	0.0138	0.0092	0.0166	0.0120	1.3877	0.159653
DNAJB14	0.0474	0.0329	0.0481	0.0350	0.0410	0.0363	0.0387	0.0387	0.0387	1.0001	0.999495
DNMT3B	0.0036	0.0089	0.0069	0.0083	0.0063	0.0089	0.0035	0.0080	0.0062	1.2857	0.339987
DUSP23	0.0608	0.0505	0.0876	0.0535	0.2125	0.1789	0.1049	0.0638	0.1655	0.38584	0.0401648*
ERH	0.0100	0.0158	0.0147	0.0135	0.0130	0.0170	0.0270	0.0147	0.0190	0.7743	0.363765
FST	0.0207	0.0089	0.0218	0.0456	0.0082	0.0584	0.1095	0.0254	0.0587	0.4337	0.345538
FTH1	0.4431	0.3332	0.2268	0.2729	0.2786	0.2467	0.1673	0.2776	0.2308	1.2026	0.359377
G3BP2	0.1561	0.0505	0.1419	0.1594	0.2034	0.1780	0.1133	0.1172	0.1649	0.7113	0.331318
HOXA5	0.0127	0.0056	0.0101	0.0057	0.0086	0.0078	0.0114	0.0071	0.0093	0.7695	0.311479
HSPC244	0.0120	0.0066	0.0088	0.0205	0.0136	0.0168	0.0109	0.0119	0.0138	0.8689	0.715753
IFITM1	0.0131	0.0053	0.0070	0.0579	0.0026	0.0056	0.0387	0.0234	0.0157	1.4929	0.728239
ITGB1	0.2874	0.0525	0.2017	0.0714	0.0972	0.1724	0.0842	0.1085	0.1179	0.9202	0.870941
KRT8	0.2144	0.1677	0.3891	0.3188	0.0811	0.1140	1.125	0.2918	0.4400	0.6633	0.692823
LOC116412	1.5410	1.5420	1.3230	1.4780	1.1510	1.0400	0.8530	1.4476	1.0146	1.4267	0.016289
MGAT4B	0.0103	0.0100	0.0106	0.0059	0.0113	0.0128	0.0131	0.0088	0.0124	0.7123	0.084350

MXD4	0.0960	0.0424	0.0378	0.0460	0.0689	0.0638	0.0434	0.0421	0.0587	0.7172	0.111288
OAS3	0.0108	0.0424	0.0651	0.1124	0.0803	0.0644	0.0350	0.0734	0.0599	1.2249	0.611863
POFUT1	0.0069	0.0044	0.0042	0.0053	0.0049	0.0110	0.0087	0.0046	0.0082	0.5660	0.118385
PPP1R3E	0.0157	0.0187	0.0128	0.0128	0.0237	0.0253	0.0119	0.0147	0.0203	0.7268	0.301884
RPL23	0.0321	0.0487	0.0594	0.0533	0.0369	0.0636	0.1108	0.0538	0.0704	0.7641	0.488735
SLC25A11	0.0305	0.0349	0.0276	0.0329	0.0379	0.0404	0.0832	0.0318	0.0538	0.5913	0.212705
SLCO1B3	0.00006	0.00154	0.00055	0.00109	0.00018	0.00020	0.00009	0.0011	0.00014	7.8272	0.034401*
SNRPN	0.0661	0.0051	0.0039	0.0094	0.0453	0.0317	0.0660	0.0061	0.0477	0.1281	0.014749*
SNURF	0.0181	0.0003	0.0002	0.0007	0.0079	0.0129	0.0149	0.0004	0.0119	0.0330	0.005323*
TJAP1	0.0029	0.0018	0.0021	0.0011	0.0068	0.0043	0.0036	0.0017	0.0049	0.3469	0.035004*
TTC7B	0.0280	0.0376	0.0698	0.1204	0.0570	0.0421	0.0668	0.2278	0.1659	1.3736	0.895792
VWA1	0.0106	0.0559	0.0372	0.0622	0.0243	0.0315	0.0624	0.0517	0.0393	1.3145	0.423633

Table 4.4 36 genes validated by qRT-PCR. Values are relative to *EF1α* and p value based on student's t-test comparing all RDEB SCC and all non-RDEB SCC samples. Genes highlighted by yellow, show the same trend of expression in qRT-PCR as in the microarray data, * denotes significant difference between mRNA expression in RDEB SCC and non-RDEB SCC keratinocytes.

In non-RDEB SCC the gene seems to be positively regulated and shows a slight although not significant increase in expression compared to NHK. Whilst in RDEB SCC, the *TJAP1* expression is negatively regulated and a significant reduction is seen when compared to non-RDEB SCC keratinocytes, with a 0.35 fold decrease in expression (*p* value 0.035). However, this reduction in mRNA expression is not significantly different between RDEB SCC and NHK.

SNRPN mRNA is consistently down regulated in all 3 RDEB SCC keratinocyte samples, compared to both NHK and non-RDEB SCC keratinocytes. There is an overall reduction in the non-RDEB SCC samples compared to NHK although not significantly. However, *SNRPN* mRNA expression is significantly reduced ($p = 0.015$) in RDEB SCC by a fold change of 0.128 in RDEB SCC compared to non-RDEB SCC keratinocytes (Figure 4.5d), confirming a down regulation of *SNRPN* in both the microarray and qRT-PCR.

The mRNA levels of *SNURF* are reduced in 2 of the 3 non-RDEB SCC keratinocyte samples compared to NHK. The level of expression is negligible in all 3 RDEB SCC samples with an average 0.033 fold reduction and a significance of *p* 0.005 (Figure 4.5e), this conforms to microarray analysis also showing a reduction in mRNA expression.

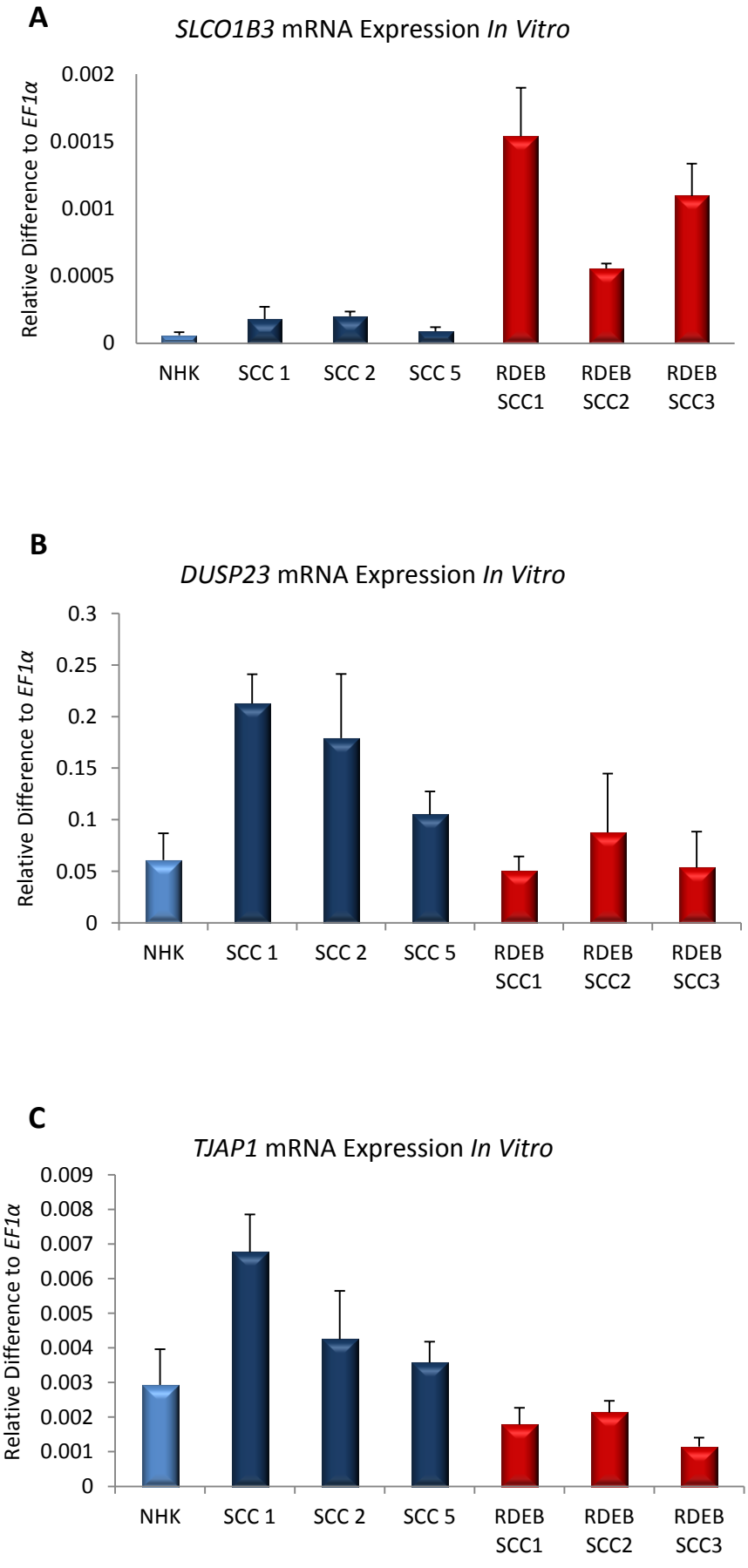
A
SLCO1B3 mRNA Expression In Vitro
Relative Difference to EF1α
0.002
0.0015
0.001
0.0005
0
NHK
SCC 1
SCC 2
SCC 5
RDEB SCC1
RDEB SCC2
RDEB SCC3
B
DUSP23 mRNA Expression In Vitro
Relative Difference to EF1α
0.3
0.25
0.2
0.15
0.1
0.05
0
NHK
SCC 1
SCC 2
SCC 5
RDEB SCC1
RDEB SCC2
RDEB SCC3
C
TJAP1 mRNA Expression In Vitro
Relative Difference to EF1α
0.009
0.008
0.007
0.006
0.005
0.004
0.003
0.002
0.001
0
NHK
SCC 1
SCC 2
SCC 5
RDEB SCC1
RDEB SCC2
RDEB SCC3

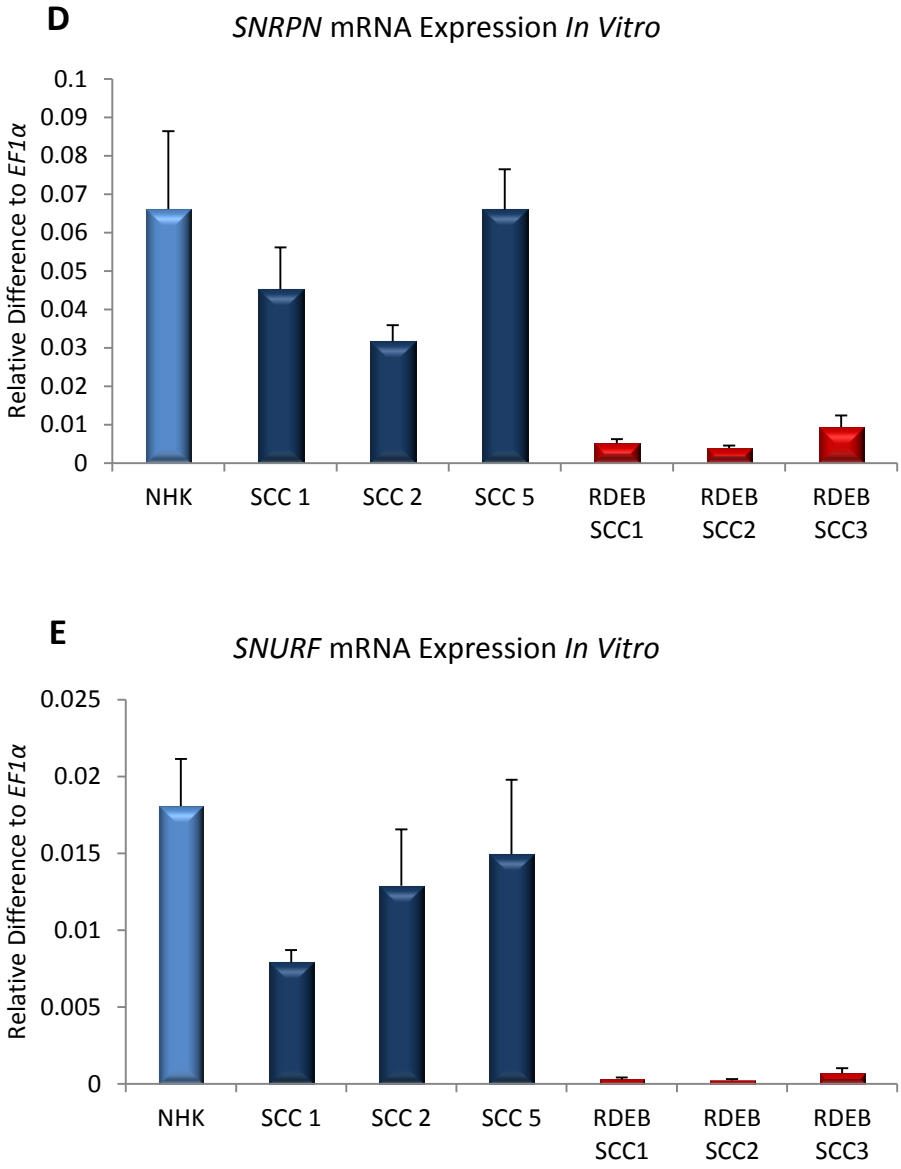

Figure 4.5 Five genes are significantly differentially expressed in RDEB SCC

qRT-PCR validation confirms 5 genes identified by microarray as being significantly differentially regulated in RDEB associated squamous cell carcinoma (RDEB SCC1-3) compared to non-RDEB SCC (SCC1,2 & 5) keratinocyte cultures. A) *SLCO1B3* is has consistently higher mRNA expression in RDEB SCC by an average of 7.8 fold increase. B) *DUSP23* has a significantly lower average mRNA expression in RDEB SCC as compared to non-RDEB SCC C) *TJAP1* expression is reduced in RDEB SCC compared to non-RDEB SCC D) *SNRPN* has significantly decreased mRNA expression in RDEB SCC E) *SNURF* also has a significantly decreased expression in RDEB SCC compared to non-RDEB SCC. Samples represent technical replicates (n=3).

4.2.5 RDEB SCC keratinocytes expressing *COL7A1* show altered expression of the 5 differentially regulated genes

Dysfunctional Type VII Collagen is the protein responsible for causing RDEB, and it has been long since suggested the lack of *COL7A1* expression is the reason why RDEB patients develop SCC. Therefore it's necessary to establish whether the dysregulation of the 5 significantly differentially expressed genes is dependent on presence of Type VII Collagen. This would identify a direct relationship between the primary disease and the tumour cells. This was tested using mRNA from RDEB SCC keratinocytes that had been retrovirally transduced to re-express Type VII Collagen (Appendices 1.3 Type VII Collagen protein expression after transduction). qRT-PCR results indicated that the mRNA expression of *SLCO1B3* is reduced to relatively normal levels comparable to NHK (Figure 4.6A). The expression of *DUSP23* is reduced in comparison to the pBabe puro empty vector control cells (PB) by an average of 2.71 fold. In all 3 cell lines the reduced expression is significant with *p* values of 0.005, 0.031, 0.007 in RDEB SCC1, 2 and 3, respectively (Figure 4.6B).

In *COL7A1* transduced RDEB SCC keratinocytes the *TJAP1* expression is reduced in 2 of the 3 RDEB SCC cell lines (Figure 4.6C). Both RDEB SCC 1 and 3, after retroviral transduction to over-express *COL7A1* show a significant decrease in mRNA expression of *TJAP1*, *p* value 0.01 and 0.02 respectively. However, in the case of RDEB SCC 3 the empty vector control has a much higher mRNA expression than NHK and somewhat different to what you would expect from the control, as the parental cell line showed a reduced expression in comparison to NHK. RDEB SCC 2 showed no significant difference between RDEB SCC keratinocytes that express *COL7A1* and those which do not, this could be as a result of continual evolution of tumour cells in culture or selection after transduction which favours clones that express more *TJAP1*.

COL7A1 re-expression in RDEB SCC keratinocytes reduces the expression of *SNRPN* mRNA further in comparison to empty vector controls (Figure 4.6D). However, only significantly so, in RDEB SCC 3, which was the sample showing the highest level of *SNRPN* in the parental cell line during the original qRT-PCR analysis. Re-expression of *COL7A1* in RDEB SCC keratinocytes, reduces the *SNURF* mRNA expression in all 3 cell lines, but only significantly in one sample (Figure 4.6E). RDEB SCC2 has a significantly decreased mRNA expression and shows a 0.11 fold change (p=0.016) when *COL7A1* in re-expressed. However, this value is against the empty vector control which showed unusually high expression of *SNURF*. Whereas it was expected to be expressed at a similar level in the control cells as the original parental cell line which demonstrated a much lower expression than NHK in the original *in vitro* qRT-PCR analysis. In this qRT-PCR, interestingly all 3 pBabe controls have similar levels of expression to the *SNURF* mRNA expression in RDEB SCC compared to NHK, suggesting that the empty vector alone maybe affecting the expression of this gene. Also, in all cases the presence of Type VII Collagen reduces the expression of all 5 genes. Paradoxically, given that if this was the mechanism that causes the dysregulation then the re-expression of *COL7A1* should switch back on the expression of these genes.

In terms of re-expressing *COL7A1* in RDEB SCC keratinocytes, it is important to consider if the changes seen in these 5 genes would be controlled by the *COL7A1* production in normal skin. In other words, another it is important to test the level expression in normal skin, normal skin keratinocytes in culture in comparison to the level of expression in the RDEB SCC keratinocytes after retroviral transduction of the cells.

A

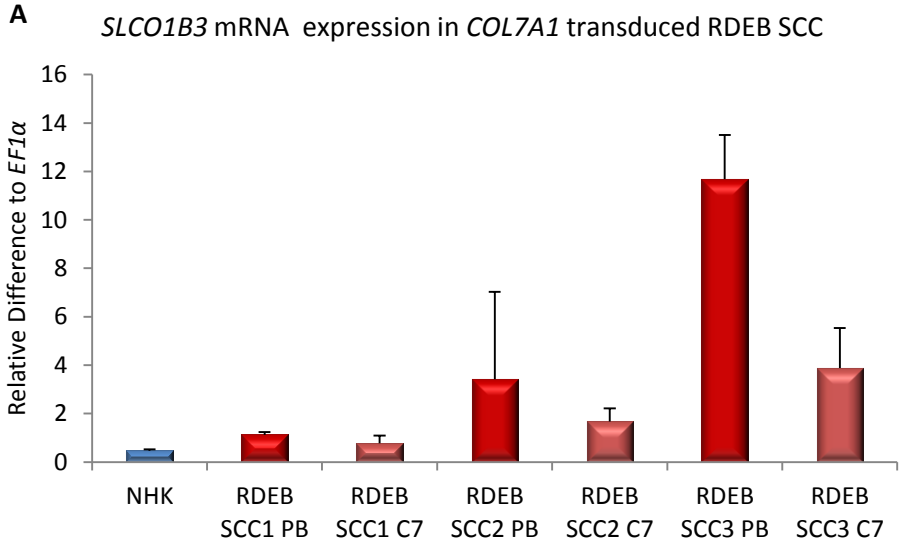
SLCO1B3 mRNA expression in COL7A1 transduced RDEB SCC
Relative Difference to EF1α
16
14
12
10
8
6
4
2
0
NHK
RDEB SCC1 PB
RDEB SCC1 C7
RDEB SCC2 PB
RDEB SCC2 C7
RDEB SCC3 PB
RDEB SCC3 C7

B

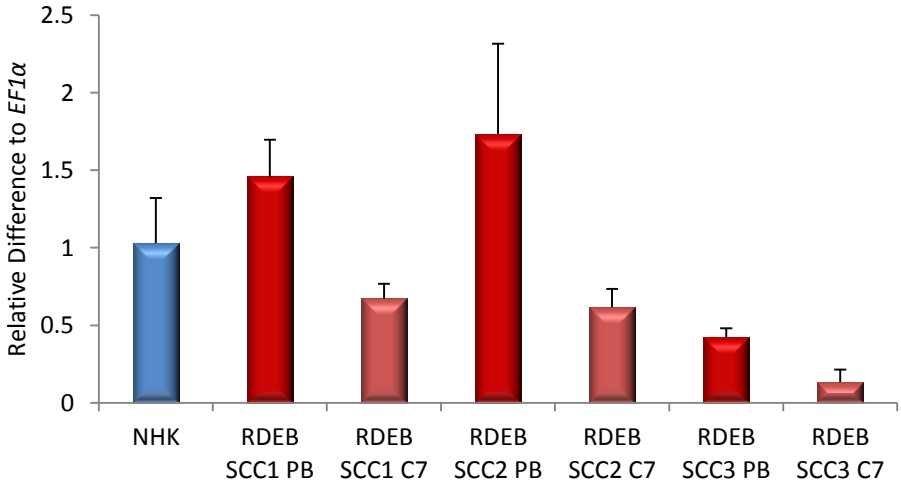
DUSP23 mRNA expression in COL7A1 transduced RDEB SCC
Relative Difference to EF1α
2.5
2
1.5
1
0.5
0
NHK
RDEB SCC1 PB
RDEB SCC1 C7
RDEB SCC2 PB
RDEB SCC2 C7
RDEB SCC3 PB
RDEB SCC3 C7

C

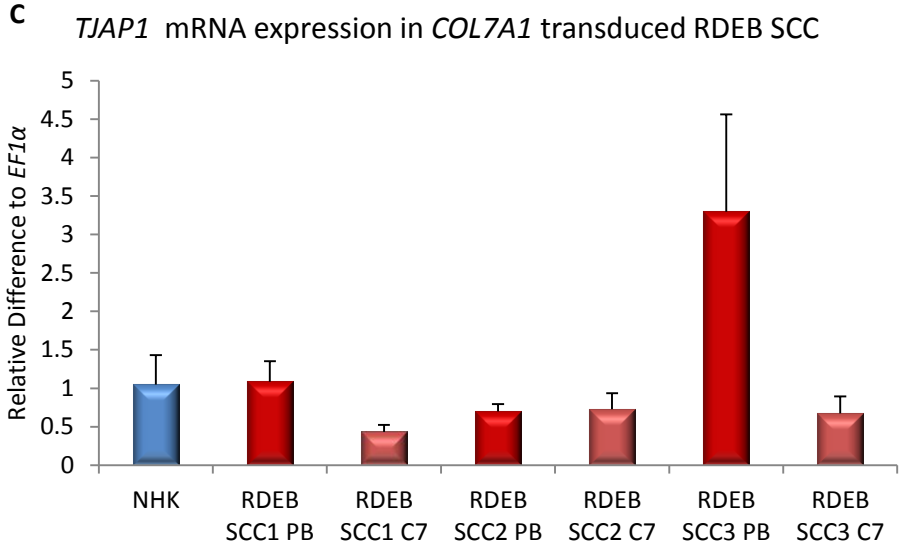
TJAP1 mRNA expression in COL7A1 transduced RDEB SCC
Relative Difference to EF1α
5
4.5
4
3.5
3
2.5
2
1.5
1
0.5
0
NHK
RDEB SCC1 PB
RDEB SCC1 C7
RDEB SCC2 PB
RDEB SCC2 C7
RDEB SCC3 PB
RDEB SCC3 C7

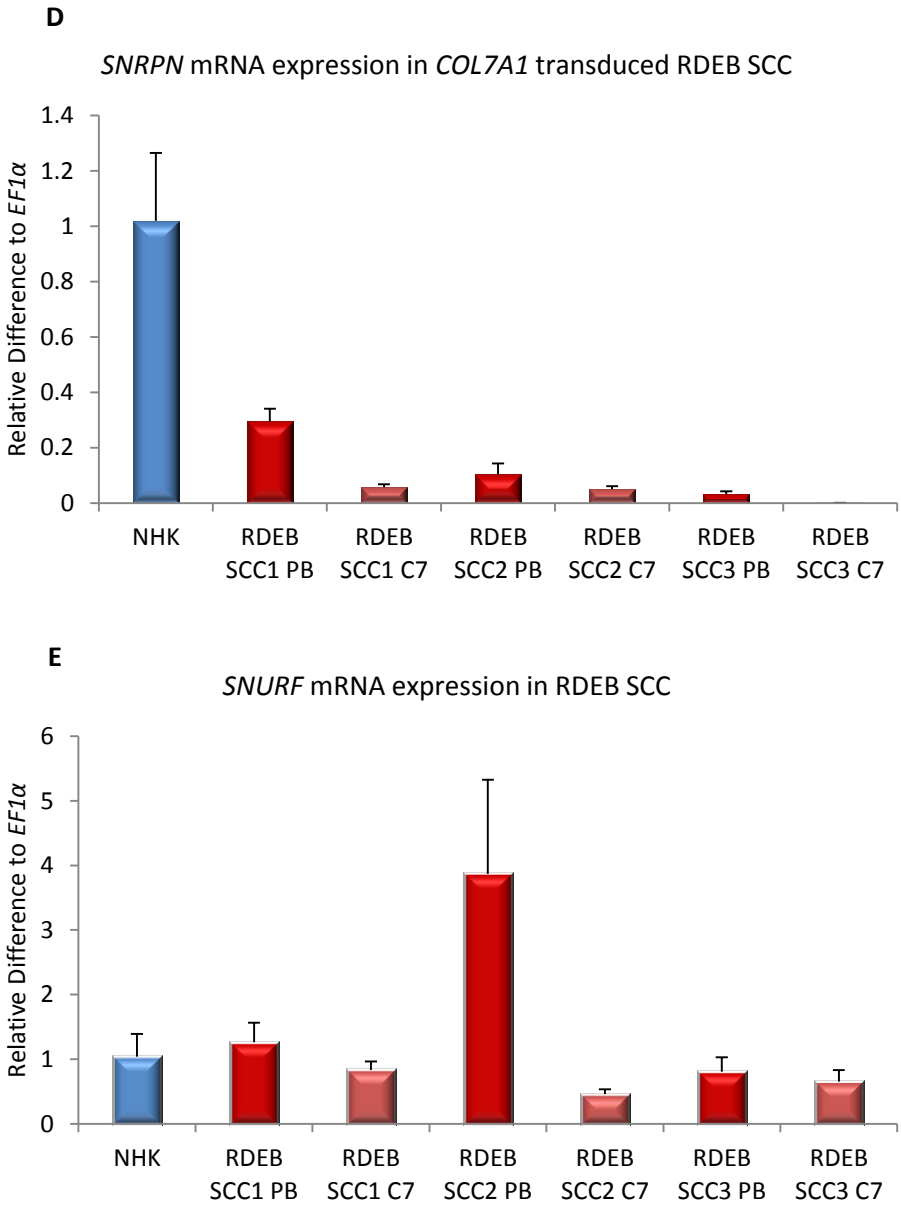

Figure 4.6 *SLCO1B3* mRNA expression is reduced when Type VII Collgan is re-expressed in RDEB SCC keratinocytes

RDEB SCC keratinocytes retrovirally transduced to express Type VII Collagen were then subjected to qRT-PCR and the mRNA expression of the 5 candidate genes tested. *SLCO1B3* mRNA expression is reduced back to a normal level of expression in RDEB SCC when Type VII Collagen is expressed (C7) in comparison to the empty vector control cultures (PB). All 5 genes tested A) *SLCO1B3*, B*) DUSP23*, C) *TJAP1*, D) *SNRPN*, E) *SNURF*, the mRNA expression is reduced in cells expressing Type VII Collagen. Samples represent technical replicates (n=3).

4.2.6 *In Vivo* mRNA expression status of the 5 *in vitro* biomarkers of RDEB SCC

To establish if the dysregulation of these 5 genes is an artefact of *in vitro* culturing of the RDEB SCC keratinocytes, RNA from normal human skin, non-RDEB SCC, RDEB skin and RDEB SCC were used to create cDNA and subjected to qRT-PCR to investigate mRNA expression levels of the *in vitro* biomarkers of RDEB SCC keratinocytes identified by the microarray and qRT-PCR analysis.

RNA was isolated from fresh frozen tissues by the NHS Tayside Tumour Bank (Dundee, UK) and assigned a RNA integrity number (RIN) based on RNA quality and quantity analysis. RIN numbers are an overall measure of RNA quality and is based on a scale of 1 to 10, the higher the number the greater the integrity of RNA. The RIN of each tissue sample used is detailed in Table 4.5, RDEB SCC samples 3, 6, 7, and 8 were eliminated from the qRT-PCR due to their poor quality RNA.

qRT-PCR using the tissue cDNA reveals *SLCO1B3* is over-expressed in 5 of 7 RDEB SCC tissues used, thus confirming the findings of the *in vitro* microarray and qRT-PCR screens. Interestingly, *in vivo* mRNA expression analysis reveals increased expression in 2 out of 3 non-RDEB SCC and RDEB skin samples (Figure 4.7A).

Tissue analysis established that the mRNA expression of *DUSP23* is higher in non-RDEB SCC *in vivo* as well as *in vitro* with all 3 non-RDEB SCC samples showing higher mRNA expression than NHK. Whilst 2 of 7 RDEB SCC samples showed a slight decrease in expression of

DUSP23, most samples show concordance with the *in vitro* data showing little difference in expression in comparison to NHK in 5 of 7 RDEB SCC tissue samples (Figure 4.7B).

Nomenclature of Tissue Samples	RIN
NH SKIN 1	8.4
SCC 1	5.7
SCC 2	6.9
SCC 3	6.5
RDEB SKIN 1	8.7
RDEB SKIN 2	8.8
RDEB SKIN 3	8
RDEB SCC 1	7
RDEB SCC 2	7.1
RDEB SCC 3	n/a*
RDEB SCC 4	7.5
RDEB SCC 5	8.4
RDEB SCC 6	1*
RDEB SCC 7	n/a*
RDEB SCC 8	1*
RDEB SCC 9	8.4
RDEB SCC 10	8.6
RDEB SCC 11	6.8

Table 4.5 Tissue Samples used for *in vivo* qRT-PCR screen

Nomenclature and RNA integrity numbers (RIN) for each sample. Only 4 samples had extremely very low RNA quality, denoted by*

TJAP1 mRNA expression was increased in 1 of 3 non-RDEB SCC tissue samples and in 2 of 7 RDEB SCC samples (Figure 4.7C). A further 4 RDEB SCC samples showed reduced expression of *TJAP1* and the final sample showed no difference. RDEB skin shows a reduction in *TJAP1* expression, along with 1 non-RDEB SCC sample. The *in vivo* study shows varied expression of *TJAP1*, with no particular pattern of expression being identified between the sample groups.

Analysis of *SNRPN* mRNA expression *in vivo* identifies increased expression in 100% of non-RDEB SCC samples. Only 50% (3 of 6) of RDEB SCC samples showed reduced expression, whilst a further 2 samples showed an increase and the final sample demonstrated no difference in expression in comparison to normal skin. Intriguingly, both RDEB skin samples showed a reduction in *SNRPN* expression *in vivo* (Figure 4.7D). *In vivo SNURF* expression was unchanged in RDEB skin and non-RDEB SCC. Only 2 of 7 RDEB SCC samples showed a reduced expression of *SNURF* in tissue (Figure 4.7E), whilst the majority of RDEB SCC samples did not conform with *in vitro* data and instead showed no difference in the mRNA expression of *SNURF*.

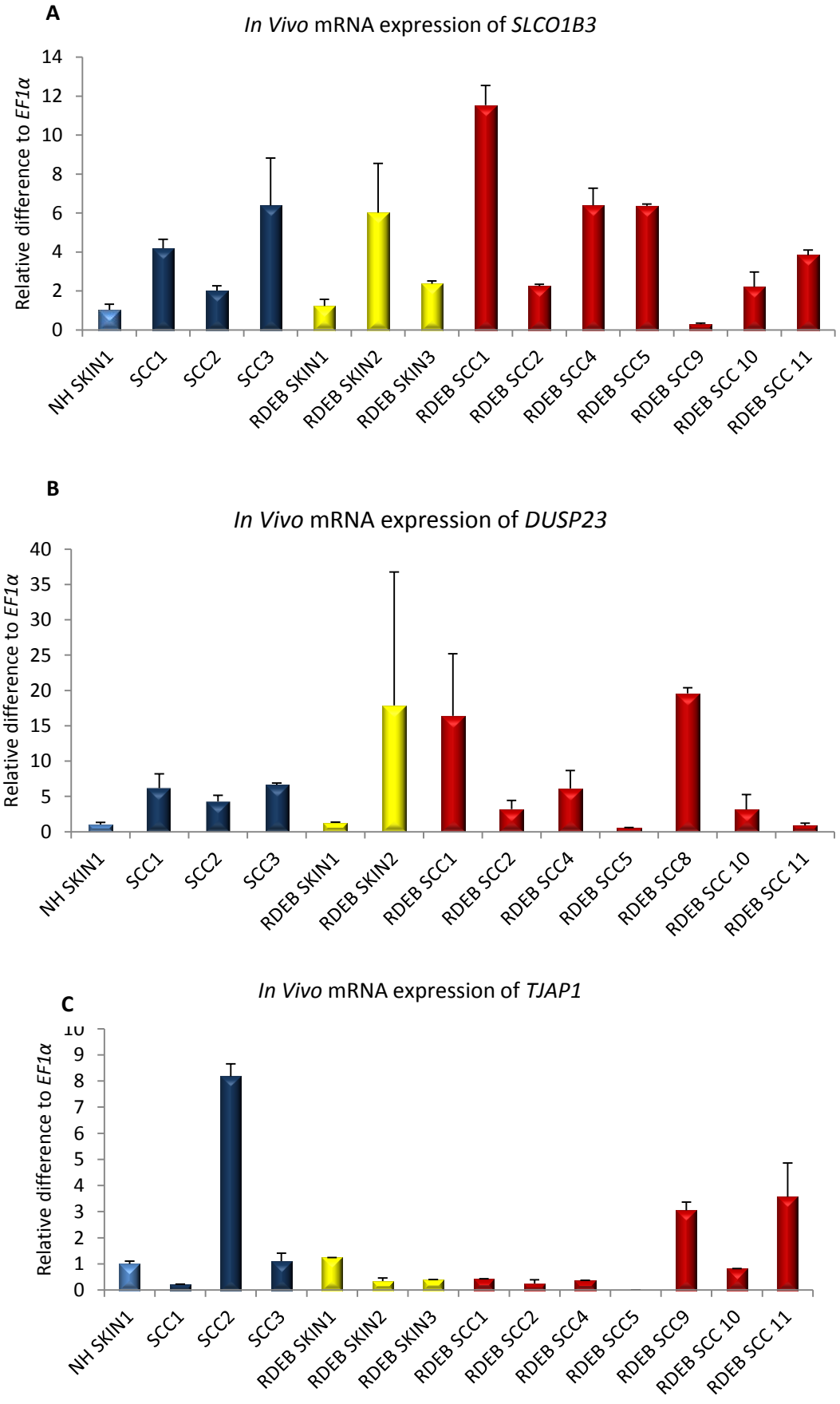
A
In Vivo mRNA expression of SLCO1B3
Relative difference to EF1α
0
2
4
6
8
10
12
14
NH SKIN1
SCC1
SCC2
SCC3
RDEB SKIN1
RDEB SKIN2
RDEB SKIN3
RDEB SCC1
RDEB SCC2
RDEB SCC4
RDEB SCC5
RDEB SCC9
RDEB SCC 10
RDEB SCC 11
B
In Vivo mRNA expression of DUSP23
Relative difference to EF1α
0
5
10
15
20
25
30
35
40
NH SKIN1
SCC1
SCC2
SCC3
RDEB SKIN1
RDEB SKIN2
RDEB SCC1
RDEB SCC2
RDEB SCC4
RDEB SCC5
RDEB SCC8
RDEB SCC 10
RDEB SCC 11
C
In Vivo mRNA expression of TJAP1
Relative difference to EF1α
0
1
2
3
4
5
6
7
8
9
10
NH SKIN1
SCC1
SCC2
SCC3
RDEB SKIN1
RDEB SKIN2
RDEB SKIN3
RDEB SCC1
RDEB SCC2
RDEB SCC4
RDEB SCC5
RDEB SCC9
RDEB SCC 10
RDEB SCC 11

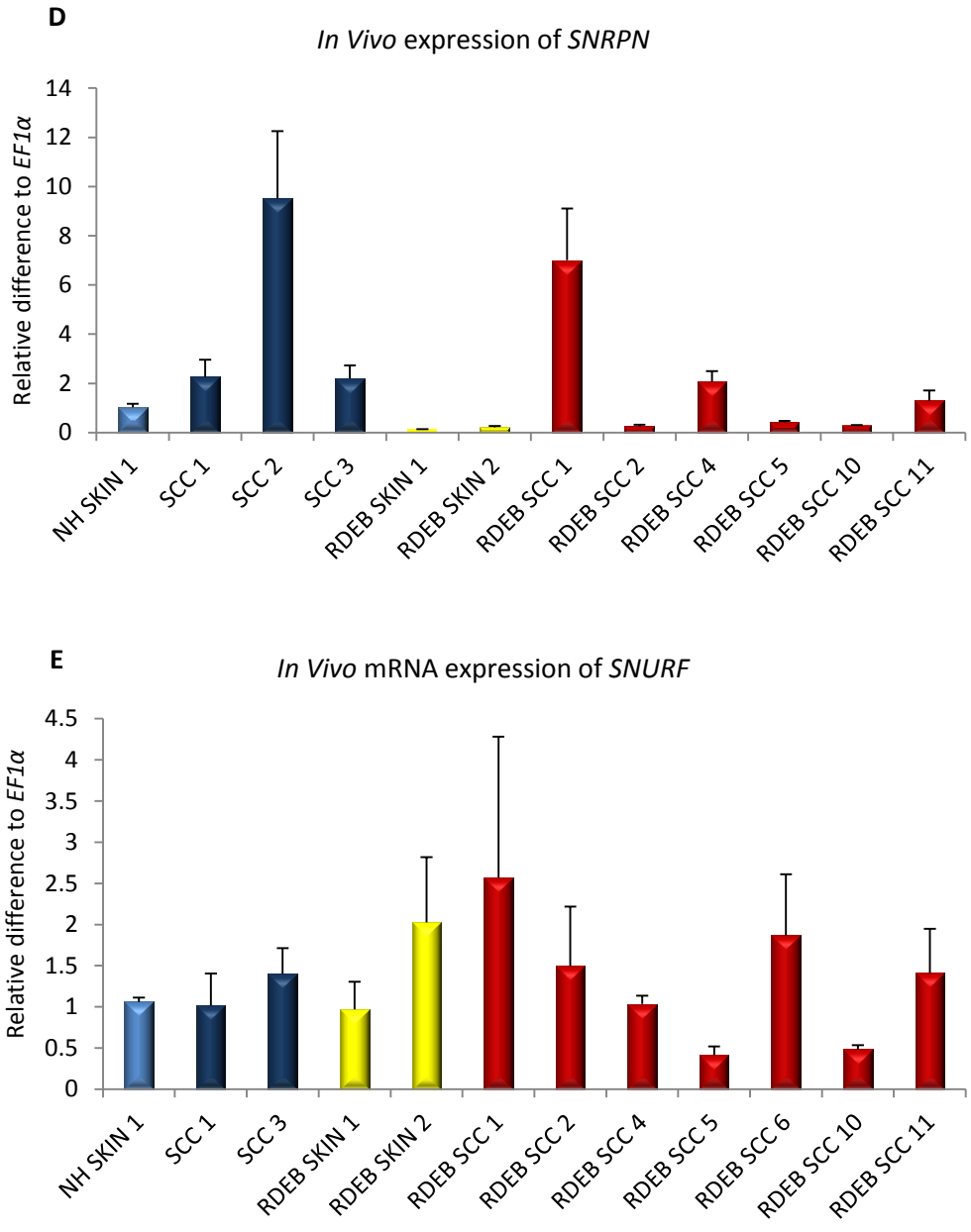

Figure 4.7 qRT-PCR revealed over-expression of *SLCO1B3* in cutaneous SCC *in vivo*.

A) *SLCO1B3* has increased expression in 71.4% of RDEC SCC samples B) *DUSP23* has higher mRNA expression in all non-RDEB SCC samples compared to NHK, and in 5 of 7 RDEB SCC samples C) *TJAP1* mRNA expression was increased in 1 of 3 non-RDEB SCC tissues and a reduction in 4 of 7 RDEB SCC samples and 2 of 3 RDEB skin samples. D) *SNRPN* expression is down in RDEB tissue, as well as in 3 of 6 RDEB SCC samples. E) *SNURF* mRNA expression is down in 2 of 7 RDEB SCC tissues, and shows no difference in expression in RDEB tissue and non-RDEB SCC tissue. Samples represent technical replicates (n=3).

4.3 Discussion

36 genes were originally identified by microarray analysis as being differentially regulated between RDEB SCC and non-RDEB SCC keratinocytes in an experiment aimed at the first steps in identifying therapeutics targets of SCC that develop in RDEB patients and understanding SCC pathology in these patients. This is a priority for research in this topic due to the aggressive nature of these tumours in RDEB patients and their resistance to conventional cancer therapies. SCC presents as a life threatening condition in RDEB patients and causes mortality in 78.7% of patients by the age of 55 (Fine et al. 2009).

The most common functional groups of genes were those involved in the regulation of transcription, which included 14.4% of the genes (Figure 4.1). This includes *HOXA5* and *ERH* both reported to be tumour related (Zafrakas et al. 2008; Yoo et al. 2010) and *MXD4* and *FST* which are both negative regulators of transcription.

4.3.1 *TGFβ* in cancer

Pathway analysis of these genes identified the *TGFβ1* to be an enriched pathway associated with several of the genes identified by the array (Figure 4.2). This could suggest that the TGFβ pathway is implicated in the development of cutaneous SCC. However the analysis doesn't determine if this pathway is more important in RDEB SCC or in non-RDEB SCC.

The TGFβ pathway includes a superfamily of cytokines that include over 30 structurally related polypeptide growth factors (Gordon and Blobe 2008) (Figure 4.8). This pathway has been implicated in many diseases including; development disorders, vascular diseases and

is the most commonly mutated signalling pathway in cancer (Akhurst 2004; Gordon and Blobe 2008). More specifically, an increase in TGFβ has been implicated in pre-eclampsia, restenosis, and hypertension and interestingly, in connective tissue and fibrotic diseases that are associated with out of control wound healing. This suggests a connection with the chronic wound healing environment and cancer develop in RDEB patients. TGFβ signalling is essential for the regulation of several cellular processes; including proliferation, migration, differentiation and survival and many physiological processes including embryonic development, angiogenesis and wound healing (Massague et al. 2000; Gordon and Blobe 2008). Therefore errors occurring within these pathways can lead to a diverse range of diseases.

TGFβ is frequently studied in sporadic cancer, and data is often paradoxical in terms of its role in the pathogenesis of human cancer (Inman 2011). In general, TGFβ acts as a tumour suppressor early on in the process of carcinogenesis, activating downstream targets such as *p21, p27*, and *p15* and leading to growth inhibition, promotion of differentiation and apoptosis (Xu and Pasche 2007). In the late stages of carcinogenesis, it has been reported that TGFβ becomes a tumour promoter and its action mimic that of an oncogene causing cell growth, increased survival, motility, invasion and metastasis (Gordon and Blobe 2008). Alterations and deletions in the TGFβ pathway often result in human disease development including; cancer, developmental disorders and vascular diseases, this is unsurprising given that this is superfamily of proteins and complex pathway are ubiquitous and essential regulators of many cellular processes.

Specifically as *TGFβ1* was identified in the pathway analysis of differentially regulated genes in RDEB SCC, this protein is synthesized and secreted into the extracellular matrix as an inactive precursor protein containing a signal peptide; the latency associated peptide (LAP) and mature TGFβ1. Activation of *TGFβ1* is thought to involve the proteolytic cleavage of LAP which can be induced by acidic environmental conditions or by an excreted extracellular proteases such as MMP2 and 9 (Wu et al. 2007).

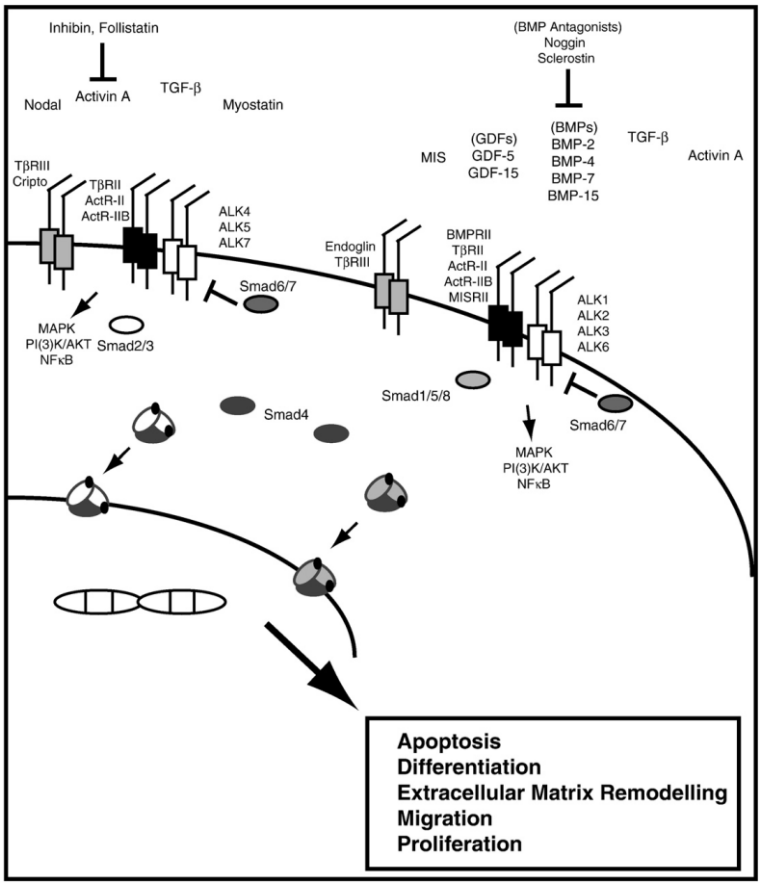

Figure 4.8 TGFβ super-family signalling pathways

The TGFβ signalling cascade is initiated when TGFβ ligands bind to their respective type I and II receptors. Once activated the type I receptor's kinase domain becomes activated by phosphorylation allowing the receptor to in turn phosphorylate Smad transcription factors. These transcription factors form complexes that accumulate within the nucleus of cells and interact with other transcription factors that affect the transcriptome. This signalling pathway leads to the regulation of a range of cellular responses including growth, motility and cell death. Figure taken from Gordon and Blobe, 2008.

The known paradoxical role of the TGFβ pathways in tumour formation and recent research into TGFβ inhibitors as cancer therapeutics would suggest the need for future work to establish if indeed the *TGFβ1* pathway specifically plays a role in RDEB associated SCC; as the protein could potentially be acting as a mutant tumour suppressor or oncogene in these patients. Further studies could initially include investigating the downstream targets of TGFβ1 to identify if there is any difference in expression, this would hopefully illuminate any changes to the pathway in this patient group. An important factor to consider would be to test both RDEB skin and RDEB SCC cells to look for early mutations and aberrations in cancer development. Furthermore, as TGFβ1 is known to play a role in wound healing this suggests there may be a direct link between the RDEB phenotype and this gene. It has been proposed that TGFβ1 can induce epidermal keratinocytes to express cell surface receptors known as Integrins such as α5β1, that facilitate cell migration in re-epithelialisation of wounds (Gailit et al. 1994). The involvement of functionally relevant proteins in the skin that are regulated by TGFβ and its potential role as a tumour promoter supports the rationale for further studies of TGFβ1 in RDEB SCC to be carried out.

4.3.2 *HNF4A* in cancer

IPA has identified *HNF4A* as being highly associated with the gene list derived from the microarray analysis (Figure 4.2). *HNF4A* encodes a transcription factor; hepatocyte nuclear factor 4α and has a key role in regulating the expression of components of cell-cell junctions, including those in adherens junctions, tight junction and desmosomes (Battle et al. 2006). Therefore, this suggests that *HNF4A* plays a part in the epithelia organization and barrier function.

A knock-out mouse model with targeted deletion of *Hnf4α* in epithelial cells of the fetal colon die perinatally (Ahn et al. 2008). There is increasing evidence in the literature that *HNF4A* could be involved in the pathogenesis of human cancer, however, the role in which *HNF4A* plays has not been elucidated as yet and literature reports are conflicting on the subject. Firstly, in several cancer cell lineages including endothelial lung carcinoma cells (Chiba et al. 2005); *HNF4A* inhibits cell proliferation suggesting that the dysregulation of this pathway would be a self protective mechanism initiated by the cell to prevent tumour progression rather than promotion. Whereas aberrations of upstream regulatory signalling cascades are associated with progression of rodent and human hepatocellular carcinoma via accelerated cell proliferation, loss of epithelial morphology, dedifferentiation and the ability to invade and metastasise (Lazarevich and Fleishman 2008).

Partial reversion of a malignant phenotype can be obtained by re-expressing *HNF4A* in dedifferentiated hepatoma cells (Yin et al. 2008). Suggesting that, if in fact this pathway is aberrant in SCC it could be used as a potential target for therapy in a similar way. *HNF4A* is described to function in a network of transcription factors including *HNF1A* and *HNF1β* which control gene expression in embryonic and adult tissues, particularly those of the liver, pancreas and kidneys (Ferrer 2002; Lucas et al. 2005). A 4.7 fold down regulation of *HNF4A* is seen in renal cell carcinoma compared to normal tissue (Lenburg et al. 2003). The different responses of the *HNF4A* pathway in various cell types suggests that there is a tissue specific response, and *HNF4A* may respond differently in various tissues in response to carcinogenesis. As mentioned earlier, *HNF4A* is associated with regulating expression of tight junction molecules, and as this chapter reports a dysregulation of *TJAP1;* a tight junction protein, this suggests a potential direct connection between these two genes in RDEB SCC. Considering that TJAP1 is reduced in RDEB SCC is could suggest that this

expression may be controlled by HNF4A and therefore causes reduced cell-cell interactions and reduced barrier function this may have an effect of the tumour cells ability to break away from the tumours and therefore increase the risk of metastasis.

The most interesting point from the IPA analysis and the identification of *HNF4A* as a hub, is its connection to *SLCO1B3*. This link was initially missed when looking at the IPA analysis however the subsequent association of the nuclear receptor *HNF4A* being able to directly influence the expression of *SLCO1B3*, makes this an attractive target in the search for a genetic target of RDEB SCC. *HNF4A* warrants further research to establish if it indeed effects the *SLCO1B3* expression in RDEB SCC keratinocytes, this could be done using a reporter assay.

4.3.3 *SLCO1B3* is highly expressed in RDEB SCC and other malignant tumours

SLCO1B3 is a member of a superfamily of sodium-independent uptake transporter proteins known as solute carrier proteins (SLCs) or Organic Anion Proteins (OATPs) (Meyer zu Schwabedissen and Kim 2009). This study is the first to report over-expression of *SLCO1B3* in cutaneous squamous cell carcinoma. *In vitro* studies, including microarray analysis and qRT-PCR have identified that the *SLCO1B3* transcript is over-expressed in 3 independent RDEB associated SCC keratinocyte samples compared to non-RDEB SCC and NHK (Figure 4.5A). *In vivo* analysis of expression also showed an up-regulation of *SLCO1B3* RDEB SCC proving this aberration in gene expression is not merely due to the culturing of RDEB SCC keratinocytes (Figure 4.7A).

The *SLCO1B3* gene encodes a protein known as OATP1B3. This family of transporters are known to transport many endogenous and xenobiotic compounds across membranes within the liver, kidney, brain, and intestine; including thyroid hormones, steroid conjugates and anti-cancer drugs (Tirona and Kim 2002). Both OATP1B1 and OATP1B3 are exclusively expressed in the liver and are localised to the basolateral membrane of hepatocytes where they are responsible for the transport of solutes from the blood to the bile via vectorial transport (Cui et al. 2001). OATP1B1 and OATP1B3 share 80% amino acid identity and there is some overlap in their substrate specificity, both can transport bile acids, Methotrexate, and steroid sulphates (Konig et al. 2000; Kullak-Ublick et al. 2001).

This investigation illustrated that *COL7A1* expression directly influences the mRNA expression of *SLCO1B3* (Figure 4.6A). This suggests that in effect, a long term reduction in *COL7A1* expression could cause the activation of transcription of *SLCO1B3*; however the mechanism responsible for *SLCO1B3* expression in RDEB SCC is unknown as yet and requires further investigation. It could be that *SLCO1B3* expression contributes to the initiation of tumourigenesis in RDEB patients or it could potentially alter cell growth, migration, and invasion and thereby enhance the aggressive nature of these tumours and increase their metastatic potential within these patients.

SLCO1B3 expression has been reported in several other cancers including gastric, colon and pancreatic cancers (Abe et al. 2001). The functional transport of small molecule drugs via OATP1B3 has not been established but as it is able to transport anti-cancer drugs such as Methotrexate into cells it could be exploited as a pathway to directly target tumour cells with cytotoxic agents already in use. Furthermore, as this gene is normally only expressed

in the liver it may be possible to use a low dose of chemotherapy to minimise the systemic toxicity to normal cells within the body, whilst targeting the cancer cells. Xenograft mouse models would be an ideal model to determine whether this is possible.

4.3.4 *DUSP23* over-expressed *in vitro* and *in vivo*

DUSP23 is a member of the Protein Tyrosine Phosphatase (PTP) family, which collectively cause reversible phosphorylation of tyrosine residues of proteins belonging to the MAPK family (Tonks and Neel 2001). More specifically *DUSP23* is part of the Dual Specificity Phosphatases (DSPs) subgroup of PTPs, which can dephosphorylate both serine/threonine residues as well as tyrosine residues (Nakamura et al. 1999; Takagaki et al. 2004). The desphosphorylation of kinases is important for the regulation of mitogenic signal transduction in response to cellular stimuli and thereby controlling the cell cycle and cell proliferation (Tonks and Neel 2001; Takagaki et al. 2004).

DUSP23 is located on chromosome 1q23, and has only two exons and 1 intron (Wu et al. 2004), its dysregulated between RDEB SCC and non-RDEB SCC keratinocytes in two independent experiments (Figure 4.5). However, the regulation of this gene between RDEB SCC and NHK is not significantly different. The up-regulation of *DUSP23* mRNA expression seen *in vitro* in 3 non-RDEB SCC keratinocytes lines, is also mimicked *in vivo* in 3 independent SCC (Figure 4.7), thus establishing this is in fact a real change within the SCC cells and is not an artefact of culturing keratinocytes *in vitro*. Furthermore, there is also evidence of increased *DUSP23* mRNA expression in some RDEB SCC tissues. Although, this gene does not provide an RDEB SCC specific target, it could be more significant as a generic genetic target of SCC, given its up-regulation both *in vitro* and *in vivo*. The apparent mRNA

up-regulation in a tumourigenic environment could suggest that it is caused in response to cellular stress. Given that DSPs are activated by specific cellular stimuli, potentially future work could investigate why *DUSP23* is expressed at higher levels in SCC, and is this due to oncogenic stimuli in tumours or a result of genetic instability of cancer cells. Kinase activity in SCC keratinocytes could be tested, to establish if this activity is affected by the *DUSP23* expression using an immune-complex assay to measure activity of kinases after the co-transfection of *DUSP23* with various MAPKs (Shen et al. 2001). One study has shown over-expression of *DUSP23* can increase the proliferative potential of human cancer cells (Tang et al. 2010).

When *COL7A1* is re-expressed in the RDEB SCC keratinocytes there is a reduction of the *DUSP23* mRNA expression, significantly so in comparison to the empty vector control cells in each of the 3 cell lines (Figure 4.6). However, due to the NHK and RDEB SCC keratinocytes expressing similar levels of *DUSP23* to begin with, the expression of *COL7A1* causes greater dysregulation of this gene in the RDEB SCC cells. This suggests that in RDEB skin the reduced expression of functional Type VII Collagen is not a contributory factor to the deregulation of this gene.

4.3.5 *TJAP1* encodes a tight junction protein dysregulated in SCC

Tight junctions (TJs) are present in epithelial cells, and form part of the physical contact between cells, creating cell-cell junctions. They have a diverse range of functions within cells by playing an essential role in adhesion, growth and proliferation (Kawabe et al. 2001). Tight junctions also act as physical barriers between cells to prevent solutes and water from passing through the paracellular pathway and provide a fence between apical and

basolateral plasma membranes in epithelial cells. These junctions are composed of transmembrane proteins such as claudin, occludin and JAM, peripheral membrane protein such as actin filament binding scaffold proteins and cell polarity molecules. *TJAP1* is a recently discovered gene which encodes a novel peripheral membrane protein identified from a cDNA library and its protein name Protein Incorporated later into TJs (PILT), aptly named as it becomes incorporated into tight junctions after the claudin-based junctional strands have been formed (Kawabe et al. 2001). However, its exact function has yet to be elucidated. It is highly expressed in tissues such as skeletal muscle and the spleen which are not rich in TJs and is conversely low in tissues which are high in TJs. PILT also localizes to the golgi so could be involved in vesicle trafficking between golgi and TJ to establish and maintain cell polarity (Kawabe et al. 2001).

PILT is incorporated in TJs at a very late stage in the wound healing process which could suggest that it is incorporated into RDEB keratinocytes more frequently as these patients have generalised skin trauma which produces chronic wound environment. qRT-PCR results suggest *TJAP1* is dysregulated in RDEB SCC however more so in non-RDEB SCC keratinocytes when compared to NHK (Figure 4.5). Although there is a significant difference between the mRNA expression of *TJAP1* in RDEB SCC when compared to non-RDEB SCC, when the expression is compared to NHK the expression is similar and not significantly different suggesting *TJAP1* is not the most appropriate target for an SCC therapeutic in RDEB specifically. This is confirmed by the *in vivo* studies which show no specific pattern of expression in RDEB SCC or non-RDEB SCC; with increased expression in 1 of 3 non-RDEB SCC samples and only 2 of 7 RDEB SCC samples, whilst 4 showed reduced expression of *TJAP1* (Figure 4.7).

4.3.6 *SNRPN* and *SNURF* encoded by the same locus and down regulated in RDEB SCC

SNURF and *SNRPN* transcripts are located within the same *SNURF-SNRPN* locus on chromosome 15. Basically, these transcripts from the microarray are in fact one gene with 10 exons, which is transcribed into a bi-cistronic mRNA transcript. Exons 1-3 encode the SNURF protein (Gray et al. 1999), whilst exons 4-10 encode SNRPN protein (Ozcelik et al. 1992), but also has 2 alternative 5' initiation of transcription sites and multiple untranslated upstream exons of unknown function (Dittrich et al. 1996). They are positioned within a gene cluster which spans an imprinted domain where genes are transcribed either from the paternal or maternal chromosome only, and their expression can occur within all cells or in a temporal or spatial manner. *SNPRN* is expressed only by the paternal allele in all tissues studied so far (Runte et al. 2001), and is functionally imprinted in both mice and humans (Leff et al. 1992; Reed and Leff 1994).

RDEB SCC keratinocytes have a significantly reduced mRNA expression of both *SNRPN* and *SNURF* which are encoded by the same locus on chromosome 15. It is also possible that these genes are simply deleted in RDEB SCC keratinocytes or perhaps a translocation has occurred, in which case this particular region of chromosome 15 has been swapped with another chromosome when the cells have divided through mitosis. This could be investigated via cytogenetic and FISH analysis to look for chromosomal abnormalities specifically in the RDEB SCC cells. Studies by Barr (1995) identified that *SNRPN* is expressed in a variety of tissues; with the highest expression occurring in the brain, but has also been identified in the heart, lungs, liver, spleen, kidneys, testis and ovary (Bar 2005). Our study identifies expression of *SNPRN* and *SNURF* in NHK, suggesting that it is expressed *in vitro*

and is also detectable in normal skin *in vivo*, as identified by the qRT-PCR screen using tissue samples (Figure 4.7).

Two upstream exons were found in the *SNRPN* gene and the first exon designated alpha, lies within a CpG island likely to be the promoter (Sutcliffe et al. 1994). This suggests that the reduced expression of *SNRPN* in RDEB SCC could be a result of hypermethylation of the promoter region. Whether or not these genes are methylated could potentially be investigated by bi-sulphite PCR, a methylation specific PCR to identify genes which are hypo- or hyper-methylated. Promoter methylation is often the cause of maternal silencing, whilst this occurs less frequently in paternal silencing as there is some evidence to suggest that the paternal genome is actively demethylated in the oocyte, and therefore other mechanisms occur to cause inactivation of the paternal chromosomes.

This imprinted domain and the loss-of-function of genes within this region are associated with 2 distinct neuro-genetic diseases; Prader-willi syndrome (PWS) and Angelmen Syndrome (AS) (Runte et al. 2004). Studies have shown uniparental disomy of chromosome 15 can result in these two disorders; with 70-80% of PWS patients having a paternal deletion of chromosome 15q11-q13 (Nicholls et al. 1989; Robinson et al. 1991), whilst 70-80% of AS patients result from the same deletion but of the maternal allele (Knoll et al. 1989; Malcolm et al. 1991). PWS results from loss of the genes expressed on paternal allele, whilst AS results from loss of genes expressed only from the maternally inherited chromosome. The lack of maternal or paternal allele expression in both AS and PWS is very similar to the UPD seen in RDEB where certain chromosomes are inherited from only one parent. Given this striking similarity between the genetic alterations between these 3

conditions it is noteworthy that AS and PWS patients do not show an increased cancer risk whilst RDEB patients do.

Future studies could include the investigation of the genes within this locus to establish if the loss is apparent before or after the initiation of malignant transformation in RDEB keratinocytes within a chronic wound environment. As SCC is very hard to distinguish from the normal blistering and chronic erosions that RDEB patients have, this gene may allow for an alternative method for assessing the tissue and tumoural margins in patients who develop SCC, as both normal and RDEB skin have expression of at least one of these transcripts. Further tests could be performed to establish how this gene is silenced in SCC. As the two upstream exons of *SNRPN* lie within CpG islands it is conceivable that methylation suppresses the transcription of this gene and this would be a plausible explanation of gene silencing. UPD is present on chromosome 15q (Chapter 3 Table 3.1) in RDEB SCC 3 and therefore could be the reason for dysregulation of *SNRPN* and *SNURF* in this sample. The other two samples could have reduced expression of these genes due to other genetic events, whereby perhaps there is a mutation in the transcript resulting in a premature termination codon and nonsense mediated decay of the transcript, or a microdeletion as mentioned in other studies surrounding PWS where part of the chromosome is simply deleted, however no losses were identified by the SNP array data on chromosome 15.

4.3.7 Cell types contributing to tissue samples

One possible explanation for the varying mRNA expression levels for the 5 genes tested in the tissue samples is that tumour tissue samples may not contain only cancer cells. It is

well known that a tumour's cell population is heterogeneous. Therefore the RNA isolated from tumour tissue samples for the experiments discussed in this chapter may also be from a combination of normal and tumour cells. This is one advantage of using the keratinocyte cell culture model for initial experiments, as the gene expression levels were taken from a homogenous cell population. One consideration for future experiments would be to microdissect tumour samples to reduce sample heterogeneity and therefore increase mRNA expression accuracy.

4.3.8 *SLCO1B3 i*s a potential candidate worth pursuing

Although 5 transcripts were identified by the microarray and qRT-PCR screening as being differentially regulated between RDEB SCC and non-RDEB SCC, *SLCO1B3* would seem to be the most intriguing gene to follow up initially due to its apparent reduction in mRNA expression when *COL7A1* is re-expressed and thus reverting the expression back to the normal mRNA levels, as seen in NHK and non-RDEB SCC keratinocytes. Furthermore, the expression is seen in some RDEB SCC tissues and some non-RDEB SCC samples but not in normal skin (Figure 4.7A). This transporter gene, could present as genetic target which is regulated in a different manner in mainly in RDEB SCC and therefore could be exploited as a potential therapeutic pathway specifically aimed at treating SCC in RDEB patients.

As *SLCO1B3* encodes an organic anion transporter that is normally only expressed in the liver and functions to transport many endogenous and exogenous proteins into the liver where they can be excreted and metabolised, this protein represents a potential pathway to directly target tumour cells and thus allow the accumulation of anti-neoplastic drugs in the tumour. OATPS have been subject to many investigations which predominantly aim to

evaluate drug disposition and metabolism in mouse models along with transport of various substrates into via these transporters (Cattori et al. 2000; Muto et al. 2007; Chen et al. 2008). Mouse models have been utilised to investigate several OATPs by knocking down their expression and then testing drug distribution in these mice (Cattori et al. 2000; Cheng et al. 2005; Chen et al. 2008). One limitation of these models in respect to OATP1B3 is that there is no ortholog in mice, the closest member is Oatp1b2 which shares a similar homology with both OATP1B1 and OATP1B3 in humans (Konig et al. 2000; Konig et al. 2006). Mouse models do however represent useful tools for understanding the role of OATPs in drug targeting and disposition in cancer cells.

OATP1B3 is capable of transporting several chemotherapeutic agents including Methotrexate and Paclitaxel. The use of chemotherapy for the treatment of SCC in RDEB patients is limited and only a few cases reports exist (Ayman et al. 2002; Arnold et al. 2009; Shivaswamy et al. 2009). This is mainly due to the systemic toxicity caused by these agents, which can increase infection rate and perturb the skin further. As OATP1B3 is only expressed in liver cells and also in tumours cells, this would theoretically allow antineoplastic drugs to be taken up by the SCC cells only in RDEB patients, and reduce the systemic toxicity as any circulating drug will be transported into the liver by OATP1B3 where it would be metabolised and excreted, thus reducing systemic toxicity to patients. This hypothesis is supported by a study undertaken by Van de Steeg and colleagues who demonstrated knockdown of *SLCO1B1* in mice drastically decreased uptake of Methotrexate and Fexofenadine and consequently increased systemic toxicity (van de Steeg et al. 2010).

Interestingly two studies have shown OATP1B3 expression to be correlated to prognosis (Muto et al. 2007; Hamada et al. 2008). Muto and colleagues demonstrated that 51 breast tumours expressed OATP1B3 which was inversely correlated to tumour size and was significantly associated with decreased risk of recurrence and improved prognosis (Muto et al. 2007). This is believed to be due to OATP1B3 being able to transport estrone 3 sulfate in to breast tumour cells in a growth dependent manner (Muto et al. 2007). Whilst Hamada and colleagues showed that prostate tumours which express wild-type OATP1B3 have poorer prognosis that those expressing the OATP1B3 334T>G or 699G>A variants. This is due to the variants having reduced transporter activity and therefore transport less testosterone into tumour cells, whilst those expressing wild-type OATP1B3 transport more testosterone into cells creating a growth advantage for the tumour cells (Hamada et al. 2008). OATP1B3 is capable of transporting estrogen into cells, which is known to be a regulator of connective tissue molecules; namely collagen (Schiffer et al. 2003). This could suggest that OATP1B3 is expressed as a result of a compensatory mechanism whereby the lack of *COL7A1* expression in RDEB patients promotes estrogen uptake by expression of OATP1B3 and thus increased collagen synthesis.

In terms of therapies for RDEB SCC, this protein presents a direct transport mechanism for the movement of anticancer drugs into tumour cells and thereby enhancing the accumulation of these drugs in tumour cells and selectively killing them. The next chapter will explore the expression of *SLCO1B3* further in RDEB SCC keratinocytes.

Chapter 5

OATP1B3 validation as a potential therapeutic target of RDEB SCC

5.1 Background

This chapter covers the validation of *SLCO1B3* as a potential therapeutic target in RDEB associated SCC. The previous chapter demonstrated that the *SLCO1B3* is one of five significantly differentially regulated genes in RDEB SCC compared to non-RDEB SCC at the mRNA level, both *in vitro* and *in vivo*. Furthermore, when *COL7A1*, the gene mutated in RDEB is retrovirally expressed in RDEB SCC keratinocytes the mRNA expression of *SLCO1B3* is reduced, thus suggesting that the extracellular matrix protein Type VII Collagen may be able to regulate the transcription of this transporter gene in RDEB SCC keratinocytes.

5.1.1 Conventional Cancer Therapies for Treatment of SCC

Cutaneous SCC is often treated via electrodessication and curettage, surgical excision, or cryosurgery, in the majority of patients with primary tumours these techniques eliminate 90% of local tumours with a low risk of recurrence and metastasis (Johnson et al. 1992). The most widely used treatment for SCC is surgical excision for patients with UV-induced SCC and is applicable to the treatment of SCC that develop in RDEB patients however even after treatment prognosis is poor. Molecular treatments of SCC are not common, although the recent study by Watt et al., illustrates two genetic targets of SCC (RDEB and non-RDEB associated SCC) and corresponding inhibitors that are currently in clinical trials can effectively reduce tumour size in mice (Watt et al. 2011).

Establishing the molecular basis of tumours is not a new concept, this research has been ongoing for decades, since the first characterisation of animal cancer viruses in the 1960s and 1970s (Huebner and Todaro 1969). Closely followed by the identification of the first oncogenes and tumour suppressor genes in the 1970s (Stehelin et al. 1976; Collins and

Workman 2006). During the 1990s studies elucidated the concept of cancer genes causing irregular signal transduction pathways to occur. Now in the 2000s the study of molecular oncology is enhancing cancer drug discovery and generating hypotheses driven by disease causing gene targets and allowing for mechanism based drug discovery.

5.1.2 Validating the Functional Characteristics of a Genetic Target

For a gene to be a true therapeutic target it must be verified as a clinically effective pathway for the delivery of anti-cancer drugs to tumour cells (Workman 2003; Collins and Workman 2006). Consequently, having identified *SLCO1B3* to be significantly differentially regulated in RDEB SCC and its expression being linked to *COL7A1*, it calls for further research to examine its potential as a therapeutic target. The natural progression of this study required these changes in expression to be confirmed and to investigate the functional and physiological consequences of *SLCO1B3* expression.

5.1.3 Drug Transporters

Cells express different types of drug transporters, which can be classified into primary, secondary and tertiary active transporters (Mizuno et al. 2003). Primary transporters are driven by ATP hydrolysis and consist of a group of ATP-binding cassette proteins which include multi-drug resistance proteins (MDR); Multidrug Resistance associated Protein (MRP) and the Breast Cancer Resistance Protein (BCRP) (Mizuno et al. 2003). These proteins are most abundantly expressed on the canicular membrane in human liver hepatocytes where they are responsible for biliary excretion of drugs and their metabolites (Hooiveld et al. 2001).

Secondary and tertiary active transporters include the following families of proteins; Organic anion Transporters (OAT), Organic Anion Transporting Polypeptides (OATP), Na^+-taurocholate cotransporting polypeptide (NTCP), Organic Cation Transporters (OCT), Novel Organic Cation Transporters (OCTN), and Peptide Transporters (PEPT) (Burckhardt and Wolff 2000; Dresser 2001). The transport of compounds by these proteins is driven by the exchange or co-transport of intracellular or extracellular ions. Secondary transporters expressed on the sinusoidal membrane of the liver and are liable for the uptake of drugs from the blood into hepatocytes (Meier et al. 1997).

5.1.4 Organic Anion Transporting Polypeptides (OATPs)

SLCO1B3 encodes the protein OATP1B3 which is a member of the OATP superfamily that include a large group of uptake carriers encoded for by SLCO genes (Konig et al. 2000; Abe et al. 2001; Cui et al. 2001). Whilst some OATPs are expressed in single organs, others are expressed ubiquitously (Hagenbuch and Gui 2008). These transporters are expressed in a variety of tissues including the liver, kidneys, intestine and brain where they are responsible for the Na+ independent movement of a broad spectrum of endogenous and xenobiotic compounds (Yamaguchi et al. 2008).

In humans, several isoforms of the OATP family have been functionally characterised (Hagenbuch & Meier 2004). They are known to mediate the transport of a range of endogenous substrates including bile acids and steroid hormones (Smith et al. 2005; Sekine et al. 2006). Of particular interest to this study are the transporters present within the liver, as OATP1B3 is a liver-specific protein and under normal circumstances is exclusively

expressed on the basolateral membrane of hepatocytes around the central vein (Muto et al. 2007).

5.1.4.1 Key functions of transporters in the Liver

Transporters present within the liver are responsible for the elimination of xenobiotics and endogenous catabolites from the systemic circulation. Once compounds have been taken up into hepatocytes, they are biotransformed into phase I and II reactions before being subsequently excreted into the bile. Bile formation is driven by vectorial secretion of bile acids from the blood, which is efficiently retained within the enterohepatic circulation by active absorption in the ileum and extraction from portal blood by hepatocytes. The major hepatocellular uptake system for bile acids is the sodium-taurocholate co-transporting polypeptide (NTCP) although there is some involvement of OATPS.

5.1.4.2 Two liver specific OATPs – OATP1B1 and OATP1B3

OAT1PB1 is the main Na+ independent bile salt uptake system in hepatocytes and is capable of transporting non-bile salt organic anions such as conjugated steroids (Abe et al. 1999; Hsiang et al. 1999; Konig et al. 2000; Kullak-Ublick et al. 2001). OATP1B1 and OATP1B3 share 80% amino acid identity and have one ortholog representing both proteins in rodents; Oatp4 (Hagenbuch and Meier 2004). OATP1B1 and OATP1B3 have overlapping substrate specificities; with some common substrates that have differences in the affinity to the transporter (Abe et al. 2001; Cui et al. 2001; Ismair et al. 2001; Kullak-Ublick et al. 2001). They are both capable of transporting bile acids such as the amphipathic steroid molecule; Chenodeoxycholic Acid (CDCA), a derivative of cholesterol catabolism which acts

as a ligand for the nuclear receptor FXR and the antifungal agent Rifampicin which inhibits transport by both proteins at varying levels (Yamaguchi et al. 2006).

5.1.4.3 OATP1B3 expression and functional characteristics

OATP1B3 is a protein of 702aa, which under normal circumstances localises to the basolateral membrane of hepatocytes (Konig et al. 2000). It has also reported to be expressed in several cancer cell lines derived from solid organ tumours including gastric, colorectal, pancreatic and hepatocellular carcinomas (Letschert et al. 2004; Smith et al. 2005) and lung, breast and colon cancer tissues (Muto et al. 2007; Lockhart et al. 2008).

OATP proteins have multiple substrate binding sites which can affect the affinity of their substrates and the compounds which they are capable of transporting. OATP1B3 is involved in the cellular uptake of steroid anions such as estradiol-17β-glucuronide and estrone-3-sulfate (Gui et al. 2008); xenobiotics including digoxin and pravastatin; oligopeptides such as cholecystokinin and thyroid hormones into hepatocytes from the portal blood (Abe et al. 2001; Kullak-Ublick et al. 2001; Jung et al. 2002; Seithel et al. 2006).

Many studies have looked at the transcriptional regulation of *SLCO1B3*. It is a polymorphic gene with 2 common SNPs, occurring at base pair 334T>G and another in 699G>A which occur as a consequence of the non-random association of alleles at two loci across chromosomes which results in the alanine residue changing to serine at amino acid 112 (S112A) and a methionine to isoleucine change at amino acid 233 (M233I), respectively (Tsujimoto et al. 2006; Smith et al. 2007). It has been shown that the polymorphic variants

of *SLCO1B3* have variable transport characteristics for some substrates (Letschert et al. 2004; Smith et al. 2005; Konig et al. 2006). The *SLCO1B3* promoter contains several hypoxia-responsive elements suggesting that up-regulation of *SLCO1B3* in tumours may also be related to anoxic conditions (Abe et al. 2001).

5.1.4.4 OATP1B3 in cancer

Research into the transport of substrates into cells via the OATP1B3 transporter is of particular interest to many research groups due to its documented over expression in tumours, and its ability to mediate uptake of many anticancer drugs including; Methotrexate, Paclitaxel, Docetaxel, SN-38 and Irinotecan (Ichihara et al. 2010). The physiological significance of OATP1B3 expression in tumour cells is unclear, but is an ongoing question for many researchers. Interestingly, in most tumours expressing OATP1B3 the change in expression is due to the induction of transcription of this gene, whilst in hepatocellular carcinoma (HCC) originating from cells where this protein is normally expressed, it has been reported to have reduced expression of OATP1B3 in 60% of HCC (Vavricka et al. 2004).

Hamada's data suggest that the over-expression of OATP1B3 is part of a complex stepwise process of cancer progression, which in the case of prostate cancer allows the cells to gain a biological advantage by up-regulating testosterone uptake and proliferation through increased androgen import (Hamada et al. 2008). They show no detectable expression of *SLCO1B3* in normal prostate tissue or benign hyperplasia, but marked expression in prostatic cancer and a statistically significant association of a specific *SLCO1B3* haplotype with survival of patients (Hamada et al. 2008).

Azathioprine has been reported to increase the transport of Methotrexate, one study showed that treatment of cancer cell lines with Azathioprine, an inhibitor of DNA methyltransferase, significantly increased the mRNA expression of OATP1B3 in HepG2 and Caco-2 cells by 18 and 14 fold, respectively (Ichihara et al. 2010). This provides a strategy that would enhance the expression of *SLCO1B3* in tumour cells prior to treatment with antineoplastic drugs that have been specifically targeted to be taken up into cells via OATP1B3 in tumours. Over-expression of OATP1B3 in RDEB SCC provides a specific pathway to deliver drugs to a specific tissue, avoiding distribution of drugs to other organs and thereby reducing the risk of toxic side effects to healthy cells. As a transporter protein it may also provide more control of drug elimination processes (Mizuno et al. 2003).

5.1.5 Aim

In any experiment conducted to identify a target suitable for therapeutic invention it is importance to prioritise the research in terms of pursuing the best target. To do this, the following points need to be considered. First, the validation of the gene targets in terms of functional validity using over expression, knock out models, and animal models; secondly the drug-ability of a given target, and finally the ability to predict toxicity from mouse models.

Understanding the extent and relevance of *SLCO1B3* in RDEB SCC is crucial to developing a therapy targeted to this protein, as the tissue distribution and organ specific entry of drugs is often facilitated by drug transporters. Essential to understanding the function in RDEB SCC is the need for efficacy and bioavailability testing of any compound used to selectively kill the tumour cells. However, before this can be done it is of utmost precedence to

establish whether *SLCO1B3* is an appropriate target for therapeutic intervention in RDEB SCC and capable of transporting compounds into cells.

Thus far we have shown only an increase in mRNA expression of *SLCO1B3* but have not demonstrated that this up-regulation of *SLCO1B3* transcription is translated to expression at the protein level. Therefore, the first aim of this chapter was to demonstrate OAT1PB3 protein expression in RDEB SCC keratinocytes and tissue.

Next, in order to assess the functional characteristics of OATP1B3 in RDEB SCC, two transporter assays were performed to establish whether OATP1B3 is an active transporter in RDEB SCC keratinocytes and is capable of transporting known substrates into cells. Two independent measures of transport were used by employing a fluorescently labelled and a radioactively labelled substrate to measure uptake in various SCC keratinocyte cell lines. Furthermore, having assessed the transporter function of OATP1B3 this chapter covers the selective killing of cells expressing OATP1B3 using a toxin produced by cyanobacteria known as Microcystin-LR which causes liver toxicity by entering cells via the OATP1B1 and OATP1B3 transporters.

5.2 Methods and Results

5.2.1 OATP1B3 is localised to the cell membranes in RDEB SCC tissue

When starting this investigation there were 3 commercially available antibodies raised against the OATP1B3 protein; D-16 and C-14, both goat-polyclonal antibodies (Santa Cruz,

California) and OATP8 mouse antibody (Novus Biologics). Immunoblotting was performed using all 3 antibodies to examine the protein expression in RDEB SCC keratinocytes. However, the initial results from immunoblotting RDEB SCC and non-RDEB SCC whole-cell lysates showed no specific bands of the expected size. Figure 5.1A demonstrates that the antibody was non-specific and produced a high background of multiple bands. There was no correlation of between the banding patterns produced and therefore were unable to confirm OATP1B3 protein expression using western blotting with this antibody. The same results were seen using the other 2 commercially available antibodies (Appendix 1.3).

It has been established that in culture the expression of the protein is gradually reduced even in hepatocytes (Jigorel et al. 2005; Richert et al. 2006), therefore the next logical step was to try and demonstrate expression of the protein in RDEB SCC tissue samples, where the expression is likely to be higher. Whilst we were unable to detect OATP1B3 in RDEB SCC keratinocytes, immunofluorescent staining of RDEB SCC tissue sections revealed some positive immuno-reactivity using the D-16 antibody (Figure 5.1B). Although the staining pattern is weak, it does imply that OATP1B3 is localised to the cell membranes as demonstrated in RDEB SCC tissue sections (Figure 5.1B). Further staining of other tissue sections showed a lower immuno-reactivity in RDEB SCC (Appendix 1.4).

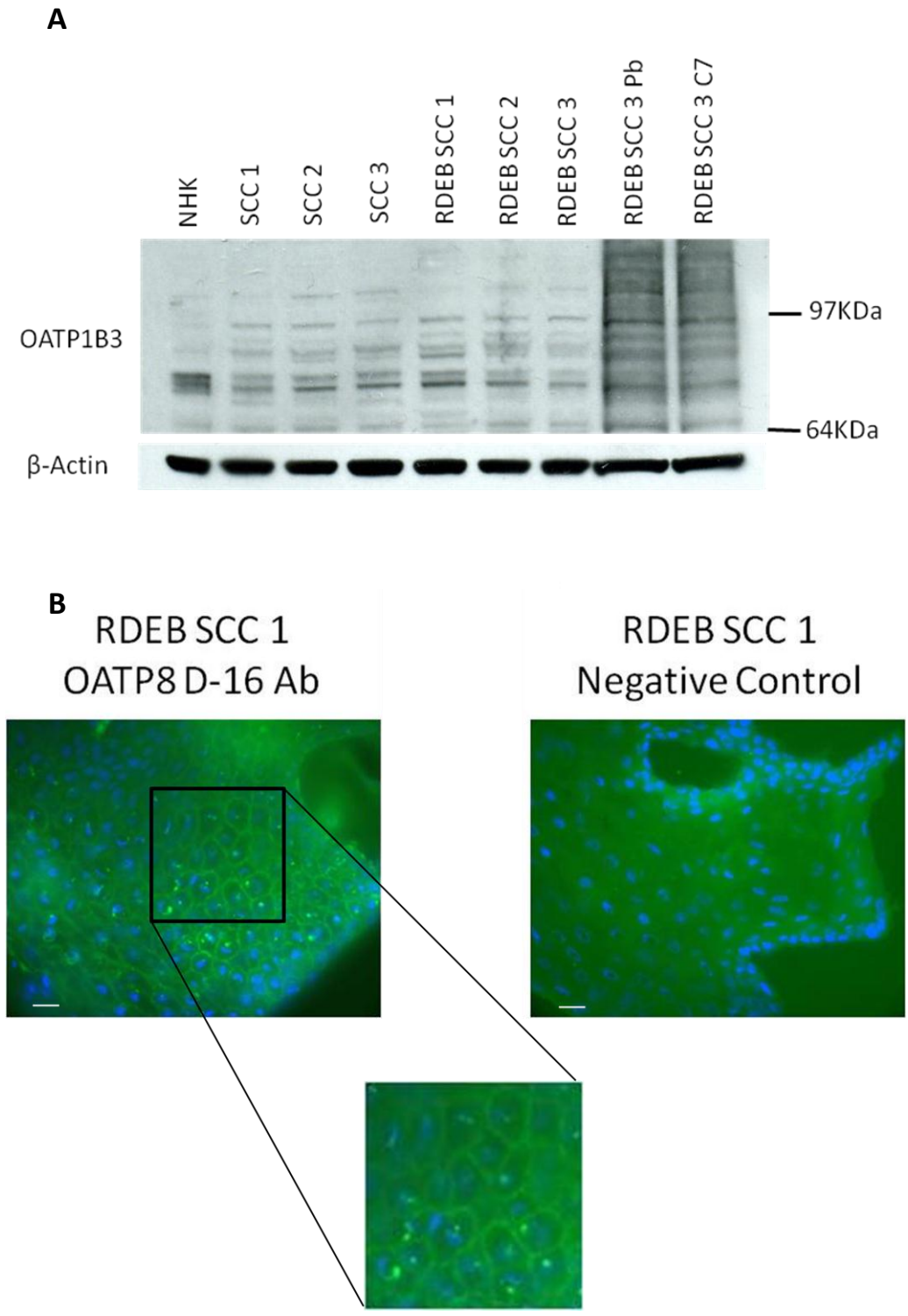

Figure 5.1 Immunofluorescent staining showing some positive membrane bound expression of OATP1B3 in RDEB SCC tissue. A) Immunoblotting cultured NHK, non-RDEB SCC (SCC), RDEB SCC, and RDEB SCC empty vector (PB) and cells over-expressing *COL7A1* (C7) does not demonstrate expression of OATP1B3. B) Immunofluorescent staining of RDEB SCC tissue using the Santa Cruz anti goat D-16 antibody (green) and Dapi nuclear staining (blue) identifies OATP1B3 membrane bound expression. Scale bar ~20µm

5.2.2 Transport assays do not show OATP1B3 specific transport in RDEB SCC keratinocytes

Having identified that OATP1B3 is localised to the cell membranes in tissue, it leads to question whether this protein can transport substrates into cells. The fluorescent calcium indicator; Fluo-3 was demonstrated by Cui and colleagues to be a substrate of OATP1B3 in MDCK cells (Cui et al. 2001). An uptake assay utilising Fluo-3 was later developed to measure the transport into cells via OATP1B1 and OATP1B3 (Baldes et al. 2006), this protocol was used to investigate OATP1B3 transport in RDEB SCC keratinocytes.

Initial results showed that a dose dependent uptake of Fluo-3 in RDEB SCC keratinocytes, when using a range of 0.125 to 20μM Fluo-3 (Figure 5.2A). As a preliminary run, two concentrations of Fluo-3 were used to look at uptake in non-RDEB SCC keratinocytes, results showed no significant difference in uptake values of 0.125μM and 5μM of Fluo-3, as the level of fluorescence was almost equal to the background fluorescence seen in cells contains no Fluo-3 (Figure 5.2A). This experiment was conducting using a HT synergy fluorimeter to measure fluorescence.

After the promising preliminary results using Fluo-3 uptake as a measure of transport activity in RDEB SCC keratinocytes, both RDEB SCC and non-RDEB SCC samples were used to look at the differences in uptake between cells expressing *SLCO1B3* and those which do not express this gene. Results showed the same dose dependent uptake of Fluo-3 in RDEB SCC 3, however using the full concentration range on non-RDEB SCC cells (SCC 3), showed that

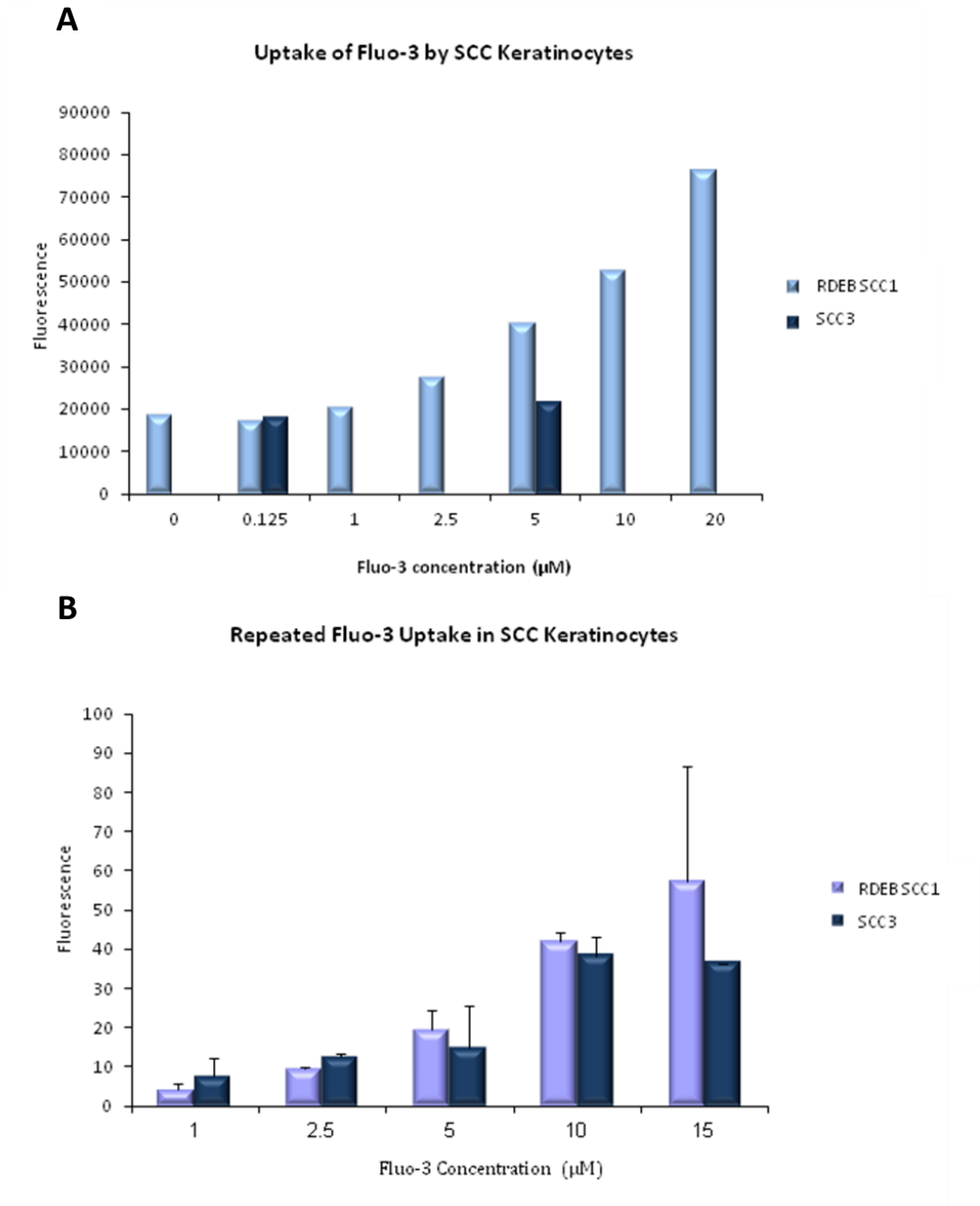

Figure 5.2 Dose dependent uptake of Fluo-3 in SCC keratinocytes

A) Initial results showed a dose dependent uptake of Fluo-3 in RDEB SCC 1 (n=1), whilst the two concentrations of Fluo-3 added to SCC 3 (n=1) showed no change in the uptake in terms of fluorescence after the cells were lysed. B) A repeat run of the uptake assay using the full range of Fluo-3 concentrations on non-RDEB SCC (SCC 3), shows a dose dependent increase in fluorescence which is proportional to the uptake in each cell line. Samples represent biological replicates (n=3). The difference in scale between the two graphs is due to using two different fluorimeters to measure fluorescence.

these cells also had an apparent dose dependent uptake of Fluo-3 based on the level of fluorescence after incubation with the substrate (Figure 5.2B). The difference in the scale used for the graphs seen in figure 5.2 A and B was due to using two different fluorimeters, the experiment performed in Figure 5.2A was performed on a LabTek Fluorimeter whilst experiments performed from Figure 5.2B onwards were performed on a Fluorimeter by Molecular Devices.

Rifampicin a known substrate of OATP which reduces the uptake of Fluo-3 through competition (Baldes et al. 2006), was used to further assess whether the transport of Fluo-3 into cells could be inhibited. Results showed that uptake of 5µM of Fluo-3 in RDEB SCC 3 cells was reduced by prior incubation with 0.5-25µM of Rifampicin, whilst the effect on uptake of 10µM Fluo-3 was variable (Figure 5.3A). RDEB SCC 3 cells pre-incubated with 0.5 to 10µM of Rifampicin, then exposed to 10µM Fluo-3, showed an increased uptake of Fluo-3, whilst, 25-50µM of Rifampicin caused no change in the uptake of 10µM Fluo-3 (Figure 5.3A).

The previous chapter showed that *SLCO1B3* mRNA expression is reduced in RDEB SCC keratinocytes that have been retrovirally transduced to re-express Type VII Collagen. Therefore, using these cells in this uptake assay would help assess whether the uptake that we see is OATP1B3 mediated transport. In RDEB SCC 3 cells that have been retrovirally transduced to express Type VII collagen the uptake of Fluo-3 was variable over the entire concentration range, where 2.5µM has a high standard deviation due to triplicate values being widely distributed in terms of fluorescence (Figure 5.3B). In RDEB SCC 3 C7, 10µM of Fluo-3 showed no uptake and 20µM shows uptake of an equal amount to 2.5µM Fluo-3

(Figure 5.3B). Whilst no significant change in uptake is seen in RDEB SCC Pb empty vector control cells. Comparing the control cells to the *COL7A1* cells, shows that 3 of the 4 concentrations of Fluo-3 (2.5, 5, and 20μM) caused slightly more uptake of Fluo-3 in *COL7A1* over-expressing cells compared to the RDEB SCC Pb cells, which is the opposite to the hypothesised result that *COL7A1* cells would have a reduced uptake of Fluo-3 as the expression of *SLCO1B3* is lower when Type VII Collagen is expressed.

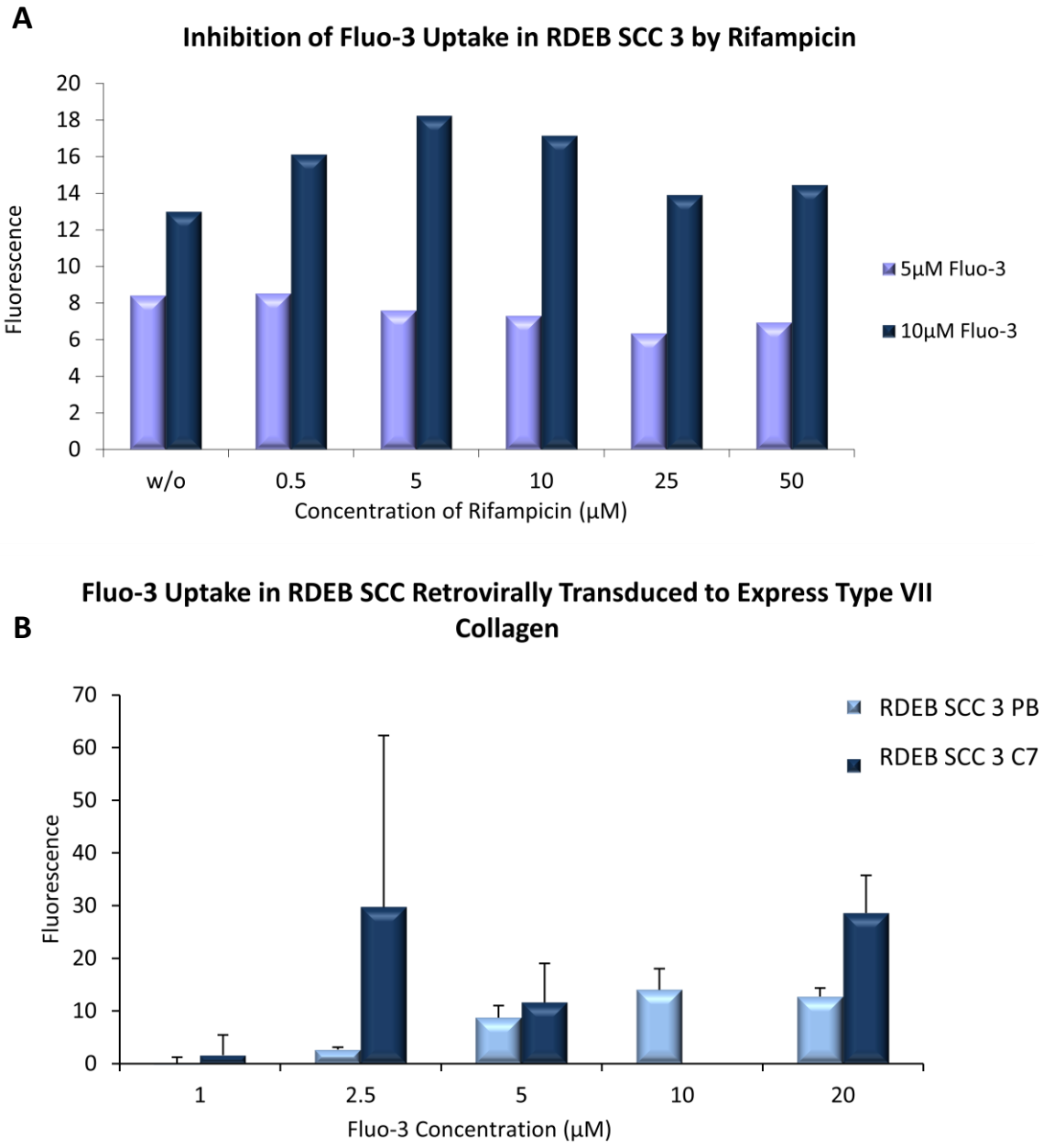

Figure 5.3 Uptake of Fluo-3 is not significantly inhibited by Rifampicin or reduced by Type VII Collagen expression. A) When RDEB SCC cells (n=1) are treated with Rifampicin prior to adding Fluo-3, there is an inhibition of Fluo-3 uptake in a Rifampicin dose dependent manner when 5µM of Fluo-3 is added. B) In RDEB SCC 3 cells that have been retrovirally transduced to express Type VII collagen the uptake is increased in RDEB SCC C7 (n=1) cells expressing Type VII Collagen, in comparison to the PB empty vector cells (n=1) in using 3 different concentrations of Fluo-3.

The Fluo-3 uptake assay although at first provided promising results to suggest *SLCO1B3* is translated into an active transporter of substrates into RDEB SCC keratinocytes, variability in assay results indicate that this assay is not a reliable predictor of transporter function in these cells. Further experiments using the same cell line demonstrated varying results, with no two experimental runs showing consistent uptake of the similar amounts of Fluo-3. Furthermore, when investigating uptake in the RDEB SCC cell lines expressing *COL7A1* in order to confirm that this assay is able to show OATP1B3 specific uptake, the results confounded the situation even more. The reason behind these baffling and unexpected results could be firstly that as we have been unable to show protein expression of OATP1B3 in these cells, that the expression of the protein is too low to show specific uptake mediated by this transporter alone, or secondly that the protein is expressed but does not act as a transporter in these cells. In addition, the experimental procedure using a fluorescently labelled substrate requires cells to be washed and then lysed before measuring the fluorescence. Variation in fluorescence levels could be attributed to the substrate being "sticky" and residual Fluo-3 remains on the plastic edges of the wells, or that insufficient lysis of cell monolayers creates inconsistent results which may be responsible for the sometimes high variability in replicate samples potentially skewing the results.

In an attempt to establish a definitive answer to the question; is OATP1B3 an active transporter in RDEB SCC keratinocytes; another OATP transport assay was used. This assay was developed by Gui and colleagues and demonstrated that tritiated estradiol-17β-glucuronide can be used to measure uptake of cells, they also demonstrated that several other substrates can enhance or attenuate the uptake of tritiated estradiol in Chinese Hamster Ovary cells over-expressing OATP1B1 and OATP1B3 (Gui et al. 2008).

Briefly, RDEB SCC 1 cells were plated out on 24-well plates at a density of 80,000 cells per well and incubated for 24 hours prior to the start of the uptake experiment. Experiment procedure for this uptake assay can be found in Chapter 2 Section 2.2.5.3. Incubating the cells with a concentration range of 1.25 to 50nM of [3H]-estradiol-17β-glucuronide for 1 hour prior to cell lysis and scintillation counting demonstrated a clear dose dependent uptake of tritiated estradiol in RDEB SCC 1 cells (Figure 5.4A), further more when cells were pre-incubated with uptake solution containing Clotrimazole, an antibiotic known to specifically enhance uptake through the OATP1B3 pathway (Gui et al. 2008), whilst inhibit uptake through the OATP1B1 pathway (Gui et al. 2008), the RDEB SCC 1 cells show increased uptake of estradiol in correlation with increasing concentrations of Clotrimazole ranging from 2.5 to 10μM (Figure 5.4B).

The assay was then repeated using NHK, three non-RDEB SCC samples and 3 RDEB SCC keratinocyte samples, to look at uptake across the whole sample range. The results showed that in all 3 RDEB SCC samples, there was uptake of [3H]-estradiol-17β-glucuronide and significantly enhanced uptake of tritiated estradiol after incubation with 10μM Clotrimazole (Figure 5.5). The enhanced uptake of the tritiated substrate in all 3 cells lines suggested that uptake was specifically OATP1B3 mediated up in the RDEB SCC cell lines expressing *SLCO1B3*. However, further investigations using NHK and 3 non-RDEB SCC cell lines, demonstrated uptake of [3H]-estradiol-17β-glucuronide, which is unsurprising as this common substrate can be transported by several transporters, but perplexingly, the pre-incubation of cells with Clotrimazole also caused an increased uptake of [3H]-estradiol-17β-glucuronide in NHK and 2 non-RDEB SCC samples (SCC 4 and 5), whilst SCC 3 showed no difference in the uptake after exposure to Clotrimazole (Figure 5.5).

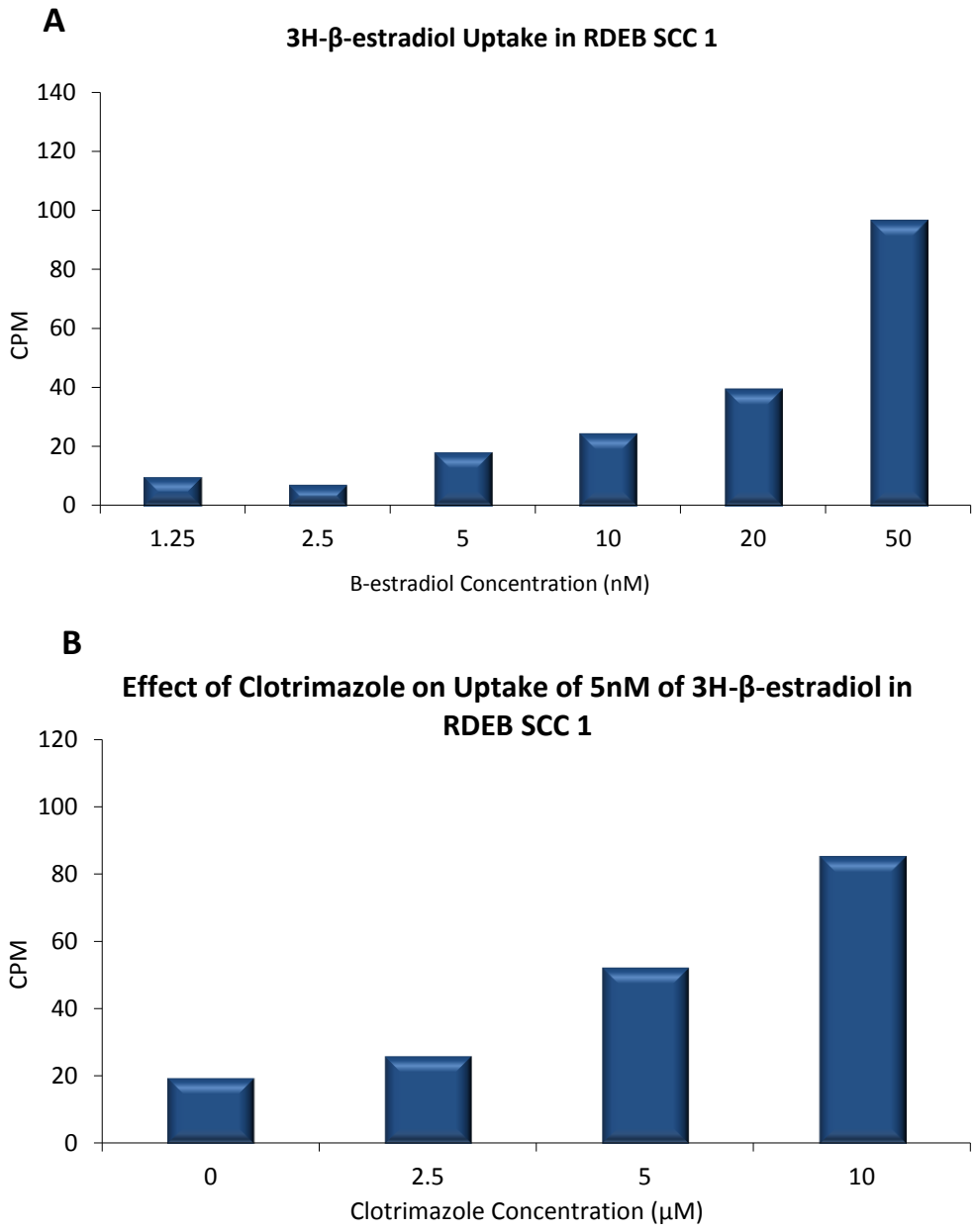

Figure 5.4 Uptake of [3H]-estradiol-17β-glucoronide is seen in a dose dependent manner in RDEB SCC 1 cells and is enhanced by Clotrimazole.

A) Tritiated estradiol was taken up in a dose dependent manner in RDEB SCC 1 cells (n=1). B) Clotrimazole enhances the uptake of 5nM of [3H]-estradiol-17β-glucoronide, in a dose dependent manner (n=1).

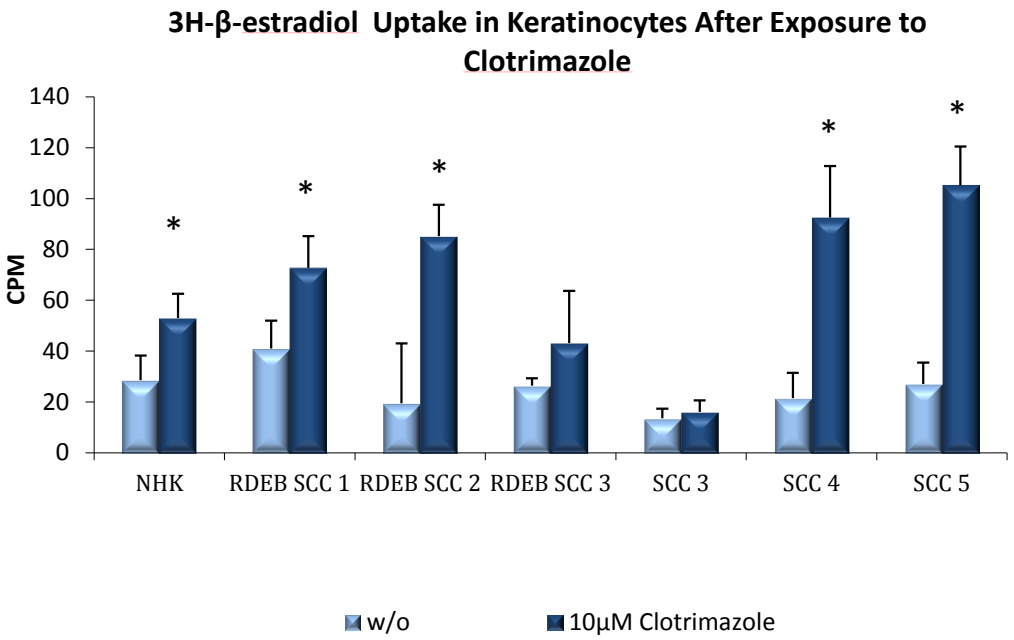

Figure 5.5 [3H]-estradiol-17β-glucuronide uptake is seen in all cell lines and enhanced in the majority of SCC cell lines. Uptake of tritiated estradiol was demonstrated in all cell lines, with all 3 non-RDEB SCC keratinocytes showing the least uptake. Pre-incubating the cells with and without (w/o) 10 µM of Clotrimazole caused the uptake of 20nM [3H]-estradiol-17β-glucurondie to be increased in all cell lines except one non-RDEB SCC cell line; SCC 3 which showed no difference in uptake of the substrate after exposure to Clotrimazole. Significance was granted >0.05 and those cell lines showing a significant difference in uptake are denoted by *(p=<0.05) R=+/- SD Student's T-Test. Samples are biological replicates (n=3).

Confounding results, still leaves the question as to whether OATP1B3 mediates uptake in RDEB SCC keratinocytes open for debate. As we have previously demonstrated that NHK and non-RDEB SCC keratinocytes do not express *SLCO1B3* at the mRNA level, but still show enhanced uptake of β-estradiol. It does suggest that, uptake in these cell lines is not dependent on expression of OATP1B3 and that other transporter mechanisms may be occurring in these cells. Therefore these results cannot be relied up on to confirm

transporter function in RDEB SCC keratinocytes as the mechanisms causing uptake in NHK and non-RDEB SCC may also be contributing to uptake in RDEB SCC keratinocytes.

This led to a change in the direction of the study, and required that a stable clone was produced that over-expressed *SLCO1B3*. This provided a much needed positive control for experiments concerning the protein expression and the functional characteristics of this transporter in RDEB SCC cells; this also creates a useful system for the validation of these experiments. In reference to the uptake assays, it's important to point out that even the OATP1B3 expression in liver tissue is low (Konig et al. 2006) and both transport assays used so far have previously only been carried out in over-expression systems where the expression of OATP1B3 is exogenous, whereas in these experiments I have been trying to demonstrate uptake of substrates by the endogenous expression of OATP1B3 which is quite probably has a low magnitude of protein expression.

5.2.3 Creating an stably over-expressing *SLCO1B3* cell line

An *SLCO1B3* image clone was purchased from Open Biosystems, and was used to amplify the *SLCO1B3* ORF using the following primers; forward primer included the KOZAK sequence: AAG CAG AGG GGC CGT CAA GG and the reverse sequence CAT GAG GCC TTA GTT GGC AGC which included an additional 3 nucleotides on the 5' end to include a STOP codon that was missing from the image clone sequence.

Prior to using PCR to amplify the ORF, the image clone was expanded by adding a pipette scraping of the glycerol stock to a universal tube containing 5ml LB Broth

and 5µl spectinomycin (100mg/ml) (Sigma Aldrich, Poole, Dorset, UK). The universal was briefly vortexed and the broth culture grown over night in a shaking incubator at 37°C. This starter culture was then used as a template for the PCR reaction, by first incubating 2µl of culture diluted in 23µl of dH_2O for 5 minutes at 95°C. 2µl of the boiled culture was then used as a template for the FastStart High Fidelity PCR reaction, and 2uL dH_2O as the NTC, and ran with an annealing temperature of 58°C. Reaction component volumes and cycling parameters are detailed in Chapter 2 Section 2.2.2.8. During the final extension, the reaction was stopped and 0.5µl SuperTaq and 0.5µl dNTPs (10mM) was added to each reaction and incubated for 5 minutes at 72°C to create AA overhangs required for subsequent cloning. Then 5.5µl of the amplified product was visualised on a 1% agarose gel (Figure 5.6).

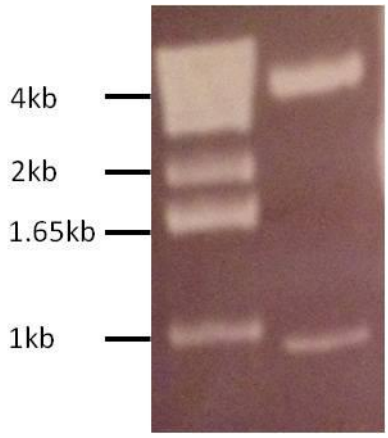

Figure 5.6 *SLCO1B3* ORF was PCR amplified and digested with BsmI. The RE digested the ORF in two places creating 2 fragments of correct size.

Next having successfully, amplified the ORF of *SLCO1B3* using the image clone as a template. The ORF was inserted into the PCR II vector included in the Invitrogen TOPO II Clone kit. Using the following technique, 0.5µl PCR, 1.5µl dH2O and 0.5uL TOPO PCRII vector, this reaction was then incubated at room temperature for 5 minutes and then placed on ice. The 0.5µl of the Topo clone reaction was added to a 2mm electroporation cuvette (PeqLab) and along with 20µl of Top10 electro-competent bugs at 1.2 volts using the GenePulse electroporator (BioRad). Each electroporation reaction should create a time constant of ~4.6. 750µl SOC medium (Invitrogen) was added to the electroporated bugs and then aliquoted into a bijou tube and recovered in a shaking incubator at 37°C for 45 minutes. 100µl of the Topo clone culture was then plated using aseptic technique onto an agar plate containing Ampicillin (0.1mg/ml) and grown overnight at 37°C. Four colonies were prepped and inoculated in 5ml LB broth and grown over night. The next day, glycerol stocks were created and the remaining culture was prepped using the Wizard plus DNA purification system, detailed methods of this kit are outline in Chapter 2 section 2.2.3.2.

500ng of the *SLCO1B3* ORF Topo clone was then digested using BstXI, by incubating at 37°C for 1 hour and visualised on a 1% agarose gel. The digested DNA showed two brighter bands one at approximately 2kb and one at 4kb, both of the correct size, a third fainter band can be seen at the top of the gel and is likely to be uncut plasmid (Figure 5.7). 1µg of the plasmid prep (*SLCO1B3* ORF Topo) and 1µg of pBabe puro retroviral vector were then digested separately with the BstXI RE over

night at 37°C. To the retroviral vector; 0.5µl of alkaline phosphatase (AP), 4.5µl dH_2O and 5µl AP Buffer was added and incubated for a further 30 minutes at 37°C, this prevents the sticky ends produced by the vector re-annealing. The ORF which is approximately 2kb was successfully excised from the Topo clone and the open linear pBabe puro vector was then purified by gel extraction. The two purified products were next ligated together using the Sigma Ligation Kit; using a ratio of 1:10 in terms of DNA concentration of vector:insert. The ligated products were then transformed into Top10 electrocompetent cells via electroporation and grown overnight at 37°C on Ampicillin agar plates. Eight colonies from the ligation cultures were prepped, starter cultures made and DNA was purified using the Wizard Plus DNA Purification kit. 200ng of DNA from each colony was digested with XbaII and HindIII by incubating DNA for 1 hour at 37°C. Figure 5.8 displays the visualised DNA digestions using the two RE. This allowed the identification of ligations that contained the ORF in the correction orientation, reading from 5' to 3' which is

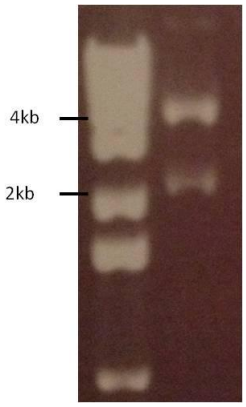

Figure 5.7 TOPO clone digestion with BstXI. Demonstrates that the ORF was efficiently inserted into the PCR II Topo vector. The BstXI RE cut the vector in two places (right hand lane), creating 2 linear pieces of DNA approximately 2kb (the inserted ORF) and 4 kb (Topo vector). A third fainter band is uncut supercoiled DNA.

required for transcription of the gene once inside the viral packaging cells. Correctly orientated ORF from 3 of the ligation colonies was confirmed by sequencing. One of the clones was then transfected into phoenix cells (packaging cell line) following the protocol in Chapter 2 Section 2.2.3.7.

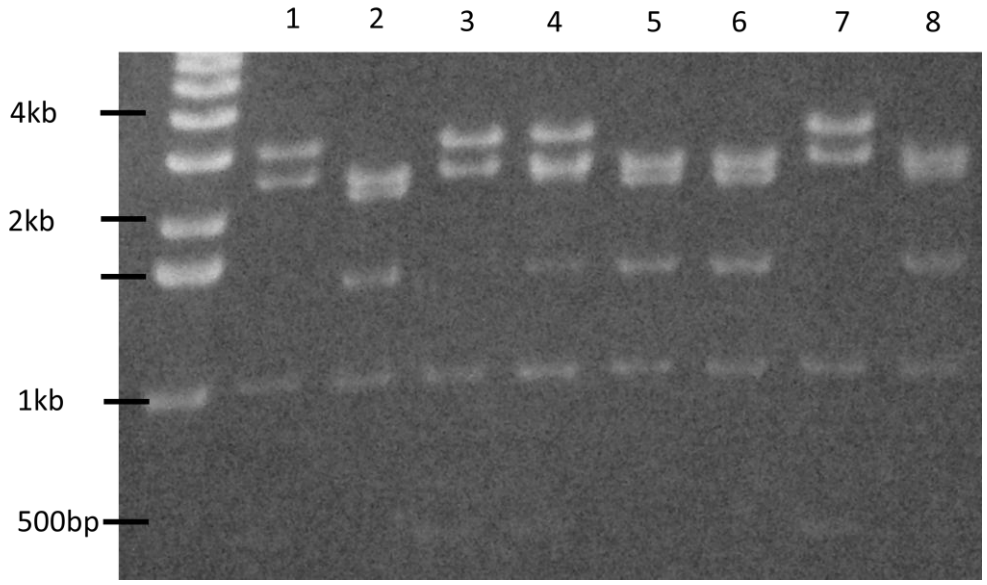

Figure 5.8 DNA from 8 ligation colonies was digested with XbaI and HindIII. The correctly orientated ORF produced a banding pattern of 1004, 1438, 2273 and 2665bp (Lanes 2,5,6 and 8) whilst the incorrect orientation produced bands of 590, 1004, 2605, 3121bp. The digestion identifies that 50% (4 of the 8) of the colonies that were prepped contained the *SLCO1B3* ORF in the correct orientation.

After retroviral transduction of RDEB SCC 1 cells with the *SLCO1B3* construct, were expanded and grown until confluency. Figure 5.9A, demonstrates that the pBabe puro (Pb) empty vector cells and the *SLCO1B3* over-expressing cells (SLC) do not show any morphological changes in the cell shape and structure. qRT-PCR using RNA isolated from the transduced cells demonstrated that the *SLCO1B3* clones; RDEB SCC 1 SLC do indeed

express higher levels of *SLCO1B3* compared to both the parental cell line RDEB SCC 1 and the empty vector control (RDEB SCC 1 PB). There was no significant difference in the mRNA expression of SLCO1B3 between the parental cell line RDEB SCC 1 and the empty vector control, RDEB SCC 1 PB (Figure 5.9). To confirm this transcript is translated into a protein, western blotting was first performed using the 3 commercially available antibodies which were documented at the beginning of this results chapter. The results showed that like cells with only endogenous *SLCO1B3* expression, there was no common band that convincingly showed the OATP1B3 protein was expressed in these samples. At this time, Professor Bruno Steiger, of University Hospital, Zurich kindly donated a custom made OATP1B3 antibody with an epitope targeted against the c-terminus of the protein. Immunoblotting confirmed that the RDEB SCC 1 SLC cells do in fact express the protein, at the expected size, using the new antibody (Figure 5.9C). The antibody was however unable to detect the endogenous expression of OATP1B3 in the empty vector control. Further confirmation of expression was seen via immunoflourescence staining of the cells using the antibody, and it clearly shows expression of OATP1B3 at cell-cell junctions and membrane of the cells (Figure 5.10).

Having created a cell line with stable expression of OATP1B3 which has been verified to express both mRNA and protein expression, this cell line was used to repeat the tritiated uptake assay. Using the parental cell line (RDEB SCC 1) and the over-expressing cells (RDEB SCC 1 SLC), I was able to show that there was no difference in the uptake of [3H]-estradiol-17β-glucuronide in the over-expressing cells (Figure 5.10). This immediately indicates that this assay does not demonstrate OATP1B3 specific uptake, as the protein level was detectable in the RDEB SCC 1 SLC cells, but not in the RDEB SCC 1 parental line. Using Clotrimazole to enhance the uptake of the tritiated substrate showed no effect on the

parental line, whilst a small increase in uptake was seen in RDEB SCC keratinocytes. Rifampicin was also used to show inhibition of uptake; which was seen slightly in both the parental cell line and *SLCO1B3* over-expressing cells.

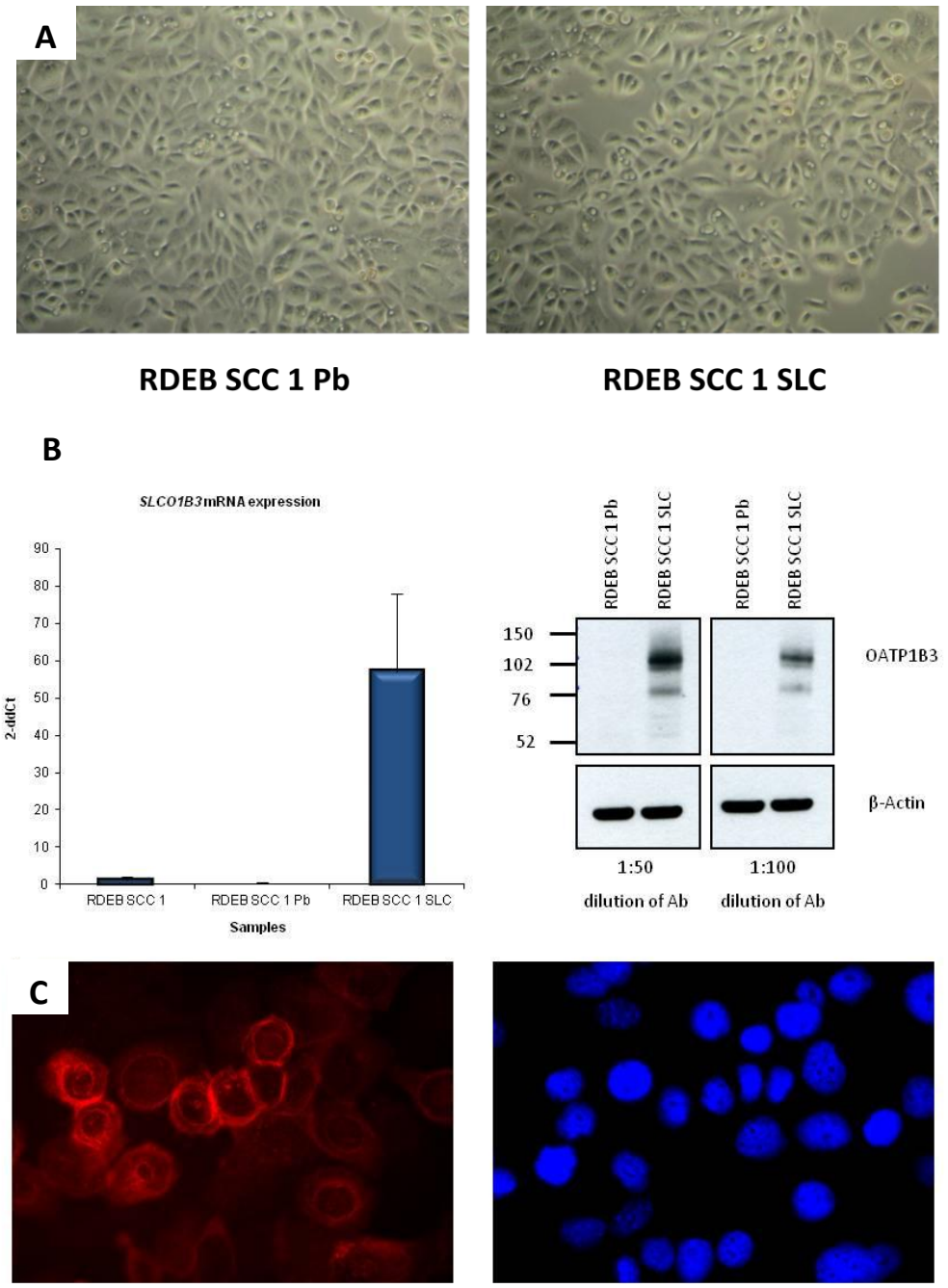

Figure 5.9 Confirmation of RDEB SCC 1 retrovirally transduced to express *SLCO1B3* show high levels of *SLCO1B3* and OATP1B3 expression. A) Confluent monolayers of both RDEB SCC 1 Pb (empty vector control cells) and RDEB SCC 1 SLC cells show no morphological differences after transduction. B) mRNA expression of *SLCO1B3* is significantly higher in RDEB SCC 1 SLC than both the parental cell line and empty vector control. Immunoblotting using a custom made OATP1B3 antibody shows expression of OATP1B3 but no detectable endogenous expression in RDEB SCC 1 PB control cells. Samples are technical replicates (n=3). C) Immunohistrochemistry confirms expression of OATP1B3 in the RDEB SCC 1 SLC cells.

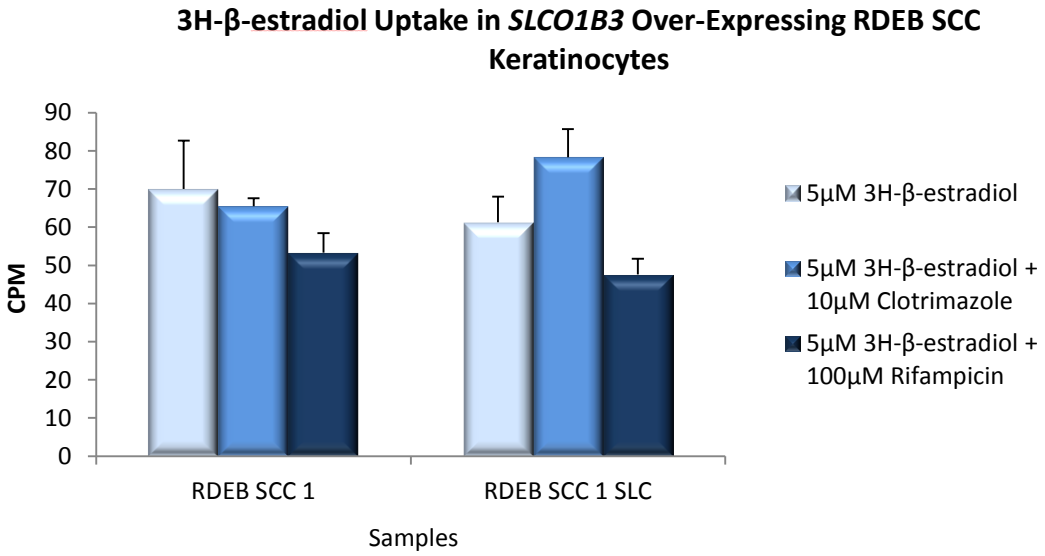

Figure 5.10 Uptake of [3H]-estradiol-17β-glucuronide in OATP1B3 over-expressing RDEB SCC 1 cells is no different to the parental cell line. RDEB SCC 1 cells over-expressing OATP1B3 showed uptake of tritiated estradiol and an enhanced uptake after incubation with Clotrimazole. Rifampicin attenuated the uptake in both the parental and over-expressing cells. The parental cell-line RDEB SCC 1 was also used, and showed that there was no significant increase in the uptake of [3H]-estradiol-17β-glucuronide between RDEB SCC 1 and RDEB SCC 1 SLC. Samples represent biological replicates (n=3).

5.2.3 Confirmation of OATP1B3 expression in RDEB SCC keratinocytes and tissue

The custom made OATP1B3 antibody was able to detect protein in the RDEB SCC 1 SLC cells. Further immunofluorescence staining, confirms the expression of OATP1B3 in the retrovirally transduced RDEB SCC 1 cells (Figure 5.11).

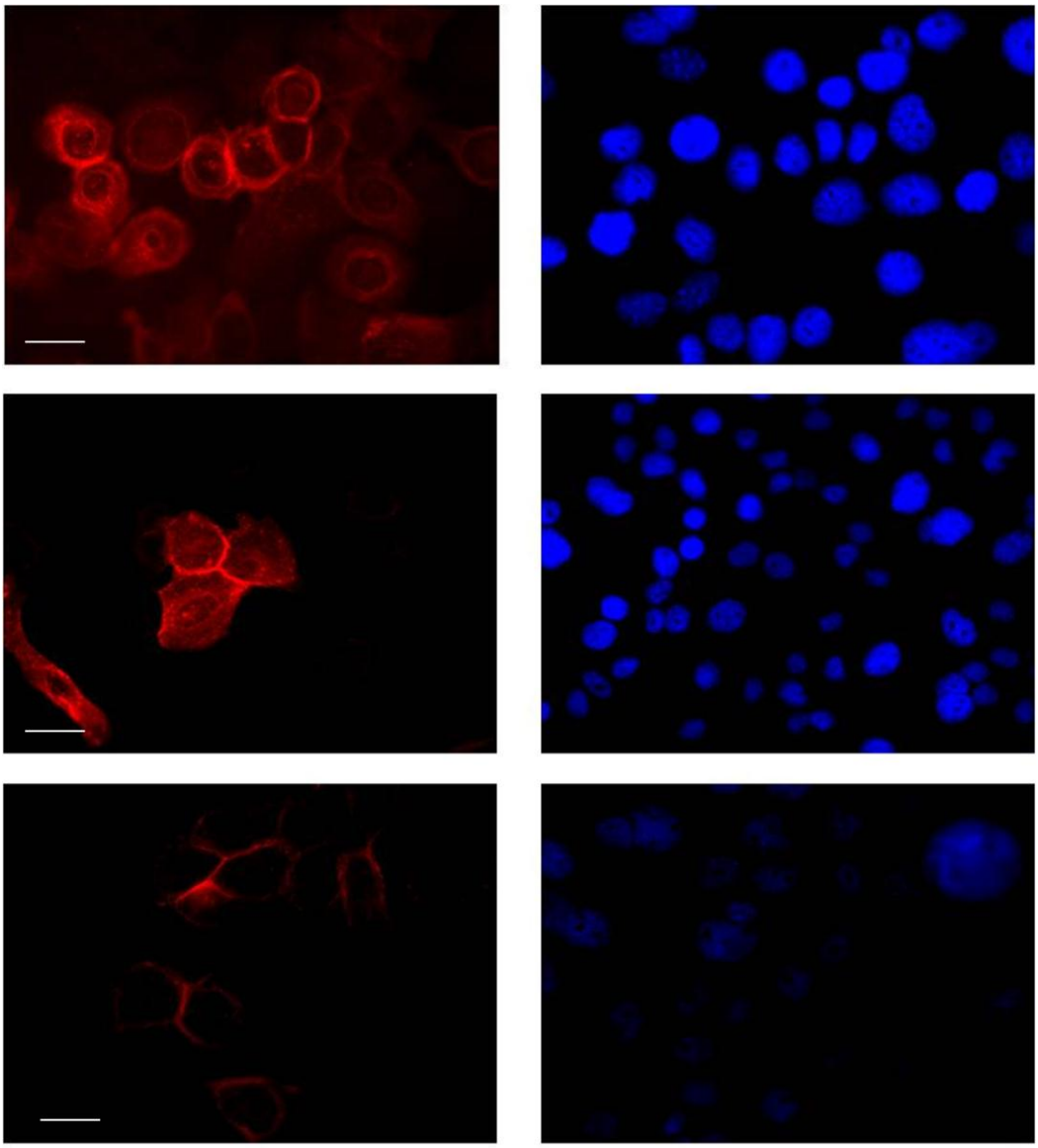

Figure 5.11 Retrovirally transduced RDEB SCC 1 cells demonstrate membrane bound expression of OATP1B3. Immunohistochemistry confirms expression of OATP1B3 at the protein level using a custom made OATP1B3 antibody, donated by Professor Bruno Stieger, University Hospital, Zurich**.** All panels on the left in Red show OATP1B3 expression. In all cases, it is clear that the protein is localised to the cell membranes. The right hand panel shows Nuclei staining in blue. Scale bar ~40µm, images taken under 65x objective.

Immunofluorescent staining performed on RDEB SCC tissue samples; include 2 RDEB SCC tissues, 1 RDEB SCC xenografts section from mouse, and a healthy skin section (Figure 5.12). Results indicated positive staining in all RDEB SCC tissues, whilst only background fluorescence was seen in normal skin. RDEB SCC7 showed hyperkeratotic whirls, which are condensed sections of keratin within the tumour sample; this made it difficult to assess the localisation of the protein in this case due to IMF background. In the RDEB43 sample and the RDEB SCC xenografts; OATP1B3 seems to localise to the cytoplasm (Figure 5.12).

Further Immunofluorescent staining was carried out on RDEB SCC and non-RDEB SCC cell lines. Results indicated that in fact the endogenous expression of OATP1B3 is detectable in RDEB SCC keratinocytes, in all 3 independent samples (Figure 5.13) whilst, the non-RDEB SCC (SCC 3) sample did not show any positive staining.

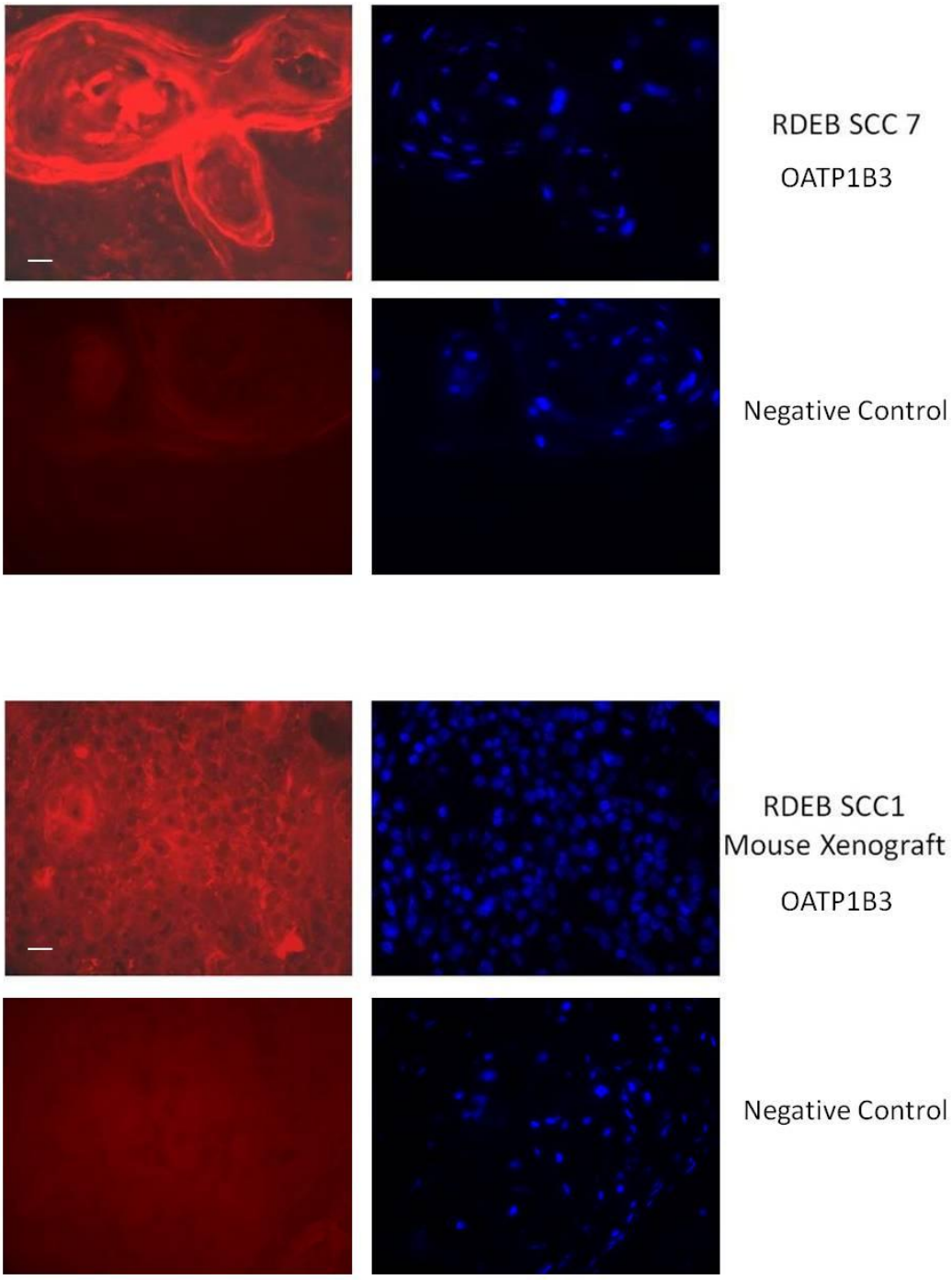
RDEB SCC 7
OATP1B3
Negative Control
RDEB SCC1
Mouse Xenograft
OATP1B3
Negative Control

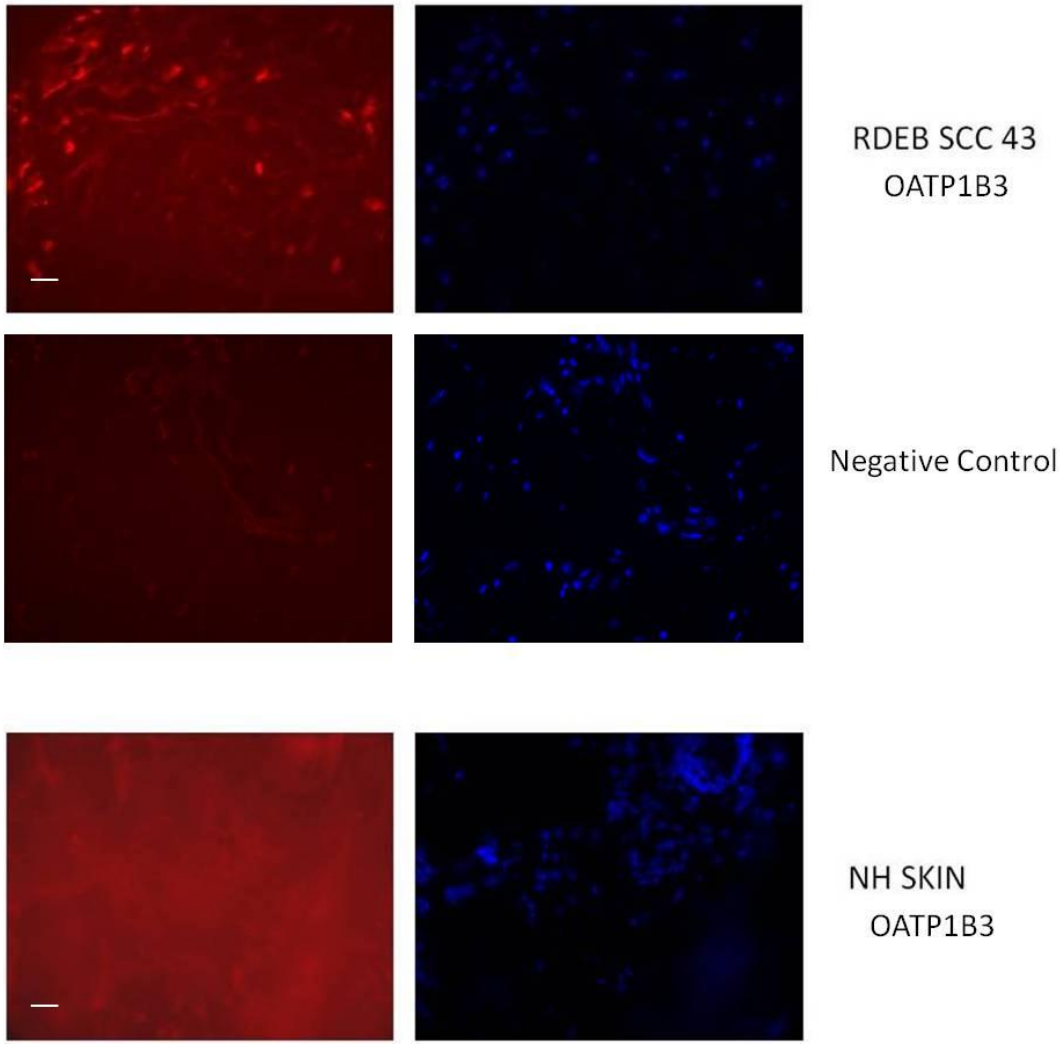

Figure 5.12 Immunofluorescence staining confirms OATP1B3 expression in RDEB SCC tissue. Tissue sections from 2 RDEB SCC tissue samples, and 1 sample taken from a mouse xenografts of RDEB SCCK 1 cells, confirms expression of OATP1B3 *in vivo*, in comparison to NH Skin which shows no specific positive staining. Scale bar ~20µm, images taken under 16x objective.

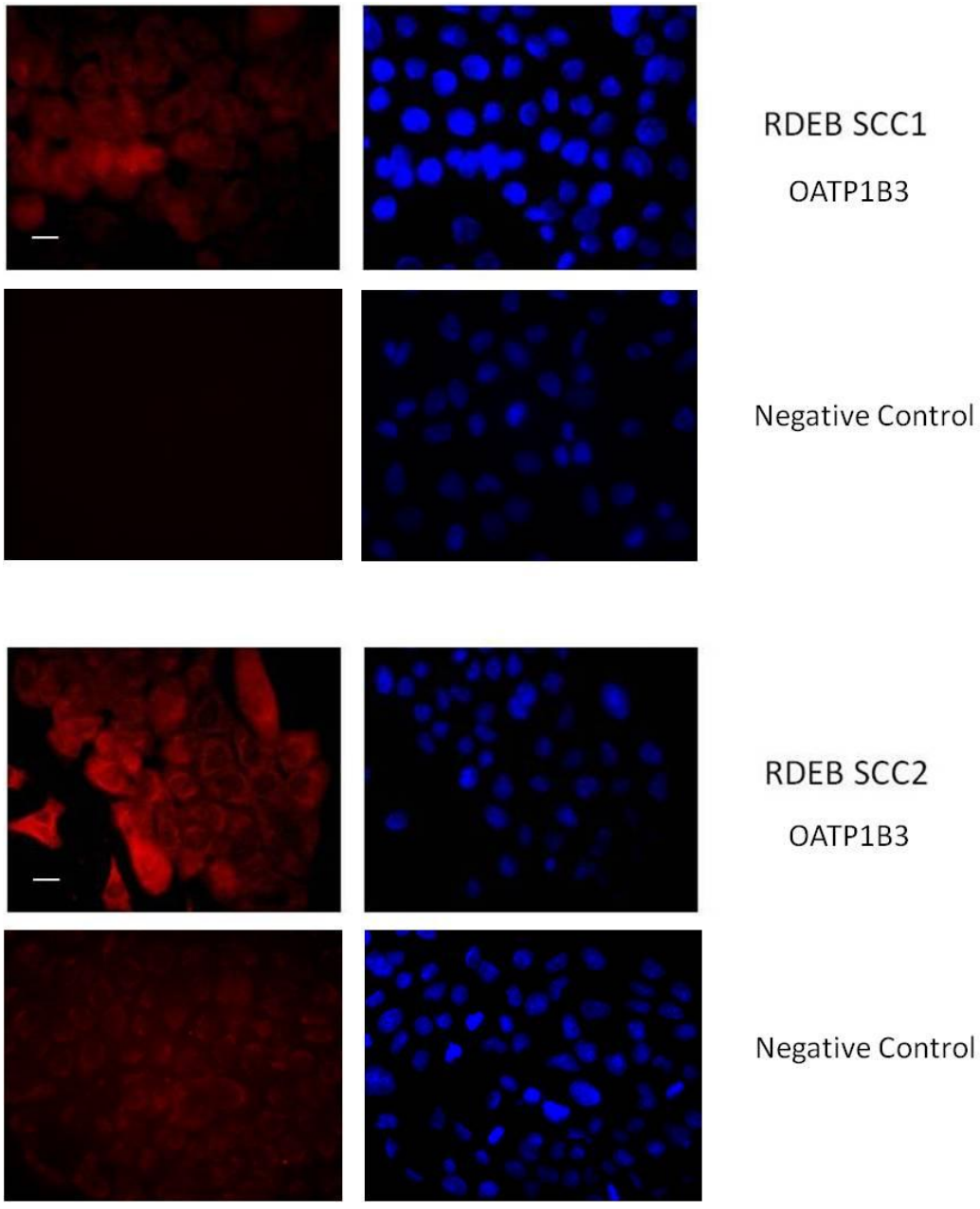
RDEB SCC1
OATP1B3
Negative Control
RDEB SCC2
OATP1B3
Negative Control

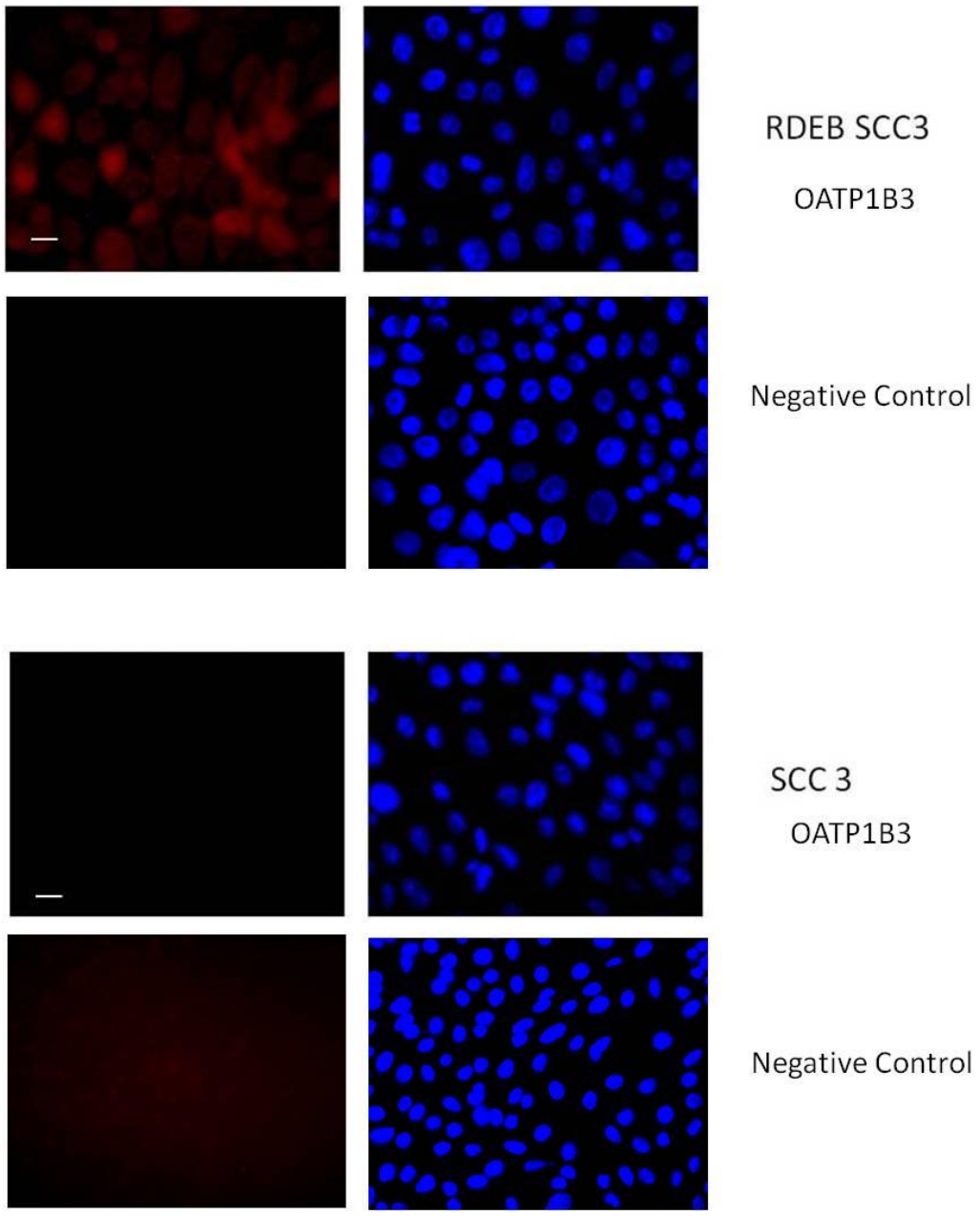

Figure 5.13 Immunofluorescence staining of 3 RDEB SCC cell lines, and 1 non-RDEB SCC cell line shows positive staining of OATP1B3 in RDEB SCC. Panels on the left show OATP1B3 positive staining in Red, with RDEB SCC 2 showing the strongest expression. Panels on the right show blue nuclei staining as a positive control. Negative control panels are used as a control, with cells exposed to the secondary antibody only. Scale bar ~20µm, images taken under 40x objective.

Having confirmed the expression of the protein in RDEB SCC, it still leaves the question; is it an active transporter in these cells, open to further investigation. The two different uptake assays used were unable to draw any OATP1B3 specific conclusions regarding the function of this transporter in RDEB SCC cells, and therefore directs our need towards a completely different and yet sensitive method for assessing OATP1B3 activity.

OATP1B1 and OATP1B3 transport the liver toxin Microcystin-LR, a toxin produced by blue green algal blooms; ingestion of which causes liver failure. Studies have shown that this toxin and other microcystin analogues are specifically transported into hepatocytes by the two liver specific OATPs (Monks et al. 2007). To further investigate to transporter function of OATP1B3 in RDEB SCC and to establish whether it is possible to selectively kill SCC cells based on their OATP1B3 expression, the MTS assay was used to measure the cell viability after exposure to Microcystin-LR (detailed methods can be found in Chapter 2 Section 2.2.5.0).

Results using the RDEB SCC 1 SLC cells over-expressing OATP1B3 and the empty vector control cells, indicates MC-LR does in fact cause cell death in RDEB SCC SLC cells, whilst the empty vector cells only show a small reduction in cell viability after exposure to 1μM MC-LR for 48 hours (Figure 5.14). These results indicate that OATP1B3 expression mediates transport of this toxin into RDEB SCC. To validate this experiment further a positive control is needed, one of two approaches could be used; firstly knock-down of *SLCO1B3* expression in the over-expressing cells to see if the toxicity of MC-LR is attenuated by lack of OATP1B3 expression or secondly use a hepatocyte cell line which is known to express OATP1B3 and transport MC-LR.

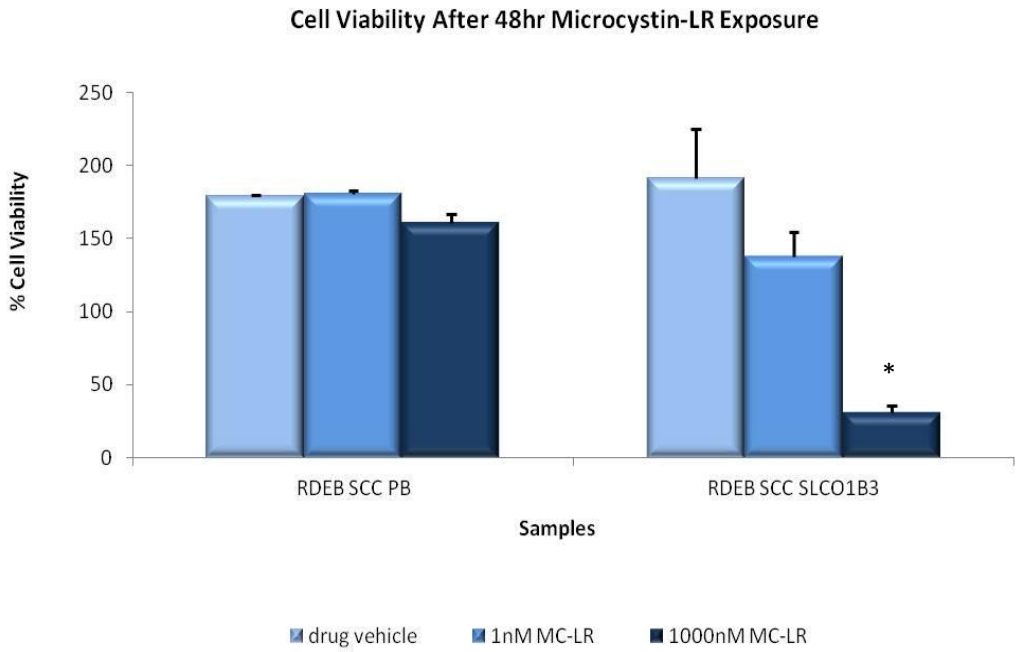

Figure 5.14 Preliminary results using the MTS assay, show that OATP1B3 over expressing cells have decreased cell viability after 48 hours exposure to 1nM and 1µM of Microcystin-LR (MC-LR). RDEB SCC 1 Pb shows a slight decrease in cell viability after 48 hrs exposure to 1µM MC-LR, whilst both 1nM and 1µM decrease cell viability in RDEB SCC 1 SLC cells. Samples represent biological replicates (n=4). Significant difference p=<0.05 denoted at *

5.2.4 Optimisation of siRNA knockdown of *SLCO1B3*

Small interfering RNA (siRNA) are short RNA sequences which can be used to transcriptionally repress genes, can provide another strategy for investigating the functional significance of OATP1B3 expression in cells. Furthermore future transport assays used to demonstrate OATP1B3 expression can be confirmed by knocking-down expression of the gene to demonstrate attenuation of the transport of a particular substrate in cells expression *SLCO1B3.* Transfecting RDEB SCC 1 cells with a pool of 3 siRNAs targeting *SLCO1B3* and culturing cells for a further 48 hours shows that *SLCO1B3* expression is

reduced by 40% at the mRNA level in comparison the untransfected control cells (Figure 5.15), the level of knockdown was measured using qRT-PCR. This reduction is also seen in comparison to the mock transfected cells and the cells transfected with a non-targeting scrambled siRNA. This assay has been optimised and could potentially be used to confirm future assay results by preventing expression of OATP1B3 and thus reducing transport in uptake assays or used in cell viability assays to prevent a reduction in cell viability after exposure to MC-LR in OATP1B3 expressing cells thus confirm that OATP1B3 mediated uptake was responsible for the intake of toxins into the cells causing apoptosis. However, time constraints have prevented these experiments being carried out. Had time not been an issue, it would also be possible to repeat the knockdown of OATP1B3 in RDEB SCC cells to establish if this alone would have an effect on the viability of the cell.

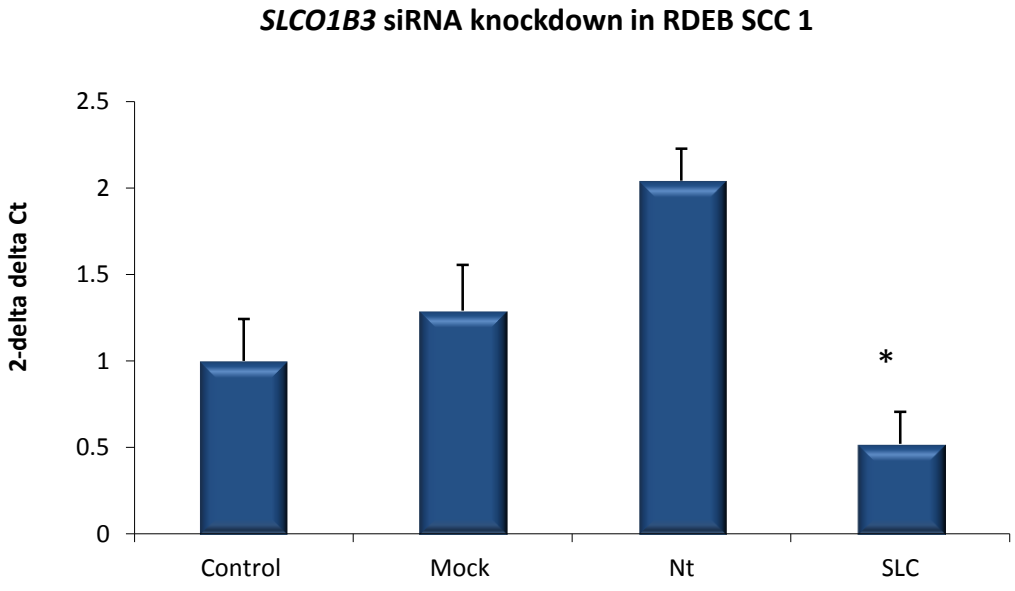

Figure 5.15 Knockdown can be achieved using a pool of 3 *SLCO1B3* specific siRNA oligonucleotides. siRNA knockdown is achieved up to 48hours after transfection of RDEB SCC 1 cells with siRNA specific to *SLCO1B3*. Knockdown is 40% lower than that of the control and mock cells. Samples represent technical replicates (n=3)

5.3 Discussion

The expression of *SLCO1B3* in RDEB SCC is an appealing therapeutic target as it is an organic anion transporter normally only expressed in the liver. In theory this would provide a physical mechanism for drug delivery, whilst minimising the off target effects and systemic toxification to other organs often seen when using common chemotherapy regimens, as the protein is only expressed in the liver.

5.3.1 *SLCO1B3* expression does translate to an OATP1B3 expression

We have been able to confirm that the OATP1B3 protein encoded by *SLCO1B3* is expressed in RDEB SCC by immunofluorescent staining of keratinocytes (Figure 5.12); furthermore OATP1B3 is expressed in RDEB SCC tissue (Figure 5.11). In RDEB SCC cultures, the cytoplasmic expression was mainly seen, whilst in the RDEB SCC keratinocytes exogenously over-expressing OATP1B3 demonstrated a membrane bound localisation. Although the cultured RDEB SCC cells lack the obvious membrane bound staining seen in liver hepatocytes and *SLCO1B3* over-expressing cells, this could be a result of the low level of expression in culture which means that the protein is undetectable in the cell membranes. Cytoplasmic expression is also seen in colon tumours which have shown a correlation between expression and prognosis based on improved 5-year survival, and with poorly differentiated tumours (Lockhart et al. 2008). This is concordant with a report that OATP1B3 expression is associated with better prognosis based on differentiation of tumours in breast cancer (Muto et al. 2007). No studies have yet determined whether the expression of OATP1B3 in the cytoplasm of tumour cells confers an altered cellular behaviour.

5.3.2 Uptake assays were an ineffective measure of transport activity

Confirming the expression of this gene at the protein level has opened up a number of questions regarding OATP1B3 tumoural expression. The normal function of OATP1B3 in hepatocytes is to transport molecules from the blood into liver cells, where it facilitates the accumulation of compounds prior to metabolising and biliary secretion (Smith et al. 2005), it is pertinent to establish if this transporter function is retained in RDEB SCC cells. Two transport assays were conducted to investigate the transport function of OATP1B3 in RDEB SCC cells. Results from both assays showed a dose dependent uptake of the substrate into RDEB SCC keratinocytes (Figures 5.2 and 5.4); however neither were able to demonstrate that the uptake of substrates was dependent and specific on OATP1B3 expression. The inability of these assays could be due to low expression of the protein, which despite its induction in RDEB SCC, it may be too low to demonstrate uptake above the background seen by natural diffusion of substrates, or movement of substrates via other transporter proteins. Also, it has been reported that SNPs that occur in *SLCO1B3* can cause changes to the transport function of OATP1B3 by direct conformational changes of the protein or be changes in affinity to certain substrates. The first SNP identified in *SLCO1B3* were within the non coding region and included a non-synonymous two now common SNPs; 334T>G and 699G>A and one rare (1546G>T) SNP (Iida et al. 2001). Functional analysis of these SNP have demonstrated that they cause alterations of the transport function and the cellular localisation of the protein (Letschert et al. 2004). Other transport assays have been developed and used in OATP studies which may be more amenable to the use with *SLCO1B3* expression in RDEB SCC, including using *Xenopus Laevis* oocytes injected with cRNA of the OATP1B3. One study, using this method was able to show the anticancer drugs Docetaxel and Paclitaxel were taken up into cells more so by OATP1B3 than OATP1B1, by a 2.2 and 3.3 fold higher, respectively (Smith et al. 2005).

In retrospect, looking at the transporter activity experiments used, it would be important to use a positive control for these experiments. This could be doing using a liver cells grown in culture, particularly a well known hepatoma cell known; HepG2. Also, when performing tritiated assays, other controls could be performed to establish the number of counts generated by the scintillation counter by directly measuring various concentrations of tritiated β-estradiol diluted in emulsifier. This would help determine if lower count numbers seen in some of the repeated assays are resulting from the experiment failing or that there is just a low count number for those particular cells in question. Further still, this would help ascertain whether the other substrates used; such as Rifampicin or Clotrimazole are having an effect on the counts in each experiment, as appropriate controls are carried out to help clarify this in each run of the assay.

Other limitations of the uptake assays are that the lysing of the cells doesn't produce a clear lysate that may affect the luminometer results for the Fluo-3 experiment. Whilst inadequate cell lysis may skew results as the substrates are not entirely released in to the lysate and therefore an inaccurate reading is taken. This is a limitation of both the Fluo-3 assay and the β-estradiol assay. Other methods of lysis could be used, and some were tried in these experiments to over-come these problems, including using different methods to homogenise the lysate, such as passing the lysate through a syringe however this did not over-come this problem.

5.3.3 Future work should involve the investigation of *COL7A1* on *SLCO1B3* promoter activity

Due to time restrictions, promoter studies to investigate the regulation of *SLCO1B3* expression via *COL7A1* were not carried out. This remains an important question in relation to the expression of *SLCO1B3* and the primary disease, RDEB. If future studies confirm that *COL7A1* does regulate the expression of *SLCO1B3* it would be interesting to see if this is then linked to cancer initiation in these patients. A simple basis to further expand this theory may to look at cell growth and proliferation using the MTS assay and cell migration using scratch wound assays to establish if *SLCO1B3* expressing cells have a growth advantage over those without expression of this transporter.

Further promoter studies that could be conducted include; DNAse I footprint analyses using RDEB SCC keratinocytes with and without *COL7A1* expression and control lysates. This would determine cell type specific binding of proteins to the promoter region (Jung et al. 2001). Site directed mutagenesis can be used to alter the minimal promoter region, and to determine the critical regions required for expression in RDEB SCC keratinocytes. It is however, possible that *COL7A1* regulates the expression of *SLCO1B3* at the post transcriptional level in which case mRNA transcription can be investigated using nuclear run on assays. Also, in relevance to RDEB, it would be important to establish if the expression of specific Type VII collagen domains are sufficient to drive the suppression of *SLCO1B3* transcriptional activity in RDEB SCC.

One could speculate that perhaps it is not *SLCO1B3* promoter that is directly affected by Type VII Collagen. It may be that the Type VII Collagen acts as a ligand to a regulator of

SLCO1B3 expression such as *PXR*, *FXR* or *HNF4A.* It could also be possible that *SLCO1B3* is expression is related to a feedback loop that is triggered by a reduction in Type VII Collagen in RDEB skin, which leads to the expression of OATP1B3 to specifically increase uptake of steroids into the skin such as estrogen which is a regulator of collagen synthesis. This mechanism could be tested by measuring estrogen levels inside keratinocytes expressing *COL7A1* at normal levels and those with a reduced expression, along with testing the differences caused by reduced and enhanced expression of *SLCO1B3*. Further work is required to elucidate the mechanism and link between *COL7A1* expression and *SLCO1B3* expression in RDEB SCC.

5.3.4 OATP1B3 is a potential target for selective killing of RDEB SCC cells

To conclude, OATP1B3 is expressed at both the mRNA and protein level in RDEB SCC and RDEB SCC tissue. Functional assay were unable to determine specific OATP1B3 mediated transport, however cell viability can be used to establish if cells can be selectively killed based on the expression of OATP1B3. These results further confirm that *SLCO1B3* represents a potential therapeutic target in RDEB SCC, and a physical pathway for delivering anti-neoplastic drugs specifically to tumour cells thus preventing systemic damage to healthy cells. It remains a pertinent question, however, to the functional consequence of OATP1B3 expression in tumours, in terms of whether this protein is creating a growth and survival advantage to the tumour cells, or is its over-expression just the result of genetic instability as a consequence of tumour development.

Chapter 6

Final Conclusion and Future Work

The main treatment regime used to tackle SCC that develop in RDEB patients is surgical excision, other conventional cancer treatments such as chemotherapy only impede the primary disease management in RDEB patients. These patients are susceptible to life threatening infections due to chronic open wounds and system toxicity induced by chemotherapy only puts pressure on their already over burdened immune system thus reducing tumour cell immune-surveillance. Therefore, adjuvant therapies are rarely used in this patient group, unlike in those who develop UV-induced SCC, who may be administered adjuvant chemotherapy in cases where patients present with an invasive and or metastatic tumour.

RDEB patients already suffer from considerable morbidity caused by their primary disease; the development of SCC is undoubtedly a “ticking time bomb” in these patients whilst clinicians and researchers are still uncertain as to the exact pathophysiology and what genetic aberrations causes the development of SCC in these patients, it is highly likely that they will develop SCC at some point in their lives, with a 75% cumulative risk by the age of 45 (Fine et al. 2009). This is hampered further by the aggressive nature and metastatic potential of these tumours which are habitually treated by surgical excision and remain the leading cause of mortality in RDEB suffers. This clearly outlines a clinical need for the research into RDEB specific therapeutic targets of SCC, in the hope to find and develop a therapeutic treatment strategy that provides a better prognosis if not a cure for SCC in these patients.

6.1 Summary of *TP53* status in RDEB SCC keratinocytes

mRNA expression analysis and direct sequencing revealed that p53 isoforms are not differentially expressed between RDEB associated SCC and non-RDEB SCC. Furthermore, the mutation spectrum is not unique in either sample set, and no common mutations were found. However, it is yet to be elucidated as to the effects of these mutations on the function of p53 and its downstream targets in these SCC samples, although with its interplay with other signalling pathways.

Given that 100% of SCC samples studied harboured p53 mutations this is an interesting gene to consider in SCC development. Especially the GOF effects of specific mutanats which could be confirmed by further experiments using siRNA knockdown of wt-p53 and mutant p53 and establishing if there are any differences in selected target genes. Further experiments could be performed to investigate the functional consequences of all the mutations identified. Another prospective avenue of investigation is to establish the p53 isoform expression in RDEB skin to determine whether p53 is an early event in the multi-step process of tumourigenesis in these patients. Also, one RDEB SCC keratinocyte sample was found to harbour a UV-signature mutation, this is somewhat unusual and unexpected. Due to the severity of the chronic wounds and generalised skin involvement in RDEB patients, they tend to have wounds bandaged and as this is where the tumours develop it seems unlikely to have been caused by UV-damage. It is most likely that the CC to TT mutation in the RDEB SCC samples was caused by other means than UV radiation.

6.2 Genome wide expression profiling and qRT-PCR suggests RDEB SCC and non-RDEB SCC are genetically similar

Analysis of the genome wide expression array identified only 36 genes with significantly different expression levels between RDEB SCC and non-RDEB SCC keratinocytes, suggesting the two SCC groups are not significantly different. However, the dysregulation of these 36 genes may hold the reason to the aggressive behaviour of these tumours and give them metastatic potential to spread. Microarray analysis and qRT-PCR has identified 14 genes that demonstrate the same trend of expression in terms of up and down regulation in RDEB SCC compared to non-RDEB SCC keratinocytes, however only 5 of which were significantly different in both experiments. This study did confirm that RDEB SCC and non-RDEB are not significantly genetically different with 22 of the genes showing opposing trends of expression in the microarray and qRT-PCR. Whilst the main aim of this thesis has been to identify candidate therapeutic targets of RDEB SCC, increasing the sample size may elaborate on whether the 11 genes that were not significantly differentially expressed in both experiments but showed the same pattern of expression are still important targets of RDEB SCC and also whether they may contribute to the highly malignant potential of the SCC keratinocytes in RDEB patients, by increasing the migration, invasion and overall metastatic potential of these cells. Functional assays could be utilised to investigate this are; siRNA screens, scratch wound assays and cell proliferation assays.

As the expression array suggests the two tumour types are more similar than different, it does question the role of the tumour microenvironment; which is the milieu of cells surrounding the tumour and may create a favourable environment which potentiates inflammation, tumour growth and progression. This has been implied by research that shows tumour-stromal fibroblasts are capable of remodelling the extracellular matrix to

favour tumour invasion (Gaggioli et al. 2007) and more recently, Erez and colleagues have shown cancer associated fibroblasts are able to support tumour growth by stimulating angiogenesis, proliferation and tumour enhancing inflammation (Erez et al. 2010).

In respect to identifying a RDEB specific therapeutics target, it is worth while considering that the RDEB keratinocytes have genes which are dysregulated in comparison to NHK. The original global expression array contained both sample groups and can be used to correlate genes which are then further dysregulated in the SCC samples and perhaps provide tumourigenic stimuli that initiate the carcinogenic conversion of keratinocytes in RDEB patients, Appendix 1.5 displays a table of genes derived from the microarray showing genes differentially regulated between NHK and EBK. A versatile study to validate these genes is to perform a siRNA screen of the tumour related genes and those which are consistently dysregulated in RDEB keratinocytes and further still in RDEB SCC keratinocytes. This method of investigation has been used to successfully identify therapeutics targets of SCC (Watt et al. 2011).

This study confirmed that in fact RDEB SCC and non-RDEB SCC are genetically similar. This has prompted research into other avenues of RDEB that could provide patients with a high risk of developing SCC. These avenues include work performed by Dr Andrew South's Laboratory; investigating the effects of *COL7A1* on RDEB SCC keratinocytes and the effect of re-expression. Also, of particular importance is whilst the genetic characterisations of RDEB SCC keratinocytes show mainly similarities that perhaps the tumour microenvironment is responsible for the high propensity of cutaneous SCC development and aggressive nature in

RDEB patient, therefore the characterisation RDEB SCC fibroblasts have become the objective of these studies.

6.2 *SLCO1B3,* an up-regulated organic anion transporter capable of transporting chemotherapeutic agents, is a potential therapeutic target of SCC specifically in RDEB patients

The most interesting finding of this investigation has been the identification of the over-expression of the organic anion transporter; *SLCO1B3* in RDEB associated SCC. Furthermore, in relation to the primary disease; RDEB, the re-expression of *COL7A1*; the gene whose genetic mutations give rise to the RDEB phenotype, reduce the expression of *SLCO1B3*. This is the first time an extracellular matrix protein has been known to possibly interact and transcriptionally suppress the expression of a membrane transporter protein. In culture the expression of *SLCO1B3* is low in comparison to tissue, and therefore using cultures cells may not have provided the ideal system to assay transport function. Even in the liver where this gene is normally expressed, serial passaging of cultured hepatocytes have been known to shown reduced and low expression of *SLCO1B3* (Konig et al. 2006).

Although the uptake studies did not successfully confirm the transport activity of OATP1B3 in RDEB SCC, this is in line with other uptake study reports that in fact use over-expression systems by creating cell lines to transiently or stably express OATP1B3 exogenously rather than performing these functional assays using the endogenous OATP1B3 expression (Cui et al. 2001; Baldes et al. 2006; Gui et al. 2008). Other uptake assays are available; such as utilizing *Xenopus laevis* oocytes as described by Ballestro and colleagues, and involves

injecting oocytes with the *SLCO1B3* cRNA so that the oocytes express the gene of interest, then perform the uptake assay (Ballestero et al. 2006).

This thesis documents the creation of an over-expression construct and stable expression of *SLCO1B3* in RDEB SCC 1 cells. This provides a cellular model that is more efficient for investigating transport of molecules via the OATP1B3 protein, and this is shown by cell viability assays using the MC-LR toxin which selectively kills cells based on the expression of *SLCO1B3*. This could also be used to investigate the transport and selective killing by chemotherapeutic agents known to be transported by *SLCO1B3*, to characterise the transport function in keratinocytes.

The over expression of *SLCO1B3* is reported in several cancers, including breast and brain tumours and has been suggested to play a role in the regulation of cellular processes such as proliferation and apoptosis (Bronger et al. 2005; Nozawa et al. 2005; Al Sarakbi et al. 2006). The underlying expression of OATP1B3 in cancer cells remains unclear, it is intriguing that a transporter protein which is more likely to be found liver and is linked to expression in tumours that have poor prognosis and lack response to available chemotherapy treatments (Ballestero et al. 2006) is expressed in cutaneous SCC in RDEB patients. The effect of the over-expression in RDEB SCC could be further investigated to establish what, if any, advantage the over-expression gives to the tumour cells. One study, has suggested that OATP1B3 over-expression in colorectal cancer cells confers anti-apoptotic mechanisms by altering the p53-dependent pathway, specifically reducing the transcriptional activity of p53 in over-expressing cells (Lee et al. 2008). This is not the case in RDEB SCC cells, as results in Chapter 1 demonstrate all 3 RDEB SCC keratinocyte cell lines

used over-express mutant p53, suggesting that other mechanisms may be occurring in these cells.

6.3 OATP1B3 as a cancer therapeutic target

As already mentioned, this transporter is known to be capable of transporting several anticancer drugs, such as Methotrexate, Paclitaxel, Docetaxel, and SN-38, an active metabolite of Irinotecan. The over-expression of OATP1B3 has been suggested to facilitate the accumulation of anti-cancer drugs in cells (Ichihara et al. 2010), given that over-expression is seen in RDEB SCC cells the accumulation of drugs delivered to cells via the OATP1B3 transporter would thereby enhance their cytotoxic effect. It has been documented in this thesis that the exogenous over-expression in RDEB SCCK mediates the uptake of MC-LR toxin into cells and effectively causes cell death.

The next step in this investigation would be to utilize the expression of OATP1B3 and the MTS assay to establish if a selection of anticancer drugs, such as Methotrexate and Paclitaxel are capable of causing cell death at low doses in RDEB SCCK in culture, and using cell lines not expressing SLCO1B3 as a control for necrotic cell death. In RDEB patients, treatment with the chemotherapeutic agent Methotrexate has been reported with limited success, and does not provide an effective treatment. Further still, the systemic side effects caused by these cancer therapeutics would be detrimental to RDEB patients. However, to establish transporter function *in vitro*, this could provide a good tool for this investigation. If this transporter proves to be a useful therapeutic target, the coupling of a pharmacological active agent to a ligand that is a substrate of OATP1B3 will create shuttle molecules that can be recognised by these transporter proteins (Tsuji 1999). When

considering using a transporter to facilitate the delivery of drugs to tumours cells, it is imperative to examine the expression of other transporters in these cells and essential to ensure drugs used are not substrates of other transporters such as MDR, MRP3, ATP binding cassette transporters and other OATP transporters. As the effect of other transporters may contribute to the failure of chemotherapy by efflux of the anticancer agents out of the cells (Leonard et al. 2003). As this study has confirmed that the SCC that develop in RDEB patients and the general population are genetically similar, further work is required to understand the mechanisms that underlie the aggressive nature of these tumours in RDEB patients.

Although the confirmation of OATP1B3 over-expression in RDEB SCC cells has identified a pathway that could be exploited to selectively target cancer cells with therapeutic agents, it could result in being more susceptible to chemotherapy resistance. This is a similar scenario to the over-expression of p-glycoprotein/MCR1 and breast cancer resistance protein/abcg2 which are known to confer chemotherapeutic resistance in malignant tumours (Perez-Tomas 2006).

To conclude, the over-expression of OATP1B3 provides a direct pathway for the delivery of drugs to cancer cells in RDEB patients. The validation of the transporter function of this protein in RDEB SCC keratinocytes will hopefully elucidate if indeed this pathway can be exploited for the therapeutic targeting of cancer cells specifically in RDEB patients whose tumours express *SLCO1B3*.

Appendices

Appendix 1.0 p53 mRNA expression by PCR amplification

A

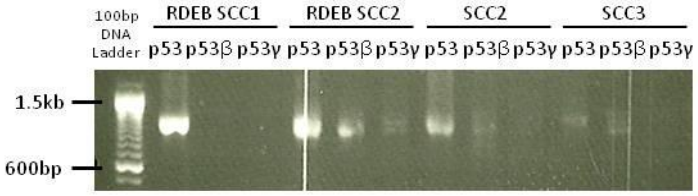

B

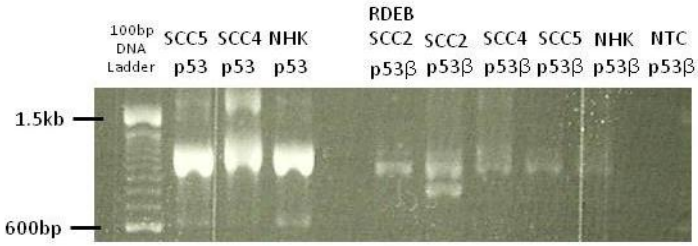

C

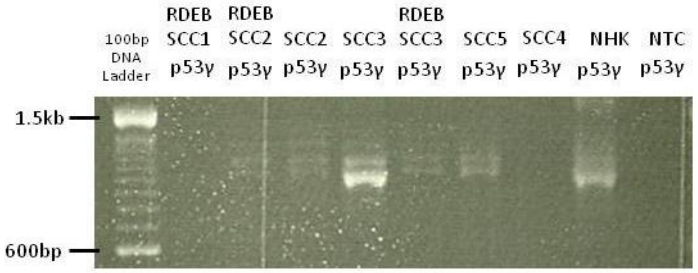

D

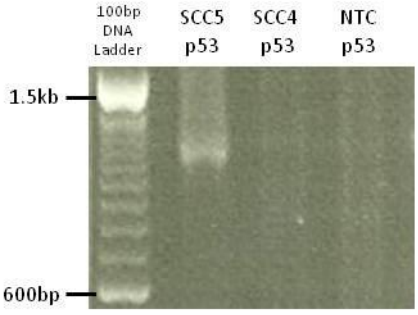

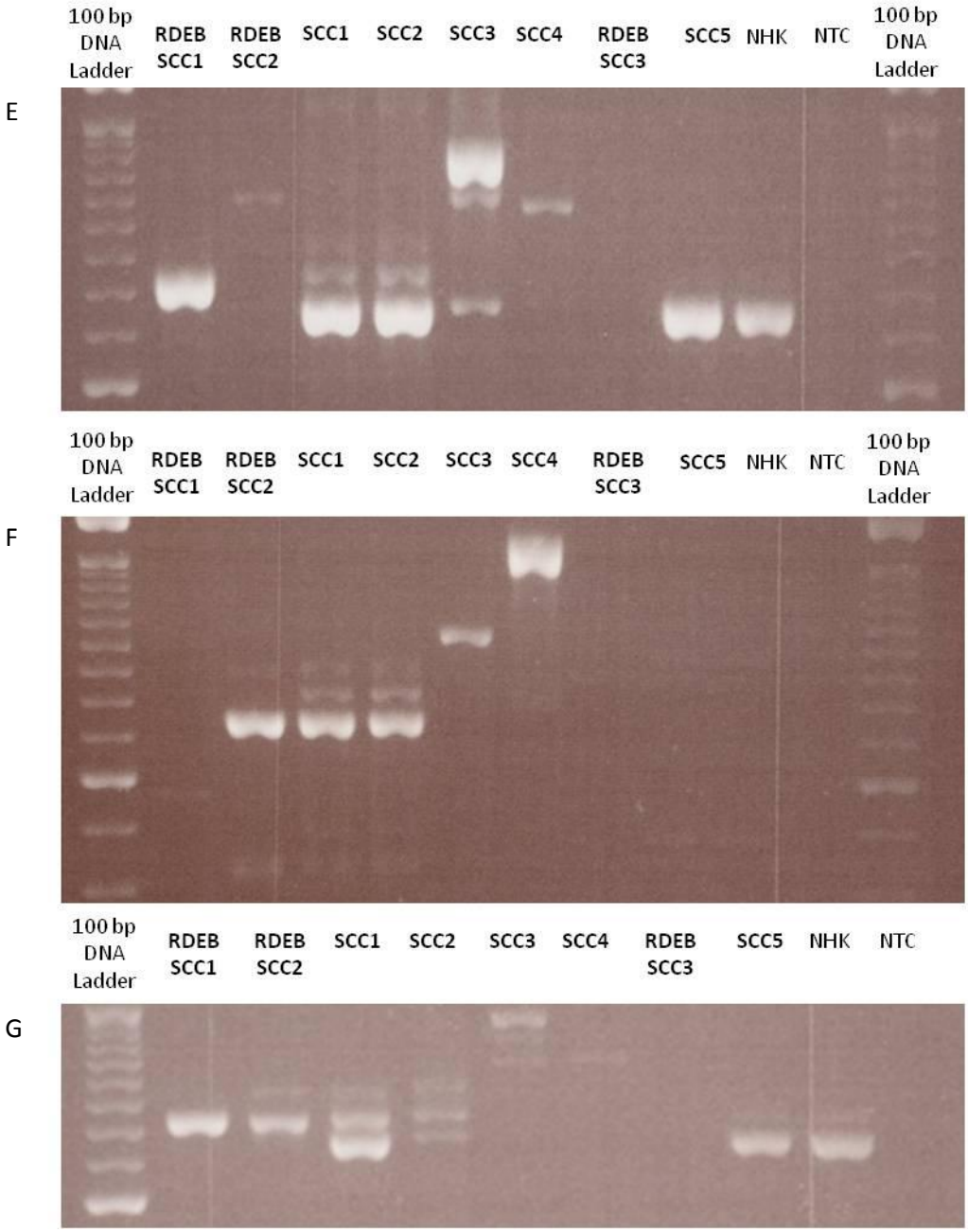

A) Amplification of p53, p53β, p53γ and in two independent RDEB SCC samples and two non-RDEB SCC samples. B) p53β was amplified in SCC (n=2) and NHK C) p53γ is amplified in RDEB SCC and non-RDEB SCC D) repeat of p53 amplification in SCC4 and SCC5 confirms no expression is seen in SCC4. E) Δp53 is amplified in 2 of 3 RDEB SCC samples and all 5 non-RDEB SCC samples. F) Δp53β was expressed in 2 of 3 RDEB SCC samples and 4 of 5 non-RDEB SCC samples G) Δp53γ is amplifiedin all non-RDEB SCC samples and only 2 of 3 RDEB SCC samples.

Appendix 1.1 p53 protein isoform expression

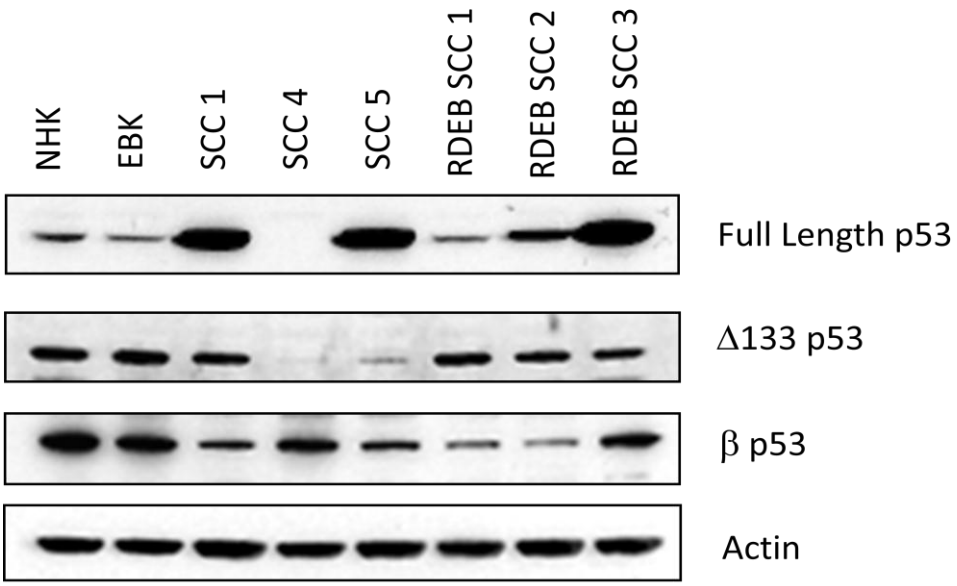

p53 protein isoform expression demonstrated by western blotting and performed by Dr Carol Hogan.

Appendix 1.2 Type VII Collagen Expression in RDEB SCC transduced cells

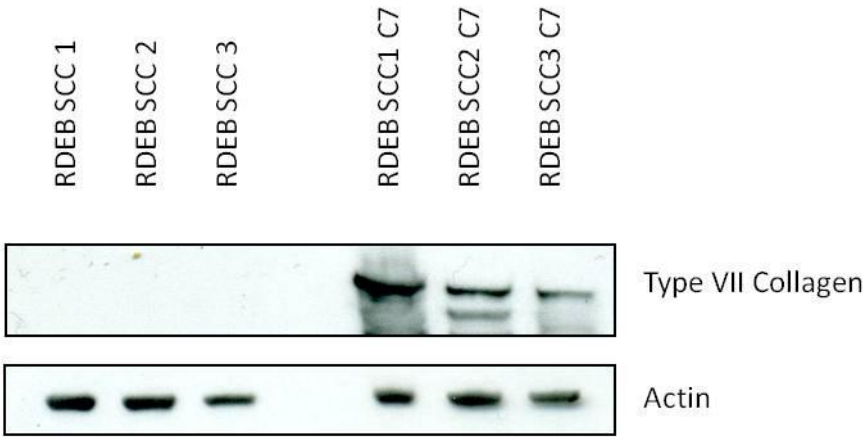

Type VII Collagen expression in RDEB SCC keratinocyte cell lines after being retrovirally transduced to re-express *COL7A* performed by Dr Celine Pourreyron.

Appendix 1.3 Commercially available antibodies used in Immunoblotting

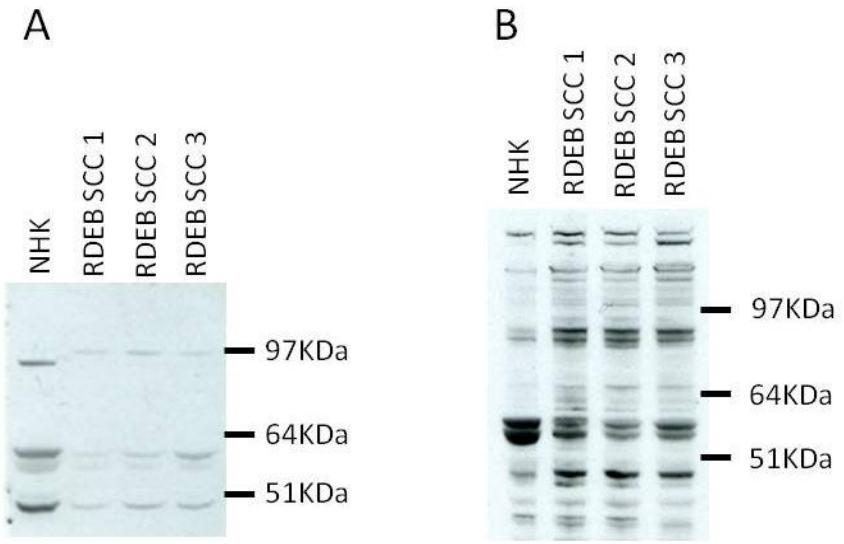

Commercially available antibodies against OATP1B3; A) Mouse OATP8 (Novus Biologicals) B) Goat C-14 (Santa Cruz), show no specific OATP1B3 bands in RDEB SCC keratinocytes.

Appendix 1.4 Immunofluorescent staining of OATP1B3 in RDEB SCC tissue

A

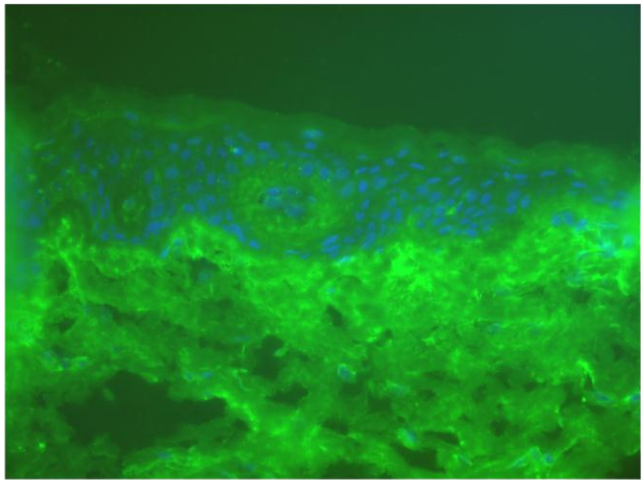

Normal skin 1/500 – dermis background

B

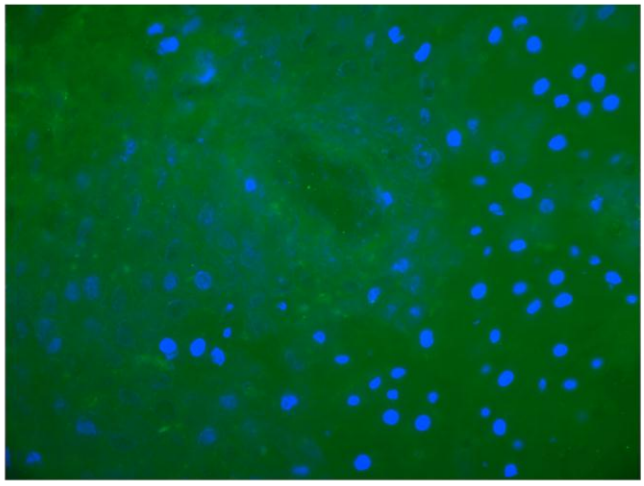

RDEB SCC8 1/500

C

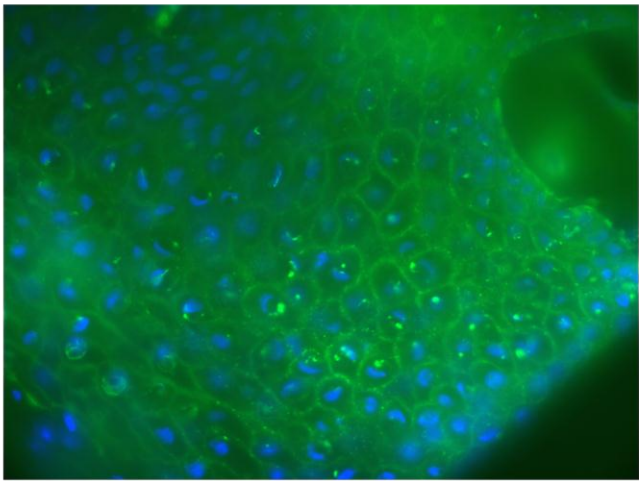

RDEB SCC37 1/500

Immunoflourescent staining using OATP1B3 D-16 antibody at a dilution of 1 in 500. A) Normal Dermis, B and C) two independent RDEB SCC tissues.

Appendix 1.5 NHK vs EBK gene list generated from the microarray analysis

GI Number	Gene Name	Chromosome	Fold Change	*p* value
GI_6138970-S	*ACP5*	19p13.3-p13.2	2.204873	0.000919
GI_4557342-S	*ALDH7A1*	5q31	2.678544	0.002105
GI_4826642-S	*ANXA3*	4q13-q22	0.367718	0.000287
GI_21361257-S	*RND3*	2q23.3	0.175303	0.000229
GI_20357534-S	*ATP6V1G1*	9q32	0.415318	0.000254
GI_40353770-S	*BOP1*	8q24.3	0.488506	0.000318
GI_8922518-S	*C14orf104*	14q22.1	1.868757	0.000485
GI_42476067-S	*C20orf30*	20p12.3	0.165571	0.000052
GI_9951924-S	*CA12*	15q22	0.547859	0.004343
GI_7706340-S	*YPEL5*	2p23.1	3.990615	0.000749
GI_11641403-S	*CKMT1*	15q15	0.517688	0.002523
GI_18765747-A	*COL18A1*	21q22.3	4.393860	0.004956
GI_38569504-A	*DDX52*	17q21.2	4.256464	0.000329
GI_19923594-S	*DDX54*	12q24.13	0.484485	0.000405
GI_41393585-A	*DGKA*	12q13.3	0.150960	0.004932
GI_30153783-S	*DNAH17*	17q25.3	2.515196	0.000471
GI_7657036-I	*DOC1*	3q12.1	0.020676	0.000020
GI_32967308-S	*EPHA1*	7q34	0.202338	0.002333
GI_10518499-S	*F3*	1p22-p21	4.169823	0.000254
GI_34304362-S	*FADS3*	11q12-q13.1	0.298760	0.000997
GI_17149847-S	*FKBP5*	6p21.3-p21.2	0.181001	0.000931
GI_39725951-S	*AGGF1*	5q13.3	4.264469	0.000130
GI_8922347-S	*TMEM39B*	1p35.1	2.987290	0.000995
GI_8922706-S	*TMEM34*	4q31.23	0.512801	0.000961
GI_40254892-S	*FLJ11273*	6q13	0.355386	0.000183
GI_31377643-S	*ATAD1*	10q23.2	0.455931	0.000103
GI_31377616-S	*HERPUD2*	7p14.2	0.322850	0.004043
GI_31542744-S	*GPR177*	1p31.3	3.431327	0.000320
GI_20127628-S	*ZNF768*	16p11.2	1.851232	0.000852
GI_44680151-S	*FOSL2*	2p23.3	2.153615	0.000065
GI_20070269-S	*G0S2*	1q32.2-q41	0.073010	0.004104
GI_45359844-S	*G3BP2*	4q21.1	0.255402	0.002283

GI_24308156-S	*GBP3*	1p22.2	0.247191	0.002699
GI_20336263-A	*GGA2*	16p12	2.585786	0.002299
GI_18104958-S	*TXNDC9*	2q11.2	2.909977	0.001516
GI_13518031-S	*GLI3*	7p13	2.962542	0.000909
GI_4759061-A	*GPSN2*	19p13.12	0.193629	0.002040
GI_31542938-S	*HPGD*	4q34-q35	0.247527	0.002128
GI_15451900-S	*KCNK1*	1q42-q43	0.383427	0.000746
GI_45267831-S	*FASTKD2*	2q33.3	0.475805	0.000079
GI_42660245-S	*KIAA1305*	14q12	2.523499	0.003401
GI_39930390-S	*DIP2B*	12q13.12	6.234034	0.000259
GI_27894338-I	*KRT23*	17q21.2	0.141580	0.004818
GI_17318577-S	*KRT5*	12q12-q13	1.727019	0.000430
GI_42734380-S	*TYW3*	1p31.1	0.292116	0.000795
GI_37059758-S	*CD300LG*	17q21.31	0.203229	0.000203
GI_42659549-S	*LOC220906*	10p12.1	0.166582	0.000631
GI_37538380-S	*MGC87042*	7p15.3	0.318666	0.000320
GI_37542995-S	*LOC341315*	12q14.2	3.148946	0.000778
GI_37546020-S	*LOC374571*	14q32.33	0.078759	0.003857
GI_29735784-S	*PPP1R3E*	14q11.2	0.411220	0.000490
GI_29789400-S	*UBE2Q2*	15q24.2	0.154882	0.000044
GI_24475622-S	*MDK*	11p11.2	0.394566	0.003858
GI_42476197-S	*CCDC104*	2p16.1	0.296648	0.000220
GI_29729561-S	*MGC21874*	4p16.1	0.292934	0.002252
GI_39930530-S	*c3orf64*	3p14.1	0.332586	0.001208
GI_19923760-S	*MINPP1*	10q23	0.275762	0.002794
GI_6912507-S	*MMD*	17q	0.233155	0.003532
GI_29826286-I	*MRPL47*	3q26.33	3.544673	0.000947
GI_31543213-S	*MT1X*	16q13	0.365543	0.000839
GI_37537693-S	*MTMR6*	13q12	0.177049	0.000047
GI_16506290-S	*OSR2*	8q22.2	0.233719	0.002691
GI_38045914-S	*PAPPA*	9q33.2	0.303215	0.004735
GI_33386694-A	*PBEF1*	7q22.2	0.365580	0.001889
GI_5031976-I	*PBEF1*	7q22.2	0.230978	0.003355
GI_25777743-S	*PGBD3*	10q11	2.743783	0.000163
GI_34147645-S	*PLOD3*	7q22	3.445257	0.001989
GI_30795205-S	*PPP2R5A*	1q32.2-q32.3	3.046272	0.004080

GI_42476154-S	*PTMS*	12p13	3.035154	0.000549
GI_24416001-S	*UBR4*	1p36.13	0.331009	0.002991
GI_34147329-S	*RRS1*	8q13.1	4.372495	0.004953
GI_8400731-S	*SFRP1*	8p12-p11.1	6.242949	0.000024
GI_20336278-A	*SLC26A6*	3p21.3	0.365709	0.001452
GI_18765730-A	*SNAP23*	15q15.1	0.192280	0.004430
GI_29893560-S	*SNN*	16p13	0.338538	0.001565
GI_33386698-S	*TMSL1*	1p34.2	0.084730	0.002729
GI_32189375-S	*TRIP4*	15q22.31	0.300121	0.000105
GI_23308730-S	*TRIP6*	7q22	1.752771	0.000041
GI_23510347-S	*TTRAP*	6p22.3-p22.1	0.170801	0.000364
GI_19718775-S	*WEE1*	11p15.3-p15.1	2.889024	0.004871
GI_23199973-A	*WTAP*	6q25-q27	0.273361	0.003192
GI_39841070-S	*ZNF322B*	9q22.33	0.239149	0.000154

Table of genes differentially expressed between EBK and NHK, identified by microarray analysis.

References

Abe, T., M. Kakyo, T. Tokui, R. Nakagomi, T. Nishio, D. Nakai, H. Nomura, M. Unno, M. Suzuki, T. Naitoh, S. Matsuno and H. Yawo (1999). Identification of a novel gene family encoding human liver-specific organic anion transporter LST-1. J Biol Chem **274**(24): 17159-63.

Abe, T., M. Unno, T. Onogawa, T. Tokui, T. N. Kondo, R. Nakagomi, H. Adachi, K. Fujiwara, M. Okabe, T. Suzuki, K. Nunoki, E. Sato, M. Kakyo, T. Nishio, J. Sugita, N. Asano, M. Tanemoto, M. Seki, F. Date, K. Ono, Y. Kondo, K. Shiiba, M. Suzuki, H. Ohtani, T. Shimosegawa, K. Iinuma, H. Nagura, S. Ito and S. Matsuno (2001). LST-2, a human liver-specific organic anion transporter, determines methotrexate sensitivity in gastrointestinal cancers. Gastroenterology **120**(7): 1689-99.

Ahn, S. H., Y. M. Shah, J. Inoue, K. Morimura, I. Kim, S. Yim, G. Lambert, R. Kurotani, K. Nagashima, F. J. Gonzalez and Y. Inoue (2008). Hepatocyte nuclear factor 4alpha in the intestinal epithelial cells protects against inflammatory bowel disease. Inflamm Bowel Dis **14**(7): 908-20.

Akhurst, R. J. (2004). TGF beta signaling in health and disease. Nat Genet **36**(8): 790-2.

Akkiprik, M., O. Sonmez, B. M. Gulluoglu, H. B. Caglar, H. Kaya, P. Demirkalem, U. Abacioglu, M. Sengoz, A. Sav and A. Ozer (2009). Analysis of p53 gene polymorphisms and protein over-expression in patients with breast cancer. Pathol Oncol Res **15**(3): 359-68.

Al Sarakbi, W., R. Mokbel, M. Salhab, W. G. Jiang, M. J. Reed and K. Mokbel (2006). The role of STS and OATP-B mRNA expression in predicting the clinical outcome in human breast cancer. Anticancer Res **26**(6C): 4985-90.

Alam, M. and D. Ratner (2001). Cutaneous squamous-cell carcinoma. N Engl J Med **344**(13): 975-83.

Almaani, N., L. Liu, P. J. Dopping-Hepenstal, J. E. Lai-Cheong, A. Wong, A. Nanda, C. Moss, A. E. Martinez, J. E. Mellerio and J. A. McGrath (2011). Identical glycine substitution mutations in type VII collagen may underlie both dominant and recessive forms of dystrophic epidermolysis bullosa. Acta Derm Venereol **91**(3): 262-6.

Altschul, S. F., T. L. Madden, A. A. Schaffer, J. Zhang, Z. Zhang, W. Miller and D. J. Lipman (1997). Gapped BLAST and PSI-BLAST: a new generation of protein database search programs. Nucleic Acids Res **25**(17): 3389-402.

Appella, E. and C. W. Anderson (2001). Post-translational modifications and activation of p53 by genotoxic stresses. Eur J Biochem **268**(10): 2764-72.

Arbiser, J. L. (2007). Why targeted therapy hasn't worked in advanced cancer. J Clin Invest **117**(10): 2762-5.

Arbiser, J. L., C.-Y. Fan, X. Su, B. O. Van Emburgh, F. Cerimele, M. S. Miller, J. Harvell and M. Marinkovich (2004). Involvement of p53 and p16 Tumor Suppressor Genes in Recessive Dystrophic Epidermolysis Bullosa-Associated Squamous Cell Carcinoma. Journal of Investigative Dermatology **123**: 788-790.

Arbiser, J. L., C. Y. Fan, X. Su, B. O. Van Emburgh, F. Cerimele, M. S. Miller, J. Harvell and M. P. Marinkovich (2004). Involvement of p53 and p16 tumor suppressor genes in recessive dystrophic epidermolysis bullosa-associated squamous cell carcinoma. J Invest Dermatol **123**(4): 788-90.

Arbiser, J. L., J. D. Fine, D. Murrell, A. Paller, S. Connors, K. Keough, E. Marsh and J. Folkman (1998). Basic fibroblast growth factor: a missing link between collagen VII, increased collagenase, and squamous cell carcinoma in recessive dystrophic epidermolysis bullosa. Mol Med **4**(3): 191-5.

Armstrong, B. K. and A. Kricker (2001). The epidemiology of UV induced skin cancer. J Photochem Photobiol B **63**(1-3): 8-18.

Arnold, A. W., L. Bruckner-Tuderman, C. Zuger and P. H. Itin (2009). Cetuximab therapy of metastasizing cutaneous squamous cell carcinoma in a patient with severe recessive dystrophic epidermolysis bullosa. Dermatology **219**(1): 80-3.

Arwert, E. N., E. Hoste and F. M. Watt Epithelial stem cells, wound healing and cancer. Nat Rev Cancer **12**(3): 170-80.

Ashton, G. H. (2004). Kindler syndrome. Clin Exp Dermatol **29**(2): 116-21.

Ashton, G. H., W. H. McLean, A. P. South, N. Oyama, F. J. Smith, R. Al-Suwaid, A. Al-Ismaily, D. J. Atherton, C. A. Harwood, I. M. Leigh, C. Moss, B. Didona, G. Zambruno, A. Patrizi, R. A. Eady and J. A. McGrath (2004). Recurrent mutations in kindlin-1, a novel keratinocyte focal contact protein, in the autosomal recessive skin fragility and photosensitivity disorder, Kindler syndrome. J Invest Dermatol **122**(1): 78-83.

Aumailley, M., C. Has, L. Tunggal and L. Bruckner-Tuderman (2006). Molecular basis of inherited skin-blistering disorders, and therapeutic implications. Expert Rev Mol Med **8**(24): 1-21.

Ayman, T., O. Yerebakan, M. A. Ciftcioglu and E. Alpsoy (2002). A 13-year-old girl with recessive dystrophic epidermolysis bullosa presenting with squamous cell carcinoma. Pediatr Dermatol **19**(5): 436-8.

Baldes, C., P. Koenig, D. Neumann, H. P. Lenhof, O. Kohlbacher and C. M. Lehr (2006). Development of a fluorescence-based assay for screening of modulators of human organic anion transporter 1B3 (OATP1B3). Eur J Pharm Biopharm **62**(1): 39-43.

Ballestero, M. R., M. J. Monte, O. Briz, F. Jimenez, F. Gonzalez-San Martin and J. J. Marin (2006). Expression of transporters potentially involved in the targeting of cytostatic bile acid derivatives to colon cancer and polyps. Biochem Pharmacol **72**(6): 729-38.

Bastin, K. T., R. A. Steeves and M. J. Richards (1997). Radiation therapy for squamous cell carcinoma in dystrophic epidermolysis bullosa: case reports and literature review. Am J Clin Oncol **20**(1): 55-8.

Battle, M. A., G. Konopka, F. Parviz, A. L. Gaggl, C. Yang, F. M. Sladek and S. A. Duncan (2006). Hepatocyte nuclear factor 4alpha orchestrates expression of cell adhesion proteins during the epithelial transformation of the developing liver. Proc Natl Acad Sci U S A **103**(22): 8419-24.

Benhamou, S. and A. Sarasin (2000). Variability in nucleotide excision repair and cancer risk: a review. Mutat Res **462**(2-3): 149-58.

Blagosklonny, M., G. Wu, K. Somasundaram and W. Eldeiry (1997). Wild-type p53 is not sufficient for serum starvation-induced apoptosis in cancer cells but accelerates apoptosis in sensitive cells. Int J Oncol **11**(6): 1165-70.

Blohme, I. and O. Larko (1990). Skin lesions in renal transplant patients after 10-23 years of immunosuppressive therapy. Acta Derm Venereol **70**(6): 491-4.

Bodemer, C., S. I. Tchen, S. Ghomrasseni, S. Seguier, F. Gaultier, S. Fraitag, Y. de Prost and G. Godeau (2003). Skin expression of metalloproteinases and tissue inhibitor of metalloproteinases in sibling patients with recessive dystrophic epidermolysis and intrafamilial phenotypic variation. J Invest Dermatol **121**(2): 273-9.

Boldrup, L., J. C. Bourdon, P. J. Coates, B. Sjostrom and K. Nylander (2007). Expression of p53 isoforms in squamous cell carcinoma of the head and neck. Eur J Cancer **43**(3): 617-23.

Bolotin, D. and E. Fuchs (2003). Cancer: More than skin deep. Nature **421**(6923): 594-5.

Bomprezzi, R., M. Ringner, S. Kim, M. L. Bittner, J. Khan, Y. Chen, A. Elkahloun, A. Yu, B. Bielekova, P. S. Meltzer, R. Martin, H. F. McFarland and J. M. Trent (2003). Gene

expression profile in multiple sclerosis patients and healthy controls: identifying pathways relevant to disease. Hum Mol Genet **12**(17): 2191-9.

Boukamp, P. (2005). Non-melanoma skin cancer: what drives tumor development and progression? Carcinogenesis **26**(10): 1657-67.

Bourdon, J.-C., K. Fernandes, F. Murray-Zmijewski, G. Liu, A. Diot, D. P. Xirodimas, M. K. Saville and D. P. Lane (2005). p53 isoforms can regulate p53 transcriptional activity. Genes Dev. **19**(18): 2122-2137.

Bourdon, J. C., K. Fernandes, F. Murray-Zmijewski, G. Liu, A. Diot, D. P. Xirodimas, M. K. Saville and D. P. Lane (2005). p53 isoforms can regulate p53 transcriptional activity. Genes Dev **19**(18): 2122-37.

Bouwes Bavinck, J. N., D. R. Hardie, A. Green, S. Cutmore, A. MacNaught, B. O'Sullivan, V. Siskind, F. J. Van Der Woude and I. R. Hardie (1996). The risk of skin cancer in renal transplant recipients in Queensland, Australia. A follow-up study. Transplantation **61**(5): 715-21.

Brash, D. E. (2006). Roles of the transcription factor p53 in keratinocyte carcinomas. British Journal of Dermatology **154**(s1): 8-10.

Brash, D. E., J. A. Rudolph, J. A. Simon, A. Lin, G. J. McKenna, H. P. Baden, A. J. Halperin and J. Ponten (1991). A role for sunlight in skin cancer: UV-induced p53 mutations in squamous cell carcinoma. Proc Natl Acad Sci U S A **88**(22): 10124-8.

Briggaman, R. A. and C. E. Wheeler, Jr. (1975). Epidermolysis bullosa dystrophica-recessive: a possible role of anchoring fibrils in the pathogenesis. J Invest Dermatol **65**(2): 203-11.

Bronger, H., J. Konig, K. Kopplow, H. H. Steiner, R. Ahmadi, C. Herold-Mende, D. Keppler and A. T. Nies (2005). ABCC drug efflux pumps and organic anion uptake transporters in human gliomas and the blood-tumor barrier. Cancer Res **65**(24): 11419-28.

Brown, C. J., C. F. Cheok, C. S. Verma and D. P. Lane (2011). Reactivation of p53: from peptides to small molecules. Trends Pharmacol Sci **32**(1): 53-62.

Brown, C. J., S. G. Dastidar, S. T. Quah, A. Lim, B. Chia and C. S. Verma (2011). C-terminal substitution of MDM2 interacting peptides modulates binding affinity by distinctive mechanisms. PLoS One **6**(8): e24122.

Brown, V. L., C. A. Harwood, T. Crook, J. G. Cronin, D. P. Kelsell and C. M. Proby (2004). p16INK4a and p14ARF tumor suppressor genes are commonly inactivated in cutaneous squamous cell carcinoma. J Invest Dermatol **122**(5): 1284-92.

Bruckner-Tuderman, L., Y. Mitsuhashi, U. W. Schnyder and P. Bruckner (1989). Anchoring fibrils and type VII collagen are absent from skin in severe recessive dystrophic epidermolysis bullosa. J Invest Dermatol **93**(1): 3-9.

Bruckner-Tuderman, L., O. Nilssen, D. R. Zimmermann, M. T. Dours-Zimmermann, D. U. Kalinke, T. Gedde-Dahl, Jr. and J. O. Winberg (1995). Immunohistochemical and mutation analyses demonstrate that procollagen VII is processed to collagen VII through removal of the NC-2 domain. J Cell Biol **131**(2): 551-9.

Burch, J. M., H. Fassihi, C. A. Jones, S. C. Mengshol, J. E. Fitzpatrick and J. A. McGrath (2006). Kindler syndrome: a new mutation and new diagnostic possibilities. Arch Dermatol **142**(5): 620-4.

Burckhardt, G. and N. A. Wolff (2000). Structure of renal organic anion and cation transporters. Am J Physiol Renal Physiol **278**(6): F853-66.

Burgeson, R. E. (1993). Type VII collagen, anchoring fibrils, and epidermolysis bullosa. J Invest Dermatol **101**(3): 252-5.

Campbell, C., A. G. Quinn, Y. S. Ro, B. Angus and J. L. Rees (1993). p53 mutations are common and early events that precede tumor invasion in squamous cell neoplasia of the skin. J Invest Dermatol **100**(6): 746-8.

Cattori, V., B. Hagenbuch, N. Hagenbuch, B. Stieger, R. Ha, K. E. Winterhalter and P. J. Meier (2000). Identification of organic anion transporting polypeptide 4 (Oatp4) as a major full-length isoform of the liver-specific transporter-1 (rlst-1) in rat liver. FEBS Lett **474**(2-3): 242-5.

Chen, C., J. L. Stock, X. Liu, J. Shi, J. W. Van Deusen, D. A. DiMattia, R. G. Dullea and S. M. de Morais (2008). Utility of a novel Oatp1b2 knockout mouse model for evaluating the role of Oatp1b2 in the hepatic uptake of model compounds. Drug Metab Dispos **36**(9): 1840-5.

Chen, M., N. Kasahara, D. R. Keene, L. Chan, W. K. Hoeffler, D. Finlay, M. Barcova, P. M. Cannon, C. Mazurek and D. T. Woodley (2002). Restoration of type VII collagen expression and function in dystrophic epidermolysis bullosa. Nat Genet **32**(4): 670-5.

Cheng, X., J. Maher, C. Chen and C. D. Klaassen (2005). Tissue distribution and ontogeny of mouse organic anion transporting polypeptides (Oatps). Drug Metab Dispos **33**(7): 1062-73.

Cheok, C. F., C. S. Verma, J. Baselga and D. P. Lane (2011). Translating p53 into the clinic. Nat Rev Clin Oncol **8**(1): 25-37.

Chiaretti, S., X. Li, R. Gentleman, A. Vitale, M. Vignetti, F. Mandelli, J. Ritz and R. Foa (2004). Gene expression profile of adult T-cell acute lymphocytic leukemia identifies distinct subsets of patients with different response to therapy and survival. Blood **103**(7): 2771-8.

Cho, J. Y., J. Y. Lim, J. H. Cheong, Y. Y. Park, S. L. Yoon, S. M. Kim, S. B. Kim, H. Kim, S. W. Hong, Y. N. Park, S. H. Noh, E. S. Park, I. S. Chu, W. K. Hong, J. A. Ajani and J. S. Lee (2011). Gene expression signature-based prognostic risk score in gastric cancer. Clin Cancer Res **17**(7): 1850-7.

Cho, Y., S. Gorina, P. D. Jeffrey and N. P. Pavletich (1994). Crystal structure of a p53 tumor suppressor-DNA complex: understanding tumorigenic mutations. Science **265**(5170): 346-55.

Chopra, V., S. K. Tyring, L. Johnson and J. D. Fine (1992). Peripheral blood mononuclear cell subsets in patients with severe inherited forms of epidermolysis bullosa. Arch Dermatol **128**(2): 201-9.

Chorny, J. A., K. R. Shroyer and L. E. Golitz (1993). Malignant melanoma and a squamous cell carcinoma in recessive dystrophic epidermolysis bullosa. Arch Dermatol **129**(9): 1212.

Christiano, A. M., D. S. Greenspan, G. G. Hoffman, X. Zhang, Y. Tamai, A. N. Lin, H. C. Dietz, A. Hovnanian and J. Uitto (1993). A missense mutation in type VII collagen in two affected siblings with recessive dystrophic epidermolysis bullosa. Nat Genet **4**(1): 62-6.

Christiano, A. M., D. S. Greenspan, S. Lee and J. Uitto (1994). Cloning of human type VII collagen. Complete primary sequence of the alpha 1(VII) chain and identification of intragenic polymorphisms. J Biol Chem **269**(32): 20256-62.

Clayman, G. L., J. J. Lee, F. C. Holsinger, X. Zhou, M. Duvic, A. K. El-Naggar, V. G. Prieto, E. Altamirano, S. L. Tucker, S. S. Strom, M. L. Kripke and S. M. Lippman (2005). Mortality risk from squamous cell skin cancer. J Clin Oncol **23**(4): 759-65.

Collins, I. and P. Workman (2006). New approaches to molecular cancer therapeutics. Nat Chem Biol **2**(12): 689-700.

Cooper, H. L., I. S. Cook, J. M. Theaker, R. Mallipeddi, J. McGrath, P. Friedmann and E. Healy (2004). Expression and glycosylation of MUC1 in epidermolysis bullosa-associated and sporadic cutaneous squamous cell carcinomas. Br J Dermatol **151**(3): 540-5.

Coulombe, P. A., M. L. Kerns and E. Fuchs (2009). Epidermolysis bullosa simplex: a paradigm for disorders of tissue fragility. J Clin Invest **119**(7): 1784-93.

Coussens, L. M. and Z. Werb (2002). Inflammation and cancer. Nature **420**(6917): 860-7.

Cruickshank, A. H., E. M. McConnell and D. G. Miller (1963). Malignancy in Scars, Chronic Ulcers, and Sinuses. J Clin Pathol **16**: 573-80.

Cui, Y., J. Konig and D. Keppler (2001). Vectorial transport by double-transfected cells expressing the human uptake transporter SLC21A8 and the apical export pump ABCC2. Mol Pharmacol **60**(5): 934-43.

Cui, Y., J. Konig, I. Leier, U. Buchholz and D. Keppler (2001). Hepatic uptake of bilirubin and its conjugates by the human organic anion transporter SLC21A6. J Biol Chem **276**(13): 9626-30.

Dajee, M., M. Lazarov, J. Y. Zhang, T. Cai, C. L. Green, A. J. Russell, M. P. Marinkovich, S. Tao, Q. Lin, Y. Kubo and P. A. Khavari (2003). NF-kappaB blockade and oncogenic Ras trigger invasive human epidermal neoplasia. Nature **421**(6923): 639-43.

Daley, G. Q., R. A. Van Etten and D. Baltimore (1990). Induction of chronic myelogenous leukemia in mice by the P210bcr/abl gene of the Philadelphia chromosome. Science **247**(4944): 824-30.

Dang, N. and D. F. Murrell (2008). Mutation analysis and characterization of COL7A1 mutations in dystrophic epidermolysis bullosa. Exp Dermatol **17**(7): 553-68.

Dazard, J. E., H. Gal, N. Amariglio, G. Rechavi, E. Domany and D. Givol (2003). Genome-wide comparison of human keratinocyte and squamous cell carcinoma responses to UVB irradiation: implications for skin and epithelial cancer. Oncogene **22**(19): 2993-3006.

De Luca, M., G. Pellegrini and F. Mavilio (2009). Gene therapy of inherited skin adhesion disorders: a critical overview. Br J Dermatol **161**(1): 19-24.

de Vries, A., E. R. Flores, B. Miranda, H. M. Hsieh, C. T. van Oostrom, J. Sage and T. Jacks (2002). Targeted point mutations of p53 lead to dominant-negative inhibition of wild-type p53 function. Proc Natl Acad Sci U S A **99**(5): 2948-53.

Dheda, K., J. F. Huggett, S. A. Bustin, M. A. Johnson, G. Rook and A. Zumla (2004). Validation of housekeeping genes for normalizing RNA expression in real-time PCR. Biotechniques **37**(1): 112-4, 116, 118-9.

Dittmer, D., S. Pati, G. Zambetti, S. Chu, A. K. Teresky, M. Moore, C. Finlay and A. J. Levine (1993). Gain of function mutations in p53. Nat Genet **4**(1): 42-6.

Dittrich, B., K. Buiting, B. Korn, S. Rickard, J. Buxton, S. Saitoh, R. D. Nicholls, A. Poustka, A. Winterpacht, B. Zabel and B. Horsthemke (1996). Imprint switching on human chromosome 15 may involve alternative transcripts of the SNRPN gene. Nat Genet **14**(2): 163-70.

Dooley, T. P., S. P. Reddy, T. W. Wilborn and R. L. Davis (2003). Biomarkers of human cutaneous squamous cell carcinoma from tissues and cell lines identified by DNA microarrays and qRT-PCR. Biochem Biophys Res Commun **306**(4): 1026-36.

Douki, T. and J. Cadet (2001). Individual determination of the yield of the main UV-induced dimeric pyrimidine photoproducts in DNA suggests a high mutagenicity of CC photolesions. Biochemistry **40**(8): 2495-501.

Dresser, M. J. (2001). The MDR1 C3435T polymorphism: effects on P-glycoprotein expression/function and clinical significance. AAPS PharmSci **3**(3): 3.

Druker, B. J., M. Talpaz, D. J. Resta, B. Peng, E. Buchdunger, J. M. Ford, N. B. Lydon, H. Kantarjian, R. Capdeville, S. Ohno-Jones and C. L. Sawyers (2001). Efficacy and safety of a specific inhibitor of the BCR-ABL tyrosine kinase in chronic myeloid leukemia. N Engl J Med **344**(14): 1031-7.

Erez, N., M. Truitt, P. Olson, S. T. Arron and D. Hanahan (2010). Cancer-Associated Fibroblasts Are Activated in Incipient Neoplasia to Orchestrate Tumor-Promoting Inflammation in an NF-kappaB-Dependent Manner. Cancer Cell **17**(2): 135-47.

Euvrard, S., J. Kanitakis and A. Claudy (2003). Skin cancers after organ transplantation. N Engl J Med **348**(17): 1681-91.

Featherstone, C. (2007). Epidermolysis bullosa: from fundamental molecular biology to clinical therapies. J Invest Dermatol **127**(2): 256-9.

Ferrer, J. (2002). A genetic switch in pancreatic beta-cells: implications for differentiation and haploinsufficiency. Diabetes **51**(8): 2355-62.

Fine, J.-D., L. B. Johnson, M. Weiner, A. Stein and C. Suchindran (2004). Chemoprevention of squamous cell carcinoma in recessive dystrophic epidermolysis bullosa: results of a phase 1 trial of systemic isotretinoin. Journal of the American Academy of Dermatology **50**(4): 563-571.

Fine, J. D. (2004). Possible role for sentinal node biopsy in the management of squamous cell carcinomas in inherited epidermolysis bullosa. Arch Dermatol **140**(8): 1012-3.

Fine, J. D., M. Hall, M. Weiner, K. P. Li and C. Suchindran (2008). The risk of cardiomyopathy in inherited epidermolysis bullosa. Br J Dermatol **159**(3): 677-82.

Fine, J. D., L. B. Johnson, M. Weiner, K. P. Li and C. Suchindran (2009). Epidermolysis bullosa and the risk of life-threatening cancers: the National EB Registry experience, 1986-2006. J Am Acad Dermatol **60**(2): 203-11.

Fleige, S. and M. W. Pfaffl (2006). RNA integrity and the effect on the real-time qRT-PCR performance. Mol Aspects Med **27**(2-3): 126-39.

Fleming, I. D., R. Amonette, T. Monaghan and M. D. Fleming (1995). Principles of management of basal and squamous cell carcinoma of the skin. Cancer **75**(2 Suppl): 699-704.

Frischmeyer, P. A. and H. C. Dietz (1999). Nonsense-mediated mRNA decay in health and disease. Hum Mol Genet **8**(10): 1893-900.

Fritsch, A., S. Loeckermann, J. S. Kern, A. Braun, M. R. Bosl, T. A. Bley, H. Schumann, D. von Elverfeldt, D. Paul, M. Erlacher, D. Berens von Rautenfeld, I. Hausser, R. Fassler and L. Bruckner-Tuderman (2008). A hypomorphic mouse model of dystrophic epidermolysis bullosa reveals mechanisms of disease and response to fibroblast therapy. J Clin Invest **118**(5): 1669-79.

Fuchs, E. and S. Raghavan (2002). Getting under the skin of epidermal morphogenesis. Nat Rev Genet **3**(3): 199-209.

Gaggioli, C., S. Hooper, C. Hidalgo-Carcedo, R. Grosse, J. F. Marshall, K. Harrington and E. Sahai (2007). Fibroblast-led collective invasion of carcinoma cells with differing roles for RhoGTPases in leading and following cells. Nat Cell Biol **9**(12): 1392-400.

Gailit, J., M. P. Welch and R. A. Clark (1994). TGF-beta 1 stimulates expression of keratinocyte integrins during re-epithelialization of cutaneous wounds. J Invest Dermatol **103**(2): 221-7.

Giaccia, A. J. and M. B. Kastan (1998). The complexity of p53 modulation: emerging patterns from divergent signals. Genes Dev **12**(19): 2973-83.

Giglia-Mari, G. and A. Sarasin (2003). TP53 mutations in human skin cancers. Hum Mutat **21**(3): 217-28.

Goh, A. M., C. R. Coffill and D. P. Lane (2010). The role of mutant p53 in human cancer. J Pathol **223**(2): 116-26.

Gordon, K. J. and G. C. Blobe (2008). Role of transforming growth factor-beta superfamily signaling pathways in human disease. Biochim Biophys Acta **1782**(4): 197-228.

Goto, M., D. Sawamura, K. Ito, M. Abe, W. Nishie, K. Sakai, A. Shibaki, M. Akiyama and H. Shimizu (2006). Fibroblasts show more potential as target cells than keratinocytes in COL7A1 gene therapy of dystrophic epidermolysis bullosa. J Invest Dermatol **126**(4): 766-72.

Gray, T. A., S. Saitoh and R. D. Nicholls (1999). An imprinted, mammalian bicistronic transcript encodes two independent proteins. Proc Natl Acad Sci U S A **96**(10): 5616-21.

Gui, C., Y. Miao, L. Thompson, B. Wahlgren, M. Mock, B. Stieger and B. Hagenbuch (2008). Effect of pregnane X receptor ligands on transport mediated by human OATP1B1 and OATP1B3. Eur J Pharmacol **584**(1): 57-65.

Hagenbuch, B. and C. Gui (2008). Xenobiotic transporters of the human organic anion transporting polypeptides (OATP) family. Xenobiotica **38**(7-8): 778-801.

Hagenbuch, B. and P. J. Meier (2004). Organic anion transporting polypeptides of the OATP/ SLC21 family: phylogenetic classification as OATP/ SLCO superfamily, new nomenclature and molecular/functional properties. Pflugers Arch **447**(5): 653-65.

Hamada, A., T. Sissung, D. K. Price, R. Danesi, C. H. Chau, N. Sharifi, D. Venzon, K. Maeda, K. Nagao, A. Sparreboom, H. Mitsuya, W. L. Dahut and W. D. Figg (2008). Effect of SLCO1B3 haplotype on testosterone transport and clinical outcome in caucasian patients with androgen-independent prostatic cancer. Clin Cancer Res **14**(11): 3312-8.

Hanahan, D. and R. A. Weinberg (2000). The hallmarks of cancer. Cell **100**(1): 57-70.

Hasford, J., M. Baccarani, V. Hoffmann, J. Guilhot, S. Saussele, G. Rosti, F. Guilhot, K. Porkka, G. Ossenkoppele, D. Lindoerfer, B. Simonsson, M. Pfirrmann and R. Hehlmann (2011). Predicting complete cytogenetic response and subsequent progression-free survival in 2060 patients with CML on imatinib treatment: the EUTOS score. Blood **118**(3): 686-92.

Hofseth, L. J., S. P. Hussain and C. C. Harris (2004). p53: 25 years after its discovery. Trends in Pharmacological Sciences **25**(4): 177-181.

Hooiveld, G. J., J. E. van Montfoort, D. K. Meijer and M. Muller (2001). Function and regulation of ATP-binding cassette transport proteins involved in hepatobiliary transport. Eur J Pharm Sci **12**(4): 525-43.

Hovnanian, A., A. Rochat, C. Bodemer, E. Petit, C. A. Rivers, C. Prost, S. Fraitag, A. M. Christiano, J. Uitto, M. Lathrop, Y. Barrandon and Y. de Prost (1997). Characterization of 18 new mutations in COL7A1 in recessive dystrophic epidermolysis bullosa provides evidence for distinct molecular mechanisms underlying defective anchoring fibril formation. Am J Hum Genet **61**(3): 599-610.

Hsiang, B., Y. Zhu, Z. Wang, Y. Wu, V. Sasseville, W. P. Yang and T. G. Kirchgessner (1999). A novel human hepatic organic anion transporting polypeptide (OATP2). Identification of a liver-specific human organic anion transporting polypeptide and identification of rat and human hydroxymethylglutaryl-CoA reductase inhibitor transporters. J Biol Chem **274**(52): 37161-8.

Huang, S. (1999). Gene expression profiling, genetic networks, and cellular states: an integrating concept for tumorigenesis and drug discovery. J Mol Med (Berl) **77**(6): 469-80.

Hudson, L. G., J. M. Gale, R. S. Padilla, G. Pickett, B. E. Alexander, J. Wang and D. F. Kusewitt (2011). Microarray analysis of cutaneous squamous cell carcinomas reveals enhanced expression of epidermal differentiation complex genes. Mol Carcinog **49**(7): 619-29.

Huebner, R. J. and G. J. Todaro (1969). Oncogenes of RNA tumor viruses as determinants of cancer. Proc Natl Acad Sci U S A **64**(3): 1087-94.

Hupp, T. R., A. Sparks and D. P. Lane (1995). Small peptides activate the latent sequence-specific DNA binding function of p53. Cell **83**(2): 237-45.

Ichihara, S., R. Kikuchi, H. Kusuhara, S. Imai, K. Maeda and Y. Sugiyama (2010). DNA methylation profiles of organic anion transporting polypeptide 1B3 in cancer cell lines. Pharm Res **27**(3): 510-6.

Iida, A., S. Saito, A. Sekine, C. Mishima, K. Kondo, Y. Kitamura, S. Harigae, S. Osawa and Y. Nakamura (2001). Catalog of 258 single-nucleotide polymorphisms (SNPs) in genes encoding three organic anion transporters, three organic anion-transporting polypeptides, and three NADH:ubiquinone oxidoreductase flavoproteins. J Hum Genet **46**(11): 668-83.

Inman, G. J. (2011). Switching TGFbeta from a tumor suppressor to a tumor promoter. Curr Opin Genet Dev **21**(1): 93-9.

Ismair, M. G., B. Stieger, V. Cattori, B. Hagenbuch, M. Fried, P. J. Meier and G. A. Kullak-Ublick (2001). Hepatic uptake of cholecystokinin octapeptide by organic anion-transporting polypeptides OATP4 and OATP8 of rat and human liver. Gastroenterology **121**(5): 1185-90.

Itoh, M., M. Kiuru, M. S. Cairo and A. M. Christiano (2011). Generation of keratinocytes from normal and recessive dystrophic epidermolysis bullosa-induced pluripotent stem cells. Proc Natl Acad Sci U S A **108**(21): 8797-802.

Jensen, P., S. Hansen, B. Moller, T. Leivestad, P. Pfeffer, O. Geiran, P. Fauchald and S. Simonsen (1999). Skin cancer in kidney and heart transplant recipients and different long-term immunosuppressive therapy regimens. J Am Acad Dermatol **40**(2 Pt 1): 177-86.

Jigorel, E., M. Le Vee, C. Boursier-Neyret, M. Bertrand and O. Fardel (2005). Functional expression of sinusoidal drug transporters in primary human and rat hepatocytes. Drug Metab Dispos **33**(10): 1418-22.

Jobard, F., B. Bouadjar, F. Caux, S. Hadj-Rabia, C. Has, F. Matsuda, J. Weissenbach, M. Lathrop, J. F. Prud'homme and J. Fischer (2003). Identification of mutations in a new gene encoding a FERM family protein with a pleckstrin homology domain in Kindler syndrome. Hum Mol Genet **12**(8): 925-35.

Joerger, A. C. and A. R. Fersht (2007). Structural biology of the tumor suppressor p53 and cancer-associated mutants. Adv Cancer Res **97**: 1-23.

Johnson, T. M., D. E. Rowe, B. R. Nelson and N. A. Swanson (1992). Squamous cell carcinoma of the skin (excluding lip and oral mucosa). J Am Acad Dermatol **26**(3 Pt 2): 467-84.

Jung, D., B. Hagenbuch, L. Gresh, M. Pontoglio, P. J. Meier and G. A. Kullak-Ublick (2001). Characterization of the human OATP-C (SLC21A6) gene promoter and regulation of liver-specific OATP genes by hepatocyte nuclear factor 1 alpha. J Biol Chem **276**(40): 37206-14.

Jung, D., M. Podvinec, U. A. Meyer, D. J. Mangelsdorf, M. Fried, P. J. Meier and G. A. Kullak-Ublick (2002). Human organic anion transporting polypeptide 8 promoter is transactivated by the farnesoid X receptor/bile acid receptor. Gastroenterology **122**(7): 1954-66.

Kadir, A. R. (2007). Burn scar neoplasm. Ann Burns Fire Disasters **20**(4): 185-8.

Kato, S., S. Y. Han, W. Liu, K. Otsuka, H. Shibata, R. Kanamaru and C. Ishioka (2003). Understanding the function-structure and function-mutation relationships of p53 tumor suppressor protein by high-resolution missense mutation analysis. Proc Natl Acad Sci U S A **100**(14): 8424-9.

Kawabe, H., H. Nakanishi, M. Asada, A. Fukuhara, K. Morimoto, M. Takeuchi and Y. Takai (2001). Pilt, a novel peripheral membrane protein at tight junctions in epithelial cells. J Biol Chem **276**(51): 48350-5.

Kern, J. S., S. Loeckermann, A. Fritsch, I. Hausser, W. Roth, T. M. Magin, C. Mack, M. L. Muller, O. Paul, P. Ruther and L. Bruckner-Tuderman (2009). Mechanisms of fibroblast cell therapy for dystrophic epidermolysis bullosa: high stability of collagen VII favors long-term skin integrity. Mol Ther **17**(9): 1605-15.

Keswani, R. N., A. Noffsinger, I. Waxman and M. Bissonnette (2006). Clinical use of p53 in Barrett's esophagus. Cancer Epidemiol Biomarkers Prev **15**(7): 1243-9.

Khromova, N. V., P. B. Kopnin, E. V. Stepanova, L. S. Agapova and B. P. Kopnin (2009). p53 hot-spot mutants increase tumor vascularization via ROS-mediated activation of the HIF1/VEGF-A pathway. Cancer Lett **276**(2): 143-51.

Kim, M. J., S. C. Lee, S. H. Kang, J. Choo and J. M. Song (2010). Quantification of UV-induced cyclobutane pyrimidine dimers using an oligonucleotide chip assay. Anal Bioanal Chem **397**(6): 2271-7.

Kinzler, K. W. and B. Vogelstein (1998). Landscaping the cancer terrain. Science **280**(5366): 1036-7.

Kivisaari, A. K., M. Kallajoki, T. Mirtti, J. A. McGrath, J. W. Bauer, F. Weber, R. Konigova, D. Sawamura, K. C. Sato-Matsumura, H. Shimizu, M. Csikos, K. Sinemus, W. Beckert and V. M. Kahari (2008). Transformation-specific matrix metalloproteinases (MMP)-7 and MMP-13 are expressed by tumour cells in epidermolysis bullosa-associated squamous cell carcinomas. British Journal of Dermatology **158**(4): 778-785.

Knoll, J. H., R. D. Nicholls, R. E. Magenis, J. M. Graham, Jr., M. Lalande and S. A. Latt (1989). Angelman and Prader-Willi syndromes share a common chromosome 15 deletion but differ in parental origin of the deletion. Am J Med Genet **32**(2): 285-90.

Knudson, A. G., Jr. (1971). Mutation and cancer: statistical study of retinoblastoma. Proc Natl Acad Sci U S A **68**(4): 820-3.

Kojima, K., M. Konopleva, I. J. Samudio, M. Shikami, M. Cabreira-Hansen, T. McQueen, V. Ruvolo, T. Tsao, Z. Zeng, L. T. Vassilev and M. Andreeff (2005). MDM2 antagonists induce p53-dependent apoptosis in AML: implications for leukemia therapy. Blood **106**(9): 3150-9.

Kong, J., D. B. Stairs and J. P. Lynch (2010). Modelling Barrett's oesophagus. Biochem Soc Trans **38**(2): 321-6.

Konig, J., Y. Cui, A. T. Nies and D. Keppler (2000). Localization and genomic organization of a new hepatocellular organic anion transporting polypeptide. J Biol Chem **275**(30): 23161-8.

Konig, J., A. Seithel, U. Gradhand and M. F. Fromm (2006). Pharmacogenomics of human OATP transporters. Naunyn Schmiedebergs Arch Pharmacol **372**(6): 432-43.

Kowal-Vern, A. and B. K. Criswell (2005). Burn scar neoplasms: a literature review and statistical analysis. Burns **31**(4): 403-13.

Kraemer, K. H. (1993). Xeroderma Pigmentosum.

Kraemer, K. H., M. M. Lee and J. Scotto (1987). Xeroderma pigmentosum. Cutaneous, ocular, and neurologic abnormalities in 830 published cases. Arch Dermatol **123**(2): 241-50.

Krepulat, F., J. Lohler, C. Heinlein, A. Hermannstadter, G. V. Tolstonog and W. Deppert (2005). Epigenetic mechanisms affect mutant p53 transgene expression in WAP-mutp53 transgenic mice. Oncogene **24**(29): 4645-59.

Kullak-Ublick, G. A., M. G. Ismair, B. Stieger, L. Landmann, R. Huber, F. Pizzagalli, K. Fattinger, P. J. Meier and B. Hagenbuch (2001). Organic anion-transporting polypeptide B (OATP-B) and its functional comparison with three other OATPs of human liver. Gastroenterology **120**(2): 525-33.

Kusters-Vandevelde, H. V., A. Van Leeuwen, M. A. Verdijk, M. N. de Koning, W. G. Quint, W. J. Melchers, M. J. Ligtenberg and W. A. Blokx (2010). CDKN2A but not TP53 mutations nor HPV presence predict poor outcome in metastatic squamous cell carcinoma of the skin. Int J Cancer **126**(9): 2123-32.

Kwa, R. E., K. Campana and R. L. Moy (1992). Biology of cutaneous squamous cell carcinoma. J Am Acad Dermatol **26**(1): 1-26.

Lane, D. P. (1992). Cancer. p53, guardian of the genome. Nature **358**(6381): 15-6.

Lane, D. P., C. F. Cheok and S. Lain (2010). p53-based cancer therapy. Cold Spring Harb Perspect Biol **2**(9): a001222.

Lane, D. P. and L. V. Crawford (1979). T antigen is bound to a host protein in SV40-transformed cells. Nature **278**(5701): 261-3.

Lanssens, S. and K. Ongenae (2011). Dermatologic lesions and risk for cancer. Acta Clin Belg **66**(3): 177-85.

Lazarevich, N. L. and D. I. Fleishman (2008). Tissue-specific transcription factors in progression of epithelial tumors. Biochemistry (Mosc) **73**(5): 573-91.

Lee, W., A. Belkhiri, A. C. Lockhart, N. Merchant, H. Glaeser, E. I. Harris, M. K. Washington, E. M. Brunt, A. Zaika, R. B. Kim and W. El-Rifai (2008). Overexpression of OATP1B3 confers apoptotic resistance in colon cancer. Cancer Res **68**(24): 10315-23.

Leff, S. E., C. I. Brannan, M. L. Reed, T. Ozcelik, U. Francke, N. G. Copeland and N. A. Jenkins (1992). Maternal imprinting of the mouse Snrpn gene and conserved linkage homology with the human Prader-Willi syndrome region. Nat Genet **2**(4): 259-64.

Leibovitch, I., S. C. Huilgol, D. Selva, D. Hill, S. Richards and R. Paver (2005). Cutaneous squamous cell carcinoma treated with Mohs micrographic surgery in Australia I. Experience over 10 years. J Am Acad Dermatol **53**(2): 253-60.

Leigh, I. M., R. A. Eady, A. H. Heagerty, P. E. Purkis, P. A. Whitehead and R. E. Burgeson (1988). Type VII collagen is a normal component of epidermal basement membrane, which shows altered expression in recessive dystrophic epidermolysis bullosa. J Invest Dermatol **90**(5): 639-42.

Lenburg, M. E., L. S. Liou, N. P. Gerry, G. M. Frampton, H. T. Cohen and M. F. Christman (2003). Previously unidentified changes in renal cell carcinoma gene expression identified by parametric analysis of microarray data. BMC Cancer **3**: 31.

Lentz, S. R., R. J. Raish, E. P. Orlowski and J. M. Marion (1990). Squamous cell carcinoma in epidermolysis bullosa. Treatment with systemic chemotherapy. Cancer **66**(6): 1276-8.

Leonard, G. D., T. Fojo and S. E. Bates (2003). The role of ABC transporters in clinical practice. Oncologist **8**(5): 411-24.

Letschert, K., D. Keppler and J. Konig (2004). Mutations in the SLCO1B3 gene affecting the substrate specificity of the hepatocellular uptake transporter OATP1B3 (OATP8). Pharmacogenetics **14**(7): 441-52.

Levine, A. J. and M. Oren (2009). The first 30 years of p53: growing ever more complex. Nat Rev Cancer **9**(10): 749-58.

Lindelof, B., B. Krynitz, F. Granath and A. Ekbom (2008). Burn injuries and skin cancer: a population-based cohort study. Acta Derm Venereol **88**(1): 20-2.

Livak, K. J. and T. D. Schmittgen (2001). Analysis of relative gene expression data using real-time quantitative PCR and the 2(-Delta Delta C(T)) Method. Methods **25**(4): 402-8.

Lockhart, A. C., E. Harris, B. J. Lafleur, N. B. Merchant, M. K. Washington, M. B. Resnick, T. J. Yeatman and W. Lee (2008). Organic anion transporting polypeptide 1B3 (OATP1B3) is overexpressed in colorectal tumors and is a predictor of clinical outcome. Clin Exp Gastroenterol **1**: 1-7.

Lozano, G. (2007). Mouse models of p53 functions. Cold Spring Harb Perspect Biol **2**(4): a001115.

Lucas, B., K. Grigo, S. Erdmann, J. Lausen, L. Klein-Hitpass and G. U. Ryffel (2005). HNF4alpha reduces proliferation of kidney cells and affects genes deregulated in renal cell carcinoma. Oncogene **24**(42): 6418-31.

Lugo, T. G., A. M. Pendergast, A. J. Muller and O. N. Witte (1990). Tyrosine kinase activity and transformation potency of bcr-abl oncogene products. Science **247**(4946): 1079-82.

Macleod, K. (2000). Tumor suppressor genes. Curr Opin Genet Dev **10**(1): 81-93.

Malcolm, S., J. Clayton-Smith, M. Nichols, S. Robb, T. Webb, J. A. Armour, A. J. Jeffreys and M. E. Pembrey (1991). Uniparental paternal disomy in Angelman's syndrome. Lancet **337**(8743): 694-7.

Malkin, D. (1993). p53 and the Li-Fraumeni syndrome. Cancer Genet Cytogenet **66**(2): 83-92.

Mallipeddi, R. (2002). Epidermolysis bullosa and cancer. Clin Exp Dermatol **27**(8): 616-23.

Mallipeddi, R., F. M. Keane, J. A. McGrath, B. J. Mayou and R. A. Eady (2004). Increased risk of squamous cell carcinoma in junctional epidermolysis bullosa. J Eur Acad Dermatol Venereol **18**(5): 521-6.

Mallipeddi, R., V. Wessagowit, A. P. South, A. M. Robson, G. E. Orchard, R. A. Eady and J. A. McGrath (2004). Reduced expression of insulin-like growth factor-binding protein-3 (IGFBP-3) in Squamous cell carcinoma complicating recessive dystrophic epidermolysis bullosa. J Invest Dermatol **122**(5): 1302-9.

Marcel, V. and P. Hainaut (2009). p53 isoforms - a conspiracy to kidnap p53 tumor suppressor activity? Cell Mol Life Sci **66**(3): 391-406.

Martinez, J. C. and C. C. Otley (2001). The management of melanoma and nonmelanoma skin cancer: a review for the primary care physician. Mayo Clin Proc **76**(12): 1253-65.

Martins, V. L., J. J. Vyas, M. Chen, K. Purdie, C. A. Mein, A. P. South, A. Storey, J. A. McGrath and E. A. O'Toole (2009). Increased invasive behaviour in cutaneous squamous cell carcinoma with loss of basement-membrane type VII collagen. J Cell Sci **122**(Pt 11): 1788-99.

Masini, C., P. G. Fuchs, F. Gabrielli, S. Stark, F. Sera, M. Ploner, C. F. Melchi, G. Primavera, G. Pirchio, O. Picconi, P. Petasecca, M. S. Cattaruzza, H. J. Pfister and D. Abeni (2003). Evidence for the association of human papillomavirus infection and cutaneous squamous cell carcinoma in immunocompetent individuals. Arch Dermatol **139**(7): 890-4.

Maskos, U. and E. M. Southern (1992). Oligonucleotide hybridizations on glass supports: a novel linker for oligonucleotide synthesis and hybridization properties of oligonucleotides synthesised in situ. Nucleic Acids Res **20**(7): 1679-84.

Massague, J., S. W. Blain and R. S. Lo (2000). TGFbeta signaling in growth control, cancer, and heritable disorders. Cell **103**(2): 295-309.

Mavilio, F., G. Pellegrini, S. Ferrari, F. Di Nunzio, E. Di Iorio, A. Recchia, G. Maruggi, G. Ferrari, E. Provasi, C. Bonini, S. Capurro, A. Conti, C. Magnoni, A. Giannetti and M.

De Luca (2006). Correction of junctional epidermolysis bullosa by transplantation of genetically modified epidermal stem cells. Nat Med **12**(12): 1397-402.

Maxwell, P. J., D. B. Longley, T. Latif, J. Boyer, W. Allen, M. Lynch, U. McDermott, D. P. Harkin, C. J. Allegra and P. G. Johnston (2003). Identification of 5-fluorouracil-inducible target genes using cDNA microarray profiling. Cancer Res **63**(15): 4602-6.

McGrath, J. A., O. M. Schofield, B. J. Mayou, P. H. McKee and R. A. Eady (1992). Epidermolysis bullosa complicated by squamous cell carcinoma: report of 10 cases. J Cutan Pathol **19**(2): 116-23.

McGregor, J. M., R. J. Berkhout, M. Rozycka, J. ter Schegget, J. N. Bouwes Bavinck, L. Brooks and T. Crook (1997). p53 mutations implicate sunlight in post-transplant skin cancer irrespective of human papillomavirus status. Oncogene **15**(14): 1737-40.

McLean, W. H., L. Pulkkinen, F. J. Smith, E. L. Rugg, E. B. Lane, F. Bullrich, R. E. Burgeson, S. Amano, D. L. Hudson, K. Owaribe, J. A. McGrath, J. R. McMillan, R. A. Eady, I. M. Leigh, A. M. Christiano and J. Uitto (1996). Loss of plectin causes epidermolysis bullosa with muscular dystrophy: cDNA cloning and genomic organization. Genes Dev **10**(14): 1724-35.

Medina, V., M. B. Calvo, S. Diaz-Prado and J. Espada (2009). Hedgehog signalling as a target in cancer stem cells. Clin Transl Oncol **11**(4): 199-207.

Meier, P. J., U. Eckhardt, A. Schroeder, B. Hagenbuch and B. Stieger (1997). Substrate specificity of sinusoidal bile acid and organic anion uptake systems in rat and human liver. Hepatology **26**(6): 1667-77.

Mellemkjaer, L., L. R. Holmich, G. Gridley, C. Rabkin and J. H. Olsen (2006). Risks for skin and other cancers up to 25 years after burn injuries. Epidemiology **17**(6): 668-73.

Mellerio (1999). Molecular pathology of the cutaneous basement membrane zone. Clinical and Experimental Dermatology **24**(1): 25-32.

Mellerio, J. E. (1999). Molecular pathology of the cutaneous basement membrane zone. Clin Exp Dermatol **24**(1): 25-32.

Meltzer, P. S. (2001). Spotting the target: microarrays for disease gene discovery. Curr Opin Genet Dev **11**(3): 258-63.

Meyer zu Schwabedissen, H. E. and R. B. Kim (2009). Hepatic OATP1B transporters and nuclear receptors PXR and CAR: interplay, regulation of drug disposition genes, and single nucleotide polymorphisms. Mol Pharm **6**(6): 1644-61.

Miller, D. L. and M. A. Weinstock (1994). Nonmelanoma skin cancer in the United States: incidence. J Am Acad Dermatol **30**(5 Pt 1): 774-8.

Milner, J. and E. A. Medcalf (1991). Cotranslation of activated mutant p53 with wild type drives the wild-type p53 protein into the mutant conformation. Cell **65**(5): 765-74.

Mizuno, N., T. Niwa, Y. Yotsumoto and Y. Sugiyama (2003). Impact of drug transporter studies on drug discovery and development. Pharmacol Rev **55**(3): 425-61.

Mohr, S., G. D. Leikauf, G. Keith and B. H. Rihn (2002). Microarrays as cancer keys: an array of possibilities. J Clin Oncol **20**(14): 3165-75.

Moller, R., F. Reymann and K. Hou-Jensen (1979). Metastases in dermatological patients with squamous cell carcinoma. Arch Dermatol **115**(6): 703-5.

Monks, N. R., S. Liu, Y. Xu, H. Yu, A. S. Bendelow and J. A. Moscow (2007). Potent cytotoxicity of the phosphatase inhibitor microcystin LR and microcystin analogues in OATP1B1- and OATP1B3-expressing HeLa cells. Mol Cancer Ther **6**(2): 587-98.

Muto, M., T. Onogawa, T. Suzuki, T. Ishida, T. Rikiyama, Y. Katayose, N. Ohuchi, H. Sasano, T. Abe and M. Unno (2007). Human liver-specific organic anion transporter-2 is a potent prognostic factor for human breast carcinoma. Cancer Sci **98**(10): 1570-6.

Nakamura, K., H. Shima, M. Watanabe, T. Haneji and K. Kikuchi (1999). Molecular cloning and characterization of a novel dual-specificity protein phosphatase possibly involved in spermatogenesis. Biochem J **344 Pt 3**: 819-25.

Nelson, M. A., J. G. Einspahr, D. S. Alberts, C. A. Balfour, J. A. Wymer, K. L. Welch, S. J. Salasche, J. L. Bangert, T. M. Grogan and P. O. Bozzo (1994). Analysis of the p53 gene in human precancerous actinic keratosis lesions and squamous cell cancers. Cancer Lett **85**(1): 23-9.

Nemunaitis, J., G. Clayman, S. S. Agarwala, W. Hrushesky, J. R. Wells, C. Moore, J. Hamm, G. Yoo, J. Baselga, B. A. Murphy, K. A. Menander, L. L. Licato, S. Chada, R. D. Gibbons, M. Olivier, P. Hainaut, J. A. Roth, R. E. Sobol and W. J. Goodwin (2009). Biomarkers Predict p53 Gene Therapy Efficacy in Recurrent Squamous Cell Carcinoma of the Head and Neck. Clin Cancer Res **15**(24): 7719-7725.

Nicholls, R. D., J. H. Knoll, M. G. Butler, S. Karam and M. Lalande (1989). Genetic imprinting suggested by maternal heterodisomy in nondeletion Prader-Willi syndrome. Nature **342**(6247): 281-5.

Nishida, N., H. Yano, T. Nishida, T. Kamura and M. Kojiro (2006). Angiogenesis in cancer. Vasc Health Risk Manag **2**(3): 213-9.

Novick, M., D. A. Gard, S. B. Hardy and M. Spira (1977). Burn scar carcinoma: a review and analysis of 46 cases. J Trauma **17**(10): 809-17.

Nozawa, T., H. Minami, S. Sugiura, A. Tsuji and I. Tamai (2005). Role of organic anion transporter OATP1B1 (OATP-C) in hepatic uptake of irinotecan and its active metabolite, 7-ethyl-10-hydroxycamptothecin: in vitro evidence and effect of single nucleotide polymorphisms. Drug Metab Dispos **33**(3): 434-9.

O'Shaughnessy, R. F. and A. M. Christiano (2004). Inherited disorders of the skin in human and mouse: from development to differentiation. Int J Dev Biol **48**(2-3): 171-9.

Olivier, M., M. Hollstein and P. Hainaut (2010). TP53 mutations in human cancers: origins, consequences, and clinical use. Cold Spring Harb Perspect Biol **2**(1): a001008.

Ortiz-Urda, S., J. Garcia, C. L. Green, L. Chen, Q. Lin, D. P. Veitch, L. Y. Sakai, H. Lee, M. P. Marinkovich and P. A. Khavari (2005). Type VII Collagen Is Required for Ras-Driven Human Epidermal Tumorigenesis. Science **307**(5716): 1773-1776.

Ortiz-Urda, S., B. Thyagarajan, D. R. Keene, Q. Lin, M. Fang, M. P. Calos and P. A. Khavari (2002). Stable nonviral genetic correction of inherited human skin disease. Nat Med **8**(10): 1166-70.

Ozcelik, T., S. Leff, W. Robinson, T. Donlon, M. Lalande, E. Sanjines, A. Schinzel and U. Francke (1992). Small nuclear ribonucleoprotein polypeptide N (SNRPN), an expressed gene in the Prader-Willi syndrome critical region. Nat Genet **2**(4): 265-9.

Pane, F., M. Intrieri, C. Quintarelli, B. Izzo, G. C. Muccioli and F. Salvatore (2002). BCR/ABL genes and leukemic phenotype: from molecular mechanisms to clinical correlations. Oncogene **21**(56): 8652-67.

Pearson, R. W. (1962). Studies on the pathogenesis of epidermolysis bullosa. J Invest Dermatol **39**: 551-75.

Peltonen, J. K., H. M. Helppi, P. Paakko, T. Turpeenniemi-Hujanen and K. H. Vahakangas (2010). p53 in head and neck cancer: functional consequences and environmental implications of TP53 mutations. Head Neck Oncol **2**: 36.

Penn, I. and T. E. Starzl (1972). Malignant tumors arising de novo in immunosuppressed organ transplant recipients. Transplantation **14**(4): 407-17.

Perez-Tomas, R. (2006). Multidrug resistance: retrospect and prospects in anti-cancer drug treatment. Curr Med Chem **13**(16): 1859-76.

Petitjean, A., E. Mathe, S. Kato, C. Ishioka, S. V. Tavtigian, P. Hainaut and M. Olivier (2007). Impact of mutant p53 functional properties on TP53 mutation patterns and tumor phenotype: lessons from recent developments in the IARC TP53 database. Hum Mutat **28**(6): 622-9.

Pfendner, E. G., A. Bruckner, P. Conget, J. Mellerio, F. Palisson and A. W. Lucky (2007). Basic science of epidermolysis bullosa and diagnostic and molecular characterization: Proceedings of the IInd International Symposium on Epidermolysis Bullosa, Santiago, Chile, 2005. International Journal of Dermatology **46**(8): 781-794.

Pfendner, E. G. and A. L. Bruckner (1993). Epidermolysis Bullosa Simplex.

Pfendner, E. G. and A. W. Lucky (1993). Junctional Epidermolysis Bullosa.

Pillay, E. (2008). Epidermolysis bullosa. Part 1: causes, presentation and complications. Br J Nurs **17**(5): 292-6.

Pittelkow, M. R. and G. D. Shipley (1989). Serum-free culture of normal human melanocytes: growth kinetics and growth factor requirements. J Cell Physiol **140**(3): 565-76.

Poumay, Y. and A. Coquette (2007). Modelling the human epidermis in vitro: tools for basic and applied research. Arch Dermatol Res **298**(8): 361-9.

Pourreyron, C., G. Cox, X. Mao, A. Volz, N. Baksh, T. Wong, H. Fassihi, K. Arita, E. A. O'Toole, J. Ocampo-Candiani, M. Chen, I. R. Hart, L. Bruckner-Tuderman, J. C. Salas-Alanis, J. A. McGrath, I. M. Leigh and A. P. South (2007). Patients with recessive dystrophic epidermolysis bullosa develop squamous-cell carcinoma regardless of type VII collagen expression. J Invest Dermatol **127**(10): 2438-44.

Preciado, D. A., A. Matas and G. L. Adams (2002). Squamous cell carcinoma of the head and neck in solid organ transplant recipients. Head Neck **24**(4): 319-25.

Purdie, K. J., S. R. Lambert, M. T. Teh, T. Chaplin, G. Molloy, M. Raghavan, D. P. Kelsell, I. M. Leigh, C. A. Harwood, C. M. Proby and B. D. Young (2007). Allelic imbalances and microdeletions affecting the PTPRD gene in cutaneous squamous cell carcinomas detected using single nucleotide polymorphism microarray analysis. Genes Chromosomes Cancer **46**(7): 661-9.

Radonic, A., S. Thulke, I. M. Mackay, O. Landt, W. Siegert and A. Nitsche (2004). Guideline to reference gene selection for quantitative real-time PCR. Biochem Biophys Res Commun **313**(4): 856-62.

Reed, M. L. and S. E. Leff (1994). Maternal imprinting of human SNRPN, a gene deleted in Prader-Willi syndrome. Nat Genet **6**(2): 163-7.

Reis-Filho, J. S. (2009). Next-generation sequencing. Breast Cancer Res **11 Suppl 3**: S12.

Remington, J., X. Wang, Y. Hou, H. Zhou, J. Burnett, T. Muirhead, J. Uitto, D. R. Keene, D. T. Woodley and M. Chen (2009). Injection of recombinant human type VII collagen

corrects the disease phenotype in a murine model of dystrophic epidermolysis bullosa. Mol Ther **17**(1): 26-33.

Richert, L., M. J. Liguori, C. Abadie, B. Heyd, G. Mantion, N. Halkic and J. F. Waring (2006). Gene expression in human hepatocytes in suspension after isolation is similar to the liver of origin, is not affected by hepatocyte cold storage and cryopreservation, but is strongly changed after hepatocyte plating. Drug Metab Dispos **34**(5): 870-9.

Rigel, D. S., R. J. Friedman and A. W. Kopf (1996). Lifetime risk for development of skin cancer in the U.S. population: current estimate is now 1 in 5. J Am Acad Dermatol **35**(6): 1012-3.

Robinson, W. P., A. Bottani, Y. G. Xie, J. Balakrishman, F. Binkert, M. Machler, A. Prader and A. Schinzel (1991). Molecular, cytogenetic, and clinical investigations of Prader-Willi syndrome patients. Am J Hum Genet **49**(6): 1219-34.

Rodeck, U., A. Fertala and J. Uitto (2007). Anchorless keratinocyte survival: an emerging pathogenic mechanism for squamous cell carcinoma in recessive dystrophic epidermolysis bullosa. Experimental Dermatology **16**: 465-467.

Rodeck, U. and J. Uitto (2007). Recessive dystrophic epidermolysis bullosa-associated squamous-cell carcinoma: an enigmatic entity with complex pathogenesis. J Invest Dermatol **127**(10): 2295-6.

Roth, J. A., D. Nguyen, D. D. Lawrence, B. L. Kemp, C. H. Carrasco, D. Z. Ferson, W. K. Hong, R. Komaki, J. J. Lee, J. C. Nesbitt, K. M. Pisters, J. B. Putnam, R. Schea, D. M. Shin, G. L. Walsh, M. M. Dolormente, C. I. Han, F. D. Martin, N. Yen, K. Xu, L. C. Stephens, T. J. McDonnell, T. Mukhopadhyay and D. Cai (1996). Retrovirus-mediated wild-type p53 gene transfer to tumors of patients with lung cancer. Nat Med **2**(9): 985-91.

Rowe, D. E., R. J. Carroll and C. L. Day, Jr. (1992). Prognostic factors for local recurrence, metastasis, and survival rates in squamous cell carcinoma of the skin, ear, and lip. Implications for treatment modality selection. J Am Acad Dermatol **26**(6): 976-90.

Runte, M., A. Huttenhofer, S. Gross, M. Kiefmann, B. Horsthemke and K. Buiting (2001). The IC-SNURF-SNRPN transcript serves as a host for multiple small nucleolar RNA species and as an antisense RNA for UBE3A. Hum Mol Genet **10**(23): 2687-700.

Runte, M., P. M. Kroisel, G. Gillessen-Kaesbach, R. Varon, D. Horn, M. Y. Cohen, J. Wagstaff, B. Horsthemke and K. Buiting (2004). SNURF-SNRPN and UBE3A transcript levels in patients with Angelman syndrome. Hum Genet **114**(6): 553-61.

Sabin, S. R., G. Goldstein, H. G. Rosenthal and K. K. Haynes (2004). Aggressive squamous cell carcinoma originating as a Marjolin's ulcer. Dermatol Surg **30**(2 Pt 1): 229-30.

Sakai, L. Y., D. R. Keene, N. P. Morris and R. E. Burgeson (1986). Type VII collagen is a major structural component of anchoring fibrils. J Cell Biol **103**(4): 1577-86.

Salasche, S. J. (2000). Epidemiology of actinic keratoses and squamous cell carcinoma. J Am Acad Dermatol **42**(1 Pt 2): 4-7.

Sawamura, D., H. Nakano and Y. Matsuzaki (2010). Overview of epidermolysis bullosa. J Dermatol **37**(3): 214-9.

Schena, M., D. Shalon, R. W. Davis and P. O. Brown (1995). Quantitative monitoring of gene expression patterns with a complementary DNA microarray. Science **270**(5235): 467-70.

Schiffer, R., M. Neis, D. Holler, F. Rodriguez, A. Geier, C. Gartung, F. Lammert, A. Dreuw, G. Zwadlo-Klarwasser, H. Merk, F. Jugert and J. M. Baron (2003). Active influx transport is mediated by members of the organic anion transporting polypeptide family in human epidermal keratinocytes. J Invest Dermatol **120**(2): 285-91.

Schuster, S. C. (2008). Next-generation sequencing transforms today's biology. Nat Methods **5**(1): 16-8.

Secchiero, P., M. G. di Iasio, A. Gonelli and G. Zauli (2008). The MDM2 inhibitor Nutlins as an innovative therapeutic tool for the treatment of haematological malignancies. Curr Pharm Des **14**(21): 2100-10.

Seithel, A., J. Karlsson, C. Hilgendorf, A. Bjorquist and A. L. Ungell (2006). Variability in mRNA expression of ABC- and SLC-transporters in human intestinal cells: comparison between human segments and Caco-2 cells. Eur J Pharm Sci **28**(4): 291-9.

Sekine, T., H. Miyazaki and H. Endou (2006). Molecular physiology of renal organic anion transporters. Am J Physiol Renal Physiol **290**(2): F251-61.

Shah, S. P., R. D. Morin, J. Khattra, L. Prentice, T. Pugh, A. Burleigh, A. Delaney, K. Gelmon, R. Guliany, J. Senz, C. Steidl, R. A. Holt, S. Jones, M. Sun, G. Leung, R. Moore, T. Severson, G. A. Taylor, A. E. Teschendorff, K. Tse, G. Turashvili, R. Varhol, R. L. Warren, P. Watson, Y. Zhao, C. Caldas, D. Huntsman, M. Hirst, M. A. Marra and S. Aparicio (2009). Mutational evolution in a lobular breast tumour profiled at single nucleotide resolution. Nature **461**(7265): 809-13.

Shalon, D., S. J. Smith and P. O. Brown (1996). A DNA microarray system for analyzing complex DNA samples using two-color fluorescent probe hybridization. Genome Res **6**(7): 639-45.

Shen, Y., R. Luche, B. Wei, M. L. Gordon, C. D. Diltz and N. K. Tonks (2001). Activation of the Jnk signaling pathway by a dual-specificity phosphatase, JSP-1. Proc Natl Acad Sci U S A **98**(24): 13613-8.

Shimizu, H., M. Sato, M. Ban, Y. Kitajima, S. Ishizaki, T. Harada, L. Bruckner-Tuderman, J. D. Fine, R. Burgeson, A. Kon, J. A. McGrath, A. M. Christiano, J. Uitto and T. Nishikawa (1997). Immunohistochemical, ultrastructural, and molecular features of Kindler syndrome distinguish it from dystrophic epidermolysis bullosa. Arch Dermatol **133**(9): 1111-7.

Shimohira-Yamasaki, M., S. Toda, Y. Narisawa and H. Sugihara (2006). Merkel cell-nerve cell interaction undergoes formation of a synapse-like structure in a primary culture. Cell Struct Funct **31**(1): 39-45.

Shivaswamy, K. N., T. K. Sumathy, A. L. Shyamprasad and C. Ranganathan (2009). Squamous cell carcinoma complicating epidermolysis bullosa in a 6-year-old girl. Int J Dermatol **48**(7): 731-3.

Siegel, D. H., G. H. Ashton, H. G. Penagos, J. V. Lee, H. S. Feiler, K. C. Wilhelmsen, A. P. South, F. J. Smith, A. R. Prescott, V. Wessagowit, N. Oyama, M. Akiyama, D. Al Aboud, K. Al Aboud, A. Al Githami, K. Al Hawsawi, A. Al Ismaily, R. Al-Suwaid, D. J. Atherton, R. Caputo, J. D. Fine, I. J. Frieden, E. Fuchs, R. M. Haber, T. Harada, Y. Kitajima, S. B. Mallory, H. Ogawa, S. Sahin, H. Shimizu, Y. Suga, G. Tadini, K. Tsuchiya, C. B. Wiebe, F. Wojnarowska, A. B. Zaghloul, T. Hamada, R. Mallipeddi, R. A. Eady, W. H. McLean, J. A. McGrath and E. H. Epstein (2003). Loss of kindlin-1, a human homolog of the Caenorhabditis elegans actin-extracellular-matrix linker protein UNC-112, causes Kindler syndrome. Am J Hum Genet **73**(1): 174-87.

Slater, S. D., J. A. McGrath, C. Hobbs, R. A. Eady and P. H. McKee (1992). Expression of mutant p53 gene in squamous carcinoma arising in patients with recessive dystrophic epidermolysis bullosa. Histopathology **20**(3): 237-41.

Smith, F. J., R. A. Eady, I. M. Leigh, J. R. McMillan, E. L. Rugg, D. P. Kelsell, S. P. Bryant, N. K. Spurr, J. F. Geddes, G. Kirtschig, G. Milana, A. G. de Bono, K. Owaribe, G. Wiche, L. Pulkkinen, J. Uitto, W. H. McLean and E. B. Lane (1996). Plectin deficiency results in muscular dystrophy with epidermolysis bullosa. Nat Genet **13**(4): 450-7.

Smith, N. F., M. R. Acharya, N. Desai, W. D. Figg and A. Sparreboom (2005). Identification of OATP1B3 as a high-affinity hepatocellular transporter of paclitaxel. Cancer Biol Ther **4**(8): 815-8.

Smith, N. F., W. D. Figg and A. Sparreboom (2005). Role of the liver-specific transporters OATP1B1 and OATP1B3 in governing drug elimination. Expert Opin Drug Metab Toxicol **1**(3): 429-45.

Smith, N. F., S. Marsh, T. J. Scott-Horton, A. Hamada, S. Mielke, K. Mross, W. D. Figg, J. Verweij, H. L. McLeod and A. Sparreboom (2007). Variants in the SLCO1B3 gene: interethnic distribution and association with paclitaxel pharmacokinetics. Clin Pharmacol Ther **81**(1): 76-82.

Song, H., M. Hollstein and Y. Xu (2007). p53 gain-of-function cancer mutants induce genetic instability by inactivating ATM. Nat Cell Biol **9**(5): 573-80.

Stahl, P. L., H. Stranneheim, A. Asplund, L. Berglund, F. Ponten and J. Lundeberg (2011). Sun-induced nonsynonymous p53 mutations are extensively accumulated and tolerated in normal appearing human skin. J Invest Dermatol **131**(2): 504-8.

Stasko, T., M. D. Brown, J. A. Carucci, S. Euvrard, T. M. Johnson, R. D. Sengelmann, E. Stockfleth and W. D. Tope (2004). Guidelines for the management of squamous cell carcinoma in organ transplant recipients. Dermatol Surg **30**(4 Pt 2): 642-50.

Stehelin, D., H. E. Varmus, J. M. Bishop and P. K. Vogt (1976). DNA related to the transforming gene(s) of avian sarcoma viruses is present in normal avian DNA. Nature **260**(5547): 170-3.

Strano, S., G. Fontemaggi, A. Costanzo, M. G. Rizzo, O. Monti, A. Baccarini, G. Del Sal, M. Levrero, A. Sacchi, M. Oren and G. Blandino (2002). Physical interaction with human tumor-derived p53 mutants inhibits p63 activities. J Biol Chem **277**(21): 18817-26.

Stratton, M. R., P. J. Campbell and P. A. Futreal (2009). The cancer genome. Nature **458**(7239): 719-24.

Subramanian, J. and R. Simon (2010). Gene expression-based prognostic signatures in lung cancer: ready for clinical use? J Natl Cancer Inst **102**(7): 464-74.

Sutcliffe, J. S., M. Nakao, S. Christian, K. H. Orstavik, N. Tommerup, D. H. Ledbetter and A. L. Beaudet (1994). Deletions of a differentially methylated CpG island at the SNRPN gene define a putative imprinting control region. Nat Genet **8**(1): 52-8.

Suzuki, N., T. Onda, N. Yamamoto, A. Katakura, J. E. Mizoe and T. Shibahara (2007). Mutation of the p16/CDKN2 gene and loss of heterozygosity in malignant mucosal melanoma and adenoid cystic carcinoma of the head and neck. Int J Oncol **31**(5): 1061-7.

Takagaki, K., T. Satoh, N. Tanuma, K. Masuda, M. Takekawa, H. Shima and K. Kikuchi (2004). Characterization of a novel low-molecular-mass dual-specificity phosphatase-3 (LDP-3) that enhances activation of JNK and p38. Biochem J **383**(Pt. 3): 447-55.

Tang, J. P., C. P. Tan, J. Li, M. M. Siddique, K. Guo, S. W. Chan, J. E. Park, W. N. Tay, Z. Y. Huang, W. C. Li, J. Chen and Q. Zeng (2010). VHZ is a novel centrosomal phosphatase associated with cell growth and human primary cancers. Mol Cancer **9**: 128.

Teh, M. T., D. Blaydon, T. Chaplin, N. J. Foot, S. Skoulakis, M. Raghavan, C. A. Harwood, C. M. Proby, M. P. Philpott, B. D. Young and D. P. Kelsell (2005). Genomewide single nucleotide polymorphism microarray mapping in basal cell carcinomas unveils uniparental disomy as a key somatic event. Cancer Res **65**(19): 8597-603.

Tirona, R. G. and R. B. Kim (2002). Pharmacogenomics of organic anion-transporting polypeptides (OATP). Adv Drug Deliv Rev **54**(10): 1343-52.

Tischfield, J. A. (1997). Loss of heterozygosity or: how I learned to stop worrying and love mitotic recombination. Am J Hum Genet **61**(5): 995-9.

Titeux, M., J. Mazereeuw-Hautier, S. Hadj-Rabia, C. Prost, L. Tonasso, S. Fraitag, Y. de Prost, A. Hovnanian and C. Bodemer (2006). Three severe cases of EBS Dowling-Meara caused by missense and frameshift mutations in the keratin 14 gene. J Invest Dermatol **126**(4): 773-6.

Titeux, M., V. Pendaries, L. Tonasso, A. Décha, C. Bodemer and A. Hovnanian (2008). A frequent functional SNP in the MMP1 promoter is associated with higher disease severity in recessive dystrophic epidermolysis bullosa. Human Mutation **29**(2): 267-276.

Tolar, J., A. Ishida-Yamamoto, M. Riddle, R. T. McElmurry, M. Osborn, L. Xia, T. Lund, C. Slattery, J. Uitto, A. M. Christiano, J. E. Wagner and B. R. Blazar (2009). Amelioration of epidermolysis bullosa by transfer of wild-type bone marrow cells. Blood **113**(5): 1167-74.

Tomlinson, A. A. (1983). Recessive dystrophic epidermolysis bullosa. The anaesthetic management of a case for major surgery. Anaesthesia **38**(5): 485-91.

Tonks, N. K. and B. G. Neel (2001). Combinatorial control of the specificity of protein tyrosine phosphatases. Curr Opin Cell Biol **13**(2): 182-95.

Tsuji, A. (1999). Tissue selective drug delivery utilizing carrier-mediated transport systems. J Control Release **62**(1-2): 239-44.

Tsujimoto, M., S. Hirata, Y. Dan, H. Ohtani and Y. Sawada (2006). Polymorphisms and linkage disequilibrium of the OATP8 (OATP1B3) gene in Japanese subjects. Drug Metab Pharmacokinet **21**(2): 165-9.

Uitto, J., L. C. Chung-Honet and A. M. Christiano (1992). Molecular biology and pathology of type VII collagen. Exp Dermatol **1**(1): 2-11.

Uitto, J., J. A. McGrath, U. Rodeck, L. Bruckner-Tuderman and E. C. Robinson (2010). Progress in epidermolysis bullosa research: toward treatment and cure. J Invest Dermatol **130**(7): 1778-84.

Uitto, J. and G. Richard (2005). Progress in epidermolysis bullosa: from eponyms to molecular genetic classification. Clin Dermatol **23**(1): 33-40.

van de Steeg, E., E. Wagenaar, C. M. van der Kruijssen, J. E. Burggraaff, D. R. de Waart, R. P. Elferink, K. E. Kenworthy and A. H. Schinkel (2010). Organic anion transporting polypeptide 1a/1b-knockout mice provide insights into hepatic handling of bilirubin, bile acids, and drugs. J Clin Invest **120**(8): 2942-52.

van Steeg, H. and K. H. Kraemer (1999). Xeroderma pigmentosum and the role of UV-induced DNA damage in skin cancer. Mol Med Today **5**(2): 86-94.

Varki, R., S. Sadowski, J. Uitto and E. Pfendner (2007). Epidermolysis bullosa. II. Type VII collagen mutations and phenotype-genotype correlations in the dystrophic subtypes. J Med Genet **44**(3): 181-192.

Vassilev, L. T., B. T. Vu, B. Graves, D. Carvajal, F. Podlaski, Z. Filipovic, N. Kong, U. Kammlott, C. Lukacs, C. Klein, N. Fotouhi and E. A. Liu (2004). In vivo activation of the p53 pathway by small-molecule antagonists of MDM2. Science **303**(5659): 844-8.

Vavricka, S. R., D. Jung, M. Fried, U. Grutzner, P. J. Meier and G. A. Kullak-Ublick (2004). The human organic anion transporting polypeptide 8 (SLCO1B3) gene is transcriptionally repressed by hepatocyte nuclear factor 3beta in hepatocellular carcinoma. J Hepatol **40**(2): 212-8.

Vendrell, X., R. Bautista-Llacer, T. M. Alberola, E. Garcia-Mengual, M. Pardo, A. Urries and J. Sanchez (2011). Pregnancy after PGD for recessive dystrophic epidermolysis bullosa inversa: genetics and preimplantation genetics. J Assist Reprod Genet **28**(9): 825-32.

Veness, M. J. (2006). Defining patients with high-risk cutaneous squamous cell carcinoma. Australas J Dermatol **47**(1): 28-33.

von Holzen, U., T. Chen, A. Boquoi, J. E. Richter, G. W. Falk, A. J. Klein-Szanto, H. Cooper, S. Litwin, D. S. Weinberg and G. H. Enders (2010). Evidence for DNA damage checkpoint activation in barrett esophagus. Transl Oncol **3**(1): 33-42.

Vousden, K. H. and D. P. Lane (2007). p53 in health and disease. Nat Rev Mol Cell Biol **8**(4): 275-283.

Vousden, K. H. and C. Prives (2005). P53 and prognosis: new insights and further complexity. Cell **120**(1): 7-10.

Watt, S. A., C. Pourreyron, K. Purdie, C. Hogan, C. L. Cole, N. Foster, N. Pratt, J. C. Bourdon, V. Appleyard, K. Murray, A. M. Thompson, X. Mao, C. Mein, L. Bruckner-Tuderman, A. Evans, J. A. McGrath, C. M. Proby, J. Foerster, I. M. Leigh and A. P. South (2011). Integrative mRNA profiling comparing cultured primary cells with clinical samples reveals PLK1 and C20orf20 as therapeutic targets in cutaneous squamous cell carcinoma. Oncogene **30**(46): 4666-77.

Wessagowit, V., R. Mallipeddi, J. A. McGrath and A. P. South (2004). Altered expression of L-arginine metabolism pathway genes in chronic wounds in recessive dystrophic epidermolysis bullosa. Clin Exp Dermatol **29**(6): 664-8.

Whittle, D. O., M. G. Lee and B. Hanchard (2010). Juvenile polyposis syndrome. West Indian Med J **59**(3): 306-8.

Wong, T., L. Gammon, L. Liu, J. E. Mellerio, P. J. Dopping-Hepenstal, J. Pacy, G. Elia, R. Jeffery, I. M. Leigh, H. Navsaria and J. A. McGrath (2008). Potential of fibroblast cell therapy for recessive dystrophic epidermolysis bullosa. J Invest Dermatol **128**(9): 2179-89.

Woodley, D. T., D. R. Keene, T. Atha, Y. Huang, K. Lipman, W. Li and M. Chen (2004). Injection of recombinant human type VII collagen restores collagen function in dystrophic epidermolysis bullosa. Nat Med **10**(7): 693-5.

Woodley, D. T., G. G. Krueger, C. M. Jorgensen, J. A. Fairley, T. Atha, Y. Huang, L. Chan, D. R. Keene and M. Chen (2003). Normal and gene-corrected dystrophic epidermolysis bullosa fibroblasts alone can produce type VII collagen at the basement membrane zone. J Invest Dermatol **121**(5): 1021-8.

Woodley, D. T., J. Remington, Y. Huang, Y. Hou, W. Li, D. R. Keene and M. Chen (2007). Intravenously injected human fibroblasts home to skin wounds, deliver type VII collagen, and promote wound healing. Mol Ther **15**(3): 628-35.

Workman, P. (2003). The opportunities and challenges of personalized genome-based molecular therapies for cancer: targets, technologies, and molecular chaperones. Cancer Chemother Pharmacol **52 Suppl 1**: S45-56.

Wu, Q., Y. Li, S. Gu, N. Li, D. Zheng, D. Li, Z. Zheng, C. Ji, Y. Xie and Y. Mao (2004). Molecular cloning and characterization of a novel dual-specificity phosphatase 23 gene from human fetal brain. Int J Biochem Cell Biol **36**(8): 1542-53.

Wu, S., S. Liang, Y. Yan, Y. Wang, F. Li, Y. Deng, W. Huang, W. Yuan, N. Luo, C. Zhu, Y. Wang, Y. Li, M. Liu and X. Wu (2007). A novel mutation of TGF beta1 in a Chinese family with Camurati-Engelmann disease. Bone **40**(6): 1630-4.

Xu, Y. and B. Pasche (2007). TGF-beta signaling alterations and susceptibility to colorectal cancer. Hum Mol Genet **16 Spec No 1**: R14-20.

Yamaguchi, H., M. Kobayashi, M. Okada, T. Takeuchi, M. Unno, T. Abe, J. Goto, T. Hishinuma and N. Mano (2008). Rapid screening of antineoplastic candidates for the human organic anion transporter OATP1B3 substrates using fluorescent probes. Cancer Lett **260**(1-2): 163-9.

Yamaguchi, H., M. Okada, S. Akitaya, H. Ohara, T. Mikkaichi, H. Ishikawa, M. Sato, M. Matsuura, T. Saga, M. Unno, T. Abe, N. Mano, T. Hishinuma and J. Goto (2006). Transport of fluorescent chenodeoxycholic acid via the human organic anion transporters OATP1B1 and OATP1B3. J Lipid Res **47**(6): 1196-202.

Yin, C., Y. Lin, X. Zhang, Y. X. Chen, X. Zeng, H. Y. Yue, J. L. Hou, X. Deng, J. P. Zhang, Z. G. Han and W. F. Xie (2008). Differentiation therapy of hepatocellular carcinoma in mice with recombinant adenovirus carrying hepatocyte nuclear factor-4alpha gene. Hepatology **48**(5): 1528-39.

Yoo, K. H., Y. K. Park, H. S. Kim, W. W. Jung and S. G. Chang (2010). Epigenetic inactivation of HOXA5 and MSH2 gene in clear cell renal cell carcinoma. Pathol Int **60**(10): 661-6.

Yuspa, S. H. and E. H. Epstein, Jr. (2005). Cancer. An anchor for tumor cell invasion. Science **307**(5716): 1727-8.

Zafrakas, M., I. Losen, R. Knuchel and E. Dahl (2008). Enhancer of the rudimentary gene homologue (ERH) expression pattern in sporadic human breast cancer and normal breast tissue. BMC Cancer **8**: 145.

Zhou, X., S. Temam, Z. Chen, H. Ye, L. Mao and D. T. Wong (2005). Allelic imbalance analysis of oral tongue squamous cell carcinoma by high-density single nucleotide polymorphism arrays using whole-genome amplified DNA. Hum Genet **118**(3-4): 504-7.

Ziegler, A., D. J. Leffell, S. Kunala, H. W. Sharma, M. Gailani, J. A. Simon, A. J. Halperin, H. P. Baden, P. E. Shapiro, A. E. Bale and et al. (1993). Mutation hotspots due to sunlight

in the p53 gene of nonmelanoma skin cancers. Proc Natl Acad Sci U S A **90**(9): 4216-20.